

Differential Equations and Depth First Search for Enumeration of Maps in Surfaces

by

Daniel Richard Laurence Brown

A thesis

presented to the University of Waterloo

in fulfilment of the

thesis requirement for the degree of

Doctor of Philosophy

in

Combinatorics and Optimization

Waterloo, Ontario, Canada, 2000

©Daniel Richard Laurence Brown 2000

I hereby declare that I am the sole author of this thesis.

I authorize the University of Waterloo to lend this thesis to other institutions or individuals for the purpose of scholarly research.

I further authorize the University of Waterloo to reproduce this thesis by photocopying or by other means, in total or in part, at the request of other institutions or individuals for the purpose of scholarly research.

The University of Waterloo requires the signatures of all persons using or photocopying this thesis. Please sign below, and give address and date.

Abstract

A map is an embedding of the vertices and edges of a graph into a compact 2-manifold such that the remainder of the surface has components homeomorphic to open disks. With the goal of proving the Four Colour Theorem, Tutte began the field of map enumeration in the 1960's. His methods included developing the edge deletion decomposition, developing and solving a recurrence and functional equation based on this decomposition, and developing the *medial bijection* between two equinumerous infinite families of maps.

Beginning in the 1980's Jackson, Goulden and Visentin applied algebraic methods in enumeration of non-planar and non-orientable maps, to obtain results of interest for mathematical physics and algebraic geometry, and the *Quadrangulation Conjecture* and the *Map-Jack Conjecture*. A special case of the former is solved by Tutte's medial bijection. The latter uses Jack symmetric functions which are a topic of active research.

In the 1960's Walsh and Lehman introduced a method of encoding orientable maps. We develop a similar method, based on depth first search and extended to non-orientable maps. With this, we develop a bijection that extends Tutte's medial bijection and partially solves the Quadrangulation Conjecture.

Walsh extended Tutte's recurrence for planar maps to a recurrence for all orientable maps. We further extend the recurrence to include non-orientable maps, and express it as a partial differential equation satisfied by the generating series. By appropriately interpolating the differential equation and applying the depth first search method, we construct a parameter that empirically fulfils the conditions of the Map-Jack Conjecture, and we prove some of its predicted properties.

Arquès and Béraud recently obtained a continued fraction form of a specialisation of the generating series for maps. We apply the depth search method with an ordinary differential equation, to construct a bijection whose existence is implied by the continued fraction.

Acknowledgements

Professor David M. Jackson supervised my research in this challenging and important area of mathematics. During his sabbatical leave, he provided much useful assistance with the writing of my doctoral thesis. In addition, my fourth year of doctoral studies was generously supported by a research assistantship from Professor Jackson.

Four years of my graduate studies were supported by a postgraduate scholarship from the Natural Sciences and Engineering Research Council of Canada. Supplemental support was provided by teaching assistantships from the University of Waterloo.

Fellow graduate students created a friendly, and thus productive, work environment. Faculty and staff members of the Department of Combinatorics and Optimization were kind and helpful to me in matters great and small. My parents provided the benefit of a home inclined to mathematics. I am extremely grateful and indebted to Aleksandra Zivkovic for her patience, sensible advice and caring support.

Contents

1	Introduction	1
1.1	Brief Overview of the Conjectures	3
1.2	Continued Fraction Bijection Problem	9
1.3	Background and Overview of the Combinatorial Methods	10
1.4	Outline of the following chapters	12
2	Preliminary Combinatorics	14
2.1	Partitions	15
2.2	Permutations	18
2.3	Maps	19
3	On the Algebraic Method	28
3.1	Group Algebras and Some Subalgebras	29
3.2	Symmetric Functions	33
3.3	Walsh's Formula	43
3.4	Summary	52
4	Depth First Search	53

CONTENTS

4.1	The Canonical Position Labelling Algorithm	56
4.2	Canonical Ordered Digraphs	65
4.3	Canonical Spanning Trees, Struts and Cuts	72
4.4	Edge Diagrams and Integer-Parenthesis Systems	82
4.5	Summary	92
5	On Extending Tutte's Medial Bijection	95
5.1	The Quadrangulation Conjecture	96
5.2	On Tutte's Medial Construction	102
5.3	Sample Computation: $\tilde{\Xi}(q_{1.2.9}) = q_{1.2.9}$	107
5.4	Formal Summary of $\tilde{\Xi}$ and Planar Restriction	121
5.5	An Example with Struts: $q_{1.2.7}$	124
5.6	Genus Non-preservation, with Possible Corrections	124
5.7	Summary	127
6	Partial Differential Equations	128
6.1	Edge Deletion Types and the Parameter β	131
6.2	A Partial Differential Equation	136
6.3	The low degree terms of D	151
6.4	Specialisations	156
6.5	A Bound on β	164
6.6	Refinements of β and corollaries	166
6.7	Rooted maps	168
6.8	Disconnected Digraphs	174

CONTENTS

6.9	Summary	178
7	On a Candidate Map-Jack Parameter	180
7.1	Small example	184
7.2	Suitability of η under specialisation of H	189
7.3	Reduction of η to Non-Separable Maps	196
7.4	Reduction of η to Digon-Free Maps	206
7.5	Doubling Construction	209
7.6	Summary	211
8	A Bijection for Continued Fractions	213
8.1	Continued Fractions and Trees	214
8.2	Ricatti Equations	218
8.3	Recursive construction of λ	228
8.4	Specialisations and Generalisations	229
8.5	Alternate expressions for $M(y, z)$	232
8.6	Summary	238
A	Further Work	240
A.1	On Double Coset Algebras	240
A.2	On $\tilde{\Xi}$	241
A.3	On β	241
A.4	On η	243
A.5	On Θ	244
A.6	On random matrices	244

CONTENTS

A.7	Products in the Category of Rooted Maps	245
A.8	On Jucys-Murphy elements	246
B	Tables of coefficients of Φ_n, for $n \leq 6$	247
B.1	Number of Edges = 1	247
B.2	Number of Edges = 2	249
B.3	Number of Edges = 3	249
B.4	Number of Edges = 4	250
B.5	Number of Edges = 5	251
B.6	Number of Edges = 6	254
C	Numbers of Rootings of Maps	259
C.1	Surface: Genus 0 ($\chi = 2$, orientable)	260
C.2	Surface: Genus 1 ($\chi = 0$, orientable)	261
C.3	Surface: Genus 2 ($\chi = -2$, orientable)	262
C.4	Surface: Genus $\tilde{1}$ ($\chi = 1$, nonorientable)	263
C.5	Surface: Genus $\tilde{2}$ ($\chi = 0$, nonorientable)	264
C.6	Surface: Genus $\tilde{3}$ ($\chi = -1$, nonorientable)	266
C.7	Surface: Genus $\tilde{4}$ ($\chi = -2$, nonorientable)	266
C.8	Surface: Genus $\tilde{5}$ ($\chi = -3$, nonorientable)	267
	Bibliography	268

List of Tables

4.1	Some canonical structures for three different rooted maps	93
5.1	Listings of $\mathcal{Q}_{1,2}$ and $\mathcal{A}_{1,2}$ such that $\tilde{\Xi}(q_{1.2.i}) = \alpha_{1.2.i}$ for $i = 1, \dots, 15$.	98
5.2	Changes in the topology through the various stages	108
5.3	Thirteen stages of the computation $\tilde{\Xi}(q_{1.2.9}) = \alpha_{1.2.9}$. (Explained in §§5.3.1–5.3.12)	109
5.4	Properties of the various stages	110
5.5	The component bijections	121
6.1	Nine deletion types of e_n and their contribution to $\frac{\partial D}{\partial z}$	135
6.2	Unrooted maps with two edges	154
6.3	Eight sets of ordered digraphs	156
6.4	Recurrence equations and solutions	157
6.5	Eight sets and nine deletion types	158
7.1	Five values of η	187
7.2	The cases of e_1 and e_2	190
8.1	The correspondences $v(\epsilon)$ for ϵ with two or less edges	227

LIST OF TABLES

8.2	Sample computation of Θ	230
B.1	Coefficients $[x_\phi y^2 b^B] \Phi_8$ for $\ell(\phi) = 3$	248

List of Figures

4.1	A planar rooted embedding of the complete graph K_4	58
4.2	The algorithm begins at the root position	58
4.3	The algorithm moves along μ_1 first	59
4.4	If $\mu_1(x)$ has been labelled, look at $\mu_2(x)$	59
4.5	First instance that μ_3 is used	60
4.6	Use letters instead of number for labels	61
4.7	Assignment of labels m, n, o, p, q and r	61
4.8	Assign label s , by backtracking from r to p	62
4.9	The trace of the algorithm around the rooted map	63
4.10	Canonical position labelling of a planar K_4 embedding (alphabetical form)	67
4.11	Canonical ordered digraph structure	68
4.12	Formal position descriptions in an ordered digraph in the Klein bottle	70
4.13	The traversed edges of a planar embedding of K_4	73
4.14	The canonical spanning subtree	74
4.15	The rooted map m , an embedding of K_5 in the torus	75

LIST OF FIGURES

4.16	The canonical labelling from depth first search	76
4.17	The canonical order of edges and the canonical tree edges	77
4.18	The first two cuts to be tested	78
4.19	The next two non-tree edges, a strut and a cut	78
4.20	Another strut and another cut	79
4.21	The backbone of the rooted embedding of K_5	80
4.22	The submap m_2 , with association of e_3 to the non-root face	81
4.23	The submap m_3 , with the association of e_6 to the new non-root face	81
4.24	The cuts e_9 and e_{10} and associated faces	82
4.25	A more convenient set of labels	85
4.26	Linearising a rooted map into an <i>edge diagram</i>	86
4.27	A rooted map in the Klein bottle	86
4.28	Adding an “ \times ” to the edge diagram of a non-orientable map	87
4.29	Forbidden sub-configurations	88
4.30	How to trace a face in an edge diagram	90
4.31	Building an integer-parenthesis system	91
5.1	A planar rooted map σ	104
5.2	A formal representation of σ	104
5.3	Superimposition of q on σ	105
5.4	The planar quadrangulation $q = M^{-1}(\sigma)$	105
5.5	Stages 1 – 2	110
5.6	Stages 2 – 3	111

LIST OF FIGURES

5.7 Shading the corners of the first (root) vertex of the Stage 3 edge diagram 113

5.8 Shading the corners of the second vertex of the Stage 3 edge diagram 113

5.9 Adding twists to the Stage 3 edge diagram to correct failures to the face-bicolouring 114

5.10 Stages 4 – 5 115

5.11 Stages 5 – 6 116

5.12 Edge diagram (Stage 7) of the projective-plane map (Stage 6) . . . 117

5.13 Replacing a twisted edge by a negatively signed edge 118

5.14 Determining the map (Stage 9) from the edge diagram (Stage 8), and carrying over the edge-signs 118

5.15 Transferring signs from the cuts of Stage 9 to the faces of Stage 10 119

5.16 The computation of $\tilde{\Xi}_{(q_{1.2.7})}$, with flagged dual-struts 123

5.17 A counterexample to preservation of g . ($g = 1$ in Stage 1 and $g = 2$ in Stage 13) 125

6.1 The unique ordered digraph of loop deletion type 139

6.2 The ordered digraph of cross-loop deletion type 140

6.3 Both ordered digraphs of link deletion type 141

6.4 A three edge ordered digraph of leaf deletion type in the torus . . 142

6.5 A border e_n between a triangle and a quadrangle in ∂ , leaves a pentagon in ∂' 144

6.6 The cross-border deletion type. Cut a large hole in a face, attach a twisted ribbon. 145

LIST OF FIGURES

6.7 Joining two faces by a handle 148

6.8 A Hasse diagram for containment between the eight sets 157

7.1 The five rooted maps m with $\phi(m) = \nu(m) = [4]$ 186

7.2 The canonical position labellings 187

7.3 The five canonical ordered digraphs 188

7.4 Deletion of e_2 189

7.5 A split vertex in the triple torus 198

7.6 Replacing a degree one face by a digon 211

8.1 A level-labelled tree 217

8.2 Ricatti decomposition for edge diagrams 219

8.3 A broken arc configuration with separating vertical lines 222

8.4 An unbroken arc configuration 222

8.5 Ricatti decomposition for edge diagrams 224

8.6 Comparison of the two Ricatti decompositions 226

8.7 An edge diagram with no arcs 235

Chapter 1

Introduction

A *map* is an embedding of a graph, with vertices sent to points and edges sent to continuous paths (joining the images of the vertices to which the edge is incident), into a closed surface without boundary (compact 2-manifold), such that the remainder of the surface has components each of which homeomorphic to an open disk. Maps are formalised combinatorially in Chapter 2. For fixed values of certain sets of parameters of maps, the number of maps is, up to isomorphism, finite.

There are three general objectives of enumeration in this thesis. The first objective is to find simple formulae for the cardinalities of finite sets in a given infinite family of sets, such as the family of finite sets of maps defined above by a certain set of parameters. As often occurs in enumeration, there is a limit to the simplicity of the formulae. But on occasion such formulae are shown to give the cardinality of sets from a different infinite family of finite sets. The second objective of enumeration is to construct a bijection between the corresponding sets

of the two families. The methods used to obtain the formula, may or may not be useful in constructing the bijection. The third objective, a converse to the first objective, is to construct an infinite family of finite sets with cardinalities given by a desired formula.

The specific topics of this thesis are the three problems from the enumeration of maps in surfaces, briefly described as follows.

- The Quadrangulation Conjecture [JV90a]: this involves constructing a bijection between rooted quadrangulations and rooted maps in arbitrary orientable surfaces.
- The Map-Jack Conjecture [GJ96a]: this involves finding a combinatorial interpretation for an indeterminate b where $1 + b$ appears as the parameter of Jack symmetric functions in the generating series for maps.
- The continued fraction bijection problem [AB97]: this involves constructing a bijection between rooted maps and a certain set of trees enumerated by continued fractions.

These three problems share certain features. Each was suggested from the development of an enumerative result whose proof contained algebraic steps which defy easy combinatorial interpretation. The problems then, are to find combinatorial, constructive solutions for each of these enumerative results. In this, very little help was forthcoming from a study of the original algebraic proof. Therefore other approaches were needed.

The approach taken in this thesis is to employ two other methods, depth first

search and edge deletion. Depth first search is used to canonically and naturally label rooted maps. These labels permit further combinatorics on rooted maps. Edge deletion is a more general operation upon maps, and facilitates inductive definitions and proofs. Edge deletion induces recurrence relations for the number of maps, and thence a differential equation for the generating series of these numbers. With these two methods, new advances, beyond the original developments of the three problems, are made here.

The advance in the Quadrangulation Conjecture is a partial solution. The advance in the Map-Jack Conjecture is a candidate solution. The advance in the continued fraction bijection problem is a complete solution.

The two conjectures are briefly reviewed in §1.1. More detailed information is provided in later chapters as needed. Implications for the solutions of these conjectures are discussed in §1.1.3. The continued fraction bijection problem is given in §1.2. The original applications and the new usage of the two combinatorial methods are briefly discussed in §1.3. An outline of the remaining chapters is provided in §1.4.

1.1 Brief Overview of the Conjectures

The *algebraic method*, developed in [JV90b, JV90a, GJ96b, GJ96a] involves encoding maps with permutations. Extensive knowledge of permutations and their algebra is then applied to map enumeration. Chapter 3 describes the algebraic method in greater depth. There the Quadrangulation Conjecture and the Map-Jack Conjecture are stated with a simple overview of their original development.

More complete definitions and details are to be found in Chapters 2 and 3.

The cycle structure of permutations can be described by partitions. The three cycle partitions of two permutations and their product, have corresponding interpretations as natural parameters of maps, the degree partitions of vertices, edges and faces. In the case of orientable maps, the centre of the group algebra of the symmetric group, $\mathbb{C}\mathfrak{S}_n$, is the algebra that we use for enumerative purposes. In the case of locally orientable maps it is another algebra spanned by permutations, the double coset algebra of the hyperoctahedral group. In both cases, the enumeration of maps with respect to vertex and face degrees, is expressible in terms of the structure constants, or connection coefficients, of these algebras.

Since the connection coefficients can be found with symmetric functions [Mac95, Sag91], maps can be enumerated by means of symmetric functions [JV90b]. Schur functions, s_λ , can be used to find characters of the symmetric group and thus its connection coefficients. The generating series for rooted orientable maps, expressed in terms of Schur symmetric functions, [JV90a] is

$$\begin{aligned} \Omega(\mathbf{x}, \mathbf{y}, \mathbf{z}) &= \sum_{\phi, \nu, n} \omega_{\phi, \nu, n} \mathbf{x}_\phi \mathbf{y}_\nu \mathbf{z}^n \\ &= 2\mathbf{z} \frac{\partial}{\partial \mathbf{z}} \log \sum_{n \geq 0} \sum_{\lambda \vdash n} H_\lambda s_\lambda(\mathbf{x}) s_\lambda(\mathbf{y}) s_\lambda(\mathbf{z}) \Big|_{\substack{p_j(\mathbf{x}) \mapsto x_j, & p_j(\mathbf{y}) \mapsto y_j \\ p_j(\mathbf{z}) \mapsto z \delta_{j,2}}} \end{aligned} \quad (1.1)$$

where: $\mathbf{x} = (x_1, x_2, \dots)$, and for partition $\phi = (\phi_1, \phi_2, \dots)$, \mathbf{x}_ϕ denotes $x_{\phi_1} x_{\phi_2} \dots$; $\omega_{\phi, \nu, n}$ is the number of rooted orientable maps with face partition, vertex partition and number of edges given by ϕ, ν and n respectively; p_j is the power sum

symmetric function $p_j(\mathbf{x}) = x_1^j + x_2^j + \dots$; and H_λ is the product of hook lengths of λ .

1.1.1 The Quadrangulation Conjecture

In [JV90a], there is a factorisation result for characters of the symmetric group. Characters are proportional to coefficients of power sum symmetric functions in Schur functions, so this factorisation may be expressed as:

$$[p_{[4^n]}] s_\lambda = \frac{1}{2^n} [p_{[2^{2n}]}] s_{\lambda^{(1)}} s_{\lambda^{(2)}} \quad (1.2)$$

which holds only for a restricted subset of partitions λ , those which are [JV90a] 2-balanced, the coefficient being zero otherwise. The partitions $\lambda^{(1)}$ and $\lambda^{(2)}$ form the 2-factorisation [JV90a] of the partition λ .

Under suitable transformations of $\Omega(\mathbf{x}, \mathbf{y}, z)$, generating series $M(u, x, y, z)$ and $Q(u, x, y, z)$ can be formed which enumerate, rooted orientable maps, and rooted quadrangulations, *i.e.* rooted face-4-regular maps, respectively. (The variables u, x, y, z mark genus, faces, vertices and edges, respectively.) The factorisation result (1.2) leads to the following relationship:

$$Q(4u^2, x, y, z) = \text{bis}_u M(4u^2, y + u, y, xz^2), \quad (1.3)$$

where $\text{bis}_u f$ denotes the even bisection $\frac{1}{2}\{f(u) + f(-u)\}$ of the formal power series f .

The result (1.3) implies existence of bijections between two sets of rooted

maps, \mathcal{Q} rooted orientable quadrangulations, and \mathcal{A} , decorated rooted orientable maps, which are defined in Chapter 5. There are pairs of corresponding weight-functions defined on \mathcal{Q} and \mathcal{A} , and the generating series equality (1.3) further implies that there exists a weight-preserving bijection $\xi : \mathcal{Q} \rightarrow \mathcal{A}$. It was not possible to combinatorialise each step of the proof of (1.3). Thus a construction of such a bijections $\xi : \mathcal{Q} \rightarrow \mathcal{A}$ does not immediately follow from the proof of (1.3).

Conjecture 1.1 (Quadrangulation Conjecture [JV90a]). *There exists a constructive, weight-preserving bijection $\Xi : \mathcal{Q} \rightarrow \mathcal{A}$ admitting an element-wise action having a combinatorial description.*

Of course, the construction in Conjecture 1.1 for the bijection Ξ , if found, would provide a new and purely combinatorial proof of (1.3).

In Chapter 5, a bijection $\tilde{\Xi} : \mathcal{Q} \rightarrow \mathcal{A}$ which preserves one of the two required weight functions is found. Thus $\tilde{\Xi}$ is a partial solution to Conjecture 1.1.

1.1.2 The Map-Jack Conjecture

A scalar product $\langle \cdot, \cdot \rangle_\alpha$ can be defined on the ring of symmetric functions by:

$$\langle \mathbf{p}_\lambda, \mathbf{p}_\mu \rangle_\alpha = \alpha^{\ell(\lambda)} z_\lambda \delta_{\lambda\mu}, \quad (1.4)$$

where $z_\lambda = \prod_i i^{m_i(\lambda)} m_i(\lambda)!$, and $\delta_{\lambda\mu}$ is the Kronecker delta function. Jack symmetric functions $J_\lambda^{(\alpha)}$ are defined as the result of orthogonalising the monomial symmetric functions m_λ with respect to this scalar product. Chapter 3 gives a more complete definition of Jack symmetric functions. Jack symmetric functions

are also described in [Mac95, Sta89].

Since $J_\lambda^{(1)} = H_\lambda s_\lambda$, Jack symmetric functions are a generalisation of Schur functions. For $\alpha = 2$, Jack symmetric functions specialise to Zonal polynomials $Z_\lambda = J_\lambda^{(2)}$. Zonal polynomials play an analogous role to Schur functions in the enumeration of locally orientable maps [GJ96b]. It follows [GJ96a] that the series:

$$\Psi^{(\alpha)}(\mathbf{x}, \mathbf{y}, \mathbf{z}) = 2\alpha \mathbf{z} \frac{\partial}{\partial \mathbf{z}} \log \sum_{n \geq 0} \sum_{\lambda \vdash n} \frac{J_\lambda^{(\alpha)}(\mathbf{x}) J_\lambda^{(\alpha)}(\mathbf{y}) J_\lambda^{(\alpha)}(\mathbf{z})}{\langle J_\lambda^{(\alpha)}, J_\lambda^{(\alpha)} \rangle_\alpha} \Bigg|_{\substack{p_j(\mathbf{x}) \mapsto x_j, & p_j(\mathbf{y}) \mapsto y_j \\ p_j(\mathbf{z}) \mapsto z_j^{\delta_{j,2}}}} \quad (1.5)$$

enumerates rooted orientable maps when $\alpha = 1$, and locally orientable maps when $\alpha = 2$. This is consistent with the following conjecture, extracted from [GJ96a]:

Conjecture 1.2 (Map-Jack Conjecture [GJ96a]). *There exists a parameter ϑ of rooted locally orientable maps, such that:*

1. *For $\phi(m)$, $\nu(m)$ and $n(m)$, the face degree partition, the vertex degree partition, and the number of edges of a map m , we have:*

$$\Psi^{(b+1)}(\mathbf{x}, \mathbf{y}, \mathbf{z}) = \sum_{m \in \mathcal{L}} b^{\vartheta(m)} x_{\phi(m)} y_{\nu(m)} z^{n(m)} \quad (1.6)$$

where \mathcal{L} is the set of rooted locally orientable maps,

2. *$\vartheta(m)$ is a non-negative integer,*
3. *$\vartheta(m) = 0$ if and only if m is orientable.*

Condition 3 suggests that the hypothetical parameter ϑ should be regarded

as a parameter associated with non-orientability.

Hitherto, the main evidence for Conjecture 1.2 has been numerical computations of the smaller coefficients of $\Psi^{(b+1)}(\mathbf{x}, \mathbf{y}, z)$, which turn out to be non-negative integers. In fact, the current theory of Jack symmetric functions only shows that coefficients $[\mathbf{x}_\phi \mathbf{y}_\nu z^n] \Psi^{(b+1)}$ are rational functions of b , while Conjecture 1.2 claims that these are polynomials in b with non-negative integer coefficients.

In Chapter 7, a parameter η of rooted maps is defined. With $\vartheta = \eta$, Conditions 2 and 3 are met, and Condition 1 holds to the extent of all the computed data. (These computations include all maps up to 4 edges, and all single vertex maps with 6 or less edges.)

1.1.3 Implications

There are several implications of the combinatorial solutions to the two conjectures. The enumerative results associated with the conjectures have been applied to two areas, 2-dimensional quantum gravity and algebraic geometry.

The enumerative result (1.3) proved [JPV96] physicist's suspected connection between the φ^4 -model and Penner model of 2-dimensional quantum gravity. The related hypothetical bijection Ξ of the Quadrangulation Conjecture could provide a physical interpretation of the connection between these two models, at the level of Feynman diagrams and mesons.

Related general applications of map enumeration to string theory and quantum field theory are given in [Hoo74, BIZ80]. In algebra, Grothendieck's theory

of Galois groups, *dessins d'enfants* [Sch94], involves enumerative aspects of maps.

The Map-Jack Conjecture is related, via Jack symmetric functions, to the Calogero-Sutherland model [LPS95] in quantum physics. The Map-Jack Conjecture also has potential applications to algebraic geometry. For $b = 0$ and $b = 1$ respectively, the enumeration of maps (especially monopoles) has been used to find the virtual Euler characteristic of the moduli space of complex [HZ86] and real algebraic curves respectively. When b is left unspecialised, there is potential application to an algebraic construction of a moduli space that interpolates between these two moduli spaces, and the hypothetical parameter ϑ would have a prominent rôle in the structure of this moduli space.

1.2 Continued Fraction Bijection Problem

In [AB97], the following result was proved.

Theorem 1.1. *Let $\omega_{k,n}$ be the number of rooted orientable maps with k vertices and n edges. Then*

$$\sum_{k,n} \omega_{k,n} y^k z^n = \frac{y}{1 - \frac{(y+1)z}{1 - \frac{(y+2)z}{1 - \dots}}} \quad (1.7)$$

The proof in [AB97] involves relating the solutions to an iterative family of Riccati equations. The Riccati equation was established by the edge deletion

method. But the iterative solution method to the Riccati equation does not give a combinatorial explanation for the continued fraction in (1.7). The problem of finding a combinatorial explanation for (1.7), in the form of a bijection, was proposed in [AB97].

In Chapter 8, such a bijection Θ is found. Advantage is taken of the depth first search method for rooted maps to construct Θ . Hence, Theorem 1.1 is provided with a bijective proof.

1.3 Background and Overview of the Combinatorial Methods

Two methods, depth first search and edge deletion, appeared early in the enumeration of maps. These methods pre-date the algebraic methods of the Quadrangulation Conjecture and the Map-Jack Conjecture, and may be regarded as more elementary than the algebraic methods.

1.3.1 Edge Deletion

Edge deletion was used by Tutte in [Tut62]. A recurrence relation was found for the number of slicings, which are certain labelled planar maps, by considering the enumerative effect of edge deletion. Later, Walsh extended this method and applied it to all labelled orientable maps.

In Chapter 6, the edge deletion method is extended to include non-orientable maps. Moreover, the recurrence is expressed in a new form, as a partial differ-

ential equation. A variable b is then introduced into the partial differential equation. This b appears to have the rôle of the Jack parameter α of the Map-Jack Conjecture.

1.3.2 Depth First Search

Depth first search is a standard, general combinatorial algorithm, with applications to optimisation and to finding strongly connected orientations of graphs. It is less frequently applied to enumeration [GW79, GS96]. In the enumeration of maps it is implicitly used in [Wal71].

The canonical integer-parenthesis system for rooted maps was developed by Lehman [Wal71]. The system was used to obtain some enumerative results, including a recurrence form of the Ricatti equation involved in the proof of a continued fraction result. (The solution (8.7) given in [Wal71] is different from the continued fraction.)

In Chapter 4, a similar system for rooted maps is defined, and the underlying mechanism is identified to be depth first search. We develop the edge diagram model of a rooted map, a combinatorial object similar to the integer-parenthesis system. The edge diagram model of a rooted map is applied to the Quadrangulation Conjecture and to the continued fraction problem.

A canonical ordered digraph, using the same depth first search method, is also defined for each rooted map, in Chapter 4. The canonical ordered digraph is then used to define η of Chapter 7, the candidate parameter for the Map-Jack Conjecture.

1.4 Outline of the following chapters

Below are listed brief summaries of the chapters and their logical dependencies.

Chapter 2 defines essential combinatorial notions for the study of maps: partitions, permutations, and of course topological and combinatorial maps.

Chapter 3 addresses the algebraic method behind the Quadrangulation Conjecture and Map-Jack Conjecture. The material is not crucial to later chapters, but rather motivates them.

Chapter 4 develops depth first search methods. Chapters 5,7 and 8 depend heavily on these methods.

Chapter 5 uses edge diagrams defined in Chapter 4, to construct a bijection $\tilde{\Xi}$ which is a partial solution to the Quadrangulation Conjecture. The construction of $\tilde{\Xi}$ involves non-orientable maps, although the domain and range consist of orientable maps.

Chapter 6 introduces the edge deletion method. A partial differential equation is obtained for the generating series of ordered digraphs. A parameter β of non-orientability of ordered digraphs is defined, which is empirically related to the Jack parameter of the the Map-Jack Conjecture.

Chapter 7 combines the depth first search method (Ch. 4) with the edge deletion method (Ch. 6) to define a parameter η , which is a candidate for the parameter ϑ of the Map-Jack Conjecture. Some properties of this parameter η will be discussed, including some invariance and additivity results,

and a summation result known to hold for any hypothetical parameter ϑ of the Map-Jack Conjecture.

Chapter 8 also combines the depth first search method (Ch. 4) with the edge deletion method, but to develop a bijection whose existence is implied by a recent continued fraction result in the enumeration of maps.

Logical sequences of chapters include: Chapters 2,3 for the motivation behind the two conjectures; Chapters 2,4,5 for the partial solution to the Quadrangulation Conjecture; Chapters 2,4,6,7 or 2,6,4,7 for the candidate solution to the Map-Jack Conjecture; and Chapters 2,4,8 for the continued fraction bijection.

Chapter 2

Preliminary Combinatorics

In the theory of combinatorial enumeration, a combinatorial definition of a map is more convenient than a topological definition, although the definitions are equivalent through the Embedding Theorem. This chapter gives both definitions.

Also given is the definition of a rooted map. Rooted maps are crucial to enumeration because their lack of nontrivial automorphisms facilitates far more effective enumeration. Most enumeration results of the following chapters concern rooted maps. Maps and rooted maps are defined in §2.3, following some preliminary combinatorial notions.

A permutation is a more basic combinatorial object than a map, but fundamental to the theory of maps. In particular, combinatorial definitions of a map are usually expressed in terms of permutations. It is through the study of the multiplicative properties of permutations that the algebraic method of Chapter 3 enumerates maps. The combinatorial definition of a map in this chapter, uses a

special type of permutation, a matching. Notational conventions for permutations are defined in §2.2.

Integer partitions will also be used extensively since they are useful in describing properties of permutations and of maps. The face partition and vertex partition of a map give information about the degrees of the faces and vertices of a map, respectively. The cycle partition of a permutation gives information about the length of its cycles. Partitions are also indices for symmetric functions of Chapter 3. Because of their use in describing features of permutations and maps, partitions are defined first, in §2.1.

2.1 Partitions

Definition 2.1. *Let n and k be nonnegative integers. An ordered k -tuple $\lambda = (\lambda_1, \lambda_2, \dots, \lambda_k)$ of non-ascending positive integers λ_i , i.e. $\lambda_1 \geq \lambda_2 \geq \dots \geq \lambda_k$, is a partition of the integer n if $n = \lambda_1 + \lambda_2 + \dots + \lambda_k$. And*

1. *The weight, $|\lambda|$, of λ is n ,*
2. *The length, $\ell(\lambda)$, of λ is k ,*
3. *To signify that λ is a partition of n specifically, write $\lambda \vdash n$,*
4. *Each λ_i is called a part of λ ,*
5. *The number of i such that $\lambda_i = j$, is the multiplicity of j in λ , denoted by $m_j(\lambda)$.*

When multiplicities are important we write

$$\lambda = [1^{m_1(\lambda)} 2^{m_2(\lambda)} \dots],$$

omitting terms of the form j^0 and superscripts 1. For example, $\alpha = (4, 2, 2, 2, 1)$ can be written as $\alpha = [12^34]$, or in the opposite (descending) order as $\alpha = [42^31]$.

The set of all partitions is denoted by \mathcal{P} ; the set of all partitions of n is denoted by \mathcal{P}_n . The unique partition of 0 is denoted by \emptyset .

In the theory of symmetric functions, the partition indexed value

$$z_\lambda = \lambda_1 \lambda_2 \lambda_3 \cdots m_1(\lambda)! m_2(\lambda)! \cdots$$

occurs frequently.

2.1.1 Lexicographic and Dominance Orders

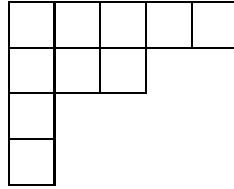
Lexicographic order of partitions of n is defined as follows. We write $\lambda < \mu$ if and only if there exists j such that $\lambda_j < \mu_j$ and $\lambda_i = \mu_i$ for $1 \leq i < j$. Lexicographic order is a total order since any two partitions of n are comparable. For partitions of $n = 5$, the order is $[1^5] < [21^3] < [2^21] < [31^2] < [32] < [41] < [5]$.

Dominance order is a partial order. We write $\lambda \prec \mu$ precisely when $\lambda_1 + \cdots + \lambda_j \leq \mu_1 + \cdots + \mu_j$ for all j . Dominance order is the same as lexicographic order for partitions of $n \leq 5$, but for $n = 6$, we have $[3^2] < [41^2]$, in the lexicographic order, but $[3^2] \not\prec [41^2]$ in the dominance order. But conversely, $\lambda \prec \mu \implies \lambda < \mu$. (The distinction becomes relevant in the theory of Jack Symmetric functions.)

2.1.2 Conjugates, Tableaux and Hook Lengths

The *conjugate (partition)* of λ is the partition λ' such that $\lambda'_i = \sum_{j \geq i} m_j(\lambda)$ for $i = 1, \dots, \lambda_1$.

The *Ferrers diagram* of a partition λ , is the set of points (i, j) with $i \leq \lambda_i$. It is represented combinatorially by an array of squares, with i indexing rows of λ_i squares and index j for columns. For example,



is the Ferrers diagram for $(5, 3, 1, 1)$. Note that λ_i is the length of the i^{th} row. The conjugate partition λ' is more simply explained as the partition whose Ferrers diagram is the transpose of the Ferrers diagram of λ , *i.e.* the reflection across the main diagonal.

For each square $s \in \lambda$, in the Ferrers diagram of λ , the *arm length*, $a_\lambda(s)$, is the number of squares to the right of s , the *leg length*, $l_\lambda(s)$, is the number of squares below s . The hook length is $h_\lambda(s) = a_\lambda(s) + l_\lambda(s) + 1$. The product of hook lengths is denoted by

$$H_\lambda = \prod_{s \in \lambda} h_\lambda(s).$$

A tableau T of shape $\text{sh } T = \lambda$ is a Ferrers diagram of λ with a positive integer assigned to each square. A tableau is semi-standard if it weakly increasing (non-

decreasing) left to right in each row, and strictly increasing downwards in each column. For example,

$$T_1 = \begin{array}{|c|c|c|c|c|} \hline 1 & 1 & 2 & 2 & 7 \\ \hline 2 & 3 & 3 & & \\ \hline 4 & & & & \\ \hline 5 & & & & \\ \hline \end{array}$$

is a semi-standard tableau of shape $(5, 3, 1, 1)$. Associated with each tableau is a monomial x^T , formed by replacing each entry i by x_i , and multiplying these together. For example, $x^{T_1} = x_1^2 x_2^3 x_3^2 x_4 x_5 x_7$.

2.2 Permutations

The set of permutations π of a finite set X is denoted by $\text{Sym}(X) = \{\pi : X \rightarrow X \mid \pi \text{ is bijective}\}$. Let $\mathfrak{S}_n = \text{Sym}(\{1, 2, \dots, n\})$. An example of a permutation $\sigma \in \mathfrak{S}_6$ is

$$\sigma = \begin{pmatrix} 1 & 2 & 3 & 4 & 5 & 6 \\ 5 & 2 & 6 & 1 & 4 & 3 \end{pmatrix} \quad (2.1)$$

which indicates that $\sigma(1) = 5$, $\sigma(2) = 2$, $\sigma(3) = 6$, and so on. A permutation has a disjoint cycle factorisation. Thus $\sigma = (1, 5, 4)(3, 6)(2)$, because σ in (2.1) interchanges 3 and 6, and sends $1 \mapsto 5 \mapsto 4 \mapsto 1$. The lengths of the cycles of a permutation π form a partition $\tau(\pi)$, its *cycle type*. For example, $\tau(\sigma) = [321]$ above. A *matching* is a permutation μ whose cycle type is of the form $\tau(\mu) = [2^n]$.

The set of matchings on a set X is $\text{Match}(X) \subset \text{Sym}(X)$.

2.3 Maps

Two definitions of a map are now provided, a topological map and a combinatorial map. These definitions are equivalent for enumerative purposes, so the term *map* on its own is used refer to either definition in the contexts where it does not matter. Similar, but more detailed, treatments of topological maps and combinatorial maps are given in [GT87] and [Tut84], respectively.

2.3.1 Topological Maps

A *locally orientable surface* [Tut84] is a compact 2-manifold. Up to homeomorphism, two parameters, the Euler characteristic $\chi \in \mathbb{Z}$ and orientability, suffice to determine locally orientable surfaces. Orientable surfaces are the sphere, the torus, the double torus and more generally the sphere with g handles, with Euler characteristics $\chi = 2, 0, -2$, and generally $2 - 2g$, respectively. The number g is the *genus* of the orientable surface. Non-orientable surfaces are the real projective plane, Klein bottle, and generally the previous two with g handles, with Euler characteristics $\chi = 1, 0$, and generally $1 - 2g$, or $-2g$, respectively.

A topological map $\mathfrak{M} = (G, S, i)$ consists of a *2-cell embedding* i of a graph G in a surface S , meaning that all the components of the topological space $S - i(G)$ are 2-cells, *i.e.* homeomorphic to open disks. The 2-cells are the *faces* of the map \mathfrak{M} . The Euler characteristic of S may be computed as $\chi = f - e + v$, where f, e, v

are the number of faces, edges and vertices of a topological map $\mathfrak{M} = (G, S, i)$.

Topological maps $\mathfrak{M} = (G, S, i)$ and $\mathfrak{M}' = (G', S', i')$ are isomorphic if there is a homeomorphism $h : S \rightarrow S'$ which preserves the images of the graphs, *i.e.* $h(i(G)) = i'(G')$. It follows that if \mathfrak{M} and \mathfrak{M}' are isomorphic, $\mathfrak{M} \cong \mathfrak{M}'$, then the underlying graphs are isomorphic, $G \cong G'$ and the underlying surfaces are homeomorphic, $S \cong S'$. The converse, however, need not be true. (For example, the graph consisting of a two edge path plus a loop incident to the middle vertex of the path, has two non-isomorphic embeddings in the sphere. On the other hand, 3-connected graphs [Tut84] have at most one embedding in the sphere.)

2.3.2 Combinatorial Maps

In preparation for the following definition consider a topological map $\mathfrak{M} = (G, S, i)$. For each edge $e \in G$, the curve $i(e)$ has two sides and two ends. Choose four points on S , each very close to one side and one end of $i(e)$. Having done this for each edge e , forming a set of such points X , let these points be the *(side-end) positions* of \mathfrak{M} . Thus, if G has n edges, then of course $|X| = 4n$.

The side-end positions are related to each other by the local topology of \mathfrak{M} . More precisely, the positions in X can be naturally paired up in three different ways.

1. Pairs in X associated with the same end of one edge but on different sides.
2. Pairs in X belonging to the same corner of a face.
3. Pairs in X associated with the same side of one edge, but at different ends.

This leads to three matchings $\mu_i, i = 1, 2, 3$ on X and to the definition given by Tutte [Tut84] of a combinatorial map, stated purely in finite terms, without reference to any topology.

Definition 2.2. *A quadruple $m = (X, \mu_1, \mu_2, \mu_3)$ is a combinatorial map if:*

1. X is a finite set,
2. μ_i is a matching on X , for $i = 1, 2, 3$,
3. The permutation product $\mu_1\mu_3$ is also a matching on X ,
4. The group $\langle \mu_1, \mu_2, \mu_3 \rangle$ acts transitively on X .

We write $m = \gamma(\mathfrak{M})$ for a combinatorial map m associated with a given topological map \mathfrak{M} , by means of the previous description.

If Condition 3 is omitted, m is called a *hypermap*. If Condition 4 is omitted, m is called a *premap*.

Definition 2.3. *A quintuple $m = (X, \mu_1, \mu_2, \mu_3, r)$ is a rooted map if $r \in X$ and (X, μ_1, μ_2, μ_3) is a combinatorial map.*

A combinatorial map or hypermap can be viewed through its matchings graph:

Definition 2.4. *The matchings graph of a map (or hypermap) $m = (X, \mu_1, \mu_2, \mu_3)$ is $\Gamma = \Gamma(m)$ with vertex set $V\Gamma = X$, and edge set*

$$E\Gamma = \{\{x, y\} : y = \mu_k(x) \text{ for some } 1 \leq k \leq 3\}.$$

The matchings graph Γ is vertex-3-regular (trivalent). The indices of the matchings μ_k provide a proper edge-3-colouring, or Tait colouring, of Γ . Any Tait-coloured trivalent graph determines a unique pre-hypermap. Condition 4 in Definition 2.2 is equivalent to $\Gamma(m)$ being connected.

For each topological map \mathfrak{M} , we have shown above how to define an associated combinatorial map $m = \gamma(\mathfrak{M})$. Vertices, edges and faces of \mathfrak{M} have the following corresponding structures in $\Gamma(m)$:

1. Faces correspond to cycles of $\Gamma(m)$ consisting of (alternating) edges from μ_2 and μ_3 .
2. Edges correspond to cycles of $\Gamma(m)$ consisting of (alternating) edges from μ_3 and μ_1 .
3. Vertices correspond to cycles of $\Gamma(m)$ consisting of (alternating) edges from μ_1 and μ_2 .

In a combinatorial map, Condition 3 in Definition 2.2 implies that cycles corresponding to the edges in item 2 above correspond to 4-cycles in the matchings graph $\Gamma(m)$.

Isomorphisms between combinatorial maps

$$m = (X, \mu_1, \mu_2, \mu_3) \text{ and } m' = (X', \mu'_1, \mu'_2, \mu'_3)$$

are bijections $\iota : X \rightarrow X'$ such that $\iota \circ \mu_k = \mu'_k \circ \iota$ for $1 \leq k \leq 3$. Two combinatorial maps m and m' arising from isomorphic topological maps \mathfrak{M} and \mathfrak{M}' are themselves isomorphic.

Let Υ denote the construction that associates with each combinatorial map m a topological map $\mathfrak{M} = \Upsilon(m)$. The three sets of cycles in $\Gamma(m)$ associated to the faces, edges and vertices, serve as boundaries to which can be attached open disks, forming a surface S , with skeleton $\Gamma(m)$. The functions Υ and γ are inverses, up to isomorphism. This result, in an equivalent form, is known as the *Embedding Theorem* [Tut84, GT87].

The Euler characteristic of a combinatorial map m is determinable from $\Gamma(m)$ by counting its cycles corresponding to the faces, edges and vertices of $\Upsilon(m)$. The next result explains how to express orientability of m in terms of $\Gamma(m)$.

Lemma 2.1. *Let $\mathfrak{M} = (G, S, i)$ be a topological map. The surface S is orientable if and only if $\Gamma(\gamma(\mathfrak{M}))$ is a bipartite graph.*

Proof. To see this, fix the global orientation of S as clockwise. Use the global orientation to assign a bipartition of X , by classifying positions at each vertex as being on the clockwise or counterclockwise side of the edge in clockwise (the global orientation) circulation of the vertex.

Conversely, given a bipartition (X_1, X_2) of the matchings graph $\Gamma(\gamma(m))$, define a global orientation of S as follows. In the neighbourhood of each vertex, the positions alternate from X_1 to X_2 . Choose a local orientation of the neighbourhood of the vertex in such a way that the positions in X_1 are on the clockwise earlier side of the edges incident to the vertex. These local orientations are consistent across the neighbourhoods of the edges, because (X_1, X_2) is a bipartition of $\Gamma(m)$. Finally, each face is contractible to a point, so the local orientation defined above for a neighbourhood of G can be extended consistently to all of S . \square

The *dual* of a map $m = (X, \mu_1, \mu_2, \mu_3, r)$ is $(X, \mu_3, \mu_2, \mu_1, r)$. The Euler characteristic and the orientability of the dual are the same as those of the original.

2.3.3 A mnemonic convention

For mnemonic convenience we can replace μ_1, μ_2, μ_3 by f, e, v respectively. One may think of μ_1 as a function which changes (at least locally) the face which contains a position, and therefore μ_1 is denoted by f . (The same vertex and edge contain positions x and $f(x)$, while x and $f(x)$ may or may not belong to the same face.) One may think of μ_2 as changing the edge containing a position, and therefore μ_2 is denoted by e . The vertex and face of the position are unaffected by e . One may think of μ_3 as changing the vertex containing a position, and therefore μ_3 is denoted by v . The face and edge containing a position are the same for positions x and $v(x)$.

The permutations ev, vf and fe are associated with faces, edges and vertices, respectively. In each permutation, there is a correspondence between a pair of disjoint cycles and faces, edges or vertices, respectively. That is, each face corresponds to a pair of cycles in ev , each vertex corresponds to a pair of cycles in the permutation fe , and each edge corresponds to a pair of cycles in vf .

2.3.4 Edge Deletion and Submaps

Given an edge e in a map $m = (X, \mu_1, \mu_2, \mu_3)$, one can form a (pre)map $m' = m - e$ by deleting e from m .

Definition 2.5. Let $m = (X, \mu_1, \mu_2, \mu_3)$ be a premap. Let e be an edge of m , i.e. a 4-

cycle in the matchings graphs $\Gamma(m)$ with edges from μ_1 and μ_3 . Let the positions in e be x_1, x_2, x_3, x_4 , where $\mu_1 : x_1 \leftrightarrow x_2, x_3 \leftrightarrow x_4$ and $\mu_3 : x_1 \leftrightarrow x_4, x_2 \leftrightarrow x_3$. Then the premap $m' = m - e$ is:

$$m' = (X', \mu'_1, \mu'_2, \mu'_3)$$

where $X' = X \setminus \{x_1, x_2, x_3, x_4\}$,

$$\mu'_2(x) = \begin{cases} (\mu_2 \circ \mu_1 \circ \mu_2)(x) & \text{if } \mu_2(x) \in \{x_1, x_2, x_3, x_4\}, \\ \mu_2(x) & \text{otherwise, and} \end{cases}$$

the other two matchings are $\mu'_1 = \mu_1|_{X'}$ and $\mu'_3 = \mu_3|_{X'}$, restrictions to X' of the matchings of m .

If multiple edges are deleted, the result does not depend on the order the edges are deleted because $(m - e_1) - e_2 = (m - e_2) - e_1$. Thus we may define $m - D$, for any set of edges D , as the result of the successive deletion of the edges in D . Since this is analogous to deletion in graphs, the following notion applies:

Definition 2.6. Let $D = \{e_1, \dots, e_d\}$ be a set of edges in a map m . Then $s = m - D = (\dots((m - e_1) - e_2) - \dots - e_d)$ is a submap of m .

2.3.5 Rotation Systems

It will be convenient to define an orientable combinatorial map in terms of a pair of permutations called a rotation system.

Definition 2.7. A rotation system with n edges, vertex partition ν and face partition ϕ is a pair (ρ, ε) with $\rho \in \mathfrak{S}_{2n}$ and $\varepsilon \in \text{Match}(\mathcal{N}_{2n})$, such that $\tau(\rho) = \nu$ and $\tau(\rho\varepsilon) = \phi$.

The encoding is done by placing a label at each end of an edge. Then ε is the matching whose pairs are the pairs of labels on each edge. The cycles of permutation ρ are formed by listing the labels in cyclic clockwise order around each vertex. This can be done consistently through the global orientation of the map. The cycles of $\rho\varepsilon$ then correspond to the faces of the map.

The resulting rotation system associated with a map is such that the permutation group $\langle \rho, \varepsilon \rangle$ generated by ρ and ε is transitive (has one orbit on the set \mathcal{N}_{2n}).

2.3.6 Generating Series for Maps

Associated with each map $m = (X, f, e, \nu)$, are two partition-valued parameters, $\phi(m)$ and $\nu(m)$, the *face (degree) partition* and *vertex (degree) partition*, respectively, and the integer parameter $n(m)$, the number of edges. In terms of a topological map, the vertex partition consists of the degrees (number of incident ends of edges) of each of the vertices, and the face partition consists of the degrees (number of incident sides of edges) of each of the faces.

In the terms of combinatorial maps, the vertex partition consists of the half-lengths of the cycles in $\Gamma(m)$ representing vertices, the *fe-cycles*. The face partition consists of the half-lengths of the cycles in $\Gamma(m)$ representing faces, the *ev-cycles*.

Let \mathcal{L} be the set of all rooted, locally orientable maps. (This includes both

orientable and non-orientable maps.) Let \mathcal{O} be the set of all rooted orientable maps (so $\mathcal{O} \subseteq \mathcal{L}$). The generating series for rooted (locally orientable) maps \mathcal{L} is defined to be

$$L = L(\mathbf{x}, \mathbf{y}, \mathbf{z}) = \sum_{\mathfrak{m} \in \mathcal{L}} \mathbf{x}_{\phi(\mathfrak{m})} \mathbf{y}_{\nu(\mathfrak{m})} \mathbf{z}^{n(\mathfrak{m})}$$

(where for any partition $\mathbf{x}_\lambda = x_{\lambda_1} x_{\lambda_2} \dots$, and \mathbf{y}_λ is similarly defined). The generating series for rooted orientable maps \mathcal{O} is defined to be

$$\Omega = \Omega(\mathbf{x}, \mathbf{y}, \mathbf{z}) = \sum_{\mathfrak{m} \in \mathcal{O}} \mathbf{x}_{\phi(\mathfrak{m})} \mathbf{y}_{\nu(\mathfrak{m})} \mathbf{z}^{n(\mathfrak{m})}.$$

For partitions $\phi, \nu \vdash 2n$, let the coefficient of $\mathbf{x}_\phi \mathbf{y}_\nu \mathbf{z}^n$ in L and Ω be $m_{\phi, \nu, n}$ and $\omega_{\phi, \nu, n}$, respectively. These coefficients are non-negative integers which count the number of either locally orientable or orientable rooted maps \mathfrak{m} with n edges, and face and vertex partitions ϕ and ν , respectively.

It was claimed that (1.5) has the specialisations $\Psi^{(1)} = \Omega$ (with $\alpha = 1$) and $\Psi^{(2)} = L$ (with $\alpha = 2$). To elaborate on the definition of (1.5) one needs the theory of symmetric functions.

Chapter 3

On the Algebraic Method

The Quadrangulation Conjecture and the Map-Jack Conjecture are based on results developed by the algebraic method of map enumeration. Although later chapters do not use the material contained here, this chapter provides a background and context with an overview of the original development. Many of the details of this development are omitted, since they are peripheral to the approach described in this thesis, and the interested reader is directed to the original sources.

The Quadrangulation Conjecture is defined in Chapter 5, together with a partial solution. This chapter outlines some of the methods in the complicated proof of [JV90a] for the enumerative result from which the Quadrangulation Conjecture arises. These methods are not required in Chapter 5, so the treatment here is to motivate the origin of the bijection.

In the case of the Map-Jack Conjecture, Chapters 6 and 7 only use the material of this chapter to support the relevance of the combinatorial parameters β and η

(to be defined in Chapters 6 and 7). The interest in these parameters derives from the computational evidence of their association with the Jack parameter α . By defining Jack symmetric functions, this chapter makes the Map-Jack Conjecture (Conjecture 1.2) precise.

This chapter also contains a re-derivation, by the algebraic method, of a result of Walsh. Walsh obtained a recurrence relation by the edge deletion method, and then solved this recurrence. Analogous steps are taken in Chapter 6 but on rather different objects. The same result is derived again in this chapter, but by the algebraic method. In the case of Walsh's formula, an algebraic method is used to re-establish a result of the edge deletion method. In later chapters, the opposite occurs: the edge deletion method is used to produce some predicted results of the algebraic method.

3.1 Group Algebras and Some Subalgebras

This section gives (without proof) the essential aspects that are needed for character theory and certain group algebras. Details are to be found in [Sag91, Irv98, Mac95, JV90b, GJ96b, GJ96a].

Let \mathfrak{S}_n be the set of permutations acting on $\mathcal{N}_n = \{1, 2, \dots, n\}$. The group algebra of \mathfrak{S}_n over \mathbb{C} is denoted $\mathbb{C}\mathfrak{S}_n$, and consists of formal linear combinations of permutations. Addition in $\mathbb{C}\mathfrak{S}_n$ is usual vector space addition $\sum_{\pi} a_{\pi}\pi + \sum_{\pi} b_{\pi}\pi =$

$\sum_{\pi} (a_{\pi} + b_{\pi})\pi$. Multiplication uses the product from the symmetric group,

$$\sum_{\pi} a_{\pi}\pi \times \sum_{\pi} b_{\pi}\pi = \sum_{\pi, \rho} a_{\pi} b_{\rho}\pi\rho = \sum_{\pi} \left(\sum_{\rho} a_{\pi\rho^{-1}} b_{\rho} \right) \pi.$$

The centre $Z(\mathbb{C}\mathfrak{S}_n)$ of the group algebra of the symmetric group consists of all $a = \sum_{\pi} a_{\pi}\pi$ such that a_{π} is constant on each conjugacy class, and hence $Z(\mathbb{C}\mathfrak{S}_n)$ is called the *class algebra*. Since a permutation's conjugacy class is determined by its cycle type, it follows that conjugacy classes \mathcal{C}_{μ} are naturally indexed by partitions. For example, the conjugacy classes of \mathfrak{S}_3 are $\mathcal{C}_{[1^3]} = \{1\}$, $\mathcal{C}_{[21]} = \{(1, 2), (2, 3), (3, 1)\}$ and $\mathcal{C}_{[3]} = \{(1, 2, 3), (1, 3, 2)\}$.

A natural basis for the class algebra is the set of class sums $C_{\lambda} = \sum_{\pi \in \mathcal{C}_{\lambda}} \pi$. The integers

$$[C_{\lambda}] C_{\mu} C_{\nu} \tag{3.1}$$

are *connection coefficients*. Connection coefficients count factorisations of permutations into permutations of specific cycle types, since

$$|C_{\lambda}| [C_{\lambda}] C_{\mu} C_{\nu} = |\{(\pi, \sigma, \tau) : \pi \in \mathcal{C}_{\lambda}, \sigma \in \mathcal{C}_{\mu}, \tau \in \mathcal{C}_{\nu}, \pi\sigma\tau = 1\}|.$$

Thus the number of rotation systems (ρ, ε) with vertex partition ν and face partition ϕ is $|C_{\phi}| [C_{\phi}] C_{[2^n]} C_{\nu}$, since $\rho \in \mathcal{C}_{\nu}$, $\varepsilon \in \mathcal{C}_{[2^n]}$ and $\rho\varepsilon \in \mathcal{C}_{\phi}$. It is therefore possible to express a generating series for rotation systems in terms of connection coef-

ficients. A generating series for rooted orientable maps can be found from the generating series for rotation systems by applying a differential operator to its logarithm.

3.1.1 Characters and Orthogonal Idempotents

For each partition $\lambda \vdash n$, the group \mathfrak{S}_n has an irreducible character $\chi^\lambda : \mathfrak{S}_n \rightarrow \mathbb{C}$, and these constitute all irreducible characters. Characters are constant on each conjugacy class. Let $\chi_\mu^\lambda = \chi^\lambda(\pi)$ for $\pi \in \mathcal{C}_\mu$. Irreducible characters can be used to express the orthogonal idempotents F_θ of $\mathbb{C}\mathfrak{S}_n$ in terms of the class sums by

$$F_\lambda = \frac{\chi_{[1^n]}^\lambda}{n!} \sum_{\mu} \chi_\mu^\lambda C_\mu. \quad (3.2)$$

Orthogonal idempotents are called so because of the property that

$$F_\lambda F_\mu = \delta_{\lambda\mu} F_\lambda. \quad (3.3)$$

Class sums are expressed in the orthogonal idempotent basis as follows:

$$C_\mu = |\mathcal{C}_\mu| \sum_{\lambda \vdash n} \frac{1}{\chi_{[1^n]}^\lambda} \chi_\mu^\lambda F_\lambda \quad (3.4)$$

From (3.2), (3.4) and (3.3), connection coefficients may be expressed in terms of characters by

$$[C_\lambda] C_\mu C_\nu = \frac{|\mathcal{C}_\mu| \cdot |\mathcal{C}_\nu|}{n!} \sum_{\theta \vdash n} \frac{\chi_\lambda^\theta \chi_\mu^\theta \chi_\nu^\theta}{\chi_{[1^n]}^\theta}. \quad (3.5)$$

Thus rotation systems may be enumerated using characters of the symmetric group. Therefore orientable rooted maps may also be enumerated. But characters of the symmetric group are themselves very difficult to compute and, in practice, character sums are often intractable. Certain special cases and special properties of characters can be used to obtain enumerative results about maps, including the enumerative result behind the Quadrangulation Conjecture. More importantly, characters of the symmetric group are an intermediate device to the introduction of symmetric functions into map enumeration.

3.1.2 Two Double Coset Algebras

Non-orientable maps cannot be encoded by rotation systems, so an algebra different from the class algebra is needed for their enumeration. This is the double coset algebra of the hyperoctahedral group, as was used [GJ96a].

Each subgroup H of a finite group G partitions the group G into *double cosets* $HgH = \{h_1gh_2 \mid h_1, h_2 \in H\}$. The *double coset algebra* $D(G, H)$ is a subalgebra of $\mathbb{C}G$, which has for a basis sums of elements in the double cosets of H . If $D(G, H)$ is a commutative algebra then (G, H) is called a *Gel'fand pair* [Mac95].

Fix a matching $\varepsilon_n = (1, 2)(3, 4) \cdots (2n - 1, 2n) \in \mathfrak{S}_{2n}$. The *hyperoctahedral group* H_n is the centraliser group of ε_n , that is all permutation commuting with ε_n . Then (\mathfrak{S}_{2n}, H_n) , is a Gel'fand pair. The double cosets of H_n may be naturally indexed by partitions, and thus, so may the corresponding basis $\{K_\lambda\}_{\lambda \vdash n}$ of $D(\mathfrak{S}_{2n}, H_n)$ [HSS92].

The structure constants $[K_\lambda] K_\mu K_\nu$, may be used to enumerate labelled locally

orientable maps, in a similar way to the way connection coefficients (3.1) enumerate rotation systems. For the double coset algebra of the hyperoctahedral group, there is also a set of scalar-valued functions which behave like characters of the symmetric group with respect to a set of orthogonal idempotents E_θ in the double coset algebra $D(\mathfrak{S}_{2n}, H_n)$.

There is another double coset algebra, described by Macdonald in [Mac95], which can be used to enumerate orientable maps and which has, moreover, a close affinity to the double coset algebra for locally orientable maps. We now digress briefly to describe it.

Let $G_n = \mathfrak{S}_n \times \mathfrak{S}_n$, considered as a subgroup of \mathfrak{S}_{2n} , acting independently on odd and even numbers. For example $(2, 8, 6)(1, 5)(3, 7) \in G_4$. Let $L_n = G_n \cap H_n$. Then (G_n, L_n) is also a Gel'fand pair. The algebra $D(G_n, L_n)$ has a double coset sum basis $\{L_\lambda\}_{\lambda \vdash n}$ indexed by partitions, which is such that $[L_\lambda]L_\mu L_\nu = [C_\lambda]C_\mu C_\nu$. Thus, theoretically the algebra $D(G_n, L_n)$ may replace the class algebra $Z(\mathbb{C}\mathfrak{S}_n)$ for the enumeration of the orientable maps. For further discussion, see §3.2.4.

3.2 Symmetric Functions

Symmetric functions are formal power series of bounded degree, over (countably) infinitely many ground variables, that are invariant under permutation of the ground variables. Let the ground variables be x_1, x_2, x_3, \dots , and let $\mathbf{x} = (x_1, x_2, \dots)$.

Each product of finitely many x_i is a monomial. The collection of degrees of the x_i in a monomial is its degree partition. Thus for the partition $\lambda = (\lambda_1, \lambda_2, \dots, \lambda_k)$,

the corresponding *monomial symmetric function* is

$$m_\lambda(\mathbf{x}) = \sum_{i_1, i_2, \dots, i_k} x_{i_1}^{\lambda_1} x_{i_2}^{\lambda_2} \cdots x_{i_k}^{\lambda_k},$$

summed over distinct monomials with degree partition λ , each appearing once.

The ring of symmetric functions is

$$\Lambda = \bigoplus_{\lambda} \mathbb{Z}m_\lambda,$$

the set of \mathbb{Z} -linear combinations of monomial symmetric functions. The rings formed by allowing other coefficients, such as the rational numbers or complex numbers, are denoted by $\Lambda_{\mathbb{Q}}$ or $\Lambda_{\mathbb{C}}$, respectively.

Other symmetric functions include the *complete symmetric functions*

$$h_n(\mathbf{x}) = \sum_{\lambda \vdash n} m_\lambda(\mathbf{x}) = \sum_{i_1 \leq \dots \leq i_n} x_{i_1} \cdots x_{i_n},$$

the *elementary symmetric functions* $e_n(\mathbf{x}) = m_{[1^n]}(\mathbf{x}) = \sum_{i_1 < \dots < i_n} x_{i_1} \cdots x_{i_n}$, and the power sum symmetric functions $p_n(\mathbf{x}) = m_{[n]}(\mathbf{x}) = x_1^n + x_2^n + \cdots$. For the partition $\lambda = (\lambda_1, \lambda_2, \dots)$, let $h_\lambda = h_{\lambda_1} h_{\lambda_2} \cdots$, $e_\lambda = e_{\lambda_1} e_{\lambda_2} \cdots$ and $p_\lambda = p_{\lambda_1} p_{\lambda_2} \cdots$.

The ring Λ has $\{h_\lambda\}$ and $\{e_\lambda\}$ as \mathbb{Z} -bases, and $\{p_\lambda\}$ is a \mathbb{Q} -basis for $\Lambda_{\mathbb{Q}}$. Moreover, $\{h_n\}$ and $\{e_n\}$ are algebraic bases for Λ , i.e.: $\Lambda = \mathbb{Z}[h_1, h_2, h_3, \dots]$. Similarly, $\{p_n\}$ is an algebraic basis for $\Lambda_{\mathbb{Q}} = \mathbb{Q}[p_1, p_2, \dots]$.

A symmetric function is homogeneous if all its monomial terms have the same total degree. The set of homogeneous symmetric functions of (total) degree n is indicated Λ^n and has $\{m_\lambda\}_{\lambda \vdash n}$, $\{h_\lambda\}_{\lambda \vdash n}$, and $\{e_\lambda\}_{\lambda \vdash n}$ as \mathbb{Z} -bases.

3.2.1 Jack Symmetric Functions

Introduce a scalar product $\langle \cdot, \cdot \rangle_\alpha$ on $\Lambda_{\mathbb{Q}(\alpha)}$, uniquely determined by:

$$\langle p_\lambda, p_\mu \rangle_\alpha = \delta_{\lambda\mu} z_\lambda \alpha^{\ell(\lambda)} \quad (3.6)$$

where

$$\delta_{\lambda\mu} = \begin{cases} 1 & \text{if } \lambda = \mu, \\ 0 & \text{if } \lambda \neq \mu, \end{cases}$$

and for partitions $\lambda = [1^{m_1(\lambda)} 2^{m_2(\lambda)} \dots]$, recall that

$$z_\lambda = \prod_i m_i(\lambda)! i^{m_i(\lambda)}.$$

Since $\{p_\lambda\}$ is a basis for $\Lambda_{\mathbb{Q}(\alpha)}$, and a scalar product is by definition linear in each of its arguments, equation (3.6) suffices to define $\langle \cdot, \cdot \rangle_\alpha$ over all of $\Lambda_{\mathbb{Q}(\alpha)}$. One has: $\langle p_{[2]}, p_{[1^2]} \rangle_\alpha = 0$, but $\langle p_{[2]}, p_{[2]} \rangle_\alpha = 2\alpha$ and $\langle p_{[1^2]}, p_{[1^2]} \rangle_\alpha = 2\alpha^2$.

Put the $\mathbb{Q}(\alpha)$ -basis $\{m_\mu\}_{\mu \vdash n}$ of $\Lambda_{\mathbb{Q}(\alpha)}^n$ into lexicographic order. Use Gram-Schmidt orthogonalisation on this ordered basis. Let $\{J_\mu^{(\alpha)}\}_{\mu \vdash n}$ be the resulting ordered basis, which satisfies the triangulation condition

$$J_\lambda^{(\alpha)} = a_{\lambda\lambda} m_\lambda + \sum_{\mu < \lambda} a_{\lambda\mu} m_\mu, \quad (3.7)$$

for some $a_{\lambda\mu} \in \mathbb{Q}(\alpha)$, the orthogonality condition

$$\left\langle J_{\lambda}^{(\alpha)}, J_{\mu}^{(\alpha)} \right\rangle_{\alpha} = 0 \quad \text{if } i \neq j,$$

and the normalisation condition

$$[m_{[1^n]}] J_{\lambda}^{(\alpha)} = n!$$

Then $J_{\lambda}^{(\alpha)}$ is a *Jack symmetric function*. (The symmetric function $J_{\lambda}^{(\alpha)}$ is called the integral form of a Jack symmetric function in [Mac95], where Jack symmetric functions are defined to be $P_{\lambda}^{(\alpha)}$ with a different normalisation condition.)

Equation (3.7) still holds if lexicographic order in (3.7) is replaced by the weaker dominance order. Moreover, Jack symmetric functions are still unique if this condition is weakened. This non-trivial result is proved by using certain differential, self-adjoint operators, the Sekiguchi-Debiard operators.

The Macdonald-Stanley Conjecture [Sta89] asserted that the $a_{\lambda\mu}$ are polynomials in α with nonnegative integer coefficients. This conjecture was proved recently independently in [KS97] and [LV95]. It is not clear how this recent result can be used to show a necessary consequence of the Map-Jack Conjecture: that $\Psi^{(b+1)}(\mathbf{x}, \mathbf{y}, z)$, from (1.5), is a non-negative integer formal power series.

We include a briefly explained calculation of $J_{[1^2]}^{(\alpha)}$ and $J_{[2]}^{(\alpha)}$ for the above definition, in the power sum basis, since these functions are so essential to the Map-Jack Conjecture. We now compute $J_{\lambda}^{(\alpha)}$ for $\lambda \vdash n \leq 2$. For $n = 1$, there is only one basis element $m_{[1]}$, so $J_{[1]}^{(\alpha)} = m_{[1]}$. For $n = 0$, one has $J_{\emptyset}^{(\alpha)} = m_{\emptyset} = 1$ by similar

reasoning. For $n = 2$, lexicographic order is $[1^2] < [2]$, so the first step of orthogonalisation is simply $J_{[1^2]}^{(\alpha)} = 2m_{[1^2]}$. Next, we must have $J_{[2]}^{(\alpha)} = a_{[2],[2]}m_{[2]} + 2m_{[1^2]}$ for some $a_{[2],[2]} = X \in \mathbb{Q}(\alpha)$, and, by orthogonality:

$$\begin{aligned}
\mathbf{0} &= \left\langle J_{[1^2]}^{(\alpha)}, J_{[2]}^{(\alpha)} \right\rangle_{\alpha} \\
&= \left\langle 2m_{[1^2]}, Xm_{[2]} + 2m_{[1^2]} \right\rangle_{\alpha} \\
&= \left\langle p_{[1^2]} - p_{[2]}, Xp_{[2]} + (p_{[1^2]} - p_{[2]}) \right\rangle_{\alpha} \\
&= (X - 1) \left\langle p_{[1^2]}, p_{[2]} \right\rangle_{\alpha} - (X - 1) \left\langle p_{[2]}, p_{[2]} \right\rangle_{\alpha} \\
&\quad + \left\langle p_{[1^2]}, p_{[1^2]} \right\rangle_{\alpha} - \left\langle p_{[1^2]}, p_{[2]} \right\rangle_{\alpha} \\
&= \mathbf{0} - (X - 1)2\alpha + 2\alpha^2 - \mathbf{0} \\
&= 2\alpha(-X + 1 + \alpha),
\end{aligned}$$

using $m_{[1^2]} = \frac{1}{2}(p_{[1^2]} - p_{[2]})$ and $m_{[2]} = p_{[2]}$. Solving yields $X = 1 + \alpha$, and therefore $J_{[2]}^{(\alpha)} = (1 + \alpha)m_{[2]} + 2m_{[1^2]}$. Consequently,

$$\begin{aligned}
J_{[2]}^{(\alpha)} &= \alpha p_{[2]} + p_{[1^2]}, \\
J_{[1^2]}^{(\alpha)} &= -p_{[2]} + p_{[1^2]}.
\end{aligned}$$

in the power sums basis. The need for expressing of Jack symmetric functions in terms of power sum symmetric functions is seen clearly in (1.5).

3.2.2 Schur Symmetric Functions

When $\alpha = 1$, Jack symmetric functions specialise, up to a scalar factor, to Schur symmetric functions since $J_{\lambda}^{(1)} = H_{\lambda}s_{\lambda}$, where, recall, H_{λ} is the product of the

hook lengths of the partition λ . Schur symmetric functions are also given by

$$s_\lambda(x_1, \dots, x_n) = \frac{\det(x_i^{\lambda_j+n-j})_{1 \leq i, j \leq n}}{\det(x_i^{n-j})_{1 \leq i, j \leq n}} \quad (3.8)$$

and

$$s_\lambda = \det(h_{\lambda_i-i+j})_{1 \leq i, j \leq n} \quad \text{for } n \geq \ell(\lambda) \quad (3.9)$$

(the equality of (3.8) and (3.9) is essentially the Jacobi-Trudi identity). Schur symmetric functions are also given by

$$s_\lambda = \sum_{|\mu|=|\lambda|} z_\mu^{-1} \chi_\mu^\lambda p_\mu \quad (3.10)$$

The above three definitions do not seem to have corresponding generalisations in terms of Jack symmetric functions. There is a combinatorial characterisation of Schur symmetric functions as

$$s_\lambda(\mathbf{x}) = \sum_{\text{sh } T=\lambda} \mathbf{x}^T \quad (3.11)$$

summed over semi-standard tableau T of shape λ . Equation (3.11) does have a generalisation to the setting of Jack symmetric functions. For further details on symmetric functions see [Mac95].

Because irreducible characters of the symmetric group appear both in (3.10) and (3.5), Schur symmetric functions may be applied to the enumeration of rotation systems and therefore to the enumeration of rooted orientable maps. In

particular, the following generating series, already seen in (1.1), for orientable rooted maps, is expressed in terms of Schur symmetric functions as

$$\Omega(\mathbf{x}, \mathbf{y}, \mathbf{z}) = 2z \frac{\partial}{\partial z} \log \sum_{n \geq 0} \sum_{\lambda \vdash n} H_\lambda s_\lambda(\mathbf{x}) s_\lambda(\mathbf{y}) s_\lambda(\mathbf{z}) \Big|_{\substack{p_j(\mathbf{x}) \mapsto x_j, p_j(\mathbf{y}) \mapsto y_j \\ p_j(\mathbf{z}) \mapsto z \delta_{j,2}}}$$

The expression (3.9) for Schur symmetric functions in terms of complete symmetric functions is useful for obtaining the factorisation (1.2), which expresses $[p_{[4^n]}] s_\lambda$ in terms of two other Schur symmetric functions $s_{\lambda^{(1)}}$ and $s_{\lambda^{(2)}}$.

This factorisation is achieved by setting $p_j = 0$ for $j \neq 4$ in the determinant $\det(h_{\lambda_i - i + j})$. Since $h_n = \sum_{\nu \vdash n} z_\nu^{-1} p_\nu$, this can be done quite simply. Entries h_n of the matrix with n not divisible by 4 become zero under this substitution. Thus the determinant may be factorised as the product of two determinants. This also means the character $\chi_{[4^n]}^\lambda$ can be expressed simply in terms of some characters $\chi_{[2^k]}^\mu$.

To restrict to quadrangulations set $\phi = [4^n]$. The number of quadrangulations may be expressed in terms of the number of all maps, by using the above factorisation. A natural bijection for this enumerative result is sought in the Quadrangulation Conjecture. More detail can be found in [JV90a].

3.2.3 Zonal Polynomials

When $\alpha = 2$, a Jack symmetric function specialises to a zonal polynomial $Z_\lambda = J_\lambda^{(2)}$. While zonal polynomials do not share all the corresponding properties of

Schur symmetric functions, they do share one property (not known to generalise to Jack symmetric functions), a property corresponding to equation (3.10),

$$Z_\lambda = |H_n| \sum_{\mu_n} z_{2\mu}^{-1} \omega_\mu^\lambda p_\mu$$

where $\omega_\mu^\lambda = \omega^\lambda(\pi)$ for any $\pi \in \mathcal{D}_\mu$, the double coset of H_n indexed by μ , and the function ω^λ is defined

$$\omega^\lambda(s) = \frac{1}{2^n n!} \sum_{h \in H_n} \chi^{2\lambda}(sh).$$

in [HSS92] with a full account of the character theory.

The same functions ω^λ occur for double coset algebra of the hyperoctahedral groups in the conversions from the double coset sum basis to the orthogonal idempotents. These ω^λ have the same rôle as characters do for the class algebra. It then follows that Zonal polynomials Z_λ may be used to enumerate locally orientable maps.

3.2.4 Symmetric Functions and Double Coset Algebras

The relationship between symmetric functions and the two double coset algebras of §3.1.2 is summarised in this section. The following applies to the class algebra $Z(\mathbb{C}\mathfrak{S}_n)$ as well, because it is related to the double coset algebra $D(G_n, L_n)$ by having equal connection coefficients $[L_\lambda] L_\mu L_\nu = [C_\lambda] C_\mu C_\nu$.

Let $D_\mu^{(1)} = \frac{1}{|L_n|} L_\mu$, and $D_\mu^{(2)} = \frac{1}{|H_n|} K_\mu$ (normalised double coset sums). For $i = 1, 2$, let $E_\lambda^{(i)}$ be the orthogonal idempotent indexed by λ , of $D(G_n, L_n)$ and $D(\mathfrak{S}_{2n}, H_n)$

respectively. Then for $i = 1, 2$ the following is true

$$\sum_{\lambda \vdash n} J_\lambda^{(i)} E_\lambda^{(i)} = \sum_{\mu \vdash n} p_\mu D_\mu^{(i)}. \quad (3.12)$$

The chosen normalisation of $D_\mu^{(i)}$ gives (3.12) its simple form. The fundamental relationship of Jack symmetric functions at $\alpha = 1$ and $\alpha = 2$ to the structure of the double coset algebras is made clear by the simplicity of (3.12). The result (3.12) will not be proven here. However, the usefulness of (3.12) is demonstrated by simultaneously outlining part of the development of symmetric function based generating series for both the set of orientable maps and the set of locally orientable maps.

By taking coefficients of each side (3.12), it is possible to change bases, either between power sums and Schur functions or zonal polynomials, or between double cosets and orthogonal idempotents. For example

$$[p_\theta] J_\psi^{(i)} = [p_\theta E_\psi^{(i)}] \sum_{\lambda \vdash n} J_\lambda^{(i)} E_\lambda^{(i)} = [p_\theta E_\psi^{(i)}] \sum_{\mu \vdash n} p_\mu D_\mu^{(i)} = [E_\psi^{(i)}] D_\theta^{(i)}.$$

More importantly,

$$\begin{aligned}
[D_\lambda^{(i)}] D_\mu^{(i)} D_\nu^{(i)} &= [p_\mu(\mathbf{x}) p_\nu(\mathbf{y}) D_\lambda^{(i)}] \left(\sum_{\theta \vdash n} p_\theta(\mathbf{x}) D_\theta^{(i)} \right) \left(\sum_{\psi \vdash n} p_\psi(\mathbf{y}) D_\psi^{(i)} \right) \\
&= [p_\mu(\mathbf{x}) p_\nu(\mathbf{y}) D_\lambda^{(i)}] \left(\sum_{\theta \vdash n} J_\theta^{(i)}(\mathbf{x}) E_\theta^{(i)} \right) \left(\sum_{\psi \vdash n} J_\psi^{(i)}(\mathbf{y}) E_\psi^{(i)} \right) \\
&= [p_\mu(\mathbf{x}) p_\nu(\mathbf{y}) D_\lambda^{(i)}] \sum_{\theta \vdash n} J_\theta^{(i)}(\mathbf{x}) J_\theta^{(i)}(\mathbf{y}) E_\theta^{(i)} \\
&= \sum_{\theta \vdash n} [p_\mu(\mathbf{x}) p_\nu(\mathbf{y})] J_\theta^{(i)}(\mathbf{x}) J_\theta^{(i)}(\mathbf{y}) [D_\lambda^{(i)} J_\theta^{(i)}(\mathbf{z})] \sum_{\tau \vdash n} J_\tau^{(i)}(\mathbf{z}) E_\tau^{(i)} \\
&= \sum_{\theta \vdash n} [p_\mu(\mathbf{x}) p_\nu(\mathbf{y})] J_\theta^{(i)}(\mathbf{x}) J_\theta^{(i)}(\mathbf{y}) [D_\lambda^{(i)} J_\theta^{(i)}(\mathbf{z})] \sum_{\tau \vdash n} p_\tau(\mathbf{z}) D_\tau^{(i)} \\
&= \sum_{\theta \vdash n} \left([p_\mu(\mathbf{x})] J_\theta^{(i)}(\mathbf{x}) \right) \left([p_\nu(\mathbf{y})] J_\theta^{(i)}(\mathbf{y}) \right) \left([J_\theta^{(i)}(\mathbf{z})] p_\lambda(\mathbf{z}) \right)
\end{aligned}$$

But

$$[J_\theta^{(\alpha)}] p_\lambda = \frac{\langle J_\theta^{(\alpha)}, p_\lambda \rangle_\alpha}{\langle J_\theta^{(\alpha)}, J_\theta^{(\alpha)} \rangle_\alpha} = \frac{\langle p_\lambda, p_\lambda \rangle_\alpha}{\langle J_\theta^{(\alpha)}, J_\theta^{(\alpha)} \rangle_\alpha} \frac{\langle J_\theta^{(\alpha)}, p_\lambda \rangle_\alpha}{\langle p_\lambda, p_\lambda \rangle_\alpha} = \frac{z_\lambda \alpha^{\ell(\lambda)}}{\langle J_\theta^{(\alpha)}, J_\theta^{(\alpha)} \rangle_\alpha} [p_\lambda] J_\theta^{(\alpha)}.$$

Therefore, for $i = 1$ and $i = 2$,

$$[D_\lambda^{(i)}] D_\mu^{(i)} D_\nu^{(i)} = z_\lambda i^{\ell(\lambda)} [p_\lambda(\mathbf{x}) p_\mu(\mathbf{y}) p_\nu(\mathbf{z})] \sum_{\theta \vdash n} \frac{J_\theta^{(i)}(\mathbf{x}) J_\theta^{(i)}(\mathbf{y}) J_\theta^{(i)}(\mathbf{z})}{\langle J_\theta^{(i)}, J_\theta^{(i)} \rangle_i} \quad (3.13)$$

For $i = \alpha = b + 1$, the right hand side of (3.13) is part of the generating series for maps $\Psi^{(b+1)}$ of (1.5) and the Map-Jack Conjecture. For $i = \alpha$, the left hand side of (3.13) has no interpretation because $D_\mu^{(\alpha)}$ has no interpretation, except at the values $\alpha = 1$ and $\alpha = 2$.

3.3 Algebraic Re-derivation of Walsh's Monopole Formula

An example is given of the use of the algebraic method to obtain an explicit result. The result is a new proof of a result of Walsh and Lehman [Wal71] obtained originally by the edge deletion method. It concerns a simple expression for the number of orientable rooted *monopoles* (map with a single vertex) with a give face partition.

The starting point of the new proof is a generating series for maps in terms of Schur symmetric functions. It is shown that in the case of monopoles, the generating series simplifies into the form discovered by Walsh and Lehman. The proof is divided between the next three subsections for convenience.

3.3.1 Walsh's formula

Walsh and Lehman obtained a formula, which is equivalent to the following expression for $\omega_{\phi, [2n], n}$, the number of orientable *monopoles* (rooted, single vertex maps) with n edges and face partition ϕ ,

$$\omega_{\phi, [2n], n} = \frac{n!}{2^n z_{\phi}} [u^{n+1}] \prod_{j=1}^{\ell(\phi)} \{(1+u)^{\phi_j} - (1-u)^{\phi_j}\}. \quad (3.14)$$

The coefficient in (3.14) may be extracted to obtain the sum

$$\omega_{\phi, [2n], n} = \frac{n!}{2^{2g-1} z_{\phi}} \sum_{\substack{i_j \geq 0 \\ i_1 + \dots + i_{\ell(\phi)} = g}} \prod_{j=1}^{\ell(\phi)} \binom{\phi_j}{2i_j + 1}$$

where $g = \frac{1}{2}(2 - \chi) = \frac{1}{2}(2 - (\ell(\phi) - n + 1)) = \frac{n+1-\ell(\phi)}{2}$ is the genus of the monopoles being enumerated by $\omega_{\phi, [2n], n}$.

For example,

$$\begin{aligned}\omega_{[321^3], [8], 4} &= \frac{4!}{2^{-1}(3 \cdot 2)3!} \left\{ \binom{3}{1} \binom{2}{1} \binom{1}{1}^3 \right\} = 8, \\ \omega_{[6, 4], [10], 5} &= \frac{5!}{2^3(6 \cdot 4)} \left\{ \binom{6}{3} \binom{4}{3} + \binom{6}{5} \binom{4}{1} \right\} = 65 \\ \omega_{[9, 2, 1], [12], 6} &= \frac{6!}{2^3(9 \cdot 2 \cdot 1)} \left\{ \binom{9}{5} \binom{2}{1} \binom{1}{1} \right\} = 1260\end{aligned}$$

which can be compared to the tables of Appendix B. In §B.4.1, §B.5.1, and §B.6.1 (respectively), these values are found in the column with $B = 0$ and in the row with $[321^3]$, $[6, 4]$ and $[9, 2, 1]$ (respectively). Incidentally, the values given in Appendix B are coefficients of the generating series Φ of Chapter 6, and are computed by a recurrence that extends the one used by Walsh originally.

3.3.2 From Walsh's formula to special Schur symmetric functions

The simple formula (3.14) is now manipulated into a form involving a special class of Schur symmetric functions s_θ : those where θ is a hook partition. To obtain a generating series $W(\mathbf{p}, z)$ for the expression (3.14), multiply by $p_\phi z^n$, and sum over all partitions ϕ , to give

$$W(\mathbf{p}, z) = \sum_{n \geq 0} z^n \sum_{\phi \vdash 2n} p_\phi \frac{n!}{2^n z_\phi} [u^{n+1}] \prod_{j=1}^{\ell(\phi)} \{(1+u)^{\phi_j} - (1-u)^{\phi_j}\}.$$

Proving the validity of Walsh's formula (3.14) is equivalent to verifying that $W(\mathbf{p}, z)$ is a generating series for orientable rooted monopoles. If the algebraic method is to be used, then $W(\mathbf{p}, z)$ should be shown to equal the expression for the generating series expressed in terms Schur symmetric functions.

Let $m_j = m_j(\phi)$. As ϕ varies over all partitions, m_j varies over all non-negative integers. So sum over all $m_j \geq 0$.

$$\begin{aligned} W(\mathbf{p}, z) &= \sum_{m_j \geq 0} \frac{n!}{2^n m_1! m_2! m_3! \dots} z^n [u^{n+1}] \prod_{j \geq 1} \left(p_j \frac{(1+u)^j - (1-u)^j}{j} \right)^{m_j} \\ &= \sum_{m_j \geq 0} n! [t^{n+1}] \prod_{j \geq 1} \frac{1}{m_j!} \left(p_j \left(\sqrt{\frac{z}{2}} \right)^j \frac{(1+t)^j - (1-t)^j}{j} \right)^{m_j} \end{aligned}$$

where $n = \frac{1}{2}(1m_1 + 2m_2 + \dots + jm_j + \dots)$ is assumed. Extraction of the coefficient of u^{n+1} and t^{n+1} may seem problematic if n is not an integer. However, the issue is resolved by letting $u = w^2$ and $t = w^2$ respectively, from which it is seen that coefficient should be zero when n is a half-integer. Let Θ_z be an operator defined by $\Theta_z : z^n \mapsto n!z^n$, and extended linearly. Then

$$\begin{aligned} W(\mathbf{p}, z) &= \Theta_z \sum_{m_j \geq 0} [t^1] \prod_{j \geq 1} \frac{1}{m_j!} \left(p_j \frac{1}{j} \left(\sqrt{\frac{z}{2t}} \right)^j ((1+t)^j - (1-t)^j) \right)^{m_j} \\ &= \Theta_z [t^1] \prod_{j \geq 1} \exp \left(p_j \frac{1}{j} \left(\sqrt{\frac{z}{2t}} \right)^j ((1+t)^j - (1-t)^j) \right) \\ &= \Theta_z [t^1] \exp \sum_{j \geq 1} \left(\frac{p_j}{j} \left(\sqrt{\frac{z}{2t}} (1+t) \right)^j - \frac{p_j}{j} \left(\sqrt{\frac{z}{2t}} (1-t) \right)^j \right) \\ &= \Theta_z [t^1] \exp \left(\log H \left(\sqrt{\frac{z}{2t}} (1+t) \right) - \log H \left(\sqrt{\frac{z}{2t}} (1-t) \right) \right) \\ &= \Theta_z [t^1] \frac{H \left((1+t) \sqrt{\frac{z}{2t}} \right)}{H \left((1-t) \sqrt{\frac{z}{2t}} \right)} \end{aligned}$$

where $H(z) = \sum_{m \geq 0} h_m z^m$. With $E(z) = \sum_{m \geq 0} e_m z^m$ below,

$$W(\mathbf{p}, z) = \Theta_z[t^1] H\left((t+1)\sqrt{z/(2t)}\right) E\left((t-1)\sqrt{z/(2t)}\right) \quad (3.15)$$

From [Mac95], it can easily be deduced that

$$H(u)E(yu) = (1+y) \sum_{\substack{0 \leq n, \\ 0 \leq k \leq n-1}} s_{[n-k, 1^k]} y^k u^n. \quad (3.16)$$

Hence (3.15), under the substitutions $u = (t+1)\sqrt{z/(2t)}$ and $y = \frac{t-1}{t+1}$ into (3.16), becomes

$$W(\mathbf{p}, z) = \Theta_z[t^1] \left(1 + \frac{t-1}{t+1}\right) \sum_{\substack{0 \leq n, \\ 0 \leq k \leq n-1}} s_{[n-k, 1^k]} \left(\frac{t-1}{t+1}\right)^k \left((t+1)\sqrt{\frac{z}{2t}}\right)^n. \quad (3.17)$$

3.3.3 Determination of the monopole series M

For orientable rooted maps, the algebraic method gives a generating series involving a sum of a product of three Schur symmetric functions. This is now specialised to include only monopoles.

$$M(\mathbf{p}(\mathbf{x}), z) = 2z \frac{\partial}{\partial z} [y] \sum_{\theta} H_{\theta} s_{\theta}(\mathbf{x}) s_{\theta}(\mathbf{y}) s_{\theta}(\mathbf{z}) \Big|_{\substack{p_j(\mathbf{y})=y \\ p_j(\mathbf{z})=z\delta_{j,2}}}, \quad (3.18)$$

where z is an ordinary marker variable for edges, and each face of degree k is marked by a factor of $p_k(\mathbf{x})$. To evaluate this begin by recalling that

$$s_\theta = \sum_{\alpha \vdash |\theta|} z_\alpha^{-1} \chi_\alpha^\theta p_\alpha \quad (3.19)$$

where, $\chi_\alpha^\theta = \langle s_\theta, p_\alpha \rangle$ is a character. Recall (3.9) which states that

$$s_\theta = \det(h_{\theta_i - i + j})_{1 \leq i, j \leq n},$$

for any $n \geq \ell(\theta)$. Since

$$h_n = \sum_{\alpha \vdash n} z_\alpha^{-1} p_\alpha$$

for $n \geq 0$, and since $h_n = 0$ for $n < 0$, with some work [Mac95] or [JV90a], it follows that

$$\chi_{[n]}^\theta = \begin{cases} (-1)^k & \text{if } \theta = [n - k, 1^k], \\ 0 & \text{otherwise,} \end{cases} \quad (3.20)$$

where $0 \leq k \leq n - 1$. Thus $\chi_{[n]}^\theta$ vanishes unless θ has a hook shape.

Therefore only those θ that are hooks contribute to the sum in (3.18). This simplifies the sum in (3.18) considerably, because only a small portion of partitions are hooks.

For $\theta \vdash n$,

$$[y] s_\theta \Big|_{p_j(y)=y} = [p_n] s_\theta$$

because when s_θ is expanded into power symmetric functions of degree n , the only term of degree one as a polynomial over the variables p_1, p_2, p_3, \dots is the term containing p_n . From (3.19)

$$[p_n] s_\theta = z_{[n]}^{-1} \chi_{[n]}^\theta.$$

Now we can use (3.20) to simplify the sum in (3.18):

$$2z \frac{\partial}{\partial z} \sum_{\substack{n \geq 0 \\ 0 \leq k \leq n-1}} H_{[n-k, 1^k]} s_{[n-k, 1^k]}(\mathbf{x}) z_{[n]}^{-1} (-1)^k \left(\sum_{m \geq 0} z^m [p_{[2^m]}] s_{[n-k, 1^k]} \right). \quad (3.21)$$

The last factor in (3.21) can be explained by observing that when s_θ is expanded into a polynomial of power symmetric functions the only nonzero terms in $s_\theta(\mathbf{z})$ arise from the terms of p_2^m in s_θ for some m , because of the condition that $p_j(\mathbf{z}) = 0$ if $j \neq 2$.

It follows that, in (3.21), n must be even. So replace n by $2n$. Then $m = n$. Hence

$$M(\mathbf{p}(\mathbf{x}), z) = 2z \frac{\partial}{\partial z} \sum_{\substack{n \geq 0 \\ 0 \leq k \leq 2n-1}} H_{[2n-k, 1^k]} s_{[2n-k, 1^k]}(\mathbf{x}) z_{[2n]}^{-1} (-1)^k z^n [p_{[2^n]}] s_{[2n-k, 1^k]}. \quad (3.22)$$

Since $z_{[2n]}^{-1} = \frac{1}{2n}$ cancels the effect of the differential operator $2z \frac{\partial}{\partial z}$ in (3.22), we

have

$$M(\mathbf{p}(\mathbf{x}), z) = \sum_{\substack{n \geq 0 \\ 0 \leq k \leq 2n-1}} (-1)^k z^n H_{[2n-k, 1^k]} S_{[2n-k, 1^k]}(\mathbf{x}) z_{[2^n]}^{-1} \chi_{[2^n]}^{[2n-k, 1^k]} \quad (3.23)$$

Clearly $z_{[2^n]}^{-1} = \frac{1}{2^{n n!}}$. From [Mac95], the value of the character indexed by a hook partition $[2n - k, 1^k]$ evaluated at a permutation with cycle partition μ may be deduced to be

$$\chi_{\mu}^{[2n-k, 1^k]} = [u^k] \frac{1}{1+u} \prod_{i \geq 1} (1 - (-u)^i)^{m_i(\mu)}.$$

In particular, when $\mu = [2^n]$,

$$\begin{aligned} \chi_{[2^n]}^{[2n-k, 1^k]} &= [u^k] \frac{1}{1+u} (1-u^2)^n \\ &= [u^k] (1-u) (1-u^2)^{n-1} \\ &= [u^k] (1-u) \left(1 - \binom{n-1}{1} u^2 + \binom{n-1}{2} u^4 - \dots \right) \\ &= [u^k] \left\{ 1 - u - \binom{n-1}{1} u^2 + \binom{n-1}{1} u^3 + \binom{n-1}{2} u^4 \right. \\ &\quad \left. - \binom{n-1}{2} u^5 - \binom{n-1}{3} u^6 + \dots \right\} \\ &= (-1)^{\lceil \frac{k}{2} \rceil} \binom{n-1}{\lfloor \frac{k}{2} \rfloor}. \end{aligned} \quad (3.24)$$

Omitting the argument (\mathbf{x}) , and by noting that $(-1)^{k+\lceil \frac{k}{2} \rceil} = (-1)^{\lfloor \frac{k}{2} \rfloor}$, (3.23) can

now be re-expressed as

$$M(\mathbf{p}, z) = \sum_{\substack{n \geq 0 \\ 0 \leq k \leq 2n-1}} (-1)^{\lfloor \frac{k}{2} \rfloor} z^n \frac{\binom{n-1}{\lfloor \frac{k}{2} \rfloor}}{2^n n!} H_{[2n-k, 1^k]} S_{[2n-k, 1^k]},$$

But the product of the hook lengths of the partition $[2n - k, 1^k]$ is $H_{[2n-k, 1^k]} = (2n)k!(2n - k - 1)!$. Therefore

$$M(\mathbf{p}, z) = \sum_{\substack{n \geq 0 \\ 0 \leq k \leq 2n-1}} (-1)^{\lfloor \frac{k}{2} \rfloor} z^n \frac{k!}{\lfloor \frac{k}{2} \rfloor!} \cdot 2^{1-n} \cdot \frac{(2n - k - 1)!}{(n - 1 - \lfloor \frac{k}{2} \rfloor)!} S_{[2n-k, 1^k]}, \quad (3.25)$$

3.3.4 Completing the equality

To complete the proof we show that $W(\mathbf{p}, z) = M(\mathbf{p}, z)$. From (3.17)

$$\begin{aligned} W(\mathbf{p}, z) &= \Theta_z [t^1] \sum_{\substack{0 \leq n, \\ 0 \leq k \leq n-1}} s_{[n-k, 1^k]} \left(\frac{(t-1)^k}{(t+1)^k} \frac{2t}{t+1} \right) \left\{ (t+1) \sqrt{\frac{z}{2t}} \right\}^n \\ &= \Theta_z [t^1] \sum_{\substack{0 \leq n, \\ 0 \leq k \leq n-1}} s_{[n-k, 1^k]} \{ (t-1)^k (t+1)^{n-1-k} (2t) \} z^{n/2} (2t)^{-n/2} \\ &= \Theta_z [t^0] \sum_{\substack{0 \leq n, \\ 0 \leq k \leq n-1}} s_{[n-k, 1^k]} \{ 2(t-1)^k (t+1)^{n-1-k} \} z^{n/2} (2t)^{-n/2} \\ &= \Theta_z \sum_{\substack{0 \leq n, \\ 0 \leq k \leq n-1}} 2s_{[n-k, 1^k]} [t^{n/2}] \{ (t-1)^k (t+1)^{n-1-k} \} (2z)^{n/2} \\ &= \sum_{\substack{0 \leq n, \\ 0 \leq k \leq n-1}} 2^{1-n/2} (n/2)! z^{n/2} s_{[n-k, 1^k]} [t^{n/2}] \{ (t-1)^k (t+1)^{n-1-k} \} \end{aligned}$$

which forces n to be even. (Again, this is made clearly rigorous by setting $t = w^2$.)

Replacing n by $2n$,

$$W(\mathbf{p}, z) = \sum_{\substack{0 \leq k \leq 2n-1 \\ 0 \leq k \leq 2n-1}} 2^{1-n} n! z^n s_{[2n-k, 1^k]} [t^n] (t-1)^k (t+1)^{2n-1-k}.$$

We need to evaluate

$$\begin{aligned} [t^n] (t-1)^k (t+1)^{2n-1-k} &= \sum_i (-1)^{k-i} \binom{k}{i} \binom{2n-k-1}{n-i} \\ &= \sum_i (-1)^k (-1)^{-i} \frac{k!}{i!(k-i)!} \frac{(2n-k-1)!}{(n-i)!(n-1-k+i)!} \\ &= \frac{k!(2n-k-1)!}{n!(n-1)!} (-1)^k \\ &\quad \times \sum_i (-1)^{-i} \frac{n!(n-1)!}{i!(n-i)!(k-i)!(n-1-k+i)!} \\ &= \frac{k!(2n-k-1)!}{n!(n-1)!} (-1)^k \sum_i (-1)^{-i} \binom{n}{i} \binom{n-1}{k-i} \\ &= \frac{k!(2n-k-1)!}{n!(n-1)!} (-1)^k [u^k] (1-u)^n (1+u)^{n-1} \\ &= \frac{k!(2n-k-1)!}{n!(n-1)!} (-1)^k [u^k] (1-u)(1-u^2)^{n-1} \end{aligned}$$

which, by (3.24),

$$\begin{aligned} &= \frac{k!(2n-k-1)!}{n!(n-1)!} (-1)^k (-1)^{\lceil \frac{k}{2} \rceil} \binom{n-1}{\lfloor \frac{k}{2} \rfloor} \\ &= \frac{k!(2n-k-1)!}{n!(n-1)!} (-1)^k (-1)^{\lceil \frac{k}{2} \rceil} \binom{n-1}{\lfloor \frac{k}{2} \rfloor} \\ &= \frac{1}{n!} \frac{k!}{\lfloor \frac{k}{2} \rfloor!} \frac{(2n-k-1)!}{(n-1-\lfloor \frac{k}{2} \rfloor)!} (-1)^{\lfloor \frac{k}{2} \rfloor} \end{aligned}$$

Hence

$$\begin{aligned}
 W(\mathbf{p}, z) &= \sum_{\substack{0 \leq k \leq 2n-1 \\ 0 \leq k \leq 2n-1}} 2^{1-n} z^n s_{[2n-k, 1^k]} \frac{(2n-k-1)!}{(n-1 - \lfloor \frac{k}{2} \rfloor)!} (-1)^{\lfloor \frac{k}{2} \rfloor} \\
 &= M(\mathbf{p}, z)
 \end{aligned}$$

This completes the proof of Walsh's formula using the algebraic method.

3.4 Summary

The algebraic method was briefly described, in order to indicate the origins of the Quadrangulation Conjecture and the Map-Jack Conjecture and to define the latter. A new application of the algebraic method was given, reproving a result of Walsh.

Chapter 4

Depth First Search

Depth first search is an essential tool in the description of the bijections $\tilde{\Xi}$ and Θ , and the parameter η . By imposing some canonical structures, depth first search on the matching graphs of rooted maps provides a starting point for the later constructions. Utilising depth first search, we introduce the following canonical structures associated with rooted maps: a canonical position labelling (§4.1), a canonical ordered digraph (§4.2) structure, a canonical edge classification (§4.3), and a canonical representation as an edge diagram (§4.4). Examples of each of these canonical structures for three different rooted maps are given at the end of this chapter in Table 4.1.

The construction of the bijection $\tilde{\Xi}$ of Chapter 5 employs both the canonical edge classifications and the canonical edge diagram representation. The construction of the parameter η of Chapter 7 is defined by a composition: first the canonical ordered digraph structure is required, followed by an evaluation of the parameter β of Chapter 6. The canonical edge diagram representation of rooted

maps is employed again in Chapter 8 in a bijective proof of a continued fraction result concerning numbers of rooted maps of without regard to genus.

According to Chapter 2, a rooted map has many different but isomorphic representations $(X, \mu_1, \mu_2, \mu_3, r)$, and should itself be regarded as the collection of all these representations. Until this chapter, we have not described a means choosing one of these representations as canonical. Such a unique and natural canonical representation expands (as we shall see) the possibilities for decompositions of rooted maps. Indeed, as will be seen in Chapters 5, 7 and 8, the canonical structures of this chapter assist in the interpretation of some previously uninterpreted enumerative results.

In particular, the canonical representation and other related canonical structures described in this chapter, may be applied to yield progress on some enumerative results formerly requiring powerful algebraic techniques. Firstly, in the original development of Conjectures 1.1 and 1.2, rooted maps were represented in a special but not unique form, namely $(X, \mu_1, \mu_2, \mu_3, r)$ with $X = \{1^-, 1^+, \dots, 2n^-, 2n^+\}$, $\mu_1 = (1^-, 1^+) \dots (2n^-, 2n^+)$, $\mu_3 = (1^-, 2^+)(1^+, 2^-) \dots$ and $r = 1^-$. There is therefore the potential consequence that even if the algebraic steps could be converted into combinatorial steps, these steps may depend on the particular representative of the rooted map. By providing canonical representations, this chapter contributes some progress on these two conjectures. Secondly, the continued fractions result of [AB97] for rooted maps uses an edge deletion decomposition for rooted maps. One step in the proof is an iterative algebraic solution of a Riccati equation, and it is this step that lacked a combina-

torial interpretation. With the canonical representations of this chapter, however, a fully combinatorial interpretation can be obtained. This is presented in Chapter 8.

It will be seen that if a certain depth first search is performed on the matchings graph of a rooted map, according to the rules of Algorithm 4.1, then the order in which the search visits the positions provides a unique canonical representation $(X, \mu_1, \mu_2, \mu_3, r)$ of the rooted map. Once a unique representation is chosen, rooted maps can be manipulated with greater ease. Element-wise actions upon rooted maps, and special properties of rooted maps, may be defined in terms of the unique representation. This more exact level of detail facilitates the precise description of complicated operations upon rooted maps.

Precise and complicated operations of this sort on rooted maps are required for expressing algorithmically the desired properties of the constructions Ξ and ϑ of Conjectures 1.1 and 1.2. By careful examination of the associated enumerative results, it can be concluded that both constructions depend on the rooting of the map, so different rootings of the same map may give different results. In addition, by their definitions, η , Θ and $\tilde{\Xi}$ are necessarily (through depth first search) root dependent operations.

Lehman's integer-parenthesis system [Wal71], as a canonical representation of rooted maps, resembles the edge diagram. In this thesis, an extension of a structure equivalent to integer-parenthesis systems (namely orientable edge diagrams) are applied for enumerative and constructive purposes. Walsh, in his thesis [Wal71], applies integer-parenthesis systems to obtain enumerative re-

sults about orientable rooted maps, so Walsh's association between orientable rooted maps and integer-parenthesis systems is analogous to the depth first search method. However, here we extend the use of depth first search to non-orientable rooted maps. Moreover, the applications to η , $\tilde{\Xi}$ and Θ , constitute a new use of depth first search.

4.1 The Canonical Position Labelling Algorithm

The following algorithm describes a canonical labelling $\ell_m : X \rightarrow \mathcal{N}_{|X|}$ of the position set of an arbitrary locally orientable, rooted map $m = (X, \mu_1, \mu_2, \mu_3, r)$.

Algorithm 4.1 (Canonical Position Labelling). *Let $m = (X, \mu_1, \mu_2, \mu_3, r)$ be a rooted map.*

1. Let $j := 1$ and $x := r$.
2. Let $x_j = x$.
3. Let $k := 1$.
4. If $\mu_k(x) \notin \{x_1, \dots, x_j\}$ then let $\text{Parent}(\mu_k(x)) = x$, $x := \mu_k(x)$, $j := j + 1$ and goto Step 2.
5. Let $k := k + 1$. If $k \leq 3$ then goto Step 4.
6. If $x \neq r$ then let $x := \text{Parent}(x)$ and goto Step 3.
7. Halt.

Let $\ell_m : x_j \mapsto j$. Then $\ell_m : X \rightarrow \mathcal{N}_{|X|}$, is the canonical position labelling of m .

An example of the execution of the algorithm upon a rooted map is given in §4.1.1. The example is general enough in the sense that the algorithm uses all of its steps, and all three values of k .

Since Algorithm 4.1 finds a unique position labelling, these labels can be used to define a unique representation $(X, \mu_1, \mu_2, \mu_3, r)$ for each rooted map:

Definition 4.1. *A rooted map $m = (\mathcal{N}_{4n}, \mu_1, \mu_2, \mu_3, 1)$ is canonical if $\ell_m(i) = i$ for all $1 \leq i \leq 4n$.*

Besides having $X = \mathcal{N}_{4n}$ and $r = 1$, a canonical map has special forms for the matchings μ_1, μ_2 and μ_3 . These forms are successively less restricted in a sense that will be seen in §4.1.2.

Algorithm 4.1 is one of the simplest ways to assign position labels canonically to a rooted map. Clearly, the method is depth first search on the matchings graph since elements accessible from the active position x are searched exhaustively before backtracking. Clearly, the method is greedy, searching with μ_1, μ_2 , and μ_3 in that order. Moreover, as discussed in §4.1.3, Algorithm 4.1 is an instance of Prim's algorithm.

4.1.1 Example of the execution of Algorithm 4.1

Consider the planar rooted map in the second column of Table 4.1(a) on page 93, as redrawn in Figure 4.1. We intend to explain how to obtain the canonical positional labelling of Table 4.1(b). The tail of the arrow in Figure 4.1 indicates the root position of this map. The root position is the starting point for the algorithm, and is assigned the label 1 in Figure 4.2.

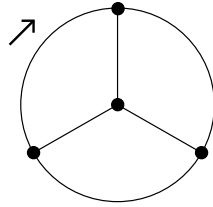
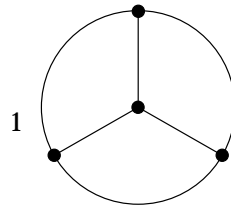
Figure 4.1: A planar rooted embedding of the complete graph K_4 

Figure 4.2: The algorithm begins at the root position

Consider the three positions adjacent to 1 in the matchings graph. These positions are $\mu_1(1)$, $\mu_2(1)$ and $\mu_3(1)$. To this point, all these positions are new in the execution of the algorithm. Thus, the algorithm next visits the first of these positions, namely $\mu_1(1)$, as in Figure 4.3.

Once a position is labelled with a 2, the positions $\mu_1(2)$, $\mu_2(2)$ and $\mu_3(2)$ are considered in order. It is found that the position $\mu_1(2)$ has already been labelled with a 1. The next position to consider is $\mu_2(2)$. This position has not been labelled, and therefore, according to the algorithm, it is labelled with a 3, as in Figure 4.4.

Continuing in this fashion, labels 4, 5, and 6 are added, alternating between μ_1 and μ_2 , as in Figure 4.5. After label 6 has been assigned, $\mu_1(6) = 1$ and $\mu_2(6) = 5$.

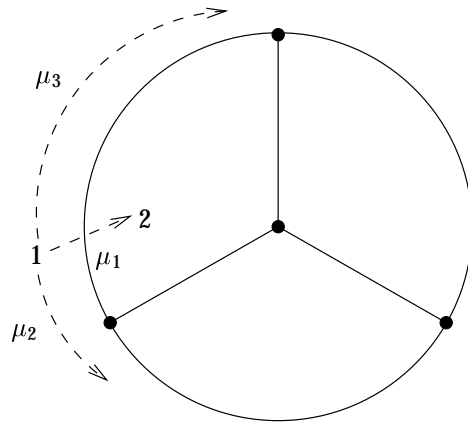


Figure 4.3: The algorithm moves along μ_1 first

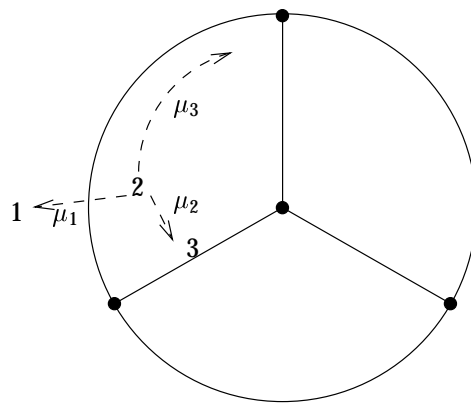


Figure 4.4: If $\mu_1(x)$ has been labelled, look at $\mu_2(x)$

Thus $\mu_3(6)$ is the only adjacent position to 6 that is not yet labelled, and therefore it receives the next label, 7, as in Figure 4.5.

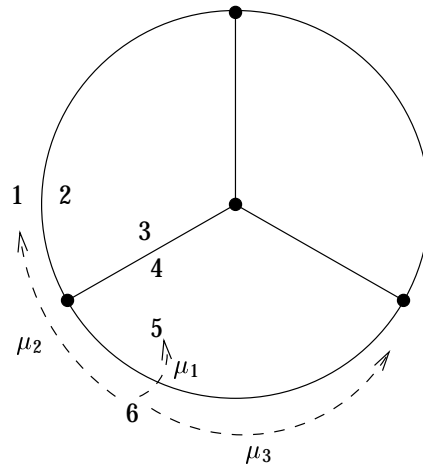


Figure 4.5: First instance that μ_3 is used

Continue assigning labels to the positions around the vertex where label 7 is located. Thus, labels 1,...,12 will be used and the result is shown in Figure 4.6(a). For convenience, in this example we replace these numerals by a, b, c, d, \dots, k, l , in alphabetical order, in Figure 4.6(b) (since there are only 24 positions in this map, we shall not run out letters).

Proceed in the same fashion, assigning letters to positions of the third vertex the algorithm visits, by taking μ_3 from position l . The first letter assigned will be m , followed by n, o, p, q, r . This is shown in Figure 4.7.

Observe that all three positions adjacent to r have been assigned labels: a, m and q . Thus backtrack to q , and check if there are any positions adjacent to q , which have not been assigned a label yet. In this case there are no such positions,

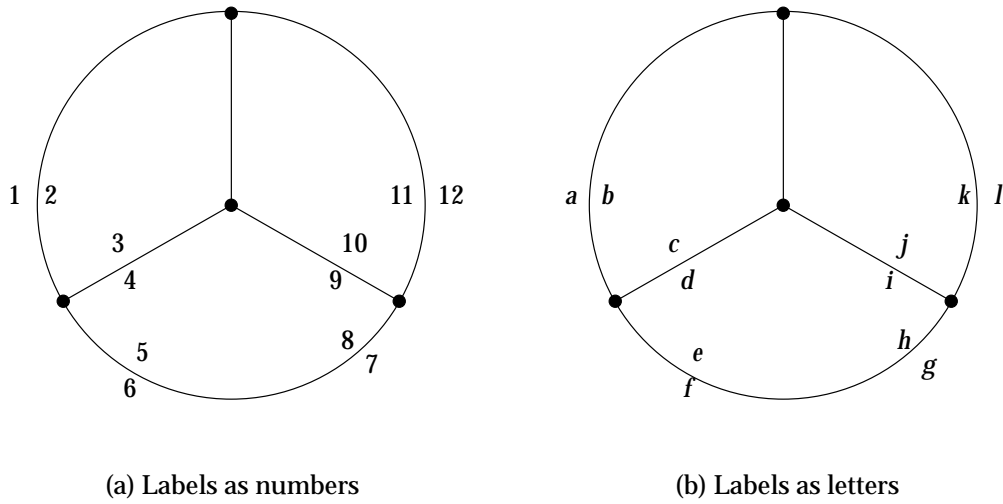


Figure 4.6: Use letters instead of number for labels

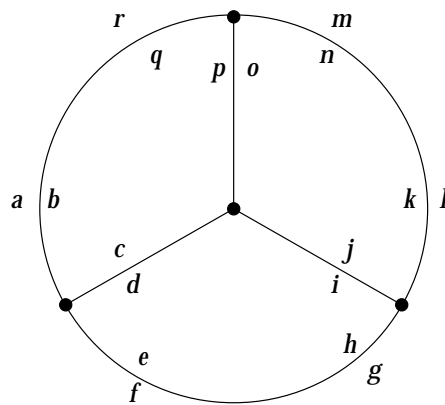


Figure 4.7: Assignment of labels m, n, o, p, q and r

because the neighbouring positions of q have already been labelled with b , p and r . Therefore, the algorithm backtracks further, to p .

In Figure 4.7, $\mu_3(p)$ has not yet been assigned a label. The next available label is s , so $s := \mu_3(p)$, as in Figure 4.8.

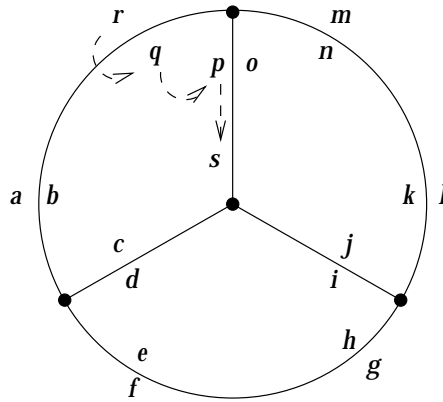


Figure 4.8: Assign label s , by backtracking from r to p .

The algorithm terminates with this map by adding labels t, u, v, w, x around the vertex where s is located, and then backtracking all the way from x to a . At a (the root position) no further backtracking is possible, so the algorithm halts.

The trace of the algorithm is indicated by the curve in Figure 4.9. Such curves can in general be drawn to trace the algorithm, without intersecting themselves.

4.1.2 Properties of Canonical Position Labellings

Let $\varepsilon_N = (1, 2)(3, 4) \cdots (2N - 1, 2N)$ and $\varepsilon_a^b = (2a + 2, 2a + 3)(2a + 4, 2a + 5) \cdots (2a + 2b, 2a + 1)$, permutations which are products of transpositions.

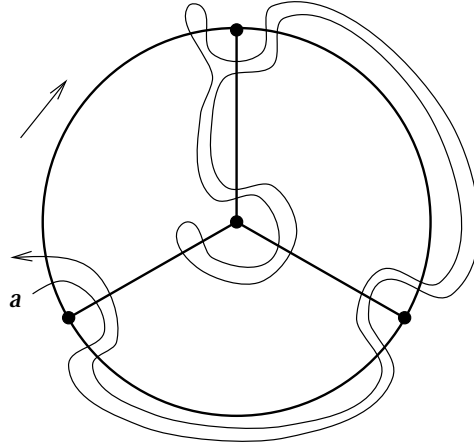


Figure 4.9: The trace of the algorithm around the rooted map

For a canonical rooted map m :

$$\mu_1 = \varepsilon_{2n} = (1, 2)(3, 4)(5, 6) \dots (4n - 1, 4n).$$

The interpretation of this is that canonical position labels at the same end of an edge are consecutive, with the odd label less than the even label.

Now, μ_2 has the form

$$\begin{aligned} \mu_2 &= \varepsilon_0^{k_1} \varepsilon_{k_1}^{k_2} \varepsilon_{k_1+k_2}^{k_3} \dots \varepsilon_{k_1+k_2+\dots+k_{v-1}}^{k_v} \\ &= \underbrace{(2, 3)(4, 5) \dots (2k_1, 1)}_{\text{first vertex}} \underbrace{(2k_1 + 2, 2k_1 + 3) \dots (2k_1 + 2k_2, 2k_1 + 1)}_{\text{second vertex}} \dots \end{aligned}$$

where v is the number of vertices of the rooted map m . The k_i are the degrees of the vertices in the order they are encountered by the algorithm. The matching μ_2 has this property because the algorithm cycles once around each vertex,

assigning a set of consecutive labels $[a, b] \cap \mathbb{N}$ to the set of positions at that vertex.

Consider the first position that Algorithm 4.1 encounters at each vertex. The parent of this position will have a smaller label, and these two will be paired by μ_3 . Therefore, for $i \geq 1$:

$$\mu_3(2k_1 + 2k_2 + \cdots + 2k_i + 1) = h_i$$

for some $h_i < 2k_1 + 2k_2 + \cdots + 2k_i + 1$. Moreover, if

$$h_i < j < 2k_1 + \cdots + 2k_i + 1 \tag{4.1}$$

then $\mu_3(j) < 2k_1 + \cdots + 2k_i + 1$, because at position j the algorithm continued backtracking to h_i before finding a position with an unlabelled neighbour.

4.1.3 Relationship to Prim's Algorithm

Let $|X| = 2m$. Let $m = (X, \mu_1, \mu_2, \mu_3, r)$ be a rooted map. Then the canonical position labelling ℓ_m of m is characterised as the unique bijection $\ell_m = \ell : X \rightarrow \mathcal{N}_{2m}$ satisfying:

1. $\ell(r) = 1$,
2. For $L = 1, \dots, 2m - 1$, let x_i be such that $\ell(x_i) = i$ for $1 \leq i \leq L$, then amongst all pairs (j, k) satisfying:
 - (a) $1 \leq j \leq L$,
 - (b) $1 \leq k \leq 3$, and

(c) $\mu_k(x_j) \notin \{x_1, \dots, x_L\}$,

there is a pair $(j, k) = (j', k')$ which

(d) maximises the value of j ,

(e) minimises the value of k , and

(f) satisfies $\ell(\mu_k(x_j)) = L + 1$.

The canonical position labelling algorithm is a *depth first search* on the matchings graph of $\Gamma = \Gamma(m)$ of a rooted map m . Because of 2(e) above, it is also a special case of Prim's algorithm acting on the matchings graph, for finding a minimum-weight spanning tree of an edge-weighted version of the matchings graph where edges associated with μ_i are given weight i .

4.2 Canonical Ordered Digraphs

Definition 4.2. An ordered digraph \mathfrak{d} with n edges is a map (X, μ_1, μ_2, μ_3) , together with the following additional information:

1. each edge is assigned a direction,
2. each edge is assigned a label from \mathcal{N}_n ,
3. each vertex is assigned a cyclic orientation.

The map $m = (X, \mu_1, \mu_2, \mu_3)$ is the *underlying map* of the ordered digraph \mathfrak{d} above. For a rephrasing of the definition of ordered digraphs, in terms of matchings, see Proposition 4.1.

Algorithm 4.2 (Canonical Ordered Digraph). Let $\mathfrak{m} = (X, \mu_1, \mu_2, \mu_3, r)$ be a rooted map. Its canonical ordered digraph $\mathfrak{d} = \delta(\mathfrak{m})$ is determined by its canonical labelling $\ell_{\mathfrak{m}}$ as the unique ordered digraph satisfying the following conditions.

1. \mathfrak{d} has the underlying map (X, μ_1, μ_2, μ_3) .
2. Each edge e of \mathfrak{m} has a pair of positions at one end with higher labels under $\ell_{\mathfrak{m}}$ than at the other end. In \mathfrak{d} , make the higher end of e its head, and its lower end the tail.
3. Each edge e has four positions, one of which maximises the value of the labelling $\ell_{\mathfrak{m}}$ over e . Use these maxima to sort the edges in \mathfrak{d} , i.e. the edge with the lowest maximum becomes e_1 and the edge with the highest maximum becomes e_n .
4. To determine the cyclic orientation of a vertex v , recall that the set of labels under $\ell_{\mathfrak{m}}$ assigned to the positions at each vertex v is a set of the form $[a, b] \cap \mathbb{N}$. Then
 - If v has degree greater than one, the cycle in the matchings graph $\Gamma(\mathfrak{m})$ can be given a cyclic orientation by starting at the $\ell_{\mathfrak{m}}$ -minimiser, and in the direction of the next lowest, around the associated cycle of $\Gamma(\mathfrak{m})$.
 - Otherwise, if v has degree one, then the cycle associated with v in $\Gamma(\mathfrak{m})$ has two edges, one associated with μ_1 and one associated with μ_2 . Direct the μ_1 edge, from the lower position to the higher position, and the μ_2 edge in the opposite direction.

Chapter 7 uses δ to define the candidate Map-Jack parameter η .

4.2.1 Example of a canonical ordered digraph

Consider once again the rooted planar embedding of the complete graph K_4 on four vertices, together with its (alphabetical) canonical position labelling in Figure 4.10.

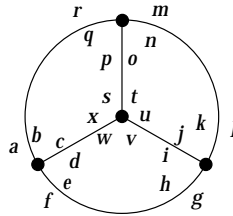


Figure 4.10: Canonical position labelling of a planar K_4 embedding (alphabetical form)

The edges sorted by their highest position label are $\{e, f, g, h\}, \dots, \{c, d, w, x\}$, so the assignments of the labels in $\{e_1, \dots, e_6\}$ to these are

$$\begin{aligned} e_1 &\leftarrow \{e, f, g, h\}, & e_2 &\leftarrow \{k, l, m, n\}, & e_3 &\leftarrow \{a, b, q, r\}, \\ e_4 &\leftarrow \{o, p, s, t\}, & e_5 &\leftarrow \{i, j, u, v\}, & e_6 &\leftarrow \{c, d, w, x\}. \end{aligned}$$

This determines how each edge is to be assigned a label from \mathcal{N}_6 .

As an example of the determination of edge directions, consider e_3 . The tail of e_3 is to contain the lower positions $\{a, b\}$, and the head the higher positions $\{q, r\}$. Thus e_3 is directed towards $\{q, r\}$.

The vertices have sets of canonical position labels

$$\{a, b, c, d, e, f\}, \{g, h, i, j, k, l\}, \{m, n, o, p, q, r\}, \{s, t, u, v, w, x\}.$$

These determine cyclic orientations of the four vertices. All four cyclic orientations are clockwise in this instance. The resulting canonical ordered digraph

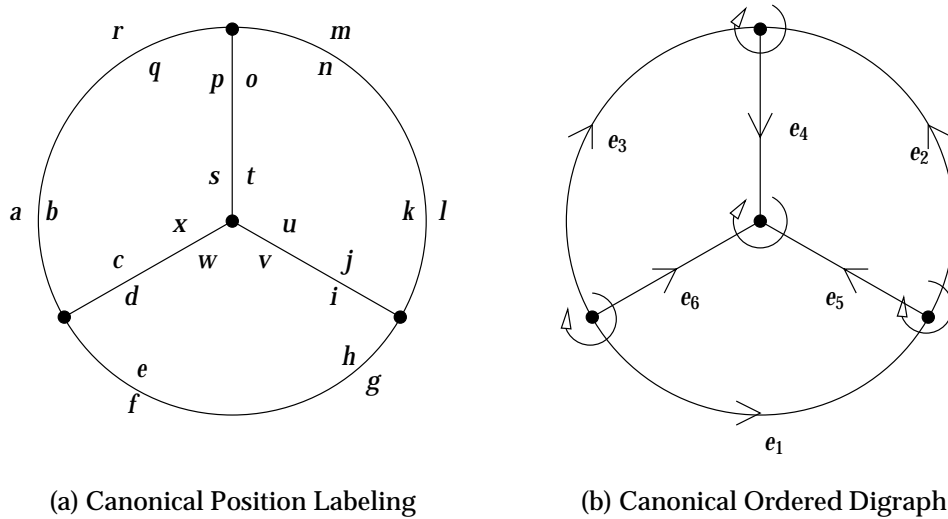


Figure 4.11: Canonical ordered digraph structure

structure is given in Figure 4.11(b).

4.2.2 An equivalent formulation in terms of triples

The definition of an ordered digraph (X, μ_1, μ_2, μ_3) may be rephrased in terms of conditions on the matchings and the set of positions X , in such a way that the additional information required for an ordered digraph is contained within (X, μ_1, μ_2, μ_3) . The set of positions is to have the form $X = \mathcal{N}_n \times \{-1, 1\} \times \{-1, 1\}$. Then, the extra information is to be interpreted as follows:

- The two positions $(i, -1, -1)$ and $(i, -1, +1)$, are the positions at the tail of the directed edge e_i .

- The two positions $(i, +1, -1)$ and $(i, +1, +1)$, are the positions at the head of the directed edge e_i .
- At a given vertex v of an ordered digraph \mathfrak{d} , the positions around v may be arranged (i_m, j_m, k_m) , in the cyclic order according to the structure of \mathfrak{d} , and will satisfy $i_{2m-1} = i_{2m}$, $j_{2m-1} = j_{2m}$ and $k_{2m-1} = -1$ and $k_{2m} = +1$.

Thus:

Proposition 4.1. *A map (X, μ_1, μ_2, μ_3) is an ordered digraph if $X = \mathcal{N}_n \times \{-1, 1\} \times \{-1, 1\}$ and:*

1. $\mu_1 : (i, j, k) \mapsto (i', j', k') \Rightarrow i' = i, j' = j, k' = -k,$
2. $\mu_2 : (i, j, k) \mapsto (i', j', k') \Rightarrow k' = -k,$
3. $\mu_3 : (i, j, k) \mapsto (i', j', k') \Rightarrow i' = i, j' = -j.$

for all $(i, j, k), (i', j', k') \in X$.

Proof. This is just a re-statement of Definition 4.2. □

Figure 4.12 gives an example by means of triples description of the positions of an ordered digraph in the Klein bottle. With this description, it is possible to define the notion of an edge e_i preserving or reversing the cyclic orientations at its ends, as follows

- Edge e_i *preserves* local cyclical orientations if $\mu_3 : (i, -1, -1) \mapsto (i, +1, +1)$.
- Edge e_i *reverses* local cyclical orientations if $\mu_3 : (i, -1, -1) \mapsto (i, +1, -1)$.

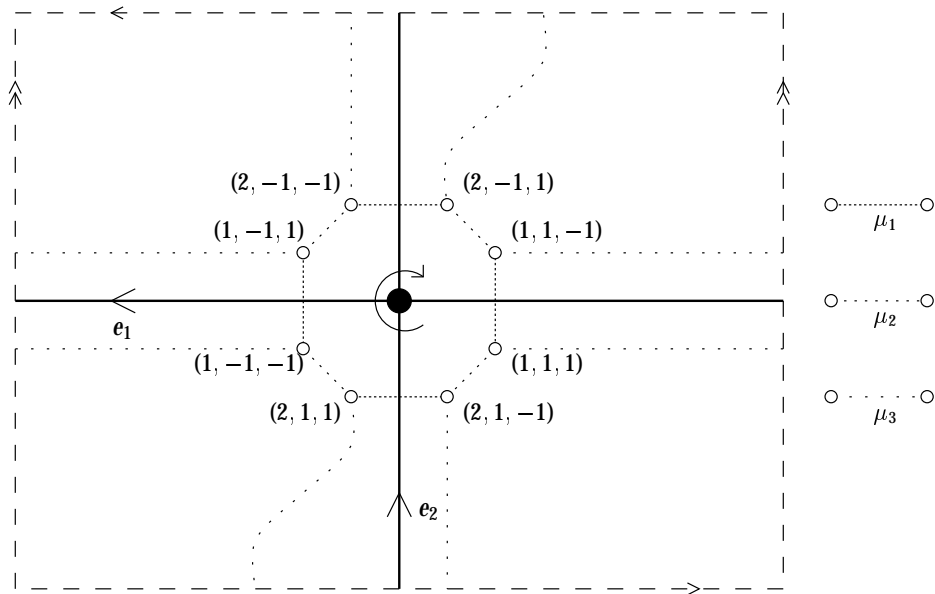


Figure 4.12: Formal position descriptions in an ordered digraph in the Klein bottle

An ordered digraph is *oriented* if all its edges preserve cyclic orientations. An ordered digraph \mathfrak{d} is *orientable* if the k -values alone can be changed so the digraph becomes oriented. An ordered digraph is orientable if and only if the surface its map is embedded in is orientable. In the digraph \mathfrak{d} of Figure 4.12, the edge e_2 reverses local cyclic orientation of \mathfrak{d} , while e_1 preserves local cyclic orientation.

Algorithm 4.2 may be rephrased as follows for ordered digraphs of Proposition 4.1.

Algorithm 4.3 (Canonical Ordered Digraph, II). *Given a rooted map $\mathfrak{m} = (X, \mu_1, \mu_2, \mu_3, r)$ with n edges, the canonical ordered digraph $\mathfrak{d} = \delta(\mathfrak{m})$ of \mathfrak{m} is computed as follows:*

1. Let $Y = \mathcal{N}_n \times \{-1, 1\} \times \{-1, 1\}$.
2. Execute Algorithm 4.1 to compute $\ell_{\mathfrak{m}}$.
3. Assume without loss of generality that \mathfrak{m} is canonical. In particular, assume that $X = \mathcal{N}_{4n}$.
4. Let e_i be the edge of X containing position $a_i < b_i < c_i < d_i$, such that $d_1 < d_2 < d_3 < \cdots < d_n$.

5. Let $\varphi : X \rightarrow Y$ be the bijection such that

$$\varphi(\mathbf{x}) = \begin{cases} (i, -1, -1) & \text{if } \mathbf{x} = a_i \\ (i, -1, 1) & \text{if } \mathbf{x} = b_i \\ (i, 1, -1) & \text{if } \mathbf{x} = c_i \\ (i, 1, 1) & \text{if } \mathbf{x} = d_i \end{cases}$$

6. Let $\nu_k = \varphi \circ \mu_k \circ \varphi^{-1}$.

Then

$$\mathfrak{d} = \delta(\mathfrak{m}) = (Y, \nu_1, \nu_2, \nu_3).$$

is the canonical ordered digraph of \mathfrak{m} .

4.3 Canonical Spanning Trees, Struts and Cuts

Most often, the occurrences of Step 4 of Algorithm 4.1 in which the re-assignment $x := \mu_k(x)$ is made, the value of k is 1 or 2, because these values are considered before the value $k = 3$. In fact, $k = 3$ for $v - 1$ of these re-assignments, because one such re-assignment $x := \mu_3(x)$ is needed each time the algorithm visits a new vertex (excluding the root vertex).

When this happens, we say that the edge of \mathfrak{m} containing the positions x and $\mu_3(x)$ has been *traversed* by Algorithm 4.1. The set of the traversed edges of the

rooted map m form a spanning subtree of the underlying graph of m . (Not the matchings graph.) This tree is the *canonical spanning subtree* of m . Its edges are called *canonical tree edges*.

For example, consider the rooted planar map of Figure 4.13, which is an embedding of the complete graph K_4 on four vertices. All the canonical position

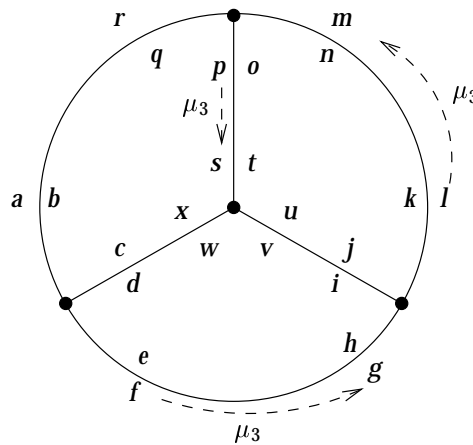


Figure 4.13: The traversed edges of a planar embedding of K_4

labels are indicated. The letters a, b, c, d, \dots indicate the order. Note that Algorithm 4.1 uses μ_3 to move to a new vertex in exactly three instances: $f \rightarrow g, l \rightarrow m$ and $p \rightarrow s$. (In the last case, the algorithm backtracks from r , explaining why s is not the immediate successor to p). Hence the canonical spanning subtree is indicated by the solid edges of Figure 4.14. Note that the canonical spanning subtree of m is also a depth first search tree.

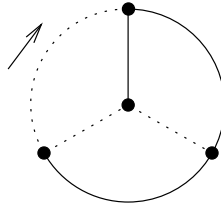


Figure 4.14: The canonical spanning subtree

4.3.1 Struts and Cuts

Recall that depth first search has been used to classify edges canonically into tree edges and non-tree edges. Later, in the construction of the bijection $\tilde{\Xi}$, we shall need a more refined classification, one which separates non-tree edges into *cuts* and *struts*. We now provide such a classification.

Algorithm 4.4 (Cuts and Struts). *Let m be a rooted map with n edges. Let $\mathfrak{d} = \delta(m)$ be its canonical ordered digraph. Determine the canonical tree edges of m . Then*

1. *Let $i := n$ and $\mathfrak{b} := m$.*
2. *If e_i is*
 - *not a canonical tree edge, and*
 - *bounds two distinct faces,*

then let $e_i \in C_m$ and let $\mathfrak{b} := \mathfrak{b} - e_i$.

3. *Let $i := i - 1$. If $i > 0$, goto Step 2.*

Then

- the edges in C_m are the cuts of m .
- the terminal value of the submap \flat is the backbone of m ,
- the edges of \flat which are not canonical tree edges are the struts of m .

There are $V - 1$ tree edges. Because each time a cut is removed from \flat the number of faces is reduced by one, there are $F - 1$ cuts. Therefore there are $2 - \chi$ struts. For orientable maps, $\chi = 2 - 2g$, so the number of struts is $2g$.

4.3.2 Example of the determination of cuts and struts

To explain the definitions of struts and cuts let us refer to a running example involving the rooted map m , which is an embedding of K_5 in the torus. The map m is given in Figure 4.15.

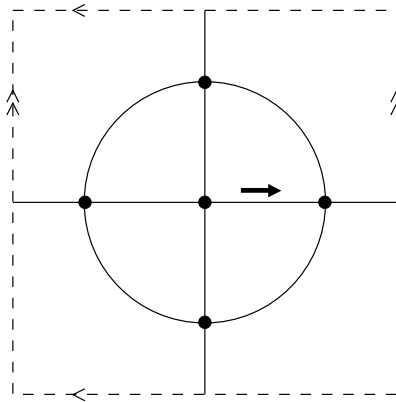


Figure 4.15: The rooted map m , an embedding of K_5 in the torus

First, perform Algorithm 4.1 on the positions of the map m , as in Figure 4.16, where, to avoid clutter, the letters a, A, b, B, \dots rather than numbers have been

assigned to the positions. Recall that edges have a canonical order, based on

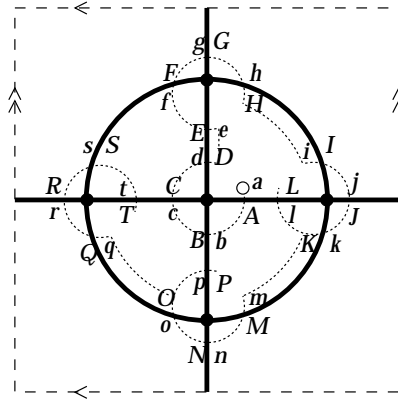


Figure 4.16: The canonical labelling from depth first search

the order of the highest letter (position) on each edge. For m , this edge order is illustrated in Figure 4.17 by the symbols e_1, e_2, \dots, e_{10} in increasing order of the subscripts. Edge order plays a prominent role in distinguishing struts from cuts.

As before, certain edges are canonical tree edges and these form a canonical spanning subtree of the underlying graph K_5 . In m , the tree edges e_1, e_2, e_4, e_7 , and are shown with thickened line segments in Figure 4.17.

The non-tree edges of m in descending order are $e_{10}, e_9, e_8, e_6, e_5, e_3$. To test which of these are struts and which are cuts, conditionally delete them in succession by descending order. Delete an edge only if it separates two distinct faces. The edges that are deleted in this process are the *cuts*. The edges that are not deleted are the *struts*. The result of this conditional deletion process is, in general, a submap of m , that

- consists of only the tree edges and struts,

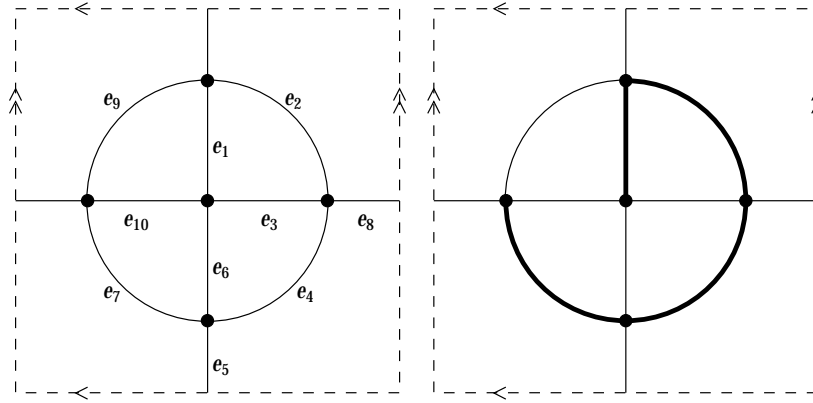


Figure 4.17: The canonical order of edges and the canonical tree edges

- has only one face, and
- has the same surface structure as m .

This submap is called the *backbone* of the rooted map m .

Figure 4.18(a) shows that e_{10} separates two distinct faces in m . Therefore, delete e_{10} from m . Figure 4.18(b) shows that e_9 separates two distinct faces in $m - e_{10}$. Therefore, delete e_9 too. Thus e_{10} and e_9 are *cuts*.

In $m - \{e_{10}, e_9\}$, the next edge to test, e_8 , does not separate two faces. Therefore e_8 is a strut. It is not deleted by the process. To emphasise that e_8 is a strut, it is now drawn with a double line, as in Figure 4.19(a). The next non-tree edge is e_6 which is another cut, Figure 4.19(b). Finally, e_5 is a strut and e_3 is a cut, for reasons similar to the previous.

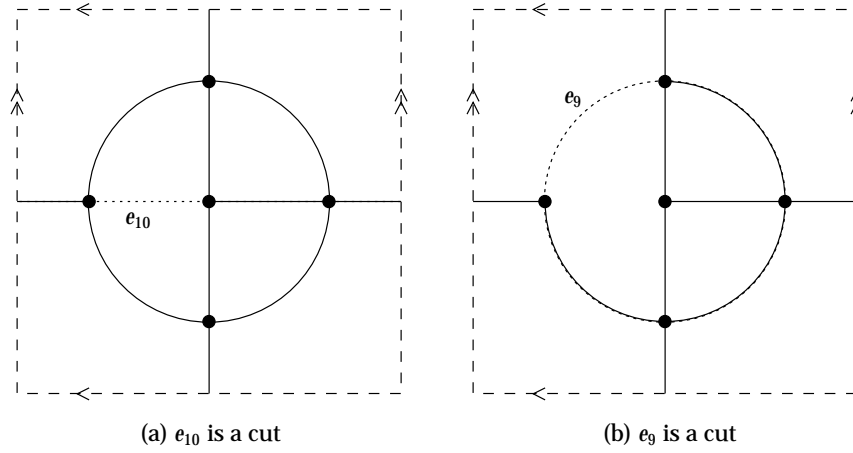


Figure 4.18: The first two cuts to be tested

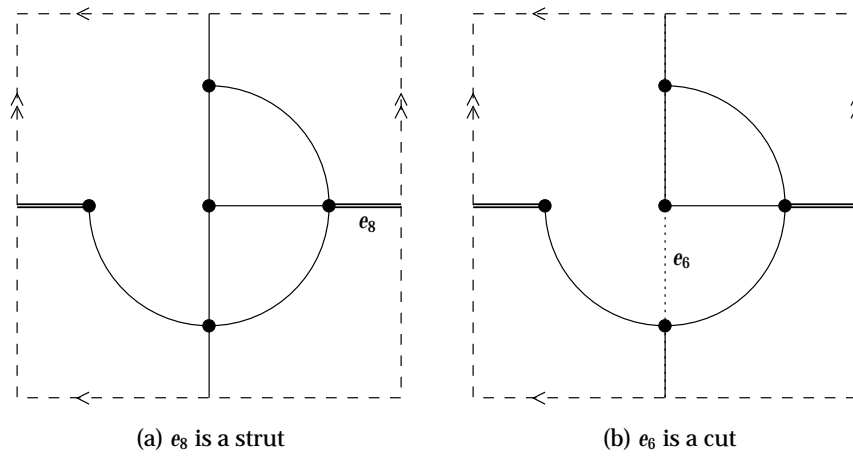


Figure 4.19: The next two non-tree edges, a strut and a cut

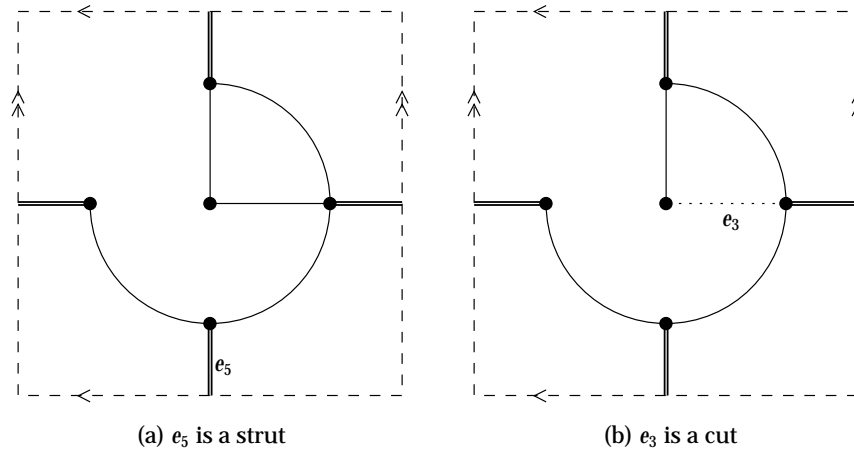


Figure 4.20: Another strut and another cut

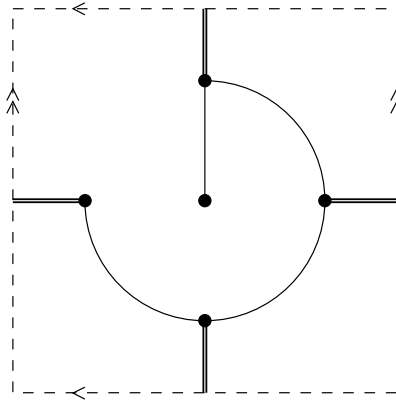
4.3.3 Associating Cuts with Non-root Faces

Recall that the backbone of a rooted map consists of the canonical tree edges and the struts (and all the vertices). In the specific example, the backbone consists of the edges $\{e_1, e_2, e_4, e_5, e_7, e_8\}$. The remaining edges are cuts.

Form submaps m_i of m by taking the backbone to be m_1 and successively adding the cuts, in *ascending* order. The resulting maps are $m_1, m_2, \dots, m_F = m$, where m has F faces. Then m_i in this sequence has i faces.

As each cut is added, it cuts an existing face into two faces. One of these faces will be considered the *new* face, in a manner to be described shortly. This new face will become associated with the cut.

Of course, subsequently, the face of m_{i+1} that is associated with the i^{th} cut, may itself be divided into faces by later cuts. Nevertheless, the association remains between the original cut, and whatever remains after new faces are cut off the

Figure 4.21: The backbone of the rooted embedding of K_5

face associated with the original cut.

The root face is treated differently. In each submap m_i , the root face R_i is the face that would have contained the root position. Note that R_i is not associated with any cuts. The root face R_i is cut into two faces, R_{i+1} and S_{i+1} . When the next cut is added to m_i to form m_{i+1} , the root face R_{i+1} has fewer edges than R_i , and the face S_{i+1} is associated with the cut just added.

With the example, $m_2 = m_1 + e_3$, the backbone with e_3 (the lowest cut) added, as in Figure 4.22. Here, e_3 cuts the root face of m_1 into two faces. Since the root position of m actually lies on e_3 itself, it is straightforward to see which of the two faces in e_3 is the non-root face. To indicate that the cut e_3 is associated with the non-root face of m_2 , an arrow is drawn in Figure 4.22, extending from one side of e_3 into the face with which it is associated.

The next cut, e_6 , cuts the face of m_2 associated with e_3 . In m_3 one of these two resulting faces is incident with e_3 and the other not. The other face is the *new*

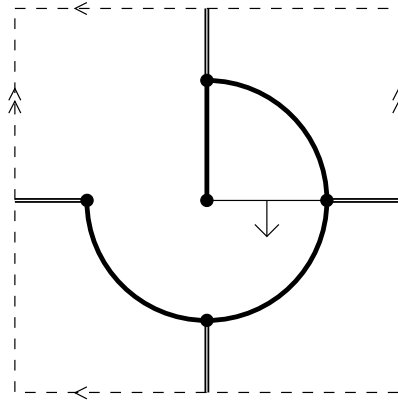


Figure 4.22: The submap m_2 , with association of e_3 to the non-root face

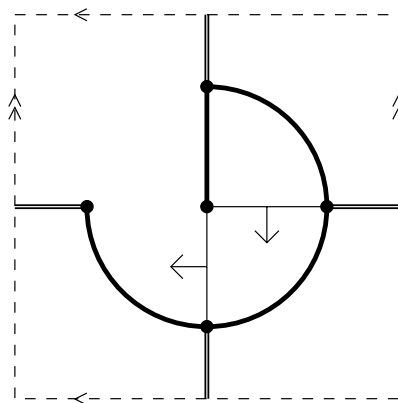


Figure 4.23: The submap m_3 , with the association of e_6 to the new non-root face

face. It is not a root face, and is not associated with any cuts. Therefore associate it with the cut e_6 . This is indicated in Figure 4.23, with an arrow on the side of e_6 .

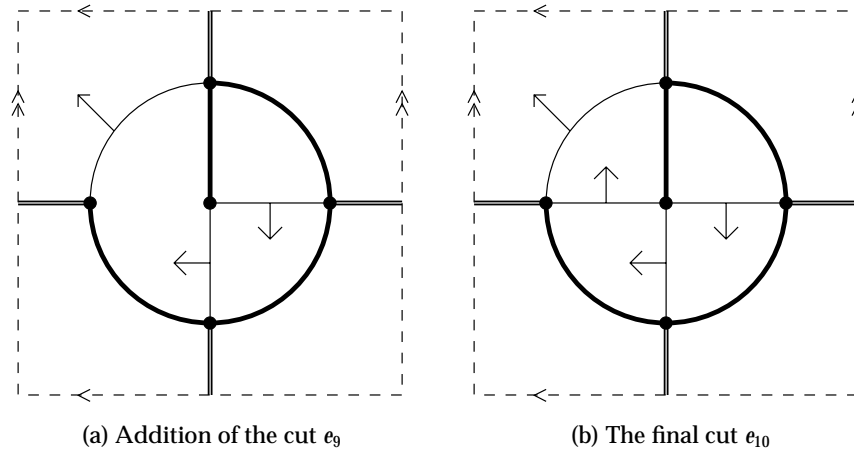


Figure 4.24: The cuts e_9 and e_{10} and associated faces

The next two cuts, e_9 and e_{10} , also cut non-root faces, so are treated similarly to e_6 . See Figure 4.24(a) for e_9 and Figure 4.24(b) for e_{10} .

4.4 Edge Diagrams and Integer-Parenthesis Systems

The canonical position labelling algorithm sorts the positions of a rooted map into linear order. The edge diagram is a *linearisation* of a rooted map, in the sense that the positions are ordered linearly on a base line. The edges are drawn as semicircular arcs from the base line to itself. Combinatorially, edge diagrams may be encoded with a single matching, together with some distinguished subsets. The pairs in the matching correspond to arcs (which represent edges) in the edge diagram.

First we introduce the notation for matchings:

Definition 4.3. Let $\mu \in \text{Match}(\mathcal{N}_{2n})$. Let $\mu^+ = \{i \in \mathcal{N}_{2n} : \mu(i) < i\}$.

Thus, μ^+ is the set of upper members of the pairs in μ .

An edge diagram consists of a system of arcs, which may be formalised as a matching μ , together with two sets of specially designated right ends of arcs: V for the vertices (associated tree edges) and T for the edges marked by an “ \times ”.

Definition 4.4. Let n be a non-negative integer. An edge diagram is a quadruple $\epsilon = (n, \mu, V, T)$ satisfying:

1. $\mu \in \text{Match}(\mathcal{N}_{2n})$,
2. $V, T \subseteq \mu^+$,
3. $V \cap T = \emptyset$,
4. If $v \in V$ and $\mu(v) < u < v$ then $\mu(u) < v$.

A quadruple (n, μ, V, T) which only satisfies Conditions 1–3 is an edge configuration.

Considering how we want to form edge diagrams $\epsilon = \epsilon(m)$, it is natural to refer to the pairs of μ (or equally well, the elements of the μ^+) as the *edges* of the edge diagram ϵ . Those edges whose right end contains a vertex (belongs to V) are *vertex-beginner* edges (called tree edges in m). Those edges whose right end bears an “ \times ”, are called *twisted* edges.

The justification for the usage of the term twisted is as follows. Given an edge diagram or configuration ϵ , we can form a topological map as follows. Form

vertices homeomorphic to open disks. Join these by ribbons corresponding to the edges. The rule for twisted edges is that a 180° twist must be introduced to the ribbon before it joins to vertices. The surface is completed by sewing discs to the boundary.

The following is a formal description of an algorithm that determines an edge diagram from a rooted map.

Algorithm 4.5 (Edge Diagram). *Given a rooted map m form its edge diagram $e = \varepsilon(m) = (n, \mu, V, T)$ as follows:*

1. Let $n = n(m)$.
2. Use Algorithm 4.1, to construct a canonical representative $(\mathcal{N}_{4n}, \mu_1, \mu_2, \mu_3, 1)$ of m .
3. For $1 \leq i \leq 2n$, let $\mu(i) = \left\lceil \frac{\mu_3(2i)}{2} \right\rceil$.
4. Let $i \in V$ if and only if $i \in \mu^+$ and $\mu_2(2i - 1) \neq 2i - 2$.
5. Let $i \in T$ if and only if $i \in \mu^+$ and $\mu_3(2i)$ is even.

In §4.4.1 below, examples are given of the application of Algorithm 4.5.

4.4.1 Example formation of an edge diagram

Consider the planar embedding of K_4 again, with its canonical position labelling in Figure 4.25(a). For what follows, it is convenient to replace the alphabetical labels a, b, c, d, \dots by the labels a, A, b, B, \dots , since doing this will cause pairs of

labels common to an end of an edge to differ only in capitalisation. This is done in Figure 4.25(b).

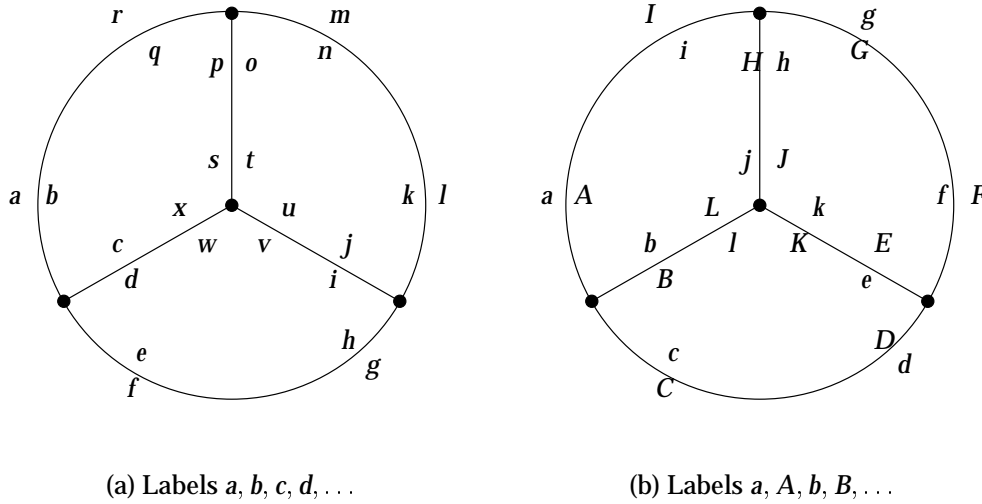
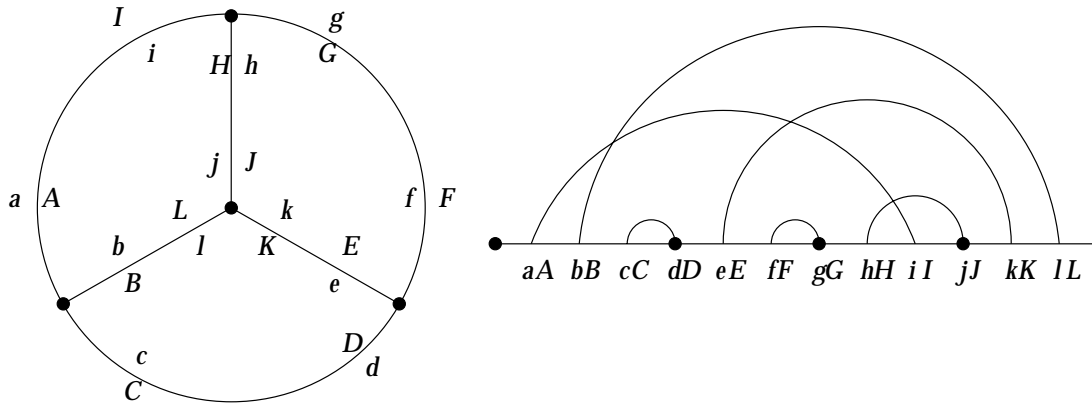


Figure 4.25: A more convenient set of labels

To draw the edge diagram, draw a base line, with the position labels a, A, b, B, \dots beneath. For each edge e_i of m , draw a semicircular arc above the base line which joins two points located above the position labels that the edge e_i contains, as in Figure 4.26(b). Place a vertex (black disc) at the left end of the base line, and at the right end of each tree edge (semicircular arc).

The edge diagram itself does not include the canonical position labels. (These are easily recovered because they appear in order a, A, b, B, \dots)

When the rooted map m is non-orientable such as in Table 4.1 (p. 93), redrawn in Figure 4.27, there is an additional consideration for each edge. Since the m is non-orientable, its matching graph is non-bipartite. This means that μ_3 sometimes pairs even (uppercase capital letter) position labels with even (uppercase



(a) Canonical position labels

(b) Edge diagram with canonical position labels

Figure 4.26: Linearising a rooted map into an *edge diagram*

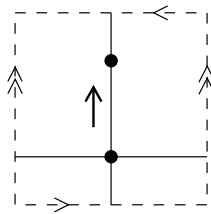


Figure 4.27: A rooted map in the Klein bottle

capital letter) position labels. In this instance we have:

$$\mu_3(A) = F.$$

To mark when this happens, place an “×” at the right end of the corresponding edge (semicircular arc). This is shown in Figure 4.28. Note that this cannot occur

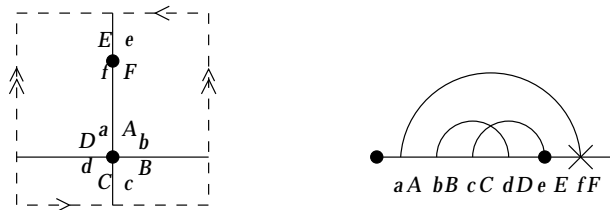


Figure 4.28: Adding an “×” to the edge diagram of a non-orientable map

in a tree edge, so “×” will not be placed on a vertex.

Up to this point it is clear that $\epsilon = \epsilon(m)$ is an edge configuration. That $\epsilon(m)$ is always an edge diagram, is seen in §4.4.2

4.4.2 Forbidden Sub-configurations

A rooted map $m = \rho(\epsilon)$ can be recovered from any edge configuration ϵ , by re-drawing the positions a, A, b, B, \dots and determining μ_1, μ_2 and μ_3 directly from the configuration. However, only edge diagrams are the images of rooted maps under ϵ . The recovery function ρ is an inverse to ϵ on the set of edge diagrams.

Condition 4 of Definition 4.4 is equivalent to the absence of one of the forms in Figure 4.29 as a sub-configuration of the edge diagram. In other words,

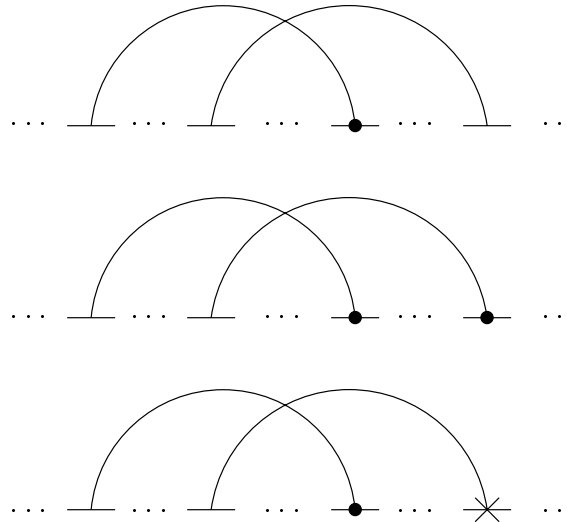


Figure 4.29: Forbidden sub-configurations

an edge diagram is an edge configuration such that no vertex-beginner edge is crossed to the right.

Forbidden sub-configurations provide a combinatorial means for distinguishing edge diagrams from edge configurations. Lemma 4.2 establishes that the function ε defined by Algorithm 4.5, always yields an edge diagram rather than an edge configuration.

Lemma 4.2. *Let m be a rooted map. Then $\varepsilon(m)$ is an edge diagram.*

Proof. It is immediate that $\varepsilon(m)$ is an edge configuration. (Any linear ordering of the ends, not just the canonical one, produces an edge configuration.)

The more substantial task is to show that the depth first search used in the canonical position labelling algorithm implies the absence of the forbidden sub-configurations (Condition 4 of Definition 4.4). Recall that if (4.1) occurs, then it

was concluded that $\mu_3(j) < 2k_1 + \cdots + 2k_l + 1$, by the nature of backtracking in the Algorithm 4.1. When linearised into an edge configuration, this inequality translates to Condition 4 of Definition 4.4. \square

4.4.3 Tracing Faces in an Edge Diagram

The number $n(m)$ of edges and the vertex partition $\nu(m)$ of a rooted map m are read off its edge diagram $\epsilon = \varepsilon(m)$. The number of semicircular arcs of ϵ gives $n(m)$, and the numbers of arc ends following each black disk (vertex) of ϵ gives the vertex degrees of m , which only need to be sorted to give $\nu(m)$.

Edge diagrams are therefore very effective in questions concerning only edges and vertices. However, for questions regarding faces, or surface structure (which requires knowledge of the number of faces), edge diagrams are less effective. Face structure is not as easily determinable from an edge diagram, as edge and vertex structure are. This difficulty in handling the face structure in edge diagrams leads to the primary defect of the bijection $\tilde{\Xi}$ of Chapter 5: the parameter associated with surface structure is not preserved.

Nevertheless, in the operation $\epsilon = \varepsilon(m)$, no information is lost (m is recoverable from ϵ). Therefore the face partition $\phi(m)$ of m is directly recoverable from the edge diagram ϵ . This can be done by tracing along edges. In Figure 4.30, two faces are traced out in a edge diagram. The rules for tracing the boundary of a face are

- trace along a side of a semicircular arc (edge),
- if the right end of the arc has an “ \times ” (it is twisted or $\in T$), then the bound-

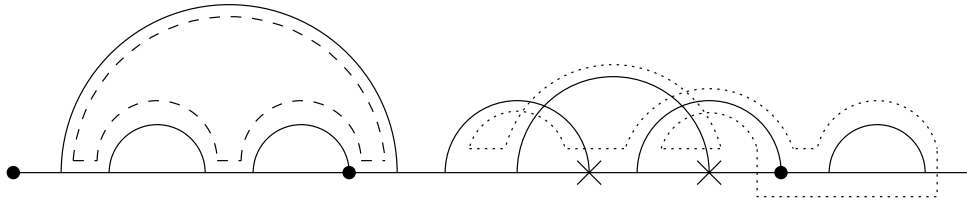


Figure 4.30: How to trace a face in an edge diagram

ary crosses the arc,

- in the gaps (corners) between the arcs trace along the base line, except when
- there is a vertex to the right of the gap, or the gap is the first or last gap, then trace underneath the base line towards the other such gap associated with the same vertex.

4.4.4 Integer-Parenthesis Systems

Lehman introduced a *integer-parenthesis* system for encoding rooted orientable maps in [Wal71]. One way to build an integer-parenthesis system from an edge diagram is, beginning from the right end and moving left, put an integer or parenthesis under every end. Vertex-beginner edges are assigned matching parentheses. Other edges are labelled with positive integers, the same label at each end. Edges are labelled in ascending order as they are first encountered moving right to left, Figure 4.31. Reverse the order of the resulting list and also reverse the parentheses. The result is an example of Lehman's integer-parenthesis sys-

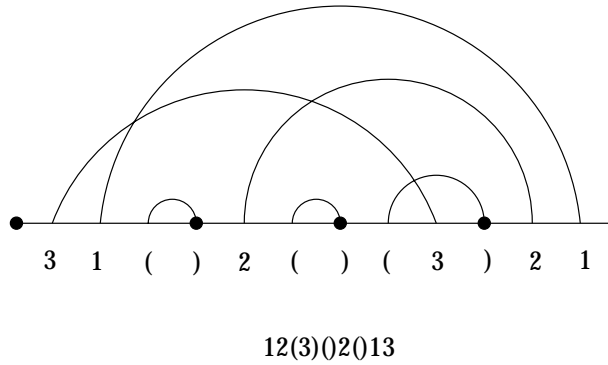


Figure 4.31: Building an integer-parenthesis system

tem.

Definition 4.5. A sequence $\sigma_1\sigma_2 \dots \sigma_{2n}$ is an integer-parenthesis system if

1. each $\sigma_i \in \{“(”, “)”, 1, 2, 3, \dots\}$,
2. for $1 \leq i \leq j$ the number of $\sigma_i = “)”$ never exceeds the number of $\sigma_i = “(”,$ for $j = 1, \dots, 2n,$
3. for $m \in \mathbb{N},$ the number of $\sigma_i = m$ is either 0 or 2,
4. $\sigma_1 = 1$ and if $\sigma_j > 1$ then for some $k < j,$ it must hold that $\sigma_k = \sigma_j - 1,$
5. the subsystem $m(m)$ is forbidden, meaning that there does not exist $i_1 < i_2 < i_3 < i_4$ with $\sigma_{i_1} = m, \sigma_{i_2} = “(”, \sigma_{i_3} = m, \sigma_{i_4} = “)”$.

An extended integer-parenthesis system is integer parenthesis system where a subset of the integer pairs $\sigma_i = \sigma_j = m \in \mathbb{N}$ is distinguished, (such pairs denoted by $\sigma_i = \sigma_j = \tilde{m}$).

For non-orientable maps m , the set $T \neq \emptyset$ in $\varepsilon(m)$. These edges become the distinguished pairs in an extended integer-parenthesis system. Note that the forbidden sub-configuration for edge diagrams (Condition 4 of Definition 4.4), is equivalent to the forbidden subsystem $i(i)$. (The parentheses are self-forbidding, as (0) is never interpreted as a beginner right-crossing a beginner, but a beginner over a beginner.)

4.5 Summary

Depth first search can be used to choose a canonical structure for a rooted map. Table 4.1 illustrates some of the canonical structures for three different rooted maps.

The following constructions:

- $\tilde{\Xi}$ of Chapter 5,
- η of Chapter 7,
- Θ of Chapter 8,

take advantage of these canonical structures (which result from depth first search). In fact, each of these constructions aims to combinatorialise an enumerative result. The original derivation of each of the three corresponding results about rooted maps involved at least one algebraic step for which no combinatorial explanation is apparent.

It would seem that depth first search is fundamental to the combinatorial treatment of rooted maps. Indeed, the only combinatorial proofs of certain enu-

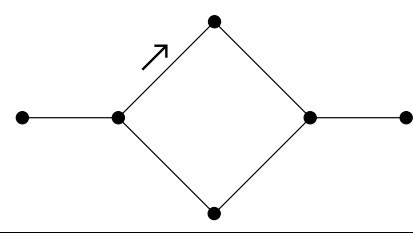
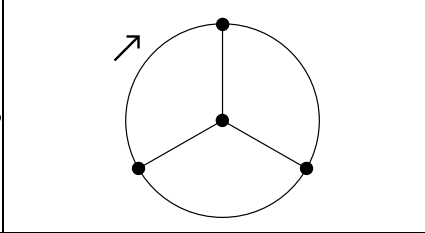
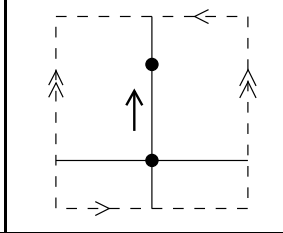
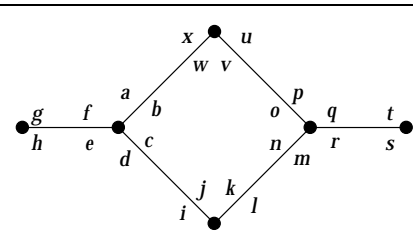
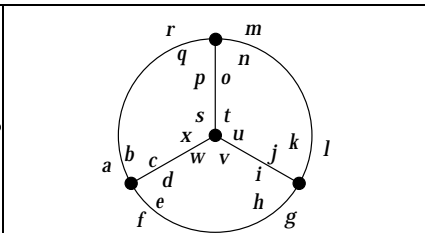
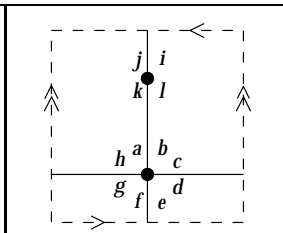
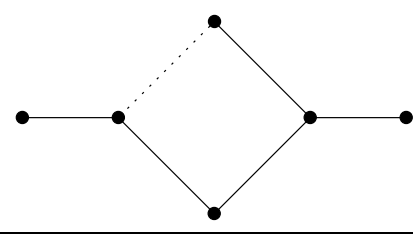
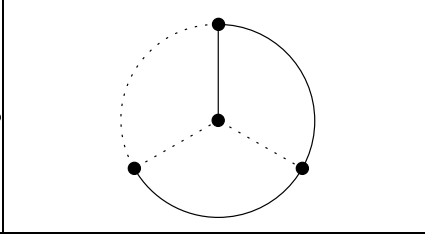
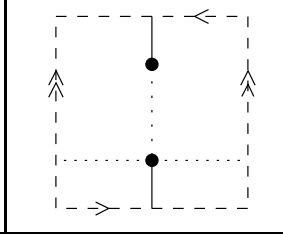
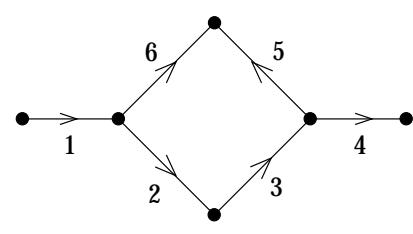
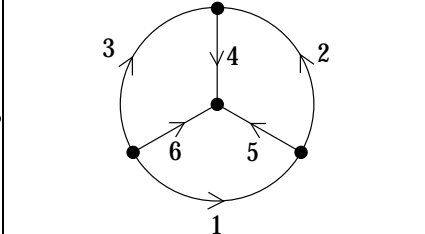
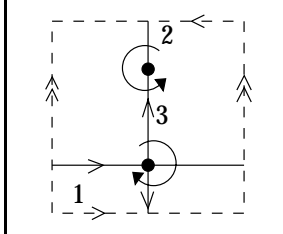
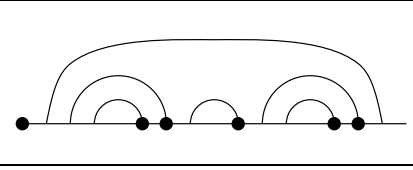
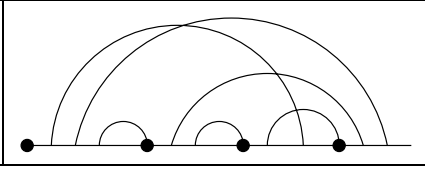
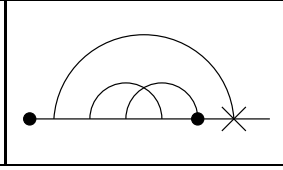
(a) Rooted Map:		
		
(b) Canonical Position Labelling:		
		
(c) Canonical Spanning Subtree:		
		
(d) Canonical Ordered Digraph: (clockwise vertex orientations for planar maps)		
		
(e) Edge Diagram:		
		
(f) Integer-Parenthesis System:		
1(0)0(0)1	12(3)02013	$\tilde{1}(2)\tilde{1}$

Table 4.1: Some canonical structures for three different rooted maps

merative results for rooted maps (results first obtained by powerful algebraic methods) make essential use of depth first search.

Chapter 5

On Extending Tutte's Medial Bijection

The Quadrangulation Conjecture (Conjecture 1.1) was developed with character theory of the symmetric group of permutations. With this character theory, [JV90a] first established the existence of a bijection $\xi : \mathcal{Q} \rightarrow \mathcal{A}$ between the set \mathcal{Q} of rooted quadrangulations and \mathcal{A} , the set of all maps with a particular decoration. The Quadrangulation Conjecture of [JV90a] then postulates that there is a bijection $\Xi : \mathcal{Q} \rightarrow \mathcal{A}$, which is *natural*, in the sense that it has combinatorial, element-wise description. In [JV99], this work is generalised to a bijection between Eulerian maps and hypermaps.

A natural bijection Ξ has not been recovered from the existence proof. No interpretation in terms of rooted maps has been found for the character theory involved in the existence proof.

Independent constructions for Ξ (not depending on the character-theoretic

existence proof) have not been found. However, a partially suitable natural bijection is presented in this chapter. Advantage is taken of the Depth First Search Algorithm, and of the resulting edge diagram model of a rooted map, to make progress towards the bijection Ξ . More precisely, a bijection $\tilde{\Xi} : \mathcal{Q} \rightarrow \mathcal{A}$ is constructed, which is natural, but only preserves one of the two desired parameters (to be defined below in §5.1) for Ξ . Moreover, $\tilde{\Xi}$ extends a bijection of Tutte, the medial bijection [Tut62, Tut63].

5.1 The Quadrangulation Conjecture

Recall that the genus of an orientable map m is $g = g(m) = \frac{1}{2}(2 - \chi)$, where the $\chi = f - e + v$ is the Euler characteristic, if m has f faces, e edges and v vertices. For any rooted map m , let $V(m)$ be its set of vertices. A *dual-strut* of m is an edge e of m whose associated edge e^∂ in the dual m^∂ is a strut. Let $S(m)$ be its set of dual-struts (a certain canonical subset of the edges).

Let \mathcal{O} be the set of rooted orientable maps. Let \mathcal{O}_n be the set of maps in \mathcal{O} with n edges.

Definition 5.1. *Let $n \geq 1$. Let $0 \leq g \leq \lfloor \frac{n+1}{2} \rfloor$. Let*

$$\mathcal{Q}_{g,n} = \{q \mid q \in \mathcal{O}, g(q) = g, \phi(q) = [4^n]\}.$$

A map $q \in \mathcal{Q}_{g,n}$ is a quadrangulation. Let

$$\mathcal{A}_{g,n} = \{(o, W, F) \mid o \in \mathcal{O}_n, W \subseteq V(o), F \subseteq S(o), \frac{|W|}{2} + g(o) = g\}.$$

An object $\alpha \in \mathcal{A}_{g,n}$ is a decorated map.

A decorated map $\alpha = (\circ, W, F)$ may be represented as the orientable map \circ with its vertices in W coloured white, the remaining vertices black, and its dual-struts in $S(\circ)$ bearing positive and negative *flags*, with F consisting of the dual-struts with negative flags. Table 5.1(b) illustrates all the decorated maps in $\mathcal{A}_{1,2}$ using this representation of coloured vertices and flagged dual-struts. Observe that since g and $g(\circ)$ are integers, the number of white vertices is even in any decorated map.

In [JV90a], $\mathcal{A}_{g,n}$ was defined without the use of flagged dual-struts (without any equivalent to F) but rather by counting maps of genus h with multiplicity 4^h . However, since a map of genus h always has $2h$ dual-struts, there are 4^h ways to assign $+/-$ flags to the dual-struts. Both definitions therefore lead to the same cardinality for $\mathcal{A}_{g,n}$.

Character factorisation leads to a proof [JV90a] that:

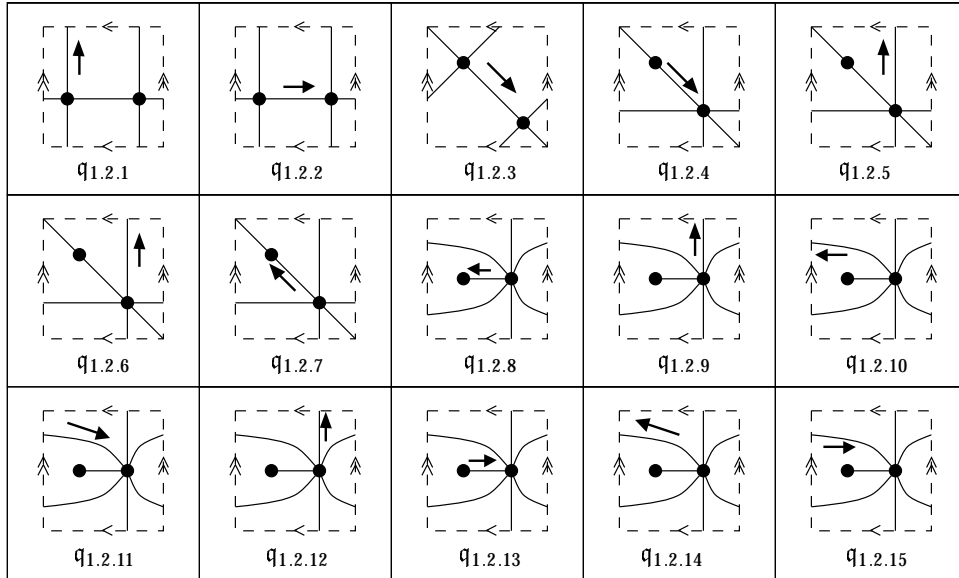
$$|\mathcal{Q}_{g,n}| = |\mathcal{A}_{g,n}|, \quad \forall g, n \tag{5.1}$$

Let $\mathcal{Q} = \bigcup_{g,n} \mathcal{Q}_{g,n}$ and $\mathcal{A} = \bigcup_{g,n} \mathcal{A}_{g,n}$. Then (5.1) implies the existence of a bijection

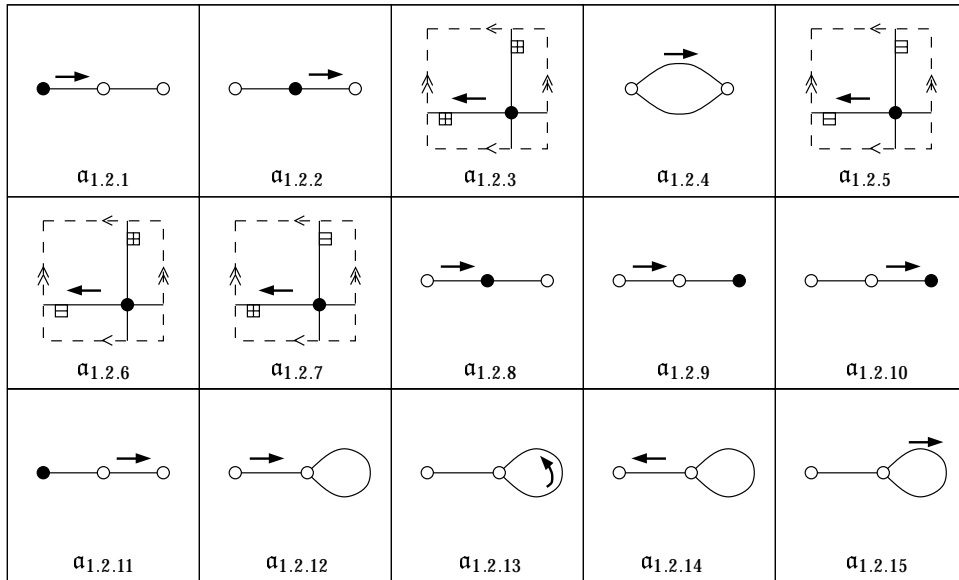
$$\xi : \mathcal{Q} \rightarrow \mathcal{A},$$

which preserves the two parameters g and n , meaning $\xi(\mathcal{Q}_{g,n}) = \mathcal{A}_{g,n}$.

Naturally, the authors in [JV90a] went on to propose what is here referred to as Conjecture 1.1, the Quadrangulation Conjecture, namely that there exists a



(a) $\mathcal{Q}_{1,2}$ — Two-faced quadrangulations of genus one



(b) $\mathcal{A}_{1,2}$ — Decorated, two-edged maps (with $w + h = 1$)

Table 5.1: Listings of $\mathcal{Q}_{1,2}$ and $\mathcal{A}_{1,2}$ such that $\tilde{\Xi}(q_{1.2.i}) = a_{1.2.i}$ for $i = 1, \dots, 15$.

natural (constructive) bijection, by which is meant a bijection with an algorithmic combinatorial element-wise action,

$$\Xi : \mathcal{Q} \rightarrow \mathcal{A},$$

which also preserves g and n . So far, all attempts at recovering a Ξ directly from the proof of (5.1) have been unsuccessful. The character factorisation is one of the primary bottlenecks which makes such a recovery so difficult.

For such a hypothetical constructive bijection, Ξ , consider a family of more specific bijections

$$\Xi_{g,n} : \mathcal{Q}_{g,n} \rightarrow \mathcal{A}_{g,n},$$

by restriction of the domain, $\Xi_{g,n} = \Xi|_{\mathcal{Q}_{g,n}}$.

In the special instance $g = 0$, prior to [JV90a], Tutte had already proven the special case $|\mathcal{Q}_{0,n}| = |\mathcal{A}_{0,n}|$, and constructed a bijection $M : \bigcup_n \mathcal{Q}_{0,n} \rightarrow \bigcup_n \mathcal{A}_{0,n}$, which preserves n . This bijection M is the *medial* construction. Then $M_n = M|_{\mathcal{Q}_{0,n}}$ serves as a valid $\Xi_{0,n}$. But, for $g \geq 1$, no general $\Xi_{g,n}$ was known. For $n \leq 2$, we can show how to provide such bijections, as restrictions of a bijection $\tilde{\Xi} : \mathcal{Q} \rightarrow \mathcal{A}$, which only preserves the parameter n .

Let $\mathcal{Q}_n = \bigcup_g \mathcal{Q}_{g,n}$ and $\mathcal{A}_n = \bigcup_g \mathcal{A}_{g,n}$. Let $\Xi_n = \Xi|_{\mathcal{Q}_n}$. No general Ξ_n is known that preserves the weight functions for g (since no Ξ is known). However, if the constraint of preserving g is lifted, then there is construction. In fact, we shall

construct a bijection

$$\tilde{\Xi} : \mathcal{Q} \rightarrow \mathcal{A}$$

which both satisfies

$$\tilde{\Xi} \Big|_{\bigcup_n \mathcal{Q}_{0,n}} = \partial \circ M, \quad (5.2)$$

where ∂ is the operation of forming the dual, thereby extending Tutte's medial construction, and

$$\tilde{\Xi}(\mathcal{Q}_n) = \mathcal{A}_n, \quad (5.3)$$

thereby preserving the weight function for n .

For $n = 1$ and $n = 2$, one has $g \leq \lfloor \frac{3}{2} \rfloor = 1$, so that

$$\mathcal{Q}_n = \mathcal{Q}_{0,n} \cup \mathcal{Q}_{1,n},$$

$$\mathcal{A}_n = \mathcal{A}_{0,n} \cup \mathcal{A}_{1,n}.$$

Since $\tilde{\Xi}$ is bijective, (5.2) and (5.3) imply that $\tilde{\Xi}(\mathcal{Q}_{1,n}) = \mathcal{A}_{1,n}$, and therefore that

$\tilde{\Xi} \Big|_{\mathcal{Q}_{1,n}}$ serves as a construction of $\Xi_{1,n}$, for $n \leq 2$.

For $n \geq 3$ though, $\tilde{\Xi}$, as it stands, is not guaranteed to yield any more constructions $\Xi_{g,n}$. In fact, $\tilde{\Xi}(\mathcal{Q}_{1,3}) \neq \mathcal{A}_{1,3}$.

Effect of $\tilde{\Xi}$ on $\mathcal{Q}_{1,2}$

Table 5.1(a) shows the set $\mathcal{Q}_{1,2}$, with labels $q_{1,2,i}$ for $i = 1, \dots, 15$. These are all orientable rooted quadrangulations with two vertices on the torus.

Table 5.1(b) shows the members of the set $\mathcal{A}_{1,2}$, with labels $a_{1,2,i}$ for $i = 1, \dots, 15$, such that $a_{1,2,i} = \tilde{\Xi}q_{1,2,i}$. For each of these rooted maps, some even number $2w$ of the vertices may be coloured white. If h is the genus of one of these maps, then $w + h = 1$. (This is part of the definition of $\mathcal{A}_{1,2}$.)

The definition of $\tilde{\Xi}$ describes how to determine the rooted map, the black and white vertex colours, and the flagged dual-struts of a decorated map $\alpha = \tilde{\Xi}(q)$ from any given quadrangulation q .

Observe that there are 15 maps in $\mathcal{Q}_{1,2}$. Thus there are 15! bijections $\xi_{1,2} : \mathcal{Q}_{1,2} \rightarrow \mathcal{A}_{1,2}$. Prior to the discovery of $\tilde{\Xi}$, the only known bijections between $\mathcal{Q}_{1,2}$ and $\mathcal{A}_{1,2}$ consisted of listing both sets in some arbitrary order. The bijectivity of such a correspondence requires the result $|\mathcal{Q}_{1,2}| = |\mathcal{A}_{1,2}|$.

The construction $\tilde{\Xi}$, on the other hand, although perhaps not the simplest construction, provides independent proof that $|\mathcal{Q}_{1,2}| = |\mathcal{A}_{1,2}|$, altogether distinct from (5.1) and from exhaustive listing of both sets.

Enumerative Clue for $\tilde{\Xi}$

By specialising a more general character-based formulae it was shown in [JV90a] that

$$|\mathcal{Q}_n| = [x^n] 4x \frac{\partial}{\partial x} \log \sum_{n \geq 0} \frac{(4n)!}{(2n)!n!16^n} x^n.$$

But it is also true that

$$L_n = |\mathcal{L}_n| = [x^n] 4x \frac{\partial}{\partial x} \log \sum_{n \geq 0} \frac{(4n)!}{(2n)!n!16^n} x^n, \quad (5.4)$$

where $\mathcal{L}_n = \{m \in \mathcal{L} \mid n(m) = n\}$ is the set of rooted, locally orientable maps with n edges. (To show (5.4) use Lemmas 8.7 and 7.2 and let $b = 1$ and $y = 1$, or use the algebraic method, or use a direct argument with matchings.)

Therefore, there exists bijections $\lambda_n : \mathcal{Q}_n \rightarrow \mathcal{L}_n$. In fact, we will construct a bijection $\Lambda : \mathcal{Q} \rightarrow \mathcal{L}$, which preserves n .

Then, we will construct a bijection $A : \mathcal{L} \rightarrow \mathcal{A}$, also preserving n , leading to a chain of bijections:

$$\mathcal{Q} \xrightarrow{\Lambda} \mathcal{L} \xrightarrow{A} \mathcal{A}$$

and

$$\tilde{\Xi} = A \circ \Lambda. \quad (5.5)$$

5.2 On Tutte's Medial Construction

Tutte's medial bijection is a natural bijection $M : \bigcup_n \mathcal{Q}_{0,n} \rightarrow \bigcup_n \mathcal{A}_{0,n}$ which preserves the parameter n . Each face of a planar quadrangulation $q \in \mathcal{Q}_{0,n}$ is an edge of its medial $\alpha = M(q)$. Suppose $\alpha = (\sigma, W, F)$, and note that $|W| = |F| = 0$,

since $\alpha \in \mathcal{A}_{0,n}$. Thus, $\alpha = (\sigma, \emptyset, \emptyset)$ is determined by the planar rooted map σ . Tutte's medial bijection, in its original form, was a bijection between (rooted) planar quadrangulations and rooted planar maps (without decorations). For the following discussion, we shall identify α with σ .

We formally define the inverse M^{-1} .

Definition 5.2. *Let $\sigma = (X, \mu_1, \mu_2, \mu_3, r)$. Then $\alpha = M^{-1}(\sigma)$ is the map*

$$\alpha = (X \times \{-1, +1\}, \mu_2^+ \mu_2^-, \mu_1^+ \mu_3^-, \sigma, (r, +1))$$

where $\sigma : (x, s) \mapsto (x, -s)$ and

$$\mu_i^\pm : \begin{cases} (x, \pm 1) & \mapsto (\mu_i(x), \pm 1), \\ (x, \mp 1) & \mapsto (x, \mp 1). \end{cases}$$

(Note that the notation μ^+ has a different meaning here than in its previous use.)

Intuitively, $\alpha = M^{-1}(\sigma)$ is constructed from σ by inserting a new vertex into each face of σ and joining this new vertex by an edge to each old vertex in the boundary of the face; then delete all the former edges of σ . The result is α . The root position of α is located at the same (old) vertex of σ , on the edge that leads into the new vertex placed in the root face of σ , and on the side of the edge nearest to the root position of σ .

As an example, consider the rooted planar map σ of Figure 5.1. It may be represented by the formal specification given in Figure 5.2.

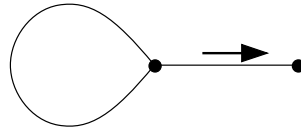


Figure 5.1: A planar rooted map σ .

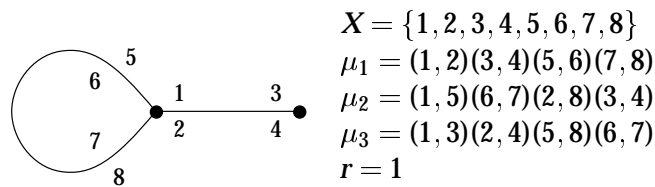
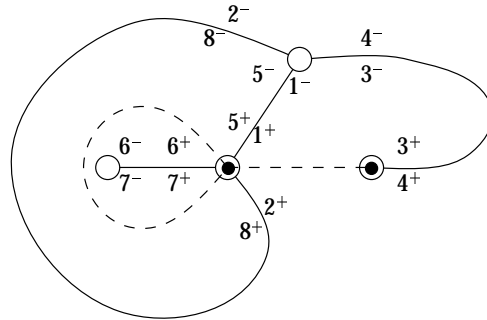


Figure 5.2: A formal representation of σ

Then $\mathfrak{q} = M^{-1}(\sigma)$, may be superimposed upon this representation of σ , as in Figure 5.3. The planar map σ appears with dashed lines for edges, and solid disks for vertices. Graphically, place a vertex of \mathfrak{q} on top of each vertex of σ and place one vertex of \mathfrak{q} into each face of σ . In Figure 5.3 the vertices of \mathfrak{q} are drawn as empty circles.

An edge of \mathfrak{q} is drawn at each corner of σ , joining vertices of \mathfrak{q} obtained from a vertex and face of σ . In Figure 5.3 the formal pairs $(x, \pm 1)$ are abbreviated as x^\pm . Then the positions x^+ of \mathfrak{q} are located at the vertices arising from vertices of σ . The positions x^- of \mathfrak{q} are located at the vertices arising from faces of σ . The resulting rooted map is given in Figure 5.4.

The domain of M^{-1} , as described above, may be extended from being only planar maps to being all rooted maps (orientable or not). Let N be this natural extension of M^{-1} . The images of N are quadrangulations (possibly non-orientable).



$$\begin{aligned}
 X &= \{1^+, 1^-, 2^+, 2^-, \dots, 8^+, 8^-\} \\
 \mu_1 &= (1^+, 5^+)(6^+, 7^+)(2^+, 8^+)(3^+, 4^+) \\
 &\quad (1^-, 5^-)(6^-, 7^-)(2^-, 8^-)(3^-, 4^-) \\
 \mu_2 &= (1^+, 2^+)(3^+, 4^+)(5^+, 6^+)(7^+, 8^+) \\
 &\quad (1^-, 3^-)(2^-, 4^-)(5^-, 8^-)(6^-, 7^-) \\
 \mu_3 &= (1^+, 1^-)(2^+, 2^-) \cdots (8^+, 8^-) \\
 r &= 1^+
 \end{aligned}$$

Figure 5.3: Superimposition of q on o

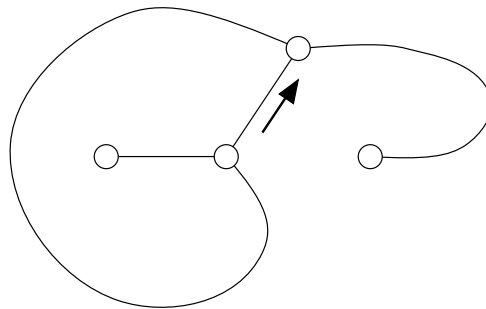


Figure 5.4: The planar quadrangulation $q = M^{-1}(o)$

However, the range does not include all quadrangulations. Observe that the vertices of $q = N(m)$, may be classified into those originating from vertices and faces of m . The edges of q only join opposite kinds of vertices in this sense. Therefore q is bipartite.

The range of N consists of all bipartite quadrangulations. The nature of N implies that $N(m)$ and m are in the same underlying topological surface. Although N^{-1} serves as a natural extension of Tutte's medial construction M , its domain only contains bipartite quadrangulations, and therefore N^{-1} cannot fulfill the role of Ξ , whose domain includes all quadrangulations.

There is another construction R , defined by $R^{-1} = N^{-1} \circ \partial$, the *radial* construction [Sch98], where ∂ is the operation of forming the dual. Its domain consists of face-bipartite quartic (vertex-4-regular) maps. The radial construction is related to the dual of the medial construction. The radial construction will arise in the construction of $\tilde{\Xi}$.

Returning to the planar case, it is not immediately evident that the range of M^{-1} includes all planar quadrangulations. It certainly includes all planar bipartite quadrangulations, since N^{-1} may be applied to these. To show that M is the desired bijection, $M: \bigcup_n \mathcal{Q}_{0,n} \rightarrow \bigcup_n \mathcal{A}_{0,n}$, it therefore suffices to show that every planar quadrangulation is bipartite. Equivalently, by duality, it suffices to prove that every planar quartic map is face-bipartite. Non-planar, non-face-bipartite quartic maps exist, so the proof must make essential use of planarity.

Lemma 5.1. *Every planar, quartic map q is face-bipartite.*

Proof. Use the Jordan curve theorem.

The edges of q may be covered by a set of closed curves, which pass through vertices at diametrically opposite edges. (This can be done whether or not the map is planar.) These curves may not be simple, they may self-intersect. Nevertheless, the Jordan curve theorem, in extended form, states that each has an inside and an outside. (This fails in the non-planar cases.) Then each face of q is either inside an even or odd number of these curves. This parity classification forms the desired bipartition of the faces. \square

5.3 Sample Computation: $\tilde{\Xi}(q_{1.2.9}) = \alpha_{1.2.9}$

We now explain the action of $\tilde{\Xi}$, given by (5.5), by referring to the example given in Table 5.3.

The table shows by a sequence of rooted maps and edge diagrams, how to compute in stages that $\tilde{\Xi}(q_{1.2.9}) = \alpha_{1.2.9}$. The rooted map (1) in the first stage is the rooted orientable quadrangulation $q_{1.2.9} \in \mathcal{Q}_{1,2}$. The following stages track the progress of the construction $\tilde{\Xi}$. The rooted map (13) of the final stage in the sequence is the decorated rooted orientable map $\alpha_{1.2.9} \in \mathcal{A}_{1,2}$.

Before getting into the details of all the intermediate stages, let us consider some more general aspects of the stages. The topology of the underlying surface changes at precisely two points in the process. (Table 5.2 tracks the surface topology in the small example.) These are from stages 3–4 and 7–8. It is not a coincidence either that stages 3,4,7 and 8 are in the form of an edge diagram. These stages use depth first search to implicitly make some changes to the sur-

face structure. Although the construction $\tilde{\Xi}$ begins and ends with orientable

Stages	Surface
1 – 3	Torus
4 – 7	Projective Plane
8 – 13	Sphere

Table 5.2: Changes in the topology through the various stages

maps, its intermediate stages usually involve non-orientable maps.

One of the key steps is to use the radial construction between stages 5 and 6, (which will usually be non-orientable maps.) It is this step that reduces the number of edges by half. Note that face and vertex partitions of stage 6 merge to form the face partition of stage 5.

The following subsections explain the twelve steps in the computation of $\tilde{\Xi}$ shown in Table 5.3. Each step is shown to be reversible (when it is not obvious) so that $\tilde{\Xi}$ and $\tilde{\Xi}^{-1}$ are well-defined, and thus $\tilde{\Xi}$ is a bijection.

5.3.1 Stages 1–2: Duality (i)

The two rooted maps in Stages 1 and 2 of Table 5.3 are duals of each other. (This is the first of two instances of duality in the construction of $\tilde{\Xi}$.) Figure 5.5 shows these two maps superimposed. Stage 1, the quadrangulation, is drawn with filled vertices and single lines for edges. Stage 2, a quartic (vertex-4-regular) map, is drawn with hollow vertices and double lines for edges.

Note that each edge of Stage 2 crosses a unique edge of Stage 1. The relation of the rootings is indicated by the arrows sharing the tail. (Recall the tail of the

<p>1-2: Duality</p>	<p>1. </p>	<p>13. </p>	<p>12-13: White: - Black: +</p>
<p>2-3: Edge diagram</p>	<p>2. </p>	<p>12. </p>	<p>11-12: Duality</p>
<p>3-4: Twist by Corner Colours</p>	<p>3. </p>	<p>11. </p>	<p>10-11: Root Face Sign by Parity</p>
<p>4-5: Edge diagram</p>	<p>4. </p>	<p>10. </p>	<p>9-10: Sign Transfer From Cuts to Associated Faces</p>
<p>5-6: Radial Construction</p>	<p>5. </p>	<p>9. </p>	<p>8-9: Edge diagram</p>
	<p>6. </p>	<p>8. </p>	<p>7-8: Twist: -</p>
	<p>6-7: Edge diagram</p>	<p>7. </p>	

Table 5.3: Thirteen stages of the computation $\tilde{\Xi}(q_{1.2.9}) = \alpha_{1.2.9}$. (Explained in §§5.3.1–5.3.12)

Stage	ϕ	ν	Orientable?	Face-Bipartite?
1.	$[4^2]$	$[71]$	Yes	No
2.	$[71]$	$[4^2]$	Yes	No
3.	$[71]$	$[4^2]$	Yes	No
4.	$[431]$	$[4^2]$	No	Yes
5.	$[431]$	$[4^2]$	No	Yes
6.	$[31]$	$[4]$	No	—
7.	$[31]$	$[4]$	No	—
8.	$[21^2]$	$[4]$	Yes	—
9.	$[21^2]$	$[4]$	Yes	—
10.	$[21^2]$	$[4]$	Yes	—
11.	$[21^2]$	$[4]$	Yes	—
12.	$[4]$	$[21^2]$	Yes	—
13.	$[4]$	$[21^2]$	Yes	—

Table 5.4: Properties of the various stages

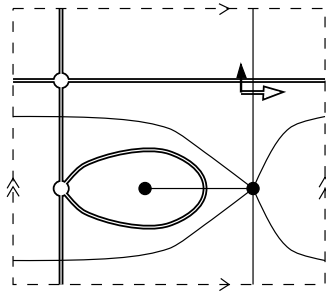


Figure 5.5: Stages 1 – 2

arrow indicates the root position.)

In general, the map in Stage 2 can be any rooted, orientable, quartic (vertex-4-regular) map.

5.3.2 Stages 2–3: Edge Diagram (I)

Stage 3 of Table 5.3 is the edge diagram of the Stage 2 map. (This step is the first of four steps in $\tilde{\Xi}$ that convert a map to its edge diagram or vice versa.) Edge diagrams are constructed by depth first search. Figure 5.6 reviews how depth first search is performed on the map of Stage 2 (on the left), the thin lines indicating the path of the search, and the letters a, A, b, B, c, \dots indicating the order in which the positions are visited. In the right of Figure 5.6, the same letters

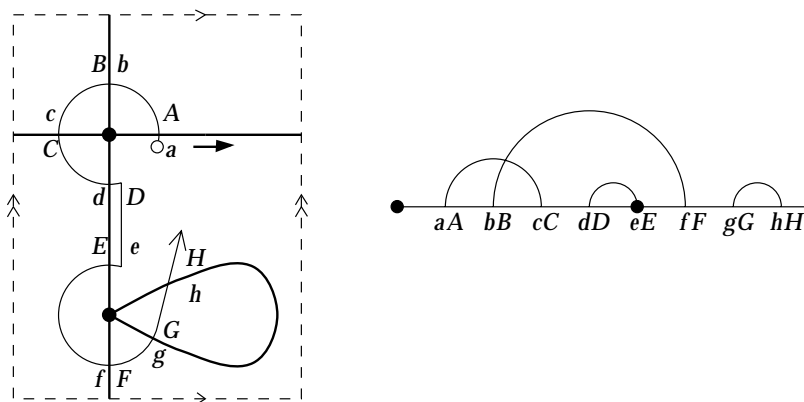


Figure 5.6: Stages 2 – 3

a, A, b, B, \dots are written in linear order beneath the edge diagram of Stage 3. Edges appear as arcs from one pair of letters to another, the same pairs joined by edges in Stage 2. At the lowest letter belonging to each vertex of Stage 2, a vertex

is drawn in the edge diagram, Stage 3.

In the opposite direction, recall that each edge diagram determines a unique rooted map.

In general, the edge diagram in Stage 3 may be any diagram that

- has no twists, and
- is quartic in the sense that vertices are located before the first end, at the fifth end, and at every fourth subsequent end, (the ninth, the thirteenth end, and so on).

5.3.3 Stages 3–4: Adding Twists

The Stage 3 edge diagram represents an orientable, but not face-bipartite map. We want to add some twists to the edge diagram in such a way that the map becomes face-bipartite. To do this, alternately shade the corners of vertices black and white, and use tree edges to initiate later vertices.

It will be easier to visualize this alternating shading procedure, if the base line of the edge diagram is replaced by a series of rectangles corresponding to the vertices, as in Figure 5.7. Then the corners, or what corresponds to corners of a map, should be more apparent. Begin by shading the corner to which the root belongs. In Figure 5.7, this first corner extends all the way underneath the first rectangle.

On top of the first rectangle, there are three more corners. The outer two of these are left white, while the inner is shaded. Thereby, the corners are alternately shaded and not shaded in the neighbourhood of the first vertex. The

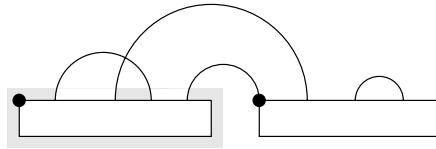


Figure 5.7: Shading the corners of the first (root) vertex of the Stage 3 edge diagram

shading provides a face-bicolouring, but only the immediate vicinity of the root vertex.

The next step is to alternately shade the corners of the second vertex. Once one corner of the second vertex is shaded, alternation determines the shading of the remaining corners.

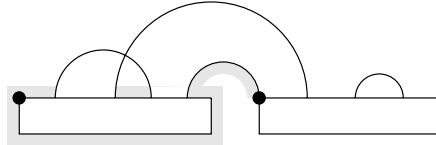


Figure 5.8: Shading the corners of the second vertex of the Stage 3 edge diagram

The first corner of the second vertex may be shaded by using the canonical tree edge joining the second vertex and first edge. Shade the entire length of the tree edge on the side determined by the shaded corner of the first vertex. The shaded side of this tree edge at the second vertex determines its first shaded corner.

Once all the corners have been shaded, the resulting shading is a face-bicolouring in the vicinity of the canonical spanning tree. Where the shading may fail as a

face-bicolouring is at the non-tree edges. The shaded corners at the ends of a non-tree edge may lie on different sides of the non-tree edge. For these edges, the face-bicoloring fails.

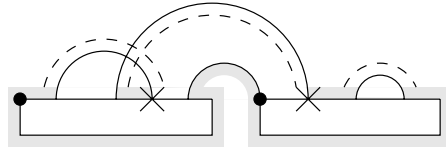


Figure 5.9: Adding twists to the Stage 3 edge diagram to correct failures to the face-bicolouring

To correct this, add a twist in the edge diagram to these failing non-tree edges. In Figure 5.9, the dashed lines drawn along the sides of non-tree edges begin at the shaded corner of the left (lower) end of the non-tree edge.

Note that dashed line of the rightmost non-tree edge arrives at a shaded corner of the right end. Therefore no twist is needed for this non-tree edge.

For the two other non-tree edges, however, the dashed lines arrive on the right at unshaded (white) corners. Therefore, twists are added in the edge diagram to these two non-tree edges. The result is the Stage 4 edge diagram.

In general, the Stage 4 edge diagram is any quartic edge diagram, for which the alternate shading procedure, when applied on the diagram without twists, results in the same set of twists. But this is equivalent in the corresponding map (Stage 5) to the edge diagram Stage 4 being face-bipartite.

To reverse this step, remove all twists to obtain an untwisted (orientable) edge diagram.

5.3.4 Stages 4–5: Edge Diagram (II)

The rooted map in Stage 5, is the map represented by the edge diagram of

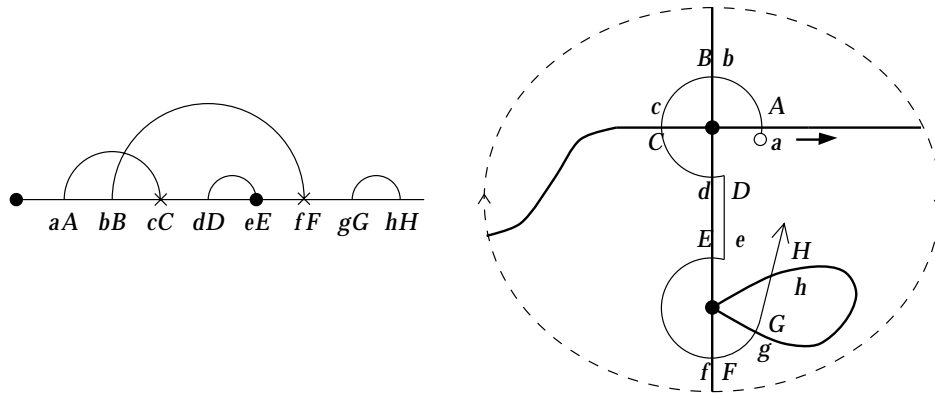


Figure 5.10: Stages 4 – 5

Stage 4. In Stage 4, the two edges on positions $\{a, A, c, C\}$ and $\{b, B, f, F\}$ are twisted. It follows that in Stage 5, that μ_3 pairs a with c , A with C , b with f and B with F (thus destroying biparticity of the matchings graph).

In Figure 5.10, Stage 5 is on the right, and is drawn on the projective plane. Any edge that arrives at the boundary of this representation, comes out on the opposite side, but with the opposite orientation. The edges $\{a, A, c, C\}$ and $\{b, B, f, F\}$ each cross this boundary once, achieving the desired twist.

5.3.5 Stages 5–6: Radial Construction

Since the rooted map of the Stage 5 is quartic and face-bipartite (by construction), the radial construction may be applied. Figure 5.11 shows Stage 6 superimposed

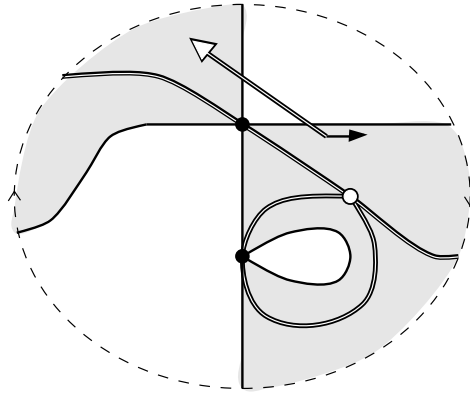


Figure 5.11: Stages 5 – 6

with a hollow vertex and double lined edges on Stage 5, shown with solid vertices and single lined edges.

Stage 6 is the radial of Stage 5. The radial of a quartic map q is the Tutte's medial of the dual of q (a quadrangulation). Each (quartic) vertex of Stage 5 is replaced by an edge of Stage 6. If the faces of Stage 5 are properly 2-coloured with the root face being shaded, then each shaded face of Stage 5 is replaced by a vertex of Stage 6. The edges of Stage 6 pass through the vertices of Stage 5, from one shaded corner to another.

As with duality, the rooting is handled pictorially by sharing of a tail.

In Figure 5.11, the root face is the only shaded face. It has degree 4. It becomes a vertex of Stage 6 of degree 4. The two unshaded faces of Stage 5 have degrees 1 and 3, and become faces of Stage 6 of degrees 1 and 3, respectively.

In general, Stage 6 can be any rooted, locally orientable map. To reverse this step (to find Stage 5) one inverts the radial construction. This involves placing

a vertex of Stage 5 on each edge of Stage 6. For each corner of Stage 6, draw an edge of Stages 5 by following the boundary of the corner closely.

Stage 6 is the halfway point in the computation $\tilde{\Xi}$. If Stage 1 is q then Stage 6 is $\Lambda(q)$.

5.3.6 Stages 6–7: Edge Diagram (III)

Stage 7 is the edge diagram of Stage 6. In Figure 5.12, these two stages are shown,

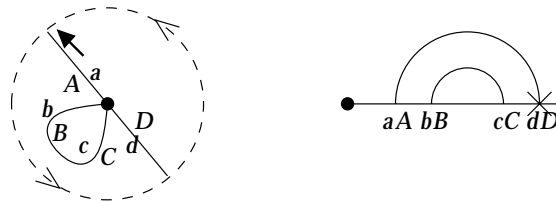


Figure 5.12: Edge diagram (Stage 7) of the projective-plane map (Stage 6)

together with alphabetical canonical position labels.

5.3.7 Stages 7–8: Twists Become Signs

The twists are removed from the edge diagram of Stage 7 to yield an orientable edge diagram for the eighth stage. Formerly twisted edges are marked by a negative sign ($-$), while untwisted non-tree edges are marked by a positive sign ($+$). Since the signs mean no information is lost, this step is reversible, as required.

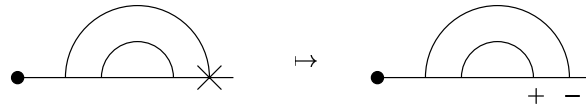


Figure 5.13: Replacing a twisted edge by a negatively signed edge

5.3.8 Stages 8–9: Edge Diagram (IV)

Stage 8 is the edge diagram of Stage 9. Note that the information of the signs of the non-tree edges is retained. (In this example, both edges happen to be non-tree edges. In a more general case, a non-tree edge would be left unsigned.) Figure 5.14, reviews this now familiar relation, with alphabetised canonical position labels.



Figure 5.14: Determining the map (Stage 9) from the edge diagram (Stage 8), and carrying over the edge-signs

Recall that depth first search also provides a canonical ordering of the edges of a rooted map. (For example in the ordered digraph structure.) The labels 1 and 2 indicate the order. The highest canonical position on e_1 is C , while on e_2 it is D . This order is relevant for the association between the non-root faces and the cuts.

5.3.9 Stages 9–10: Sign the Non-root Faces

In our example there are no tree edges, and no struts. Both edges are cuts. Figure 5.15 shows how to transfer the signs from the two cuts to the two non-root faces.

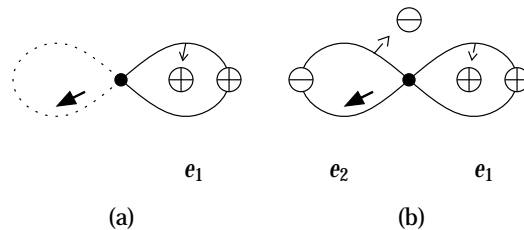


Figure 5.15: Transferring signs from the cuts of Stage 9 to the faces of Stage 10

Recall that cuts are naturally associated with non-root faces. The edge that has become e_1 under the canonical edge order of rooted maps, is the first cut. In Stage 9, e_1 carries a $+$ sign. But e_1 is a cut, and in fact separates the root face (of the single vertex map) into two faces. In Figure 5.15(a), the submap consisting of the edge e_1 is shown. (The edge e_2 is drawn dotted, in order to keep track of the root position.) Of these two faces one is the non-root face, and this non-root face is where the sign of e_1 is transferred.

In Figure 5.15(b), the edge e_2 has been added, again separating the root face into two faces. It is the non-root face of these two, that the $-$ sign of e_2 is transferred to.

The root face is left unsigned for the moment.

To reverse directions, one has only to determine the cuts of the rooted map, and their associations to non-root faces, and then transfer the non-root face signs

to their associated edges.

5.3.10 Stages 10–11: Sign the Root Face

In Stage 10, all the faces carry a sign except the root face. To arrive at Stage 11, the root face is assigned the unique sign which makes the product of all the face signs positive. Equivalently, the root face sign is to be the unique sign that makes the number of negative signs even.

To reverse this step, simply remove the root face sign.

5.3.11 Stages 11–12: Duality (ii)

Stage 12 is the dual map to Stage 11 map. The signs of faces becomes the signs of vertices.

In our example there are no struts, because the genus is zero. In a general example of genus h , there is $2h$ struts, and each of these edges carries a sign in Stage 11. These signs are carried over to Stage 12, using the natural correspondence between edges in dual maps.

5.3.12 Stages 12–13: Signs to Colours

Replace negative vertices by white vertices, and positive vertices by black vertices. The number of white vertices is necessarily an even number $2w$.

There is still $2h$ signed struts, where h is the genus. The signed struts may be ignored, but then the map are counted with multiplicity $2^{2h} = 4^h$.

5.4 Formal Summary of $\tilde{\Xi}$ and Planar Restriction

Recall that $\tilde{\Xi} = A \circ \Lambda$, for certain bijections $\Lambda : \mathcal{Q} \rightarrow \mathcal{L}$ and $A : \mathcal{L} \rightarrow \mathcal{A}$. These bijections are composed of simpler bijections (corresponding to the steps between the stages of Table 5.3), as follows:

$$\Lambda = R \circ \varepsilon^{-1} \circ \varphi \circ \varepsilon \circ \partial$$

$$A = \omega \circ \partial \circ \pi \circ \kappa \circ \varepsilon^{-1} \circ \psi \circ \varepsilon$$

where Table 5.5 summarises these bijections.

∂	dualize
ε	form edge diagram
φ	face-bipartise (by adding twists in edge diagram)
R	radial construct
ψ	sign and untwist (in edge diagram)
κ	cuts (move their signs to faces)
π	parity of root face sign
ω	white vertices (from negative vertices)

Table 5.5: The component bijections

It is worth noting that

- Only φ and ψ alter the underlying topological surface
- Only R changes the number of edges. (It halves them.)

Let $q \in \mathcal{Q}$ be planar. Simplify $\Lambda(q)$ as follows. First, note that $\partial(q)$ is planar and quartic. Then by Lemma 5.1, $\partial(q)$ is face-bipartite. Therefore φ does not

twist any edges of the edge diagram of $\partial(q)$. Hence

$$\Lambda(q) = R \circ \partial(q) = M(q)$$

It follows that $\Lambda(q)$ is planar.

In particular $\Lambda(q)$ is orientable so, more generally, let σ be some orientable rooted map, and consider $A(\sigma)$. Since σ is orientable, its edge diagram has no twists, and thus ψ has no effect on the edge diagram other than to assign $+$ to each edge. Since all the edge signs are $+$, then κ makes all the non-root face signs $+$, and π then makes the root face sign $+$.

At this point (Stage 11), there is a rooted orientable map with all positive faces and all positive struts. Applying ∂ leaves all the signs positive, and leaves the map orientable. Then ω produces no white vertices, because there are no negative signs.

The final result, $\alpha = A(\sigma)$, has black vertices and positive dual-struts. Thus $\alpha = (\sigma', \emptyset, \emptyset)$. In fact, $\sigma' = \partial(\sigma)$, because none of the operations κ , π and ω affects the underlying map, while ψ does not affect the underlying map because there was nothing to untwist in the edge diagram of σ .

Thus $A(\sigma) = (\partial(\sigma), \emptyset, \emptyset)$. In particular, when q is planar, then $\tilde{\Xi}(q) = A \circ \Lambda(q) = (\partial \circ \Lambda(q), \emptyset, \emptyset) = (\partial \circ M(q), \emptyset, \emptyset)$.

Therefore $\tilde{\Xi}$ extends Tutte's medial construction.

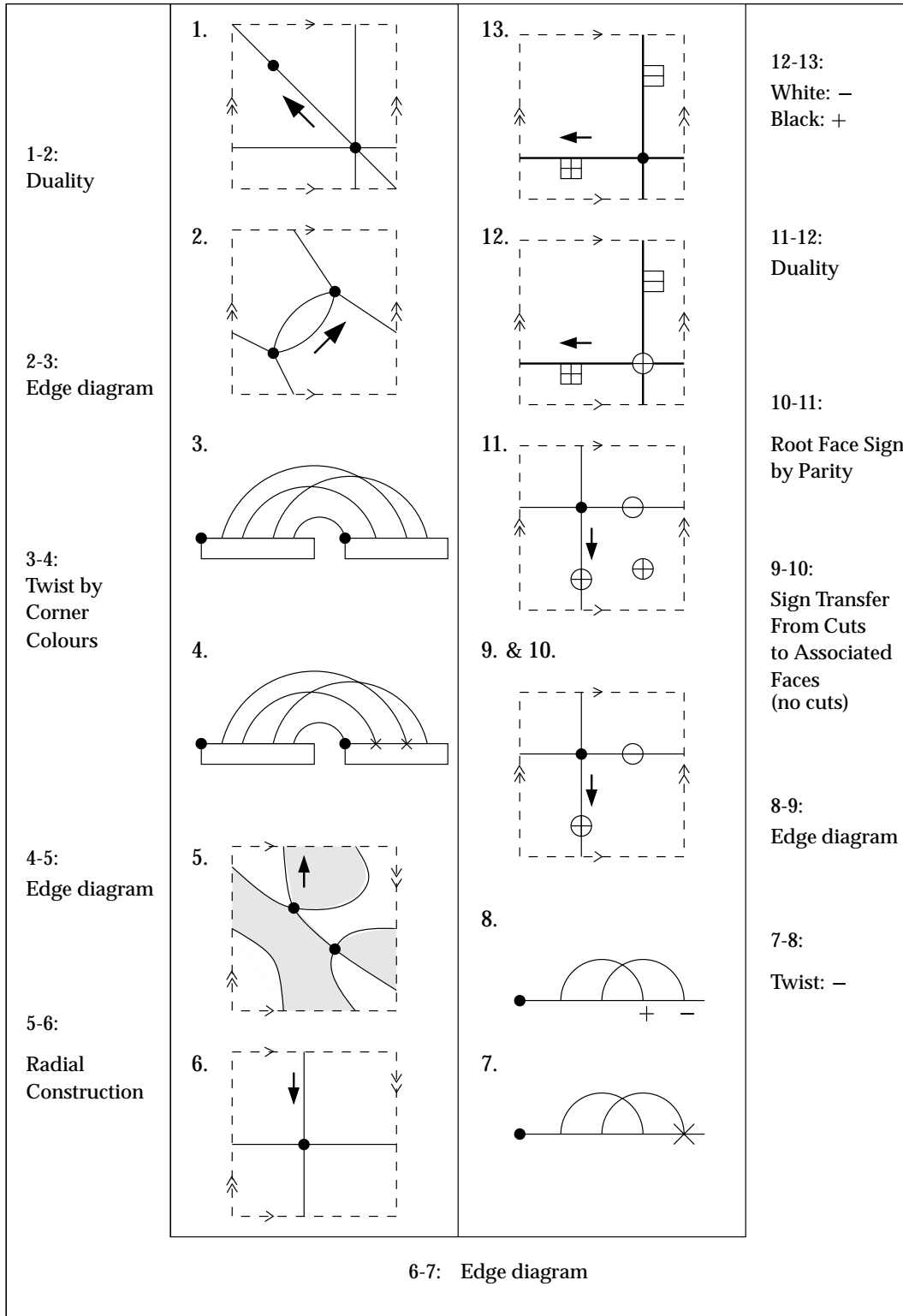


Figure 5.16: The computation of $\tilde{\Xi}(q_{1.2.7})$, with flagged dual-struts

5.5 An Example with Struts: $q_{1.2.7}$

The decorated map $\alpha_{1.2.7}$ provides an example with flagged dual-struts. Whereas $\alpha_{1.2.9}$ had no dual-struts (being planar it has 0 dual-struts), $\alpha_{1.2.7}$ has two dual-struts (having genus 1), and so in the calculation of $\tilde{\Xi}(q_{1.2.7})$ some of the edges will retain their signs.

Figure 5.16 portrays all the stages in the computation of $\tilde{\Xi}(q_{1.2.7})$.

In fact, this calculation is simpler than $\tilde{\Xi}(q_{1.2.9})$, because of the absence of cuts in Stage 9. It follows that Stage 9 is the same as Stage 10.

5.6 Genus Non-preservation, with Possible Corrections

When $n = 3$, the parameter $g \in \{0, 1, 2\}$. As we have shown, $\tilde{\Xi}$ preserves the parameter when $g = 0$. But there are quadrangulations $q \in \mathcal{Q}_{1,3}$ such that $\tilde{\Xi}(q) \in \mathcal{A}_{2,3}$, such as the quadrangulation in Stage 1 of Figure 5.17.

Therefore, for $n = 3$, the parameter g is not preserved by $\tilde{\Xi}$ unless it is zero.

Observe that $|\mathcal{Q}_3| = |\mathcal{L}_3| = |\mathcal{A}_3| = 297$, and that $\tilde{\Xi}$ puts these 297 objects in bijection with each other. The pre-image and image sets, and their sizes, which

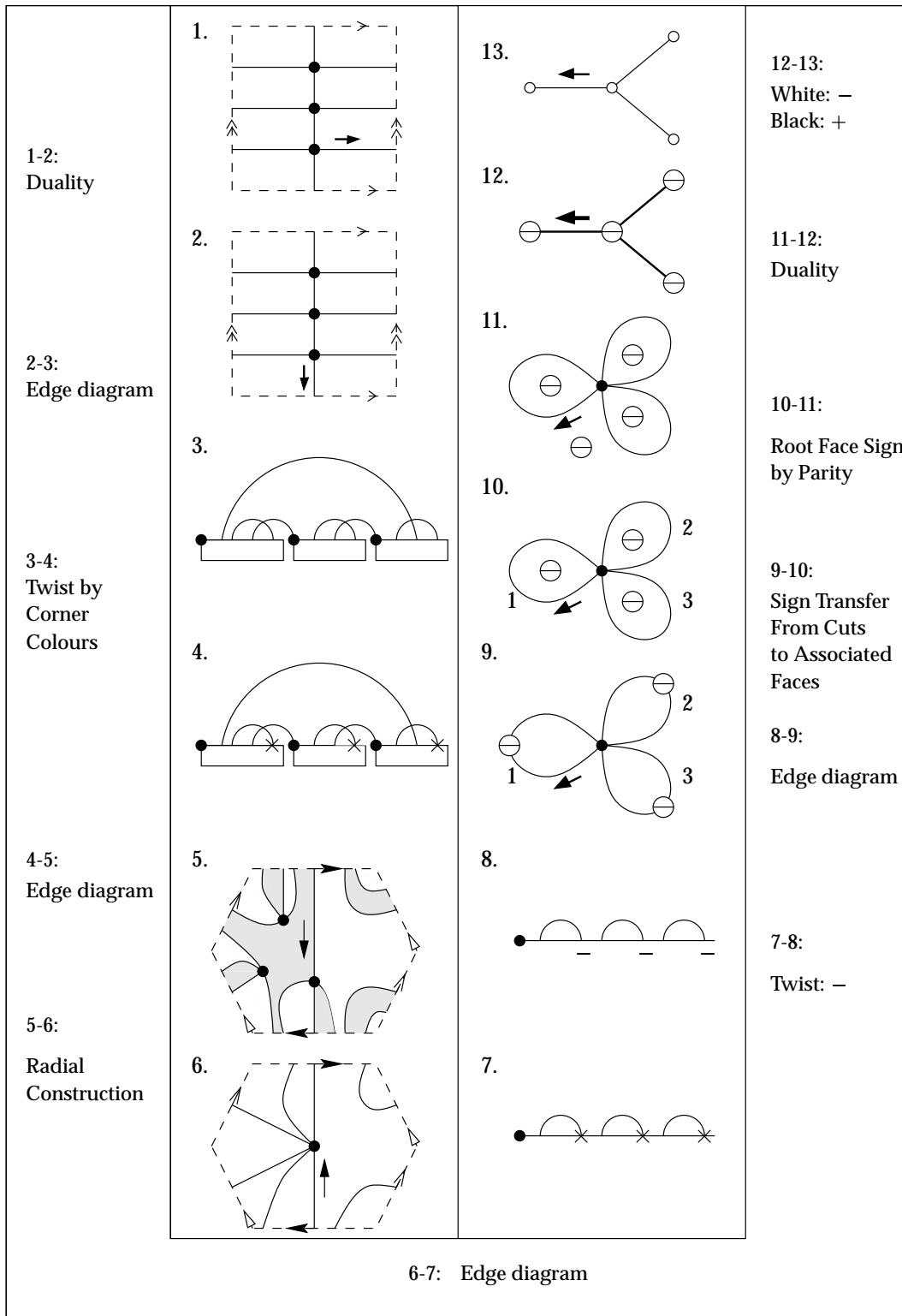


Figure 5.17: A counterexample to preservation of g . ($g = 1$ in Stage 1 and $g = 2$ in Stage 13)

are meant to be preserved by Ξ , are

$$|\mathcal{Q}_{0,3}| = |\mathcal{A}_{0,3}| = 54,$$

$$|\mathcal{Q}_{1,3}| = |\mathcal{A}_{1,3}| = 198,$$

$$|\mathcal{Q}_{2,3}| = |\mathcal{A}_{2,3}| = 45.$$

Then we may note $\tilde{\Xi}$ provides a bijection between $\mathcal{Q}_{1,3} \cup \mathcal{Q}_{2,3}$ and $\mathcal{A}_{1,3} \cup \mathcal{A}_{2,3}$, which are sets of cardinality $243 = 198 + 45$. But $\tilde{\Xi}$ combines up some of the 198 elements of one set with the 45 elements of the other set. However, Ξ must not separate these elements.

It is conceivable that $\tilde{\Xi}$ can be corrected to become the bijection Ξ that we seek. The case of $n = 3$ is first case where $\tilde{\Xi}$ fails, and therefore should be the starting point of a thorough investigation of how to correct $\tilde{\Xi}$.

For example, consider bijections $\hat{\Xi} = A \circ \Pi \circ \Lambda$, where $\Pi : \mathcal{L} \rightarrow \mathcal{L}$ is a bijection of locally orientable, rooted maps. If Π preserves n (the number of edges) and preserves planarity, then $\hat{\Xi}$ will share the properties of $\tilde{\Xi}$: it preserves n and $g = 0$. However, it may be that there is some particular choice of Π that causes $\hat{\Xi}$ to preserve all values of g . This observation applies to every stage of the computation $\tilde{\Xi}$: one may insert a permutation amongst the class of rooted maps (or edge diagrams) of that stage.

The strategy to correct $\tilde{\Xi}$, in the case of $n = 3$ and hopefully thereby all $n \geq 3$, should be to analyse the pattern of failures of $\tilde{\Xi}$ (instances $\tilde{\Xi}$ does not preserve g), with the hope that some corrective, natural permutation, such as Π above, becomes evident.

5.7 Summary

A partial solution $\tilde{\Xi}$ to the Quadrangulation Conjecture was constructed. This bijection preserves one of the two parameters required in the Quadrangulation Conjecture. The bijection $\tilde{\Xi}$ extends Tutte's medial bijection.

Chapter 6

Partial Differential Equations

Tutte obtained many enumerative results for planar maps in his study of the Four Colour Problem. Among these is the medial construction. In this chapter, we focus attention on a particular one of his results, namely the one for Eulerian planar slicings [Tut62], which we generalise here. A *slicing* is a map in which the vertices are labelled and for each vertex v one of the edges incident to v is selected. The equivalence of this definition to Tutte's original definition of slicings has been given by Walsh [Wal71]. The result states that the number of Eulerian planar slicings with n edges, k vertices and vertex partition ν is

$$\frac{(n-1)!}{(n-k+2)!} \prod_{i=1}^k \frac{\nu_i!}{\left(\frac{\nu_i}{2}\right)! \left(\frac{\nu_i}{2}-1\right)!}. \quad (6.1)$$

Tutte proved this result as the solution of a recurrence equation for all planar slicings that he derived by the method of edge deletion. This recurrence equation was extended by Walsh to include all orientable maps. (Walsh also used his

recurrence equation to obtain an explicit solution for the number of orientable monopoles (3.14).)

Note that the results (6.1) and (3.14) give information about the numbers of maps with a given vertex partition ν or given face partition ϕ , but not both. This limitation is inherent to the edge deletion analysis that gave the recurrence equation and its extension. The algebraic method does not have this limitation. However, edge deletion is effective in the development of the parameter β in this chapter.

We note in passing that the edge deletion method gives a recurrence equation that permits greater computational efficiency than does the algebraic method using symmetric functions or characters.

In this chapter, Walsh's extension of Tutte's recurrence equation is extended further to include all locally orientable maps. The recurrence equation is expressed in the form of the partial differential equation (6.2). A parameter b is introduced into the differential equation which interpolates between separate differential equations for the orientable and locally orientable cases. Thus b appears to emulate the rôle of the parameter α in the Jack symmetric function in the algebraic method of map enumeration. In fact, in the computations of the lower degree coefficients of the generating series (corresponding to the enumeration of maps with 4 or fewer edges and monopoles with 6 or fewer edges) the two methods produce identical results if $b + 1$ is substituted with α .

The recurrence equation (and therefore the partial differential equation), is proved by the edge deletion method, introduced and used by Tutte, and used

again by Walsh. In this method, maps with n edges are counted by considering the deletion of a certain edge to obtain a map with $n - 1$ edges. Then, since by induction with maps $n - 1$ edges have been counted, it is a matter of determining how many ways a map with $n - 1$ edges can be obtained from a map with n edges by edge deletion. This relationship, once determined, forms the recurrence equation, which then may be expressed as a partial differential equation that the generating series satisfies.

Summarising, we achieve two goals:

- extending and expressing Tutte's recurrence equations in partial differential equation form,
- introduction of a new parameter β defined on ordered digraphs, and marked by a variable b in the differential equations. The β and b appear to be related to the hypothetical parameter ϑ and the Jack parameter α , respectively.

Furthermore, we discuss: how (6.2) specialises to smaller sets of maps; a bound on the parameter β ; refinements of β which lead to further properties of β ; and a partial proof that the differential equation has a solution which could be a generating series for rooted maps (rather than just for the ordered digraphs over which β is defined).

A discussion of a parameter η of rooted maps, a parameter which we put forward as a candidate for the parameter ϑ , is delayed until Chapter 7. However, since η is defined as a composition involving the parameter β , the material of this chapter is a prerequisite for work on η , the candidate Map-Jack parameter.

6.1 Edge Deletion Types and the Parameter β

The recurrence equation proven in this chapter depends on an edge deletion decomposition for ordered digraphs. Tutte and Walsh both proved special cases of this recurrence by working with an equivalent decomposition for slicings and dicings, respectively (dicings are the duals of slicings and both slicings and dicings are maps with similar decorations to ordered digraphs). Here we shall work with ordered digraphs (see Definition 4.2), since they permit the more convenient manipulation of non-orientable maps. All ordered digraphs are considered in this chapter, canonical or otherwise.

Let $\mathfrak{d} \in \mathcal{D}$ be an ordered digraph, with $n \geq 2$ edges e_1, e_2, \dots, e_n . Let $\mathfrak{d}' = \mathfrak{d} - e_n$. Either \mathfrak{d}' is an ordered digraph, or has two components which, with re-indexing of edge labels, become two ordered digraphs \mathfrak{d}_1 and \mathfrak{d}_2 . For the decomposition used in this chapter, we need to classify digraphs \mathfrak{d} according to the relationship between \mathfrak{d} and \mathfrak{d}' . In particular, we are concerned with the relationship between the face partition of \mathfrak{d} and \mathfrak{d}' , and the following classification indicates the possible types of relationships between $\phi(\mathfrak{d})$ and $\phi(\mathfrak{d}')$.

Definition 6.1 (Deletion Type, Exhaustive Analysis). *Let $\mathfrak{d} \in \mathcal{D}$ be an ordered digraph with n edges. The deletion type of the ordered digraph \mathfrak{d} , which is determined by the following (clearly exhaustive) case analysis:*

1. *If $n = 1$, and:*
 - (a) *If \mathfrak{d} has one vertex, and:*
 - i. *is orientable, then \mathfrak{d} has loop deletion type.*

ii. *is non-orientable, then ∂ has cross-loop deletion type.*

(b) *If ∂ has two vertices, then ∂ has link deletion type.*

2. *If $n > 1$, and:*

(a) *If there is a vertex of degree 1 incident to the edge e_n , then ∂ has leaf deletion type.*

(b) *If e_n is not incident to a vertex of degree 1, and:*

i. *If the ends e_n are incident to two different faces in ∂' , and:*

A. *If ∂' has two components, then ∂ has bridge deletion type.*

B. *If ∂' has one component, and:*

• *If ∂' is orientable, and:*

– *If global orientation of ∂' is preserved by e_n , then ∂ has handle deletion type.*

– *If global orientation of ∂' is reversed by e_n , then ∂ has cross-handle deletion type.*

• *If ∂' is non-orientable, and:*

– *If vertex orientation in ∂ is preserved by e_n , then ∂ has handle deletion type.*

– *If vertex orientation in ∂ is reversed by e_n , then ∂ has cross-handle deletion type.*

ii. *If both ends of e_n are incident to the same face f in ∂' , and:*

A. *The face f is divided in two by e_n , then ∂ has border deletion type.*

B. The face f is not divided in two by e_n , then the ∂ has cross-border deletion type.

The highest labelled edge e_n of ∂ has the same *deletion type* as the ordered digraph ∂ . The deletion type of a general edge e_i of ∂ is defined inductively as the deletion type of e_i as an edge of $\partial' = \partial - e_n$. If ∂' has two components ∂_1, ∂_2 , then the deletion type of e_i in ∂ is the deletion type of e_i in ∂_j , where the component ∂_j contains e_i .

Digraphs ∂ of each these nine deletion types are given in Table 6.1. (The other information in the table relates to the partial differential equation is to be ignored for the moment.) We gather below, as a convenient check list, the deletion types of a digraph ∂ with n edges as follows:

Loop deletion type: ∂ consists of a planar map with one vertex and one edge (which is therefore a loop).

Cross-loop deletion type: ∂ consists of a map in the projective plane with one vertex and one edge (which is therefore a loop).

Link deletion type: ∂ consists of a planar map with two vertices linked by one edge.

Leaf deletion type: ∂ consists of ∂' having a extra vertex of degree 1 adjoined by e_n .

Border deletion type: ∂ consists of ∂' and e_n , where e_n separates one of the faces of ∂ .

Cross-border deletion type: \mathfrak{d} consists of \mathfrak{d}' and e_n , where a cross-cap has been added to one of the faces of \mathfrak{d}' , and e_n passes through the cross-cap.

Handle deletion type: \mathfrak{d} consists of \mathfrak{d}' and e_n , where a handle has joined two of the faces of \mathfrak{d}' , and e_n has been embedded into the handle.

Cross-handle deletion type: \mathfrak{d} consists of \mathfrak{d}' and e_n , where an orientation-reversing handle has joined two of the faces of \mathfrak{d}' , and e_n has been embedded in the (surface of the) handle.

Bridge deletion type: \mathfrak{d} consists of two ordered digraphs $\mathfrak{d}_1, \mathfrak{d}_2$, with a face from each joined together by a cylinder. Edge e_n is embedded into (drawn onto) the cylinder. Edges are monotonically re-labelled such that the set of combined edge labels becomes $\{e_1, \dots, e_n\}$ (as required for the ordered digraph \mathfrak{d}).

More detailed analysis of these deletion types and the relationship between $\phi(\mathfrak{d})$ and $\phi(\mathfrak{d}')$ follows in §6.2.

We now define the parameter β of ordered digraphs.

Definition 6.2. *Let \mathfrak{d} be an ordered graph with n edges. If $n = 1$ then*

$$\beta(\mathfrak{d}) = \begin{cases} 0 & \text{if } \mathfrak{d} \text{ has loop or link deletion type,} \\ 1 & \text{if } \mathfrak{d} \text{ has cross-loop deletion type.} \end{cases}$$

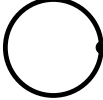
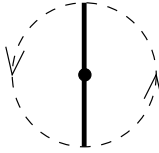

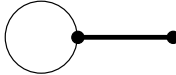
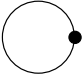
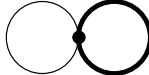
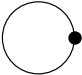
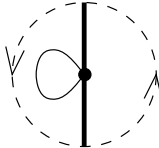
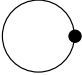
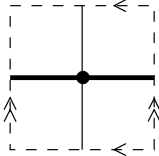
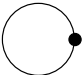
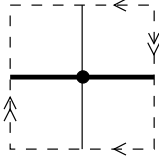
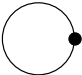
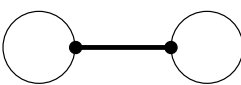
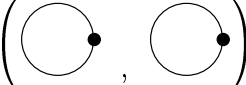
Deletion Type	Term of $\frac{\partial D}{\partial z}$	Example ∂ (edge e_n in bold)	Corresponding $\partial - e_n$
Loop	$p_1^2 v$		\emptyset
Cross-loop	$bp_2 v$		\emptyset
Link	$2p_2 tv^2$		\emptyset
Leaf	$\sum_{i \geq 1} 4ip_{i+2} tv \frac{\partial D}{\partial p_i}$		
Border	$\sum_{i, j \geq 1} (i + j - 2) p_i p_j \frac{\partial D}{\partial p_{i+j-2}}$		
Cross-border	$\sum_{i, j \geq 1} b(i + j - 2) p_{i+j} \frac{\partial D}{\partial p_{i+j-2}}$		
Handle	$\sum_{i, j \geq 1} ij p_{i+j+2} \frac{\partial^2 D}{\partial p_i \partial p_j}$		
Cross-handle	$\sum_{i, j \geq 1} bij p_{i+j+2} \frac{\partial^2 D}{\partial p_i \partial p_j}$		
Bridge	$\sum_{i, j \geq 1} 2ij p_{i+j+2} t \frac{\partial D}{\partial p_i} \frac{\partial D}{\partial p_j}$		

Table 6.1: Nine deletion types of e_n and their contribution to $\frac{\partial D}{\partial z}$

If $n > 1$ then

$$\beta(\partial) = \begin{cases} \beta(\partial') & \text{if } \partial \text{ has leaf, border, handle deletion type} \\ \beta(\partial_1) + \beta(\partial_2) & \text{if } \partial \text{ fits the bridge deletion type,} \\ \beta(\partial') + 1 & \text{if } \partial \text{ has cross-border or cross-handle deletion type.} \end{cases}$$

Equivalently, β counts the number of edges whose deletion type is among cross-loop, cross-border, and cross-handle. None of these deletion types of edges e_i in ∂ can occur if ∂ is orientable. Hence, if ∂ is orientable then $\beta(\partial) = 0$. Conversely, if $\beta(\partial) = 0$, then ∂ is orientable. Therefore β is associated with non-orientability, or more precisely, a departure from orientability.

6.2 A Partial Differential Equation

With deletion types defined, we now study the effect of edge deletion on the face partition for each deletion type. This results in a new recurrence for locally orientable maps which is succinctly expressed as a partial differential equation for a generating series of ordered digraphs, which we now define.

Edges of ∂ that are classified as a link, a leaf or a bridge, constitute *tree edges*, and all other edges are *non-tree edges*. Let $\tau(\partial)$ be the number of tree edges of a digraph ∂ . By induction, it can be seen that the tree edges form a spanning subtree of the underlying graph of ∂ . Hence the number of tree edges is $\tau(\partial) = V - 1$, where $V = \ell(\nu(\partial))$ is the number of vertices of ∂ .

Definition 6.3. *The generating series D for ordered digraphs is:*

$$D = D(\mathbf{b}, \mathbf{p}, t, \mathbf{v}, \mathbf{z}) = \sum_{\mathfrak{d} \in \mathcal{D}} \mathbf{b}^{\beta(\mathfrak{d})} \mathbf{p}_{\phi(\mathfrak{d})} t^{\tau(\mathfrak{d})} \mathbf{v}^{\ell(\nu(\mathfrak{d}))} \frac{\mathbf{z}^{n(\mathfrak{d})}}{n(\mathfrak{d})!}$$

where $\mathbf{p}_{\phi} = p_{\phi_1} p_{\phi_2} \dots$, for a partition ϕ , and \mathbf{p} represents the infinite set of indeterminates p_1, p_2, \dots .

Vertices and edges in D are marked by \mathbf{v} and \mathbf{z} , respectively. Faces of degree i , are marked by p_i , which may be (but need not be) regarded as power sum symmetric functions. The generating series D is exponential in the variable \mathbf{z} since the ordered digraph has labelled edges and these labels have a significant rôle in the edge deletion decomposition.

The variable t captures no extra information in the generating series D , because t marks $V - 1$ and \mathbf{v} marks V . All terms of D will have the factors $\mathbf{v}^V t^{V-1}$. But t is included in D to permit later substitutions $t = \frac{\mathbf{b}+1}{2}$ involved in transforming D to enumerate rooted maps. The variable t enables fractions to be avoided in the generating series D for ordered digraphs.

We now state and prove a partial differential equation for D .

Theorem 6.1. *The generating series for ordered digraphs, D , satisfies the follow-*

ing partial differential equation:

$$\begin{aligned} \frac{\partial}{\partial \mathbf{z}} D &= (p_1^2 v + b p_2 v + 2 p_2 t v^2) + \sum_{i \geq 1} 4 i p_{i+2} t v \frac{\partial D}{\partial p_i} \\ &\quad + \sum_{i, j \geq 1} (i + j - 2) \{ p_i p_j + b p_{i+j} \} \frac{\partial D}{\partial p_{i+j-2}} \\ &\quad + i j p_{i+j+2} \left\{ 2 t \left(\frac{\partial D}{\partial p_i} \right) \left(\frac{\partial D}{\partial p_j} \right) + (b + 1) \frac{\partial^2 D}{\partial p_i \partial p_j} \right\} \quad (6.2) \end{aligned}$$

Proof. The proof involves the enumerative consequences of the case analysis of edge deletion. The left hand side of (6.2) is

$$\frac{\partial}{\partial \mathbf{z}} D = \sum_{\vartheta \in \mathcal{D}} b^{\beta(\vartheta)} p_{\phi(\vartheta)} t^{\tau(\vartheta)} v^{\ell(\nu(\vartheta))} \frac{z^{n(\vartheta)-1}}{(n(\vartheta) - 1)!}.$$

The right hand side of (6.2) is obtained by summing over

- all nine deletion types (see p.133), and then for each of these deletion types:
- all instances of the digraph $\vartheta' = \vartheta - e_n$, (or pairs $(\vartheta_1, \vartheta_2)$ in the bridge deletion type), and then for each possible ϑ' :
- all ways that e_n can be added to ϑ' to form ϑ .

To complete the proof it suffices to verify that the contributions to $\frac{\partial D}{\partial \mathbf{z}}$ of each of the nine deletion types of e_n are exactly as given in Table 6.1

Loop Deletion Type

In this deletion type $n = 1$ and ϑ has one vertex and is orientable. Then $\chi = F - E + V = F$. But the sums of the degree of the faces is twice the number of

edges. Hence $\phi(\partial) = [1, 1]$ or $[2]$. In the latter case, $F = 1$ which would mean $\chi = 1$, violating the fact that orientable surfaces have even characteristic.

Therefore $\phi(\partial) = [1, 1]$, and $\chi = 2$. The underlying surface is the sphere. By definition $\beta(\partial) = 0$. The edge of ∂ is not classified as a tree edge, because it does not have leaf, link or bridge deletion type. There is one vertex and two faces of degree 1, so any ∂ belonging to this deletion type is marked by $p_1^2 v$. There is a unique ordered digraph, up to isomorphism, of the loop deletion type. Therefore the contribution of the loop deletion type to $\frac{\partial D}{\partial z}$ is

$$p_1^2 v \tag{6.3}$$

as given in Table 6.1.

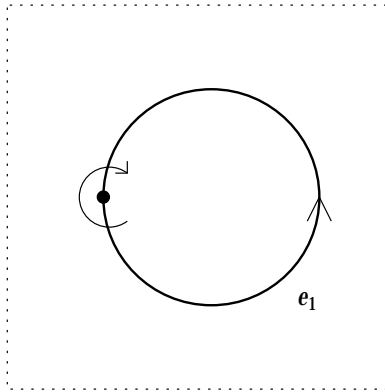


Figure 6.1: The unique ordered digraph of loop deletion type

Cross-Loop Deletion Type

Given one vertex and one edge then, according to the analysis of the loop deletion type, $\phi(\vartheta) = [2]$, because $\phi(\vartheta) = [1, 1]$ implies the loop deletion type. Then indeed $\chi = F = 1$, whose oddness implies non-orientability (as desired).

The edge of ϑ is a non-tree edge, and $\beta(\vartheta) = 1$ by definition, so any ϑ belonging to the cross-loop deletion type is marked by bp_2v .

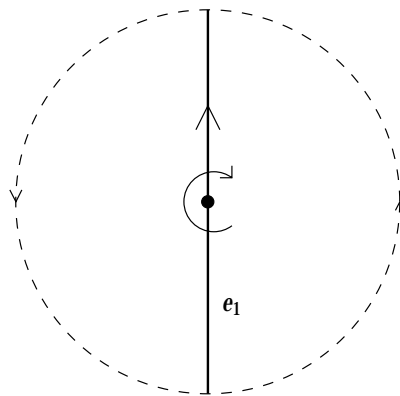


Figure 6.2: The ordered digraph of cross-loop deletion type

The ordered digraph ϑ of the cross-loop deletion type is unique. Therefore the contribution of digraphs ϑ of cross-loop deletion type to $\frac{\partial D}{\partial z}$ is

$$bp_2v \tag{6.4}$$

as given in Table 6.1.

Link Deletion Type

When $E = n = 1$ and $V = 2$, one has $\chi = F - E + V = F + 1$. Since $\chi \leq 2$, one has $F \leq 1$. And $\phi(\partial) \vdash 2n = 2$, so it follows that $\phi(\partial) = [2]$.

Hence ∂ lies on the sphere. By definition its edge is a tree edge so $\tau(\partial) = 1$, and $\beta(\partial) = 0$. Hence ∂ is marked by tp_2v^2 in the generating series D .

There are, however, *two* possible ordered digraphs belonging to the link deletion type. Recall that there are two vertices, and associated to each of these vertices is some cyclical orientation. Then as one moves from one to the other by means of the edge either these orientations are preserved or reversed. (In fact, since the surface is orientable, either one orientation is consistent or inconsistent with the other as it is extended globally over the whole surface.)

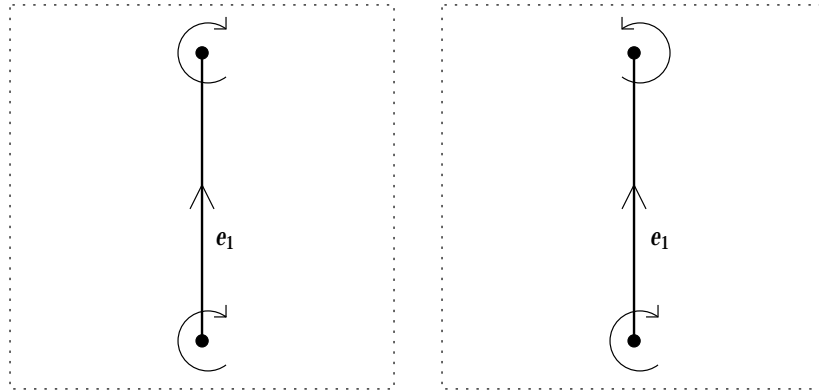


Figure 6.3: Both ordered digraphs of link deletion type

Therefore the contribution of this deletion type to $\frac{\partial D}{\partial z}$ is the term

$$2p_2tv^2 \tag{6.5}$$

as given in Table 6.1.

Leaf Deletion Type

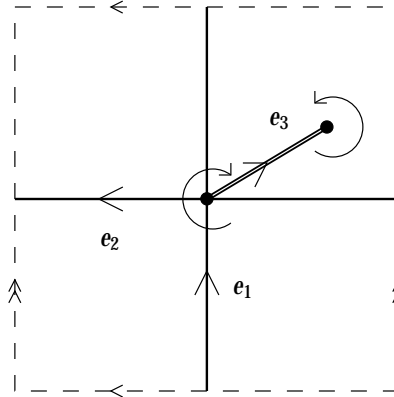


Figure 6.4: A three edge ordered digraph of leaf deletion type in the torus

When e_n has leaf deletion type, e_n must be attached to a corner of a face of the digraph $\partial' = \partial - e_n$. Let i be the degree of this face. This face of degree i in ∂' is, once edge e_n is added, transformed into a face of degree $i + 2$ in ∂ .

To account for this action enumeratively, $p_{i+2} \frac{\partial D}{\partial p_i}$ represents the replacement of a face marked with p_i by a face marked with a face marked with p_{i+2} . If ∂' has 3 faces of degree i , then the factor p_i^3 appears in its weighted contribution to D . Then p_i^3 is replaced by $3p_i^2 p_{i+2}$, the factor of three accounting for the three different choices of faces of degree i in ∂' to which e_n can be attached to form ∂ .

Each face of degree i has i corners to which e_n may be attached. This introduces a factor i .

By definition, e_n is classified as a tree edge, so the factor of t must be intro-

duced, since $\tau(\vartheta) = \tau(\vartheta') + 1$. Also, at the opposite end of e_n from ϑ' is a new vertex, which must be accounted for with a factor v .

The edge e_n in ϑ is a directed edge. It has two possible directions, towards ϑ' or away from ϑ' . This introduces a factor of 2.

Recall that ϑ is an ordered digraph, so that the new vertex of e_n must be given a cyclic orientation. This orientation may be locally consistent (along e_n) with the cyclic orientation in ϑ' of the other vertex of e_n , or it may not be. These two possibilities introduce a second and final factor of 2.

Each value of $i \geq 1$ corresponds to a distinct set of ordered digraph ϑ of link deletion type. The total contribution to $\frac{\partial D}{\partial z}$ is

$$\sum_{i \geq 1} 4ip_{i+2}tv \frac{\partial D}{\partial p_i} \quad (6.6)$$

as given in Table 6.1.

Border Deletion Type

If ϑ has border deletion type, then e_n is on the boundary of two distinct faces of ϑ , as in shown in Figure 6.5, where the dashed line represents e_n . Let the faces on either side of e_n are f_1 and f_2 . Let f_1 be the face which is earlier with respect to the vertex-local cyclical orientation at the tail of e_n . Let f_1 and f_2 have degrees i and j , respectively.

Then in $\vartheta' = \vartheta - e_n$, the removal of e_n , merges f_1 and f_2 into a single face f of degree $i + j - 2$.

For each face of f of each ϑ' , having degree $i + j - 2$, there are $i + j - 2$ corners

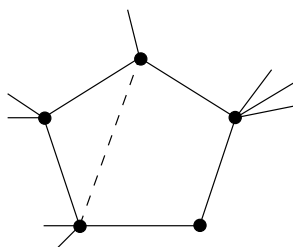


Figure 6.5: A border e_n between a triangle and a quadrangle in \mathfrak{d} , leaves a pentagon in \mathfrak{d}'

where the tail of e_n may be attached.

Therefore, using D to enumerate the choices for \mathfrak{d}' , differentiating by p_{i+j-2} selects and removes some face f in \mathfrak{d}' as above, yielding $\frac{\partial D}{\partial p_{i+j-2}}$; then, multiplying by $(i+j-2)p_i p_j$ accounts for the faces in f_1 and f_2 , and the number of choices for the position of the tail of e_n in the face of f ; then, one must consider all possible values of the degrees i and j , yielding the final contribution to $\frac{\partial D}{\partial z}$ of

$$\sum_{i,j \geq 1} (i+j-2)p_i p_j \frac{\partial D}{\partial p_{(i+j-2)}} \quad (6.7)$$

as given in Table 6.1.

Observe that for indices $i = j = 1$, there is a zero contribution to the sum (6.7). These degenerate values were already accounted for by the loop deletion type, where two adjacent faces of degree one in \mathfrak{d} were separated by $e_n (= e_1)$.

Cross-Border Deletion Type

In $\mathfrak{d}' = \mathfrak{d} - e_n$, the corners to which e_n attaches will belong again to a single face, say f .

To construct ∂ topologically, cut a circular hole out of the interior of f . Insert a *cross-cap* into this hole. This is done by topologically identifying the circular boundary of this hole with the circular boundary of a Möbius band. Then draw e_n in the resulting surface, by travelling through the cross-cap that has resulted from gluing the Möbius band to the hole.

Alternatively, attach a narrow ribbon from one segment to another segment of the boundary of the circular hole, and add a twist to the ribbon. Draw e_n along this ribbon. The new surface for f still has a single hole with one circular topological boundary, to which we attach a disk.

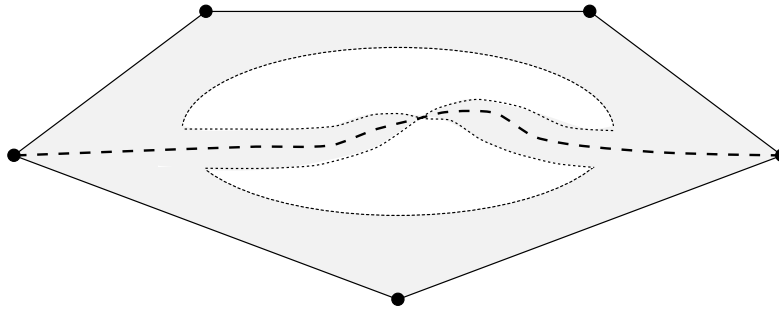


Figure 6.6: The cross-border deletion type. Cut a large hole in a face, attach a twisted ribbon.

Suppose that the single change was made to the way e_n was added to ∂' , to make e_n have border deletion type. For example, suppose that the extra twist were not applied to the ribbon. Then f would become two faces, of degrees say i and j , determined by the number of sides of f between the two corners where e_n is attached. But in the cross-border deletion type, e_n does not divide the face f , but makes a new face of degree $i + j$. The edge e_n occurs twice on the boundary

of a single face, *i.e.* the same face is incident to e_n on both sides. Hence e_n is an *isthmus*.

Nevertheless, each pair of positive values of i and j , still represents a distinct possibility for ∂ , so we still sum over all $i, j \geq 1$. As in the border deletion type, there are still $i + j - 2$, choices of a corner in f for the tail of e_n .

By definition $\beta(\partial) = \beta(\partial') + 1$, so a factor of b is introduced to account for the increase in this parameter. The parameter τ does not change.

Therefore the total contribution to $\frac{\partial D}{\partial z}$ digraphs ∂ having the cross-border deletion type is

$$\sum_{i, j \geq 1} b p_{i+j} \frac{\partial D}{\partial p_{i+j-2}} \quad (6.8)$$

as given in Table 6.1.

Handle Deletion Type

The edge e_n is again an isthmus. In $\partial' = \partial - e_n$, the single face decomposes into two faces. The corners of ∂' to which e_n 's head and tail are attached belong to distinct faces f^+ and f^- , of degrees say i and j , respectively.

Topologically, one may add a handle to the surface of ∂' . The ends of the handle are inserted into the faces f^+ and f^- . There are two topologically distinct ways to do this, depending on the choice of circular direction the ends of the handle are glued to the surface. We shall shortly determine how to decide which one applies in this deletion type. As in Figure 6.7, the edge e_n is drawn from the given corner of the former face f^- , along the length of the handle, to the given

corner of the face f^+ .

The handle therefore joins the faces f^- and f^+ , into a single face, say f , of ∂ . The degree of f is $i + j + 2$, the sum of the degrees of f^- and f^+ , plus two, for the two sides of e_n .

So far, we have explained a contribution of $p_{i+j+2} \frac{\partial^2 D}{\partial p_i \partial p_j}$. But observe that in ∂' , the face f^+ has i corners, to any of which e_n could be attached (in some ∂). Similarly, there are j choices of a corner for f^- . Thus we must multiply by ij , to account for all possible ∂ that can be obtained from each ∂' .

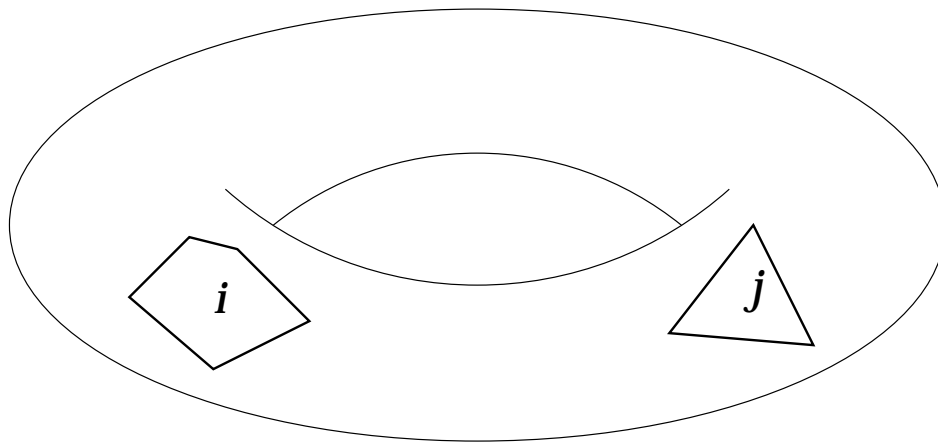
The faces f^+ and f^- may have any positive integer degrees. Therefore we must sum over $i, j \geq 1$. The total contribution to $\frac{\partial D}{\partial z}$ of digraphs ∂ of handle deletion type is

$$\sum_{i,j \geq 1} ij p_{i+j+2} \frac{\partial^2 D}{\partial p_i \partial p_j} \quad (6.9)$$

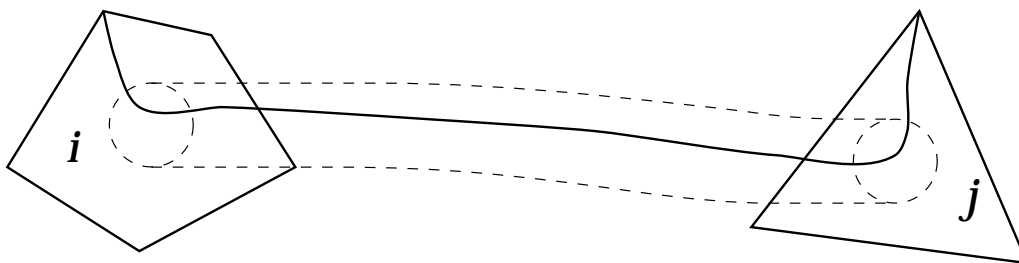
as given in Table 6.1.

The rule for topological glueing of the handle, or topological cylinder, to the surface of ∂' is as follows. First cut circular holes out of the surface of ∂' . The ends of the topological cylinder are identified with the circular boundaries of these two holes. Once the first end is attached, the second end may be attached in two ways according to the cyclical direction used to identify the circular boundaries.

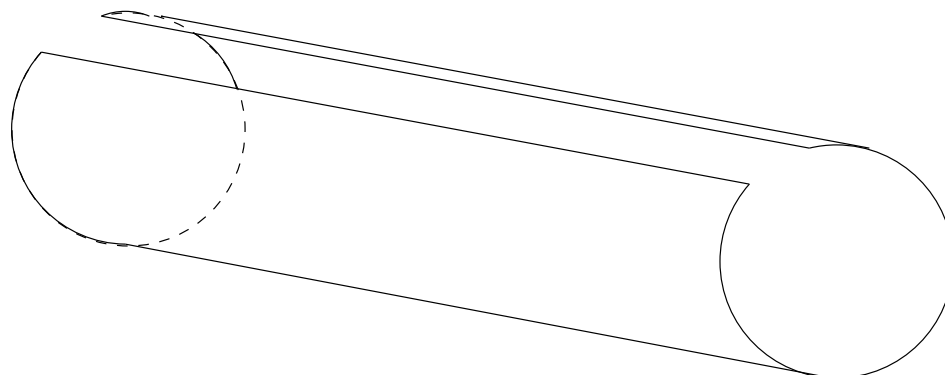
The correct direction to identify these circular boundaries in this case is the direction that causes the path along e_n in ∂ to preserve the global orientation if ∂ is orientable, and otherwise to preserve the local cyclic orientations of the vertices at both ends of e_n if ∂ is non-orientable.



(a) Distinct faces of degree i and j in a map on the torus.



(b) Attach a *handle*, and draw an edge along it.



(c) A cut cylinder is homeomorphic to a disk.

Figure 6.7: Joining two faces by a handle

Cross-Handle Deletion Type

This deletion type is identical to the handle deletion type, except that:

- The edge e_n must reverse the orientations that would be preserved for e_n of handle deletion type.
- The contribution is multiplied by b , because $\beta(\partial) = \beta(\partial') + 1$.

Hence the contribution to $\frac{\partial D}{\partial z}$ of the cross-handle deletion type is b times the contribution of the handle deletion type,

$$\sum_{i,j \geq 1} b i j p_{i+j+2} \frac{\partial^2 D}{\partial p_i \partial p_j} \quad (6.10)$$

as given in Table 6.1.

Bridge Deletion Type

In the bridge deletion type, two ordered digraphs, say ∂^- and ∂^+ , are the components $\partial - e_n$, where ∂^- and ∂^+ contain the corner to which is attached e_n 's tail and head, respectively.

The reasoning is similar to the handle and cross-handle deletion types: two faces of degrees i and j in $\partial - e_n$, are joined to form a face of degree $i + j + 2$. There are the same number ij of choices for the corners of attachment. However, the differences are:

- The joining cylinder is from one surface, that of ∂^- , to another surface, that of ∂^+ .

- The edge e_n is a tree edge, so a factor of t must be introduced.
- Both directions of attachment must be considered, the one that preserves the local orientations of the end-vertices of e_n along its length, and the one that reverses them. This leads to a factor of 2.
- The edges in ∂^- and ∂^+ must be re-labelled so that the union of the labels is $\{1, 2, \dots, n-1\}$. Enumeratively, this relabelling is taken care of by the Product Lemma for exponential generating series, since edges in D are marked exponentially by the variable z .

Thus the contribution to $\frac{\partial D}{\partial z}$ of ordered digraphs ∂ of the bridge deletion type is

$$\sum_{i,j \geq 1} 2tj p_{i+j+2} \frac{\partial D}{\partial p_i} \frac{\partial D}{\partial p_j} \quad (6.11)$$

as given in Table 6.1.

Summing (6.3)–(6.11) to get the right hand side of (6.2) completes the proof of Theorem 6.1. \square

Theorem 6.1 is presented as a natural enumerative context for the parameter β . The apparent relation of β to the Jack parameter α is another reason for presenting the recurrence equation as a partial differential equation, since Jack symmetric functions are eigenfunctions of a similar partial differential equation.

Some low degree coefficients of D are determined explicitly in §6.3 by means of the differential equation, as a concrete example of the application of Theorem 6.1.

6.3 The low degree terms of D

To illustrate the combinatorial action and computational applicability of the edge deletion method in Theorem 6.1, some coefficients of the generating series D are now computed in two ways. In §6.3.1 the coefficients $[z^1] D$ and $[z^2/2!] D$ are calculated by means of the partial differential equation (6.2). Although the computations involve many terms, all the algebraic manipulations are straightforward. In §6.3.2, the equality between the computed coefficient $[z^2/2] D$ and the defined contribution to D from the set of 80 ordered digraphs with $n = 2$ edges, and their values of the parameters ϕ , k , n and β (the parameter associated with the Jack parameter α and departure from orientability) is confirmed. The corresponding equality for the coefficient $[z^1] D$ is found directly in the proof of Theorem 6.1.

The partial differential equation for D implies a recurrence equation for its coefficients. With the symbolic algebra package `Maple` a recurrence equation in differential operator form was used to compute more coefficients of D . These coefficients of D were used to compute the coefficients of Φ , a transformation of D for rooted maps defined in §6.7. The results are tabulated in Appendix B.

6.3.1 Calculations with the partial differential equation

Write D in the form $D = \sum_{n \geq 1} D_n \frac{z^n}{n!}$. Since $[z^0] \frac{\partial}{\partial z} D = D_1$,

$$D_1 = p_1^2 v + b p_2 v + 2 p_2 t v^2 \quad (6.12)$$

by noting that, in the coefficient of z^0 in the right hand side of (6.2), all the terms with D vanish. Thus there are four ordered digraphs with one edge. In the link deletion type (one edge two vertices) the orientations of the two vertices may be preserved or reversed along the length of the edge. This accounts for the factor of 2 in the last term of (6.12).

In general, (6.2) yields a recursion for D_{n+1} in terms of differential operators evaluated at D_k for $1 \leq k \leq n$.

For example, $D_2 = [z] \frac{\partial}{\partial z} D$, so we need the coefficient of z in the right hand side of (6.2). We may discard the first group of three terms because they do not involve z . Then all remaining occurrences of D may be replaced by D_1 . (Note that $[z]$ and $\frac{\partial}{\partial u}$ commute.) The quadratic in D also vanishes, because its smallest power of z is two. Next note that $\frac{\partial D_1}{\partial p_i} = 0$ if $i \geq 3$, and the second order derivative of D_1 vanishes unless $i = j = 1$. It follows that

$$\begin{aligned}
 D_2 = & \underbrace{4p_3tv \frac{\partial D_1}{\partial p_1} + 4 \cdot 2p_4tv \frac{\partial D_1}{\partial p_2}}_{\text{leaf deletion type: } i=1 \text{ and } i=2} + \underbrace{2(1+2-2)(p_1p_2 + bp_3) \frac{\partial D_1}{\partial p_1}}_{\text{border deletion type: } \{i,j\} = \{1,2\}} \\
 & + \underbrace{(2+2-2)(p_2^2 + bp_4) \frac{\partial D_1}{\partial p_2}}_{\text{border deletion type: } i=j=2} + \\
 & \underbrace{2(1+3-2)(p_1p_3 + bp_4) \frac{\partial D_1}{\partial p_2}}_{\text{border deletion type: } \{i,j\} = \{1,3\}} + \underbrace{p_4(b+1) \frac{\partial^2}{\partial p_1^2} D_1}_{\text{handle and cross-handle deletion types: } i=j=1} \quad (6.13)
 \end{aligned}$$

Evaluating the partial derivatives:

$$\begin{aligned}
 D_2 = & 4p_2p_1^2v + 4p_2^2tv^2 + 16p_3p_1tv^2 + 16p_4t^2v^3 \\
 & + 2bp_2^2v + 8bp_3p_1v + 4bp_4tv^2 + 16bp_4tv^2 \\
 & + 2(1 + b + 3b^2)p_4v
 \end{aligned} \tag{6.14}$$

Confirmation of this is given in the next subsection.

6.3.2 Maps with two edges

We now examine ordered digraphs with two edges, to confirm that D_2 in (6.14) is correct. There are 11 distinct unrooted maps with two edges, 24 distinct rooted maps with two edges, and 80 distinct ordered digraphs with two edges. Polygonal representations of the 11 distinct unrooted maps u_1, \dots, u_{11} are given in Table 6.2.

Also in Table 6.2 is the information about the parameter ϕ (the face partition), k (the number of vertices), n (the number of edges, 2), the value of $2^{n+k-2}(n-1)!$, the number of rootings, and finally the contribution, with respect to the parameter β , of all of the ordered digraphs associated with the unrooted map u_i to the generating series D . It follows the product of the numbers in the third to last and second to last columns equals the value of the last column under the substitution $b = 1$, because both are the number of ordered digraphs associated with the unrooted map u_i .

We now compute the values of β for two edge ordered digraphs \mathfrak{d} according to the unrooted map u_i of Table 6.2 with which they are associated.

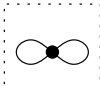

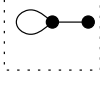
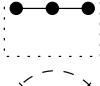



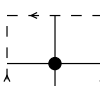
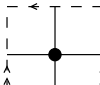
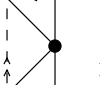
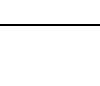
Unrooted Map	ϕ	k	n	$2^{n+k-2} \times (n-1)!$	# of Rootings	Contribution to $[p_\phi v^k \frac{z^n}{n}] D$
u_1 	[21 ²]	1	2	2	2	4
u_2 	[2 ²]	2	2	4	1	4
u_3 	[31]	2	2	4	4	16
u_4 	[4]	3	2	8	2	16
u_5 	[2 ²]	1	2	2	1	2b
u_6 	[31]	1	2	2	4	8b
u_7 	[4]	2	2	4	1	4b
u_8 	[4]	2	2	4	4	16b
u_9 	[4]	1	2	2	1	2
u_{10} 	[4]	1	2	2	2	2b + 2b ²
u_{11} 	[4]	1	2	2	2	4b ²
Totals: (at $b = 1$)					24	80

Table 6.2: Unrooted maps with two edges

u_1-u_4 : The unrooted maps in these rows are planar, and therefore orientable. It follows that $\beta(\vartheta) = 0$ for all the ordered graphs ϑ associated with these four unrooted maps.

u_5 : Let ϑ be one of the two ordered digraphs associated with this unrooted map. Then e_1 has cross-loop type, and e_2 has border type, so $\beta(\vartheta) = 1$.

u_6 : Let ϑ be one of the eight ordered digraphs associated with this unrooted map. Then e_1 and e_2 have either cross-loop and border types respectively or loop and cross-border types respectively. In either case $\beta(\vartheta) = 1$.

u_7 : Let ϑ be one of the four ordered digraphs associated with this unrooted map. Then e_1 and e_2 have link and cross-border types respectively. Thus $\beta(\vartheta) = 1$.

u_8 : Let ϑ be one of the sixteen ordered digraphs associated with this unrooted map. Then e_1 and e_2 have either link and cross-border types respectively or cross-loop and leaf types respectively. In either case $\beta(\vartheta) = 1$.

u_9 : This unrooted map is in the torus, and therefore is orientable. It follows $\beta(\vartheta) = 0$ for all ordered digraphs associated with this map.

u_{10} : Let ϑ be one of the four ordered digraphs associated with this unrooted map. Then e_1 and e_2 have either link and cross-handle types respectively or cross-loop and cross-border types respectively. In the former case $\beta(\vartheta) = 1$, and in the latter case $\beta(\vartheta) = 2$.

u_{11} : Let δ be one of the four ordered digraphs associated with this unrooted map. Then e_1 and e_2 have cross-loop and cross-border types respectively. Thus $\beta(\delta) = 2$.

6.4 Specialisations

The partial differential equation (6.2) has eight specialisations which enumerate eight different sets of ordered digraphs $\mathcal{D}, \mathcal{O}, \mathcal{P}, \mathcal{B}, \mathcal{T}, \mathcal{M}, \mathcal{W}, \mathcal{U}$, whose descriptions are given in Table 6.3. The containments among these sets is given by Fig-

\mathcal{D}	Locally orientable	\mathcal{O}	Orientable	\mathcal{P}	Planar
\mathcal{B}	Bipartite planar	\mathcal{T}	Trees	\mathcal{M}	Monopoles
\mathcal{W}	Orientable monopoles	\mathcal{U}	Planar monopoles		

Table 6.3: Eight sets of ordered digraphs

ure 6.8. Note that $\mathcal{M} \cap \mathcal{O} = \mathcal{W}$, $\mathcal{M} \cap \mathcal{P} = \mathcal{U}$, and $\mathcal{M} \cap \mathcal{B} = \emptyset$.

To place the earlier results in this context, note that Tutte exhibited [Tut62] a recurrence equation for \mathcal{P} (or more precisely, for the version of \mathcal{P} consisting of slicings — the enumeration of which differs only by a trivial scaling factor from that of ordered digraphs) and found an explicit solution for $\mathcal{B} \subset \mathcal{P}$. Walsh extended [Wal71] the recurrence equation to include all of \mathcal{O} , and found an explicit solution for $\mathcal{W} \subset \mathcal{O}$. This information is summarised in Table 6.4. Since $\mathcal{W} \cap \mathcal{B} = \emptyset$, these two explicit formulae do not have specialisations to a common set, despite the similarities in their forms.

These eight sets may be enumerated by means of the partial differential equa-

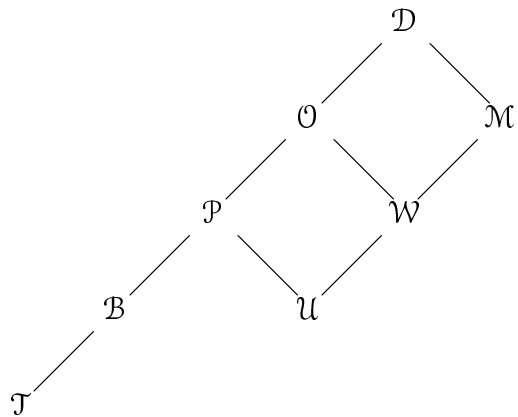


Figure 6.8: A Hasse diagram for containment between the eight sets

	[Tut62]	[Wal71]
explicit solution	\mathcal{B}	\mathcal{W}
recurrence equation	\mathcal{P}	\mathcal{O}

Table 6.4: Recurrence equations and solutions

tion, by eliminating the contribution of certain terms from (6.2). Recall that each term is associated with a particular edge deletion type. This leads to eight different partial differential equations, each of whose solutions enumerate one of restricted subsets $\mathcal{D}, \mathcal{O}, \mathcal{P}, \mathcal{B}, \mathcal{T}, \mathcal{W}, \mathcal{M}, \mathcal{U}$ of the set of ordered digraphs \mathcal{D} . Which deletion types to retain for which sets is summarised in Table 6.5. We now discuss the restrictions.

Edge deletion type	Set							
	\mathcal{D}	\mathcal{O}	\mathcal{P}	\mathcal{B}	\mathcal{T}	\mathcal{M}	\mathcal{W}	\mathcal{U}
link	✓	✓	✓	✓	✓			
leaf	✓	✓	✓	✓	✓			
bridge	✓	✓	✓	✓	✓			
border	✓	✓	✓	*		✓	✓	✓
loop	✓	✓	✓			✓	✓	✓
handle	✓	✓				✓	✓	
cross-handle	✓					✓		
cross-border	✓					✓		
cross-loop	✓					✓		

✓ Include the contribution of this deletion type
 * Include a modified contribution

Table 6.5: Eight sets and nine deletion types

We can impose restrictions on the topological surfaces of the ordered digraphs:

- to \mathcal{D} , ordered digraphs in all locally orientable surfaces (not really a restriction of sets), by setting $b = 1$ in the differential equation (6.2). (Thereby ignoring the parameter β .)
- to \mathcal{O} , ordered digraphs in orientable surfaces, by eliminating the cross-loop,

cross-border and cross-handle deletion type, or equivalently, simply by setting $b = 0$ in the differential equation (6.2). (Any of these cross-deletion types lead to a non-orientable surface for any edge e_i , which subsequent edge additions cannot correct.)

- to \mathcal{P} , ordered digraphs on planar surfaces, by eliminating the cross-loop, cross-border, cross-handle deletion types as for \mathcal{O} and, additionally, the handle deletion type. (Any edge e_i which fits the handle deletion type leads to a non-planar surface, which subsequent edge additions cannot correct.)

In a bipartite map, all the face degrees must be even. If the map is planar, then the converse of this is true. Evenness of face degrees can be ensured algebraically by setting $p_1 = p_3 = p_5 = \dots = 0$.

- For \mathcal{B} , bipartite planar ordered digraphs, we must modify the border deletion type to ensure that an even face is not separated into two odd faces by a border.
- For \mathcal{T} , ordered digraphs which are trees (characterised by being planar and one-faced) we must eliminate the border deletion type, because it creates an extra face, which subsequent edges cannot eliminate.

(Note the generating series for non-planar, even-faced ordered digraphs cannot easily be given a differential equation by the restriction $p_1 = p_3 = \dots = 0$ because, in the handle deletion type, it is possible for two odd faces to unite to form an even face. Therefore, ordered digraphs with odd faces must be included to account for all even-faced maps.)

To restrict to the sets $\mathcal{M}, \mathcal{W}, \mathcal{U}$, which are the monopole (single vertex) versions of $\mathcal{D}, \mathcal{O}, \mathcal{P}$, we must prevent those edge deletion types which lead to the creation of extra vertices:

- For the sets $\mathcal{M}, \mathcal{W}, \mathcal{U}$, additionally eliminate the link, leaf and bridge deletion types, from the the deletion types that remain for the set $\mathcal{D}, \mathcal{O}, \mathcal{P}$, respectively.

We now write out the explicit differential equations for each of the eight sets $\mathcal{D}, \mathcal{O}, \mathcal{P}, \mathcal{B}, \mathcal{J}, \mathcal{M}, \mathcal{W}, \mathcal{B}$. (We set $b = 1$ for \mathcal{D} , but for \mathcal{M} , we consider both b generally and $b = 1$.)

Surface restrictions

To count all locally orientable ordered digraphs, but without regard to the parameter β , we set $b = 1$ in (6.2). Let $A = D|_{b=1}$. Then A satisfies the partial differential equation

$$\begin{aligned} \frac{\partial A}{\partial z} = & (p_1^2 v + p_2 v + 2p_2 t v^2) + \sum_{i \geq 1} 4i p_{i+2} t v \frac{\partial A}{\partial p_i} \\ & + \sum_{i, j \geq 1} (i + j - 2) \{ p_i p_j + p_{i+j} \} \frac{\partial A}{\partial p_{i+j-2}} \\ & + i j p_{i+j+2} \left\{ 2t \left(\frac{\partial A}{\partial p_i} \right) \left(\frac{\partial A}{\partial p_j} \right) + 2 \frac{\partial^2 A}{\partial p_i \partial p_j} \right\} \quad (6.15) \end{aligned}$$

To count orientable ordered digraphs \mathcal{O} , set $b = 0$ in (6.2). This eliminates terms from the cross-loop, cross-border and cross-handle deletion types. Let

$O = D|_{b=0}$. Then O satisfies the following partial differential equation

$$\begin{aligned} \frac{\partial O}{\partial z} &= (p_1^2 v + 2p_2 tv^2) + \sum_{i \geq 1} 4ip_{i+2} tv \frac{\partial O}{\partial p_i} \\ &+ \sum_{i,j \geq 1} (i+j-2) p_i p_j \frac{\partial O}{\partial p_{i+j-2}} + ijp_{i+j+2} \left\{ 2t \left(\frac{\partial O}{\partial p_i} \right) \left(\frac{\partial O}{\partial p_j} \right) + \frac{\partial^2 O}{\partial p_i \partial p_j} \right\} \end{aligned} \quad (6.16)$$

A recurrence equation form of (6.16) was first obtained in [Wal71] (except slicings, rather than ordered digraphs, were enumerated).

To count planar ordered digraphs \mathcal{P} , take (6.16) and further eliminate the handle term. Let P be the generating series for planar ordered digraphs, then P satisfies the following differential equation:

$$\begin{aligned} \frac{\partial P}{\partial z} &= (p_1^2 v + 2p_2 tv^2) + \sum_{i \geq 1} 4ip_{i+2} tv \frac{\partial P}{\partial p_i} \\ &+ \sum_{i,j \geq 1} (i+j-2) p_i p_j \frac{\partial P}{\partial p_{i+j-2}} + ijp_{i+j+2} \left\{ 2t \left(\frac{\partial P}{\partial p_i} \right) \left(\frac{\partial P}{\partial p_j} \right) \right\} \end{aligned} \quad (6.17)$$

A recurrence equation form of (6.17) was first obtained in [Tut62] (except slicings, rather than ordered digraphs, were enumerated). Since $\mathcal{P} \subset \mathcal{O}$, the recurrence equation of Walsh corresponding to (6.16) extends the recurrence equation of Tutte corresponding to (6.17).

To count bipartite planar ordered digraphs \mathcal{B} , we take (6.17) and modify the term associated with border deletion type and eliminate the term from loop deletion type. We also re-index the summation, since only variables p_{2i} appear. Let B be the generating series for bipartite planar ordered digraphs. Then B satisfies

the following differential equation:

$$\begin{aligned} \frac{\partial B}{\partial z} = & 2p_2tv^2 + \sum_{i \geq 1} 8ip_{2i+2}tv \frac{\partial B}{\partial p_{2i}} \\ & + \sum_{i,j \geq 1} (2i+2j-2)p_{2i}p_{2j} \frac{\partial B}{\partial p_{2i+2j-2}} + 4ijp_{2i+2j+2} \left\{ 2t \left(\frac{\partial B}{\partial p_{2i}} \right) \left(\frac{\partial B}{\partial p_{2j}} \right) \right\} \end{aligned} \quad (6.18)$$

Since $\mathcal{B} \subset \mathcal{P}$, (6.18) is a restriction of (6.17). Tutte used the recurrence equation form of (6.18) to numerically compute the coefficients of B . He then surmised an expression for these coefficients and verified by induction that this expression satisfied the recurrence equation.

To enumerate the set \mathcal{T} , those ordered digraphs which are trees, take (6.18) and eliminate the term arising from the border deletion type. Let T be the generating for \mathcal{T} , then T satisfies the following differential equation:

$$\frac{\partial T}{\partial z} = 2p_2tv^2 + \sum_{i \geq 1} 8ip_{2i+2}tv \frac{\partial T}{\partial p_{2i}} + \sum_{i,j \geq 1} 4ijp_{2i+2j+2} \left\{ 2t \left(\frac{\partial T}{\partial p_{2i}} \right) \left(\frac{\partial T}{\partial p_{2j}} \right) \right\} \quad (6.19)$$

Note that the generating series T is straightforward and has the explicit form:

$$T = \sum_{n \geq 1} \frac{1}{n+1} \binom{2n}{n} 2^{2n-1} (n-1)! p_{2n} t^n v^{n+1} \frac{z^n}{n!}.$$

Monopoles

Let $M = [v^1] D$. Thus $M = M(b, \mathbf{p}, z)$ is the generating series for those ordered digraphs with a single vertex, \mathcal{M} , those which are monopoles. The variable b

marks β . Since $M = \frac{D}{v}|_{v=0}$, we can divide both sides of (6.2) by v , and set $v = 0$, to form the simpler equation

$$\frac{\partial M}{\partial z} = (p_1^2 + bp_2) + \sum_{i,j \geq 1} (i+j-2) \{p_i p_j + bp_{i+j}\} \frac{\partial M}{\partial p_{i+j-2}} + (b+1)ijp_{i+j+2} \frac{\partial^2 M}{\partial p_i \partial p_j}. \quad (6.20)$$

To enumerate \mathcal{M} without regard to the parameter β , set $b = 1$ in (6.20) above.

A further simplified equation holds for $W = [b^0] M$, which enumerates orientable ordered digraphs of a single vertex, the set \mathcal{W} .

$$\frac{\partial W}{\partial z} = p_1^2 + \sum_{i,j \geq 1} (i+j-2) p_i p_j \frac{\partial W}{\partial p_{i+j-2}} + ij p_{i+j+2} \frac{\partial^2 W}{\partial p_i \partial p_j} \quad (6.21)$$

In [Wal71], an expression for the coefficient of W is proven by inductively verifying it satisfies a recurrence equation form of (6.21).

Finally, to enumerate the set \mathcal{U} of planar single-vertex ordered digraphs, specialise (6.21) by eliminating the term from deletion of a handle deletion type edge.

$$\frac{\partial U}{\partial z} = p_1^2 + \sum_{i,j \geq 1} (i+j-2) p_i p_j \frac{\partial U}{\partial p_{i+j-2}}$$

6.5 A Bound on β

Evidently, we have $\beta(\mathfrak{d}) = 0$ for orientable ordered digraphs \mathfrak{d} and $\beta \geq 1$ for non-orientable ordered digraphs \mathfrak{d} (and of course $\beta(\mathfrak{d}) \in \mathbb{Z}$). It is natural to consider next if there are upper bounds on β . There are, as in the following lemma.

Lemma 6.2. *Let \mathfrak{d} be an ordered digraph. Then*

$$\beta(\mathfrak{d}) \leq 2 - \chi(\mathfrak{d})$$

where $\chi(\mathfrak{d})$ is the Euler characteristic of \mathfrak{d} .

Proof. Assume that \mathfrak{d} has F faces, E edges, and V vertices. Each of the E edges of \mathfrak{d} falls into one of the nine deletion types (see p.133). Sorting edges into these deletion types, will eliminate a number that cannot contribute to $\beta(\mathfrak{d})$. Since there are V vertices and the tree edges of \mathfrak{d} form a spanning subgraph, there are $V - 1$ links, leaves and bridges. None of these $V - 1$ edges contributes to $\beta(\mathfrak{d})$ (hence $\beta(\mathfrak{d}) \leq E - V + 1$). As edges are deleted from \mathfrak{d} and subsequent smaller ordered digraphs, multiple components may be created. Let \mathcal{C}_i , be the (ordered) collection of ordered digraphs during a process of successive edge deletion, with a total of i edges. Then \mathcal{C}_E has just one component, \mathfrak{d} itself. (For counting purposes, recognise as components those trivial ordered digraphs obtained from the deletion of the edge in a single edged ordered digraph.)

Let F_i and K_i be the total number of faces and components, respectively, in the collection \mathcal{C}_i . Let $G_i = F_i - K_i$. Then $G_0 = F_0 - K_0 = 0$ (because each edgeless map has one face) and $G_E = F_E - K_E = F - 1$.

Let $g_i = G_i - G_{i-1}$. Then $F - 1 = g_1 + \cdots + g_E$. But

$$g_i = \begin{cases} 1 & \text{if } e_i \text{ is a loop or border,} \\ 0 & \text{if } e_i \text{ is a leaf, link, bridge, cross-loop, or cross-border,} \\ -1 & \text{if } e_i \text{ is a handle, cross-handle.} \end{cases} \quad (6.22)$$

Thus the number of loops plus borders is at least $F - 1$. Since a link, leaf, or bridge cannot be a loop or border, the number of links, leaves, bridges, loops and borders is at least $(V - 1) + (F - 1)$.

Therefore $\beta \leq E - (V - 1) - (F - 1) = 2 - \chi$. \square

This bound $\beta \leq 2 - \chi$, depends on a fundamental topological parameter of the surface, χ , the Euler characteristic. This suggests that the parameter β could have a more topological characterisation.

Note that Lemma 6.2 implies that the coefficients $[p_\phi v^k \frac{z^n}{n!}] D$, which are polynomials in b , have degree at most $2 - \ell(\phi) + n - k$ in b . In fact, it follows from the proof of Lemma 6.2 that the degree in b of $[p_\phi v^k \frac{z^n}{n!}] D$ is exactly $2 - \chi = 2 - \ell(\phi) + n - k$. The same holds for the coefficients of the transformation Φ of the generating series D (see §6.7). If, as the evidence supports, $\Phi = \Psi^{(b+1)}|_{y_j \rightarrow y}$, then $\Psi^{(b+1)}|_{y_j \rightarrow y}$ shares the same property. If true, it would mean that the hypothetical parameter ϑ of Conjecture 1.2 would also satisfy the same bound $\vartheta \leq 2 - \chi$.

6.6 Refinements of β and corollaries

The parameter β can be expressed as a sum of two more refined parameters:

1. the number β_1 of edges with cross-loop or cross-border deletion type, and
2. the number β_2 of edges with cross-handle deletion type.

Thus $\beta(\partial) = \beta_1(\partial) + \beta_2(\partial)$. These parameters are refinements of β . A formal power series $D^*(b_1, b_2, \mathbf{p}, t, v, z)$ is straightforwardly a solution to an appropriate modification of the partial differential equation (6.2). In $D^*(b_1, b_2, \mathbf{p}, t, v, z)$, the two different variables b_1 and b_2 mark the two parameters β_1 and β_2 , respectively.

The handle and cross-handle terms may be combined into a single term

$$(b_2 + 1) \sum_{i,j \geq 1} i j p_{i+j+2} \frac{\partial^2 D^*}{\partial p_i \partial p_j}.$$

Thus D^* is a generating series in b_1 and $h = b_2 + 1$. In particular, let $\gamma(\partial)$ be the number of handles and cross-handles of an ordered digraph ∂ . Then D^* is also the generating series for \mathcal{D} with β_1 marked by b_1 , and γ marked by $h = (b_2 + 1)$.

Recall that the number of non-tree edges is $E - V + 1$, (where F, E and V are the number of faces, edges and vertices, respectively). The non-tree edges may be further divided as:

1. ζ loop or border edges,
2. β_1 cross-loop or cross-border edges,
3. γ handle or cross-handle edges.

Hence $\zeta + \beta_1 + \gamma = E - V + 1$. But according to equation (6.22),

$$F - 1 = \zeta - \gamma$$

Therefore $2 - \chi = (E - V + 1) - (F - 1) = \beta_1 + 2\gamma$. Thus terms of D^* always have factors of the form $b_1^{2-\chi-2\gamma} h^\gamma$. In other words, we have proved the following assertion.

Lemma 6.3. *The coefficients $[p_\alpha t^{V-1} v^V z^E] D^*$ are homogeneous polynomials of degree $\lfloor \frac{2-\chi}{2} \rfloor$ in b_1^2 and $(b_2 + 1)$, times a correction factor of b_1 when χ is odd.*

But $D = D^*|_{b_1, b_2=b}$, so the same coefficients of D are homogeneous polynomials of b^2 and $b + 1$, with the correction factor of 1 or b . This structure of the coefficients of D has the immediate corollaries:

Corollary 6.4. *The series $D|_{b=-1}$ enumerates only fully non-orientable ordered digraphs \mathfrak{d} , (those for which $\beta(\mathfrak{d}) = 2 - \chi(\mathfrak{d})$), with a sign factor of $(-1)^\chi$.*

Corollary 6.5. *The series $D|_{b=-\frac{1}{2}}$ enumerates all (locally orientable) ordered digraphs with the weight factor of $(-2)^{\chi-2}$.*

More generally:

Corollary 6.6. *The series D satisfies:*

$$D|_{b \rightarrow \frac{-b}{b+1}} = (b+1)^2 D \Big|_{\substack{p_i \rightarrow -(b+1)p_i, \\ z \rightarrow -(b+1)z}, \quad v \rightarrow -(b+1)v} \quad (6.23)$$

Note that the transformation of b in the left hand side of (6.23), corresponds to the transformation $\alpha \mapsto \frac{1}{\alpha}$. For Jack symmetric functions this transformation is understood [Mac95], and its effect on $\Psi^{(b+1)}$ is consistent with the right hand side of (6.23).

6.7 Rooted maps

Up to this point in the chapter, only ordered digraphs have been considered. Generally however, the focus of attention in map enumeration is rooted maps. A simple multiplicity factor, namely the number $2^{n+k-2}(n-1)!$ of ordered digraphs per rooted map with n edges and k vertices, suffices to switch from the enumeration of ordered digraphs to rooted maps. For generating series, this factor is reproduced by some elementary substitutions of the arguments of D and this leads to the following definition of a series Φ :

$$\Phi = \Phi(b) = \Phi(b, \mathbf{x}, y, z) = 2(b+1)z \frac{\partial}{\partial \mathbf{z}} D \Bigg|_{\substack{2t \mapsto b+1, & p_j \mapsto x_j \\ v \mapsto \frac{y}{b+1}, & z \mapsto z/2}}. \quad (6.24)$$

However, this does not imply Φ is a generating series of rooted maps where b marks an explicit invariant of rooted maps, because β is not defined for rooted maps. Moreover, (6.24) does not imply that Φ is a formal power series with non-negative integer coefficients in its arguments, because of the substitution $v \mapsto y/(b+1)$. But, if β is ignored by setting $b = 0$ or $b = 1$, then, as shown in §6.7.1, $\Phi(0)$ is a generating series of orientable rooted maps and $\Phi(1)$ is a generating series of locally orientable rooted maps (where, in both cases, the variable x_i

marks faces of degree i , the variable y marks vertices and the variable z marks edges).

Numerical computations of the low degree coefficients of the Jack symmetric function based generating series Ψ and the coefficients of Φ lead to the following conjecture.

Conjecture 6.1. *Let Ψ be as in (1.5).*

$$\Phi = \Psi^{(b+1)}(\mathbf{x}, \mathbf{y}, z)|_{y_j \mapsto y} \quad (6.25)$$

This is closely related to the Map-Jack Conjecture (Conjecture 1.2). It differs in two ways. First, the substitution $y_j \mapsto y$ means it concerns a less refined generating series. Second, since it is not apparent what the variable b marks in Φ because β (marked by b in D) is defined for ordered digraphs not rooted maps, Conjecture 6.1 does not yet propose a candidate for the Map-Jack parameter ϑ . (A Map-Jack parameter is proposed in Chapter 7.)

If the Map-Jack Conjecture and Conjecture 6.1 are true, then Φ is a formal power series with non-negative integer coefficients. It is not apparent whether the fact that D satisfies differential equation (6.2) implies algebraically that Φ is a formal power series with non-negative integer coefficients.

6.7.1 Rooted maps with $b = 0$ and $b = 1$

The parameter β , although a natural combinatorial parameter on \mathcal{D} , does not immediately induce a parameter on \mathcal{L} , the set of locally orientable rooted maps. A barrier to this is that the series D is exponential in z , whereas Φ is ordinary in z . In other words, a multiple of $(n - 1)!$ objects in \mathcal{D} correspond to one object in \mathcal{L} , and there are cases where β is not constant over these multiple of $(n - 1)!$ objects. Nevertheless, the following theorem about Φ , the transformation of D given by (6.24), supports the truth of Conjecture 6.1.

Theorem 6.7. *With $\Phi(b)$ defined as in (6.24), and $\widehat{\Psi}(b) = \Psi^{(b+1)}(\mathbf{x}, \mathbf{y}, z)|_{y_j \rightarrow y}$, the right hand side of (6.25),*

1. $\Phi(0) = \widehat{\Psi}(0)$, a generating series for orientable rooted maps,
2. $\Phi(1) = \widehat{\Psi}(1)$, a generating series for locally orientable rooted maps,
3. $[z^n] \Phi(b) = [z^n] \widehat{\Psi}(b)$, for $n = 1, 2, 3, 4$ and 5 and $[z^6 y] \Phi(b) = [z^6 y] \widehat{\Psi}(b)$.

Proof. For the first part, begin by noting that

$$\Phi(0) = 2z \frac{\partial}{\partial z} D|_{b=0} \left| \begin{array}{l} 2t \rightarrow 1, \\ v \rightarrow y, \end{array} \right. \begin{array}{l} p_j \rightarrow x_j \\ z \rightarrow z/2 \end{array} \quad (6.26)$$

and that $D|_{b=0}$ enumerates \mathcal{O} , orientable ordered digraphs, as implied by (6.16). The remaining transformations and substitutions of (6.26), ensure that orientable rooted maps instead of orientable ordered digraphs are enumerated. The relation is that there are $2^{n+k-2}(n - 1)!$ orientable ordered digraphs for every orientable rooted map. According to the algebraic method, $\widehat{\Psi}(0)$ also enumer-

ates orientable rooted maps (with respect to the same parameters). Therefore $\Phi(0) = \widehat{\Psi}(0)$.

The second point follows the same argument as the first point, except that all (locally orientable) ordered digraphs and rooted maps are enumerated.

The third point has been established with computer assistance. The `Maple` package `SF` of John Stembridge, described in [Ste95], was used to compute Jack symmetric functions for the determination of $[z^n]\widehat{\Psi}(b)$. The limit of this computation was $n = 5$. Similarly, the coefficients $[z^n]\Phi(b)$ were determined by `Maple`, and found to equal the coefficients $[z^n]\widehat{\Psi}(b)$. These coefficients are listed in Appendix B, up to $n = 6$. (With the recurrence equation form of (6.2), these coefficients can be computed much more efficiently than with symmetric functions.) □

A weaker result than Conjecture 6.1 is to establish that Φ has non-negative integer coefficients. Some progress in establishing this is made in §6.7.2, where advantage is taken of some simple properties of β and depth first search.

6.7.2 Towards showing the coefficients of Φ are integers

Let $D_{n,k}$ and $\Phi_{n,k}$ be given by

$$D = \sum_{n \geq 1} \sum_{k=1}^{n+1} D_{n,k}(b, \mathbf{p}) t^{k-1} v^k \frac{z^n}{n!},$$

$$\Phi = \sum_{n \geq 1} \sum_{k=1}^{n+1} \Phi_{n,k}(b, \mathbf{p}) y^k z^n.$$

The $D_{n,k}$ are polynomials in b, p_1, p_2, \dots with nonnegative integers for coefficients. We would like to establish that $\Phi_{n,k}$ has the same property.

The relation between $D_{n,k}$ and $\Phi_{n,k}$ is

$$\Phi_{n,k}(b, \mathbf{p}) = \frac{D_{n,k}(b, \mathbf{p})}{2^{n+k-2}(n-1)!}. \quad (6.27)$$

Therefore it suffices to prove that $2^{n+k-2}(n-1)! \mid D_{n,k}$ to demonstrate that $\Phi_{n,k}$ has integer coefficients. (Non-negativity is now implied by non-negativity of $D_{n,k}$ and (6.27).)

From the combinatorial interpretation of $D_{n,k}$ as a generating series for ordered digraphs, it is straightforward to show part of this divisibility criterion.

Lemma 6.8. $2^{n-1} \mid D_{n,k}(b, \mathbf{p})$.

Proof. Consider the effect of ignoring the edge directions in an ordered digraph \mathfrak{d} , except the direction of e_1 .

First, note that exactly 2^{n-1} distinct ordered digraphs \mathfrak{d}' will have the same resulting structure after this operation. This is because, each of the remaining $n-1$ edges could have been directed in two possible ways; and maintaining the direction of e_1 prevents any new symmetries from forming.

Second, observe that parameters β, τ and ϕ are independent of the edge directions. Therefore each of the 2^{n-1} ordered digraphs equivalent in the above sense make the same contribution to $D_{n,k}$. \square

As a next step to achieving the divisibility criterion, we would like find a further factor of 2^{k-1} . The idea is ignore the local cyclic orientations of all the

vertices, except v_1 which is defined by the vertex at the tail of e_1 .

Lemma 6.9. $2^{n+k-2} \mid D_{n,k}(b, \mathbf{p})$.

Proof. As above ignore all edge directions except that of e_1 and local cyclic orientations at all vertices except at v_1 , the vertex at the tail of e_1 . Note that τ and ϕ do not depend either on edge directions, or on cyclic orientations at vertices. But β does depend on the cyclic orientations of an ordered digraph \mathfrak{d} . This dependency is restricted to the handle and cross-handle deletion types. To overcome this problem, define a new parameter of non-orientability β' for ordered digraphs. For the ordered digraph \mathfrak{d} , where we have ignored all but one edge direction, and one cyclic orientation, we may define a rooted map τ , as follows.

The root position is defined to be the position at the tail of e_1 , on the side that is cyclically earlier in the local orientation of v_1 . Then, recall that upon this rooted map τ may be imposed a canonical digraph structure \mathfrak{d}' by using depth first search. The edge labels of \mathfrak{d}' may be different from those of \mathfrak{d} so ignore them. But consider the local vertex orientations. Add these to \mathfrak{d} to form an ordered digraph $\hat{\mathfrak{d}}$. These may differ from \mathfrak{d} too, but we may use them in spite of this to define a new parameter β' .

Consider the choice of $\mathfrak{d} - e_n$, where we are adding a handle or cross-handle at specific locations. There are two ways to add e_n , one incrementing β , the other not. Using β' instead, there are two further ways to add e_n , one incrementing β' and one not. Whether e_n preserves or reverses the orientations of its end-vertices in $\widehat{\mathfrak{d} - e_n}$, determines whether or not to increment β' .

For all other deletion types of e_n , the behaviour β' is identical to that of β .

Therefore, D and thus $D_{n,k}(b, \mathbf{p})$ serves as the generating series for the replacement of the parameter β by β' .

But $2^{(n-1)+(k-1)} = 2^{n+k-2}$, ordered digraphs \mathfrak{d} will be treated exactly the same by β' , since the all edge directions and vertex orientations are ignored, except for those of e_1 and v_1 , respectively. \square

The apparent next step in proving the divisibility criterion would be to additionally ignore all the edge labels of an ordered digraph \mathfrak{d} , except for the label e_1 . In effect, then we would be considering rooted maps. But a proof was not forthcoming, as it was for the previous two lemmas, in part because any other edge could serve as e_n , significantly altering the edge deletion type which \mathfrak{d} has.

6.8 PDE's for Vertex-Labelled Disconnected Ordered Digraphs

Let \mathcal{F} be the set of disconnected ordered digraphs with labelled vertices. Allow components of $\mathfrak{f} \in \mathcal{F}$ consisting of a single vertex. Let \mathcal{F}_o denote the set of those $\mathfrak{f} \in \mathcal{F}$ all of whose components are orientable. Since $\mathfrak{f} \in \mathcal{F}$ consists of unordered collections of components in $\{\bullet\} \cup \mathcal{D}$, it is easy to form a generating series F for \mathcal{F} from the generating series D for \mathcal{D} .

The motivation for considering F is its resemblance to an intermediate generating series of the algebraic method. Recall that the algebraic method begins with a generating series for disconnected collections of maps. A logarithm is then applied to the generating series in order to restrict to the connected case.

This section demonstrates a partial differential equation for F . The significance of doing this is that it is a step towards a potential proof of Conjecture 6.1, because it bypasses the complication of the logarithm. Conjecture 6.1 is equivalent to proving that

$$F = \sum_{\theta} \frac{J_{\theta}^{(b+1)}(\mathbf{x}) J_{\theta}^{(b+1)}(\mathbf{y}) J_{\theta}^{(b+1)}(\mathbf{z})}{\left\langle J_{\theta}^{(b+1)}, J_{\theta}^{(b+1)} \right\rangle_{b+1}} \Bigg|_{\substack{p_j(\mathbf{x}) \mapsto p_j, & p_j(\mathbf{y}) \mapsto y \\ p_j(\mathbf{z}) \mapsto z \delta_{j,2}}} \quad (6.28)$$

The data support this equality with F .

Let F be defined by

$$F = F(b, p_0, p_1, p_2, \dots, y, z) = \exp\{p_0 y + D\} \Bigg|_{\substack{2t \rightarrow b+1 \\ v \rightarrow \frac{y}{b+1}}}$$

Then $F|_{b=0}$ and $F|_{b=1}$ have the following interpretations as generating series:

$$F|_{b=0} = \sum_{f \in \mathcal{F}_o} p_{\phi'(f)} \frac{y^{k(f)}}{k(f)!} \frac{z^{n(f)}}{n(f)!},$$

$$F|_{b=1} = \sum_{f \in \mathcal{F}} p_{\phi'(f)} \frac{y^{k(f)}}{k(f)!} \frac{z^{n(f)}}{n(f)!}$$

where $\phi'(f)$ is the union of the face partitions of the ordered digraph of components of family f with a zeros to indicate each isolated vertices. For example, $\phi'(\bullet \bullet) = [0, 0]$, (where $\bullet \bullet$ indicates the element of \mathcal{F} consisting of two isolated vertices). The parameters $k(f)$ and $n(f)$ are the numbers of vertices and edges, respectively. Note that F is now exponential in the variable y because the vertices are labelled.

By (6.2), F satisfies the differential equation in the following lemma. Combinatorially, the distinction between the bridge deletion type and the handle and cross-handle deletion type is ignored in the differential equation for F .

Lemma 6.10. *With F as above we have*

$$\frac{\partial}{\partial z} F = \Delta(F) \quad (6.29)$$

where Δ is the differential operator:

$$\begin{aligned} \Delta = & \frac{2}{b+1} \left\{ (p_1^2 + bp_2) \frac{\partial}{\partial p_0} + p_2 \frac{\partial^2}{\partial p_0^2} \right\} + \sum_{i \geq 1} 4ip_{i+2} \frac{\partial^2}{\partial p_0 \partial p_i} \\ & + \sum_{i, j \geq 1} \left\{ 2(i+j-2)(p_i p_j + bp_{i+j}) \frac{\partial}{\partial p_{i+j-2}} + 2(b+1)ijp_{i+j+2} \frac{\partial^2}{\partial p_i \partial p_j} \right\}. \end{aligned} \quad (6.30)$$

Proof. Since $\frac{\partial}{\partial z} F = F \times \left(\frac{\partial D}{\partial z} \Big|_{\substack{2t \rightarrow b+1 \\ v \rightarrow \frac{y}{b+1}}} \right)$, we can use (6.2) to expand $\frac{\partial D}{\partial z}$ in the left hand side of (6.29) and then compare this to the right hand side.

To evaluate the right hand side, we need to understand the effect of $\frac{\partial}{\partial p_i}$ upon F . Observe that $\frac{\partial}{\partial p_0} F = yF$ and that for $i \geq 1$, we have

$$\frac{\partial}{\partial p_i} F = F \times \left(\frac{\partial D}{\partial p_i} \Big|_{\substack{2t \rightarrow b+1 \\ v \rightarrow \frac{y}{b+1}}} \right). \quad (6.31)$$

There is a second order derivative term in Δ which must be applied to F .

Using (6.31) twice, we have

$$\begin{aligned} \frac{\partial^2}{\partial p_i \partial p_j} F &= \frac{\partial}{\partial p_i} \left\{ F \times \left(\frac{\partial D}{\partial p_i} \Big|_{\substack{2t \rightarrow b+1 \\ v \rightarrow \frac{y}{b+1}}} \right) \right\} \\ &= F \times \left\{ \frac{\partial D}{\partial p_i} \frac{\partial D}{\partial p_j} + \frac{\partial^2 D}{\partial p_i \partial p_j} \right\} \Big|_{\substack{2t \rightarrow b+1 \\ v \rightarrow \frac{y}{b+1}}}. \end{aligned}$$

It therefore follows that

$$\begin{aligned} \Delta(F) &= F \times \left[\frac{2}{b+1} \{ (p_1^2 + bp_2)y + p_2y^2 \} + \sum_{i \geq 1} 4ip_{i+2}y \left(\frac{\partial D}{\partial p_i} \Big|_{\substack{2t \rightarrow b+1 \\ v \rightarrow \frac{y}{b+1}}} \right) \right. \\ &\quad + \sum_{i, j \geq 1} \left\{ 2(i+j-2)(p_i p_j + bp_{i+j}) \left(\frac{\partial D}{\partial p_{i+j-2}} \Big|_{\substack{2t \rightarrow b+1 \\ v \rightarrow \frac{y}{b+1}}} \right) \right. \\ &\quad \left. \left. + 2(b+1)ijp_{i+j+2} \left\{ \frac{\partial D}{\partial p_i} \frac{\partial D}{\partial p_j} + \frac{\partial^2 D}{\partial p_i \partial p_j} \right\} \Big|_{\substack{2t \rightarrow b+1 \\ v \rightarrow \frac{y}{b+1}}} \right\} \right] \quad (6.32) \end{aligned}$$

Comparing the right hand side of (6.2) to the right hand side of (6.32), we have

$$\Delta(F) = F \times \left(\frac{\partial D}{\partial z} \Big|_{\substack{2t \rightarrow b+1 \\ v \rightarrow \frac{y}{b+1}}} \right)$$

and hence $\frac{\partial F}{\partial z} = \Delta(F)$. □

Although the differential equation (6.29) for F suggests that there may be a way of lifting the parameter β for \mathcal{D} to a parameter for \mathcal{F} , this has not been found. So (6.29) is more interesting for its algebraic potential to prove that (6.28) is true, than for its combinatorial interpretation on \mathcal{F} .

6.9 Summary

We proved a recurrence equation for (locally orientable) ordered digraphs (maps with certain decorations). This recurrence equation is stated as a partial differential equation for generating series. This recurrence equation extends that of Walsh's [Wal71] which, in turn, extends that of Tutte's [Tut62]. We identified how to specialise the partial differential equation to these former two recurrence equation as well as others. Furthermore, we parameterised the partial differential equation with a variable b . Combinatorially, in the generating series, b marks a parameter β which we defined for ordered digraphs. This parameter β appears to be associated with the departure of an ordered digraph from orientability, because $\beta(\mathfrak{d}) = 0$ if and only \mathfrak{d} is orientable and otherwise, if \mathfrak{d} is non-orientable, $\beta(\mathfrak{d})$ is a positive integer.

We computed the small terms of the generating series with β , both by using the definition of β and by using the partial differential equation. This exhibits, for small cases, how the partial differential equation accounts for the process of edge deletion.

We analysed a few properties of β and the generating series D for ordered digraphs. We presented a transformation Φ of D which appears to equal $\Psi^{(b+1)}$ of Conjecture 1.2, the Map-Jack Conjecture. We gave partial proof that Φ has the form conjectured for $\Psi^{(b+1)}$. This has to do with the enumeration of rooted maps (rather than ordered digraphs).

We continue to use β quite extensively in Chapter 7. There, another parameter η is defined, applicable to rooted maps, in terms of a composition of two

functions, one of which is β .

Chapter 7

On a Candidate Map-Jack Parameter

Conjecture 1.2, the Map-Jack Conjecture, postulates the existence of a parameter ϑ that is associated with the non-orientability of rooted maps. This conjecture is based on extensive empirical evidence and is defined in terms of Jack symmetric functions. Jack symmetric functions, part of an active area of research in algebraic combinatorics, also arise in such diverse areas as the Calogero-Sutherland model in quantum physics [LPS95] (n particles in the unit circle acting under a certain quantum potential). More closely related to map enumeration is the determination of the Euler characteristic of the moduli spaces of real and complex algebraic curves [GHJ99]. The Jack parameter α provides a way to interpolate between these two Euler characteristics that is natural in the sense that it is reasonable to suppose that b has a geometric interpretation in this context. An interpretation for this interpolation is very desirable. The parameter ϑ may well have a major rôle in this interpretation. Thus, the hypothetical parameter ϑ is an object of considerable interest to combinatorics, to mathematical physics and to

algebraic geometry.

The candidate parameter for ϑ is the composition $\eta = \beta \circ \delta$, where β and δ are the given as follows.

- Let m be any rooted map. Then $\delta(m)$ is its canonical ordered digraph, as defined Chapter 4.
- Let \mathfrak{d} be any ordered digraph. Then $\beta(\mathfrak{d})$ is the non-orientability parameter, as defined in Chapter 6.

Convincing empirical evidence for the suitability of η is provided by a computational comparison of coefficients of the generating series $\Psi^{(b+1)}$, computed up to terms with z^5 , with the corresponding coefficients from the generating series for rooted maps with up to five edges, where b marks the parameter η . For coefficients involving z^b and higher degrees, the amount of computation required is prohibitive for either generating series.

The status of the coefficients $\psi_{\phi, \nu, n} = [x_{\phi} y_{\nu} z^n] \Psi^{(b+1)}$ is that

- they have been computed and found to be:
 - polynomials in b , with
 - non-negative integer coefficients,

but,

- no proofs of the above properties are known, and therefore, of course
- no suitable parameter ϑ of rooted maps has been found which proves the above properties.

The parameter η is the first instance of a parameter that meets these conditions for at least those rooted maps with five or fewer edges. However, in [GJ96a], two parameters (statistics) are exhibited that work for infinite sets of hypermaps. These sets are hypermaps with hyperedge partition $[1^{2n}]$ and with $[21^{2n-2}]$. Since maps may be regarded as hypermaps with hyperedge partition $[2^n]$, the two parameters in [GJ96a] are not applicable to maps.

It has been computed that the parameters η, ϕ, ν and n partition rooted maps into sets whose cardinalities equal $[b^m]\psi_{\phi, \nu, n}$, for $n \leq 4$. To see the significance of the extent of this computational verification, note that there are 214 triples (ϕ, ν, n) with $\phi, \nu \vdash 2n$ and $0 \leq n \leq 4$ and $\ell(\phi) - n + \ell(\nu) \leq 2$. The parameter η reproduces each of the coefficients of each of the polynomials $\psi_{\phi, \nu, n}$.

With the above favourable, finite amount of computation, but no complete proof of the suitability of η in sight, this chapter contains proofs of some properties of η . If η is the correct parameter for ϑ , these properties should be deducible from the formulation of $\Psi^{(b+1)}$ in terms of Jack symmetric functions. By considering several properties of η , it is hoped that the analogues of some of these properties can be proven for $\Psi^{(b+1)}$. Proof of these analogous properties requires the theory of Jack symmetric functions and would provide additional confirmation of the suitability of η for the Map-Jack Conjecture.

In fact, one of the properties of η , discussed in §7.2, is already an analogue of an existing property [GJ96a] of the coefficients $\psi_{\phi, \nu, n}$, regarding

- a simple form for the *marginal sums* of the coefficients.

This is further positive evidence for the suitability of η . Although perhaps not

as convincing as the extensive but finite collection of data discussed above, this shared property does provide confirmation across the whole of the infinite set of rooted maps.

We present three other properties of η . Each of these properties may be expressed as a decomposition for rooted maps, which preserves information about the parameter η . The three decompositions are:

- A decomposition of rooted maps into *non-separable* rooted maps.
- A decomposition to remove *digons* (faces of degree two) from rooted maps.
- A decomposition that relates two sets of rooted maps with two faces, one set where one of the faces is a digon, and the other set where one of faces is a degree one face.

Potential analogues of these properties may be expressed either in terms of particular coefficients $\psi_{\phi,\nu,n}$ or in terms of the entire series $\Psi^{(b+1)}$, although they are not proven.

The suitability of $\eta = \beta \circ \delta$ as the hypothetical parameter ϑ is phrased in terms of generating series in the following conjecture.

Conjecture 7.1. *Let*

$$H = \sum_{m \in \mathcal{L}} b^{\eta(m)} x_{\phi(m)} y_{\nu(m)} z^{\eta(m)}. \quad (7.1)$$

Then

$$H = \Psi^{(b+1)}. \quad (7.2)$$

Hence H is generating series for locally orientable, rooted maps m , with b marking the parameter η . We recall the definition (1.5) of $\Psi^{(b+1)}$ which states that

$$\Psi^{(b+1)} = 2(b+1)z \frac{\partial}{\partial z} \log \sum_{n \geq 0} \sum_{\theta \vdash n} \frac{J_{\theta}^{(b+1)}(\mathbf{x}) J_{\theta}^{(b+1)}(\mathbf{y}) J_{\theta}^{(b+1)}(\mathbf{z})}{\langle J_{\theta}^{(b+1)}, J_{\theta}^{(b+1)} \rangle_{b+1}} \Bigg|_{\substack{p_j(\mathbf{x}) \rightarrow x_j \\ p_j(\mathbf{y}) \rightarrow y_j \\ p_j(\mathbf{z}) \rightarrow z \delta_{j,2}}}$$

7.1 Small example

We now consider a coefficient of $\Psi^{(b+1)}$ of lowest degree in z , for simplicity, whose value implies that the hypothetical parameter ϑ has to depend on the root. We explain why this coefficient implies that ϑ depends on which position is the root in a rooted map, by examining the relevant rooted maps. We then demonstrate how η replicates the corresponding coefficient of H . This particular coefficient is

$$[x_{[4]}y_{[4]}z^2] \Psi^{(b+1)} = 3b^2 + b + 1 \tag{7.3}$$

The reason that this coefficient indicates the root dependence of the hypothetical parameter ϑ is that of the five rooted maps m with $\phi(m) = [4]$ and $\nu(m) = [4]$, there is only one whose associated unrooted map has a unique rooting. The

other four are partitioned as unrooted maps into two pairs by their isomorphism type, as we shall show. But (7.3) indicates that there is a single rooted map with $\vartheta(m) = 0$ and a single rooted map with $\vartheta(m) = 1$. Thus, for the other three rooted maps, the parameter ϑ must have the value of 2. It follows that for one of the above two pairs of rooted maps, the parameter ϑ has the value 2 for one member and the value 0 or 1 for the other member. These two rooted maps differ only by their root, but have different values of ϑ . This demonstrates that ϑ is root dependent.

Therefore any candidate for ϑ depends on the rooting of map. We verify below that η is indeed root dependent, for the five rooted maps mentioned above and confirm that

$$[x_{[4]}y_{[4]}z^2] H = 3b^2 + b + 1 \quad (7.4)$$

By setting $b = 1$ in (7.3) we find that there are five rooted maps m with $\phi(m) = \nu(m) = [4]$. These are given in Figure 7.1. Observe that $\chi = \ell(\phi) - n + \ell(\nu) = 1 - 2 + 1 = 0$, so the underlying surfaces of these maps are either the torus or the Klein bottle. The rooted map a in Figure 7.1(a) is embedded in the torus, and the maps b , c , d and e in Figures 7.1(b)-(d) are embedded in the Klein bottle.

Recall that root positions are indicated by rooting arrows along the root edge. (The side of the root edge on which the root position is located is the side of the root edge where the rooting arrow is drawn. The end of the root edge where the root position is located is the end of the root edge which is nearest the tail

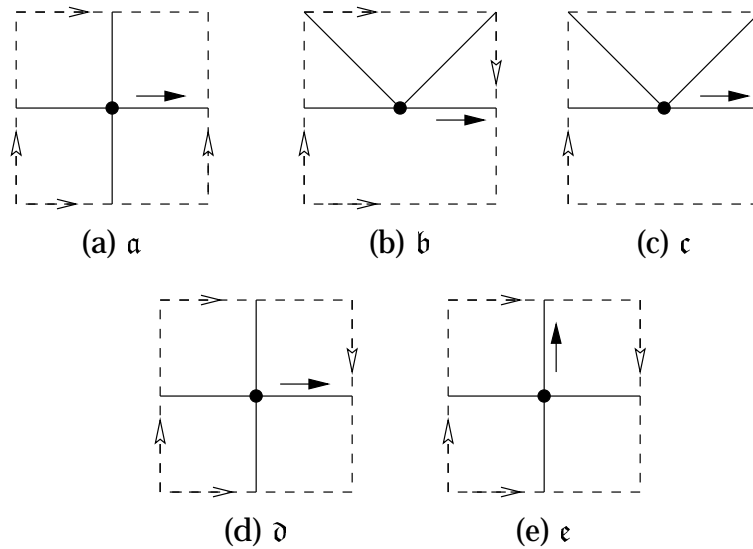


Figure 7.1: The five rooted maps m with $\phi(m) = \nu(m) = [4]$

of the rooting arrow.) Observe that rooted maps b, c of Figures 7.1(b) and (c) are the two different rootings of the same unrooted map. The same holds for d, e of Figures 7.1(d) and (e).

The five computations of η

We now confirm the suitability of η in the above sense, in that it yields (7.4). For this, compute the value of parameter of η for each of the five rooted maps a, b, c, d and e given in Figure 7.1. These values are given in Table 7.1. Since $\eta(m) = \beta(\delta(m))$, we first determine $\delta(m)$, the canonical ordered digraph for each of these five rooted maps. In order to determine $\delta(m)$, we execute Algorithm 4.1 to find the canonical position labelling ℓ_m of each rooted map. This is shown in Figure 7.2. For each of the five rooted maps, the execution of Algorithm 4.1 is

m	$\eta(m)$
a	0
b	2
c	2
d	2
e	1

Table 7.1: Five values of η

straightforward. It begins with a label 1 at the root, cycles around the sole vertex, placing labels, backtracks to the root and then terminates.

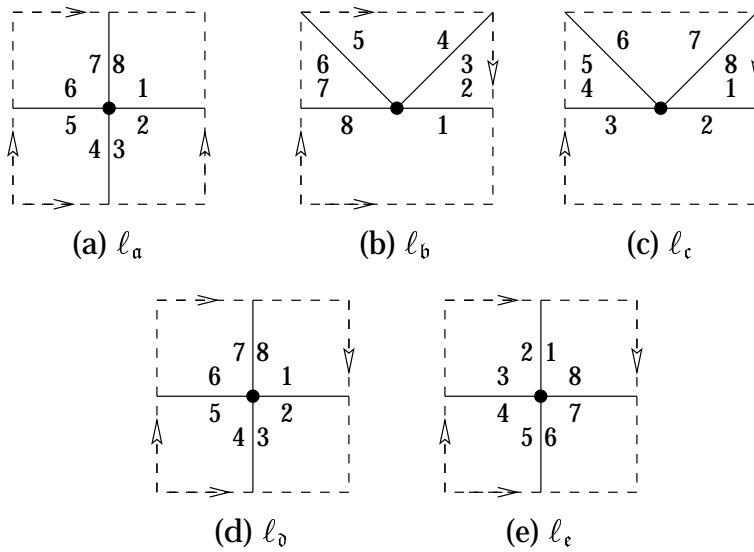


Figure 7.2: The canonical position labellings

Given l_m , the canonical ordered digraph $\delta(m)$ can be determined. The cyclic order of the canonical position labels around vertices determines the cyclic orientation of each vertex. The highest canonical position labels on the edges de-

termine their directions and the ordering. This is shown for all the maps α , b , c , ϑ and ϵ in Figure 7.3.

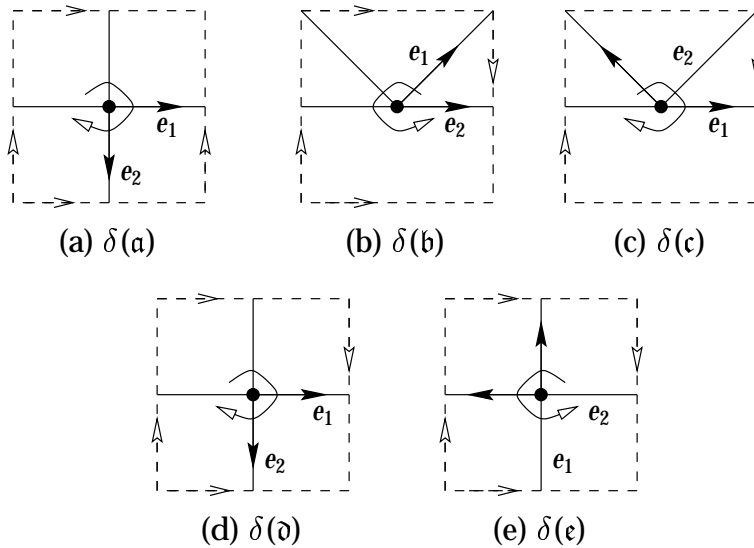


Figure 7.3: The five canonical ordered digraphs

In order to compute the value of β on each of these five ordered digraphs $\delta(m)$, we must consider the ordered digraphs $\delta(m) - e_2$ and, by doing this, determine to which of nine types the edges e_1 and e_2 belong. The five ordered digraphs $\delta(m) - e_2$ are given in Figure 7.4, in which dotted lines indicate where the ends of e_2 are to be attached. The two ordered digraphs in Figures 7.4(a) and (e) are embeddings in the sphere and show that e_1 has loop type. The three ordered digraphs of Figures 7.4(b)-(d) are embeddings in the projective plane and show that e_1 has cross-loop type.

The types which e_2 has, in each of the five ordered digraphs are:

- the handle type for e_2 in $\delta(\alpha)$,

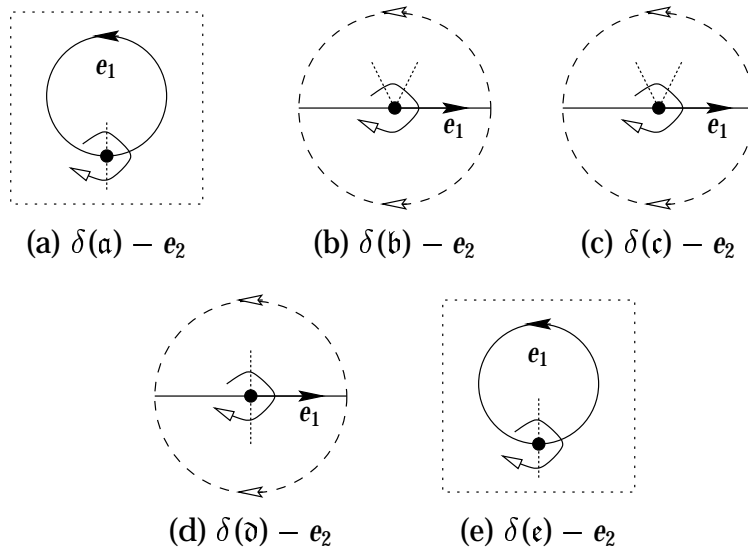


Figure 7.4: Deletion of e_2

- the cross-border type for e_2 in both of $\delta(b)$ and $\delta(c)$,
- the cross-border type for e_2 in $\delta(d)$,
- the cross-handle type for e_2 in $\delta(e)$.

We summarise these intermediate results and compute the final results in Table 7.2.

7.2 Suitability of η under specialisation of H

We now prove that η is suitable (as the Map-Jack parameter) to the extent that H and $\Psi^{(b+1)}$ are equal under the specialisation of ignoring the face partition. Equivalently, sums of the coefficients of H over all face partitions $\phi \vdash 2n$ and

m	e_1	$\beta(\delta(m) - e_1)$	e_2	$\eta(m)$
a	loop	0	handle	0
b	cross-loop	1	cross-border	2
c	cross-loop	1	cross-border	2
d	cross-loop	1	cross-border	2
e	loop	0	cross-handle	1

Table 7.2: The cases of e_1 and e_2

fixed vertex partition $\nu \vdash 2n$, are equal to the corresponding sums of coefficients of $\Psi^{(b+1)}$.

Such sums were first considered in [GJ96a], where *connection series* are defined

$$c_{\mu\nu}^\lambda(b) = \left[t^n \frac{p_\lambda(\mathbf{x}) p_\mu(\mathbf{y}) p_\nu(\mathbf{z}) |\mathcal{C}_\lambda|}{n!(1+b)^{\ell(\lambda)}} \right] \sum_{\theta \in \mathcal{P}} \frac{J_\theta^{(b+1)}(\mathbf{x}) J_\theta^{(b+1)}(\mathbf{y}) J_\theta^{(b+1)}(\mathbf{z}) t^{|\theta|}}{\langle J_\theta^{(b+1)}, J_\theta^{(b+1)} \rangle_{b+1}}.$$

These $c_{\mu\nu}^\lambda(b)$ were conjectured to be polynomials of b with non-negative integer coefficients, and are closely related to the coefficients $\psi_{\phi,\nu,n}$, both being defined as coefficients of expressions involving sums of Jack symmetric functions. (The generating series for the two families of coefficients differ by an application of a logarithm, a differential operator, and a specialisation of some of the Jack symmetric functions.)

In [GJ96a], the connection series are proven to sum as follows:

$$\sum_{\nu \vdash n} c_{\mu\nu}^\lambda(b) = |\mathcal{C}_\mu| (1+b)^{n-\ell(\lambda)}.$$

The fact that these sums of connection series are polynomials of b with non-negative integer coefficients supports the conjecture that $c_{\mu\nu}^\lambda(b)$ are polynomials with non-negative integer coefficients.

A closely related result is that the marginal sums of $\psi_{\phi,\nu,n}$ also have a similar form (7.5). For the following lemma, let $\psi_{\phi,\nu,n}(b) = \psi_{\phi,\nu,n}$. The proof is adapted from [GJ96a].

Lemma 7.1. *Let $n \geq 1$ and $\nu \vdash 2n$. Then*

$$\sum_{\phi \vdash 2n} \psi_{\phi,\nu,n}(b) = (1+b)^{n-\ell(\nu)+1} \sum_{\phi \vdash 2n} \psi_{\phi,\nu,n}(0). \quad (7.5)$$

Proof. Let

$$Q(b) = \sum_{n \geq 0} \sum_{\nu \vdash 2n} \left\{ \sum_{\phi \vdash 2n} \psi_{\phi,\nu,n}(b) \right\} y_\nu z^n$$

It suffices to prove that

$$Q(b) = (b+1)Q(0) \Big|_{\substack{y_j \rightarrow y_j/(b+1) \\ z \rightarrow (b+1)z}}.$$

On the other hand,

$$Q(b) = \Psi^{(b+1)} \Big|_{x_j \rightarrow 1}$$

Let $\mathbf{e}_1 = (1, 0, 0, \dots)$. Then $p_j(\mathbf{e}_1) = 1^j + 0^j + \dots = 1$. Thus $p_\phi(\mathbf{e}_1) = 1$ for all

partitions ϕ . The composition of the substitutions $x_j \mapsto p_j(\mathbf{x})$ and $\mathbf{x} \mapsto \mathbf{e}_1$ is $x_j \mapsto 1 = p_j(\mathbf{e}_1)$. Hence

$$Q(b) = 2(b+1)z \frac{\partial}{\partial z} \log \sum_{m \geq 0} \sum_{\theta \vdash m} \frac{J_\theta^{(b+1)}(\mathbf{e}_1) J_\theta^{(b+1)}(\mathbf{y}) J_\theta^{(b+1)}(\mathbf{z})}{\left\langle J_\theta^{(b+1)}, J_\theta^{(b+1)} \right\rangle_{b+1}} \Bigg|_{\substack{p_j(\mathbf{y}) \mapsto y_j \\ p_j(\mathbf{z}) \mapsto z_j^{\delta_{j,2}}} \quad (7.6)$$

But it is known [GJ96a] that $J_\theta^{(b+1)}(\mathbf{e}_1) = 0$ unless $\ell(\theta) = 1$. Therefore, we may delete such terms from (7.6), giving

$$Q(b) = 2(b+1)z \frac{\partial}{\partial z} \log \sum_{m \geq 0} \frac{J_{[m]}^{(b+1)}(\mathbf{e}_1) J_{[m]}^{(b+1)}(\mathbf{y}) J_{[m]}^{(b+1)}(\mathbf{z})}{\left\langle J_{[m]}^{(b+1)}, J_{[m]}^{(b+1)} \right\rangle_{b+1}} \Bigg|_{\substack{p_j(\mathbf{y}) \mapsto y_j \\ p_j(\mathbf{z}) \mapsto z_j^{\delta_{j,2}}}}$$

It is also known [GJ96a] that

$$\begin{aligned} J_{[m]}^{(b+1)} &= \sum_{\lambda \vdash m} (b+1)^{m-\ell(\lambda)} m! z_\lambda^{-1} p_\lambda, \\ J_{[m]}^{(b+1)}(\mathbf{e}_1) &= (b+1)^m \left(\frac{1}{b+1} \right)^{(m)}, \\ \left\langle J_{[m]}^{(b+1)}, J_{[m]}^{(b+1)} \right\rangle_{b+1} &= (b+1)^{2m} m! \left(\frac{1}{b+1} \right)^{(m)}, \end{aligned}$$

where $u^{(m)} = u(u+1) \dots (u+m-1)$ is the rising factorial notation.

So,

$$Q(b) = 2(b+1)z \frac{\partial}{\partial z} \log \sum_{m \geq 0} \sum_{\mu, \kappa \vdash m} \frac{(b+1)^{2m - \ell(\mu) - \ell(\kappa)} m!^2 p_\mu(\mathbf{y}) p_\kappa(\mathbf{z})}{(b+1)^m m! z_\mu z_\kappa} \Bigg|_{\substack{p_j(\mathbf{y}) \mapsto y_j \\ p_j(\mathbf{z}) \mapsto z \delta_{j,2}}} \quad (7.7)$$

Note that $p_\kappa(\mathbf{z})|_{p_j(\mathbf{z}) \mapsto z \delta_{j,2}} = 0$, unless $\kappa = [2^k]$ for some k , implying that $m = 2k$, so m is even. Now (7.7) may be simplified to

$$\begin{aligned} Q(b) &= 2(b+1)z \frac{\partial}{\partial z} \log \sum_{k \geq 0} \sum_{\mu \vdash 2k} \frac{(b+1)^{2k - \ell(\mu) - k} (2k)! y_\mu z^k}{z_\mu 2^k k!} \\ &= (b+1) \left\{ 2z \frac{\partial}{\partial z} \log \sum_{k \geq 0} \sum_{\mu \vdash 2k} \frac{(2k)! \frac{y_\mu}{(b+1)^{\ell(\mu)}} \{z(b+1)\}^k}{z_\mu 2^k k!} \right\} \\ &= (b+1) Q(0) \Bigg|_{\substack{y_j \mapsto y_j / (b+1) \\ z \mapsto z(b+1)}} \end{aligned}$$

as required. □

If $H = \Psi^{(b+1)}$, which we conjecture, then there is a corresponding relation between sums of coefficients $h_{\phi, \nu, n} = [x_\phi y_\nu z^n] H$ of H . We now prove such a relation.

Lemma 7.2. *Let $n \geq 0$ and $\nu \vdash 2n$.*

$$\sum_{\phi \vdash 2n} h_{\phi, \nu, n}(b) = (b+1)^{n - \ell(\nu) + 1} \sum_{\phi \vdash 2n} h_{\phi, \nu, n}(0). \quad (7.8)$$

Proof. Let \mathcal{E}_ν be the set of edge diagrams whose corresponding rooted maps have n edges and vertex partition ν . The sum in the left hand side of (7.8) is the gen-

erating series for the set \mathcal{E}_ν , with a single variable b which marks the parameter η . (Let $\eta(\epsilon) = \eta(\epsilon^{-1}(\epsilon))$ for any edge diagram ϵ .)

Let $\sigma : \mathcal{E}_\nu \rightarrow \mathcal{E}_\nu^o : (n, \epsilon, V, T) \mapsto (n, \epsilon, V, \emptyset)$, which deletes twists from edge diagrams, and therefore gives edge diagrams of orientable maps. We claim that for each twist-free (orientable) edge diagram $\epsilon_o = (n, \epsilon, V, \emptyset) \in \mathcal{E}_\nu^o$, the generating series for its pre-image set $\sigma^{-1}(\epsilon_o)$, where b marks η , is

$$(b + 1)^{n - \ell(\nu) + 1}. \quad (7.9)$$

To prove (7.8) it suffices to prove the claim (7.9), because the right hand side of (7.8) is (7.9) multiplied by the number of edge diagrams in \mathcal{E}_ν^o . This claim is proven by induction on the number of arcs n .

Suppose $n > 1$. Let $\epsilon \in \sigma^{-1}(\epsilon_o)$. Let a and a_o be the rightmost arcs of the edge diagrams ϵ and ϵ_o respectively. Let $\epsilon' = \epsilon - a$ and $\epsilon'_o = \epsilon_o - a_o$. Then $\sigma(\epsilon') = \epsilon'_o$. There are two cases to consider, either a and a_o possess vertices or they do not.

Case (a): The arc a possesses a vertex. It follows that the edge associated with a is classified into the leaf type by the parameter β . Therefore, $\eta(\epsilon) = \eta(\epsilon')$. This holds for all $\epsilon \in \sigma^{-1}(\epsilon_o)$. Therefore the generating series for $\sigma^{-1}(\epsilon_o)$ equals the generating series for $\sigma^{-1}(\epsilon'_o)$, which equals $(b + 1)^{(n-1) - \ell(\nu) + 1}$ by induction. This proves (7.9) for this case.

Case (b): The arc a does not possess a vertex. Now either a does or does not carry a twist. Then, depending on the classification by β of the edge associated

with a ,

$$\eta(\epsilon) = \begin{cases} \eta(\epsilon') & \text{if } a \text{ has border or handle deletion type,} \\ \eta(\epsilon') + 1 & \text{if } a \text{ has cross-border or cross-handle deletion type.} \end{cases}$$

Let $\tilde{\epsilon}$ be the edge diagram identical to ϵ except in its rightmost arc \tilde{a} which is twisted if a is not, and is not twisted if a is. Clearly this operation is a pairing, $\tilde{\tilde{\epsilon}} = \epsilon$ and the effects of deletion of a and \tilde{a} are the same, $\tilde{\epsilon}' = \epsilon'$. In fact, ϵ and $\tilde{\epsilon}$ are the unique two edge diagram solutions f determined by $f' = \epsilon'$ and $o(f) = \epsilon_o$.

Now note that a is a border if and only if \tilde{a} has cross-border type, and a is a handle if and only if \tilde{a} has cross-handle type. Thus for all $\epsilon \in \sigma^{-1}(\epsilon_o)$:

$$b^{\eta(\epsilon)} + b^{\eta(\tilde{\epsilon})} = (b + 1) \times b^{\eta(\epsilon')}.$$

Therefore the generating series for $\sigma^{-1}(\epsilon_o)$ is

$$\sum_{\epsilon \in \sigma^{-1}(\epsilon_o)} b^{\eta(\epsilon)} = (b + 1) \sum_{\epsilon' \in \sigma^{-1}(\epsilon'_o)} b^{\eta(\epsilon')}.$$

By the inductive hypothesis, this equals

$$(b + 1) \times (b + 1)^{(n-1)-\ell(\nu')+1}$$

and the proof is complete. □

7.3 Reduction of η to Non-Separable Maps

We present a useful property of η : its additivity across non-separable blocks of a map. Since maps naturally decompose into non-separable maps, this is further evidence that the parameter η is natural. An inherent enumerative limitation of this natural decomposition into non-separable maps is that the vertex and face partitions are lost. However, the number of faces and the number of vertices are preserved by the decomposition.

Thus, for the generating series, we may set $x_1 = x_2 = x_3 = \dots = x$ and $y_1 = y_2 = \dots = y$. Then the decomposition leads to a simple functional equation relating the generating series for all maps to the generating series for non-separable maps. To define the decomposition and non-separability, we first define a split-vertex.

7.3.1 Split-Vertices

In a connected graph a cut-vertex is a vertex whose removal separates the graph into two or more components. Walsh [Wal71] defined a split-vertex as a map's analogue of a graph's cut-vertex. We use the notion of the matchings graph $\Gamma(m)$ of a map m to extend Walsh's definition of a split-vertex to include non-orientable maps.

Definition 7.1. *A vertex v of a map $m = (X, \mu_1, \mu_2, \mu_3)$ is a split-vertex of m , if each of the following holds:*

1. *there exists non-empty disjoint sets P, Q , with $P \cup Q = X$,*

2. $\mu_1(P) = P$ and $\mu_3(P) = P$,
3. $\mu_2(P) \oplus P = \{p_1, p_2, q_1, q_2\}$, the symmetric difference, where $p_i \in P$ and $q_i = \mu_2(p_i) \in Q$, and
4. p_1, p_2, q_1 and q_2 are on the cycle of $\Gamma(m)$ associated with the vertex v .

We say that the sets P and Q are separated at v . The positions p_1 and p_2 are the separators for the set P .

A split-vertex of a map m is a cut-vertex of its underlying graph. The converse is not true in general. The two edges $\{p_1, q_1\}$ and $\{p_2, q_2\}$ comprise an edge cutset of the matchings graph $\Gamma(m)$.

A topological characterisation of a split-vertex v of a map m is the existence of a closed curve C in the underlying surface of S of the map m , that

1. passes once through v , entering and leaving from different corners,
2. does not pass through any other edges or vertices,
3. when removed, cuts the surface S into two components.

An example of such a curve is illustrated on a triple torus is given in Figure 7.5. A split-vertex may also be characterised as being the contraction, in the sense of [Tut84] of an edge whose deletion separates the map (a cut edge in graph theory terminology).

To determine the effect of η on a rooted map m with a split-vertex, first we show how the canonical position labelling ℓ_m is affected.

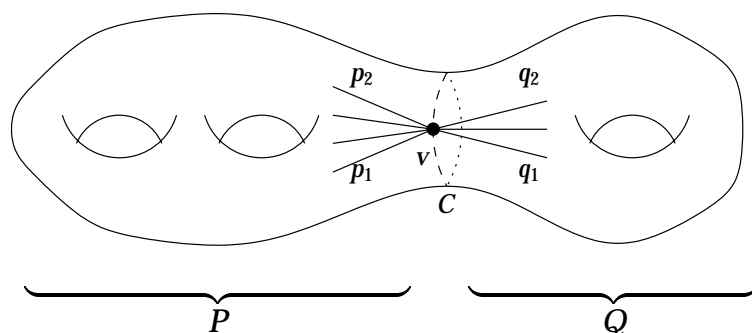


Figure 7.5: A split vertex in the triple torus

Lemma 7.3. 1. Let P and Q be separated at the split-vertex v of the rooted map $m = (X, \mu_1, \mu_2, \mu_3, r)$, where $r \in P$. Let ℓ_m be the canonical position labelling of m . Then,

$$\ell_m(Q \setminus v) = [a, b] := \{a, a + 1, \dots, b\}$$

for some $a, b \in \mathbb{N}$, where $Q \setminus v$ indicates those positions of Q not incident with the vertex v .

2. Moreover, if m_P and m_Q are the rooted submaps of m induced by the position sets P and Q , and if $P = \{r_1, r_2, \dots\}$ with $\ell_m(r_1) < \ell_m(r_2) < \dots$ and $Q = \{s_1, s_2, \dots\}$ with $\ell_m(s_1) < \ell_m(s_2) < \dots$, then $\ell_{m_P}(r_i) = i$ and $\ell_{m_Q}(s_i) = i$.

Proof. Consider the action of Algorithm 4.1 on the rooted map m . Assume the first position visited in Q is q_1 . The algorithm then cycles around v to q_2 . If there are still unvisited positions at v , then the algorithm leaves Q and visits these.

Algorithm 4.1 cannot return to Q until it backtracks to q_2 . It then visits posi-

tions in Q and eventually backtracks to q_1 , after which it visits no further positions of Q . \square

Now we are ready to show the additivity of η under splitting rooted maps at vertices.

Lemma 7.4. *With the same hypotheses as Lemma 7.3, we have*

$$\eta(m) = \eta(m_P) + \eta(m_Q)$$

Proof. The canonical ordered digraphs, $\partial_P = \delta(m_P)$ and $\partial_Q = \delta(m_Q)$ are precisely the induced ordered sub-digraphs of $\partial = \delta(m)$, by Lemma 7.3. (Thus the edges are labelled in the same order.)

Consider edge e_i of ∂ . Recall that its type is the deletion type of the component ∂_i of $\partial - \{e_{i+1}, \dots, e_n\}$ containing e_i . If ∂_i is a component of $\partial_P - \{e_{i+1}, \dots, e_n\}$ or $\partial_Q - \{e_{i+1}, \dots, e_n\}$, then e_i has the same type in ∂_P or ∂_Q , whichever it belongs to, as it has in ∂ . Otherwise ∂_i has a split-vertex v_i induced by the split-vertex v of ∂ . Precisely, there are $P_i \subset P$ and $Q_i \subset Q$, which are separated at v_i in ∂_i . Then $(\partial_i)_{P_i}$ is a component of $\partial_P - \{e_{i+1}, \dots, e_n\}$.

Suppose the edge $e_i \in (\partial_i)_{P_i}$. Then the deletion type of ∂_i is the same as $(\partial_i)_{P_i}$, except if e_i is the only edge incident to v_i in $(\partial_i)_{P_i}$. Then the deletion types of ∂_i and $(\partial_i)_{P_i}$ are, respectively, the members of the following pairs:

- bridge and leaf,
- leaf and link,

- border and loop,
- cross-border and cross-loop.

Therefore the type e_i in ∂ is one of cross-loop, cross-border or cross-handle, if and only if the type of e_i in ∂_P is one of cross-loop, cross-border or cross-handle. This applies to every edge, so $\beta(\partial) = \beta(\partial_P) + \beta(\partial_Q)$. \square

By iterating Lemma 7.4, it is possible to express $\eta(m)$ as a sum over η evaluated at several rooted submaps, until there are no further split-vertices. Thus the computation of η is reduced by this process to the special set of maps given by the following definition.

Definition 7.2. *A map m is non-separable if it has no split-vertices.*

7.3.2 Block decomposition

In the same way that graphs may be decomposed into cut-vertices and blocks (subgraphs without cut-vertices, or 2-connected subgraphs), maps may be decomposed into non-separable submaps joined at split-vertices. First, we show how to partition the set of positions.

Lemma 7.5. *Let $m = (X, \mu_1, \mu_2, \mu_3)$ be a map. Let \sim be the relation on X determined by $p \sim q$ if and only if there does not exist P, Q and v such that*

1. $p \in P$ and $q \in Q$, and
2. P and Q are separated at v .

Then \sim is an equivalence relation.

Proof. Since separated P and Q are disjoint, $p \sim p$.

The sets P and Q are separated at v , if and only if Q and P are. Thus $p \sim q \implies q \sim p$.

Suppose $p \sim r \sim q$, but $p \not\sim q$. Then there is some P, Q separated at v , with $p \in P$ and $q \in Q$. Either $r \in P$ implying $r \not\sim q$, or $r \in Q$ implying $r \not\sim p$, a contradiction. Therefore $p \sim r \sim q \implies p \sim q$. \square

The relation \sim induces a decomposition of a map into its blocks.

Definition 7.3. Let $m = (X, \mu_1, \mu_2, \mu_3)$ be a map. Let the equivalence classes of X under \sim be X_1, X_2, \dots, X_s . The blocks of m are the submaps induced by the X_i , namely

$$b_i = (X_i, \mu_1^{(i)}, \mu_2^{(i)}, \mu_3^{(i)})$$

where $\mu_k^{(i)} = \mu_k|_{X_i}$ for $k = 1, 3$ and $\mu_2^{(i)}$ is evaluated for $x \in X_i$

$$\mu_2^{(i)}(x) = (\mu_2 \mu_1)^j \mu_2(x)$$

with $j \geq 0$ is chosen to be as small as possible while meeting the constraint $\mu_2^{(i)}(x) \in X_i$,

Blocks of a map are its maximal non-separable submaps.

Let m be a rooted map. There is a natural way to assign roots to each of its blocks: this is choosing the minimum position under the canonical labelling ℓ_m of m to be the root position of each block.

Theorem 7.6. If a rooted map m has rooted non-separable blocks b_1, b_2, \dots, b_c ,

then

$$\eta(m) = \eta(b_1) + \eta(b_2) + \cdots + \eta(b_c).$$

In other words, η is additive over decomposition into non-separable submaps.

Proof. Follows immediately from Lemma 7.4. □

In particular, the study of η over rooted maps is reduced by these means to the study of η over non-separable rooted maps, and advantage is now taken of this.

7.3.3 Enumeration of non-separable maps

Now, we relate the two generating series

$$M(b, x, y, z) \quad \text{and} \quad N(b, x, y, z)$$

for the set of rooted maps and the set of non-separable, rooted maps respectively, where the variables b, x, y and z mark η , the number of faces, the number of vertices and number of edges respectively. (Thus, in contrast to some previous generating series, $M(b, x, y, z)$ does not record any information about the face and vertex partitions apart from their lengths.) We use a decomposition of rooted maps, related to the block decomposition, to prove the following result.

Corollary 7.7. *Let $M(z) = M(b, x, y, z)$ and $N(z) = N(b, x, y, z)$. Then*

$$M(z) = N\left(z\left(\frac{M(z)}{xy}\right)^2\right) \quad (7.10)$$

Proof. We do this with another decomposition of rooted maps. Take the root block b of a rooted map m (the block containing the root position). Then m consists of b with a rooted map (possibly edgeless) adjoined to every corner.

A rooted map $m = (X, \mu_1, \mu_2, \mu_3, r)$ may be partitioned into non-separable blocks, as we have seen. One of these non-separable submaps, say

$$b_1 = (X_1, \mu_1^{(1)}, \mu_2^{(1)}, \mu_3^{(1)}),$$

contains the root position of m .

Suppose that b_1 has m edges. Then it has $2m$ corners c_1, \dots, c_{2m} . At each of these corners c_i of b_1 , given by some pair of positions $\{p, p'\} \subset X_1$ with $p' = \mu_2^{(1)}(p)$, either $p' = \mu_2(p)$ or p and p' are separators for position sets P_i, Q_i , with $X_1 \subset P_i$. In the latter case, assign a root q to the induced submap $m_i = m_{Q_i}$, where q minimises ℓ_m over Q_i .

This decomposition between rooted maps and rooted, non-separable maps with two (arbitrary) rooted maps attached per edge.

Moreover $\eta(m) = \eta(b_1) + \eta(m_1) + \dots + \eta(m_{2m})$. Note, that the root vertices and faces of the maps m_i do not introduce new vertices or faces into m . (Thus we divide by xy in (7.10). \square)

This generalises a result of Walsh [Wal71] and a result of Brown and Tutte [BT64].

With the functional equation (7.10), N can be determined from M . More precisely, the coefficients $N_n = [z^n]N(x, y, z, b)$ can be expressed in terms of the coefficients $M_n = [z^n]M(x, y, z, b)$. We use Lagrange's Implicit Function Theorem to determine $N(z)$. For the following, it is convenient to write $M(x, y, z, b) = M_{x,y,b}(z) = M(z)$ and $N(x, y, z, b) = N_{x,y,b}(z) = N(z)$, and let $M_\alpha = M_{\alpha_1}M_{\alpha_2} \cdots$ where $\alpha = (\alpha_1, \alpha_2, \dots)$. Let

$$F(z) = z \left(\frac{M(z)}{xy} \right)^2,$$

then the functional equation can be written as, $M(z) = N(F(z))$. Let $G(z) = F^{\langle -1 \rangle}(z)$ be the compositional inverse of $F(z)$, which exists since $[z^0]F(z) = 0$ and $[z^1]F(z) \neq 0$. So now we have $[z^n]N(z) = [z^n]M(G(z))$ and G satisfies the functional equation

$$z = F(G(z)) = G(z) \left(\frac{M(G(z))}{xy} \right)^2$$

or, equivalently

$$G(z) = z \left(\frac{xy}{M(G(z))} \right)^2.$$

Lagrange's theorem gives:

$$\begin{aligned} [z^n]N(z) &= [z^n]M(G(z)) \\ &= \frac{1}{n} [s^{n-1}]M'(s) \left(\frac{xy}{M(s)} \right)^{2n} \end{aligned}$$

Some elementary manipulations express the coefficient of N as sum indexed by partitions involving coefficients of M :

$$\begin{aligned}
[z^n] N(z) &= \frac{1}{n} [s^{n-1}] \frac{-1}{2n} \frac{d}{ds} \left(\frac{M(s)}{xy} \right)^{-2n+1} \\
&= [s^n] \frac{-1}{2n} \left(\frac{M(s)}{xy} \right)^{-(2n-1)} \\
&= -\frac{1}{2n} [s^n] \sum_{j=0}^{\infty} \binom{-(2n-1)}{j} \left(\frac{M_1}{xy} s + \frac{M_2}{xy} s^2 + \dots \right)^j \\
&= -\frac{1}{2n} [s^n] \sum_{j=0}^{\infty} \binom{-(2n-1)}{j} \sum_{\mu \in \mathcal{P}, \ell(\mu)=j} \frac{\ell(\mu)!}{m_1(\mu)! m_2(\mu)! \dots (xy)^j} \frac{M_\mu}{s^{|\mu|}} \\
&= -\frac{1}{2n} \sum_{\mu \vdash n} \binom{-(2n-1)}{\ell(\mu)} \frac{\ell(\mu)!}{m_1(\mu)! m_2(\mu)! \dots (xy)^{\ell(\mu)}} \frac{M_\mu}{s^{|\mu|}} \\
&= \sum_{\mu \vdash n} (-1)^{\ell(\mu)-1} \frac{(2n)^{\ell(\mu)-1} M_\mu}{m_1(\mu)! m_2(\mu)! \dots (xy)^{\ell(\mu)}},
\end{aligned} \tag{7.11}$$

with the notations $M_\mu = M_{\mu_1} M_{\mu_2} \dots$, the rising factorial $n^{(k)} = n(n+1) \dots (n+k-1)$, and the multiplicity $m_i(\mu)$ of the part i in the partition μ .

Note that M is a specialisation of H . If $H = \Psi^{(b+1)}$, as conjectured, then the corresponding specialisation of $\Psi^{(b+1)}$ equals M . A functional equation may be solved to an expression similar to (7.11) with occurrences of coefficients of M replaced by coefficients of the corresponding specialisation of $\Psi^{(b+1)}$. Since, according to the conjecture, this would equal N , we expect this expression, a sum involving Jack symmetric functions, to be a polynomial in b with non-negative integer coefficients. An independent proof of this, using the theory of symmetric functions, would provide further evidence in support of Conjecture 7.1 that $H = \Psi^{(b+1)}$.

7.4 Reduction of η to Digon-Free Maps

The additivity proven in §7.3 of η for the natural decomposition into non-separable blocks supports the assertion that η is a natural parameter. Further evidence that the parameter η is natural is provided by the value it attains on maps with *digons* (faces of degree two). Digons in a map may be *deleted* topologically by removing from the surface of the map the open disk corresponding to the face of degree two. Then the two edges which make up the boundary of the digon are glued together by identification. Deleting a digon is equivalent to deleting one of the edges in its boundary.

Digon deletion is easily reversed: replace an edge with two edges bounding a single face. We call this process *digon insertion*. (The operation dual to digon insertion is more familiar in graph theory as *subdividing* an edge.) A *digon-free* map is a map without digons. Each map can be reduced to a unique digon-free map by a sequence of digon deletions and insertions. (Dually, each map is a subdivision of a map without bivalent vertices.)

A significant property of η is that it is invariant under digon deletion. Consequently, the computation of η can be reduced to digon-free maps. Moreover, this invariance property implies a simple functional equation for the generating series H of rooted maps.

7.4.1 Proof for digon deletion invariance

Lemma 7.8. *Let m' be a rooted map with digon bounded by edges e and e' . Let $m = m' - e'$. Then $\eta(m) = \eta(m')$.*

Proof. There are two cases to consider: (a) e is a canonical tree edge of m , or (b) e is a canonical non-tree edge of m .

Case (a): Canonical Tree Edge. When e is a tree edge of m , it follows that either e or e' is a tree edge of m' . Without loss of generality, assume that e is a canonical tree edge of m' . Since depth first search uses e to travel from a vertex u to a vertex v , when backtracking past e' at v , it does not travel to u , which has already been seen, nor does it backtrack along e' from u to v . Therefore e' is a canonical non-tree edge.

Suppose m' has the following canonical descending chain of rooted submaps:

$$m' = m'_{n+1} \succ m'_n \succ \cdots \succ m'_1.$$

Assume that e is the high edge of m'_i and e' the high edge of m'_j . Then $i < j$, depth first search first visits v by travelling from u along e . The end of e' at v is visited after depth first search cycles around the vertex v .

Consider the addition of e' to m'_{j-1} . The rooted map m'_{j-1} already has the edge e . In m'_j , edge e' forms a digon with e . On the other side of e' , is a face, say f' . This face arises from a face f in m'_{j-1} . Indeed e' is attached to two adjacent corners of f . In fact, e' cuts the face f into two faces: f' and the digon. Therefore the edge e' is an border edge of $\delta(m'_j)$. Since e and e' are canonical tree edges, they are either link or leaf edges of $\delta(m_i)$ and $\delta(m_j)$ respectively. Thus, e and e' make a contribution of 0 to $\eta(m')$, as does e to $\eta(m)$.

Case (b): Canonical Non-tree Edge. When e is not a canonical tree edge of m ,

neither of e or e' are canonical tree edges of m' .

Let m have the canonical descending chain of rooted submaps $m = m_n \succ \cdots \succ m_1$. If e is the high edge of submap m_i , then e and e' are the high edges of m'_i and m'_{i+1} , and without loss of generality respectively so.

Then e and e' fall into the same of the nine (eight excluding the bridge) possible cases, therefore making identical contributions to $\eta(m)$ and $\eta(m')$ respectively. As before e' belongs to the border case, therefore making no contribution to $\eta(m')$. \square

For the purpose of describing the decomposition it is convenient to use the term *bundle of adjacent digons* to mean the dual of a path of adjacent bivalent vertices. Since each map decomposes into a digon-free map with its edges replaced by bundles of adjacent digons, we get a decomposition of the generating series H for rooted maps as follows.

7.4.2 Enumeration of Digon-Free Maps

Recall that $H(b, \mathbf{x}, \mathbf{y}, z) = H(b, x_1, x_2, \dots, y_1, y_2, \dots, z)$ is an ordinary generating series for rooted maps, where b marks η , x_i marks faces of degree i , y_i vertices of degree i , and z marks edges. The generating series for digon-free rooted maps is $H|_{x_2=0}$. Every rooted map decomposes into a digon-free rooted map with its edges replaced by bundles of adjacent digons, we can express H in terms of $H|_{x_2=0}$ with a substitution as follows.

Lemma 7.9. *Writing $H(x_2, z) = H(b, \mathbf{x}, \mathbf{y}, z)$, the following holds:*

$$H(x_2, z) = H\left(0, \frac{z}{1 - x_2 z}\right)$$

Proof. The right hand side is the functional composition of $z \mapsto H(0, z)$ with $z \mapsto z/(1 - x_2 z)$. But $H(0, z)$ enumerates digon-free maps. If each edge, marked by z , is replaced by a bundle of adjacent digons, then z should be replaced by $z + x_2 z^2 + x_2^2 z^3 + \cdots = z/(1 - x_2 z)$.

But the set of all rooted maps, enumerated by $H(x_2, z)$, decomposes into the set of digon-free rooted maps with these bundles of adjacent digons substituting edges. Thus the left hand side equals the right hand side. \square

Presumably, $\Psi^{(b+1)}$ can be shown to have the similar property, but it is not immediate from the established theory of Jack symmetric functions.

7.5 Doubling Construction

On numerical examination of the coefficients of $\Psi^{(b+1)}$, one can find many striking apparent patterns. The section addresses a simple one of these. As in the previous two sections, we do not prove the property of $\Psi^{(b+1)}$, but do prove it for H by combinatorial considerations concerning η .

For a partition $\phi \vdash 2n$, let $\psi_{\phi, k} = \sum_{\nu \vdash 2n, \ell(\nu)=k} \psi_{\phi, \nu, n}$, where $\psi_{\phi, \nu, n} = [x_{\phi} y_{\nu} z^n] \Psi$,

a polynomial in b . The relationship

$$\psi_{[2n-1,1],k} = 2\psi_{[2n-2,2],k}.$$

holds from the numerical data (which is for $n \leq 5$). The corresponding relationship for coefficients of H , as determined by the parameter η , can be proven combinatorially.

Lemma 7.10. *Let H be as in (7.1). Let $h_{\phi,k} = \sum_{\nu \vdash 2n, \ell(\nu)=k} [x_{\phi} y_{\nu} z^n] H$. Then*

$$h_{[2n-1,1],k} = 2h_{[2n-2,2],k}.$$

Proof. A map m with k vertices, and face partition $\phi(m) = [2n-1, 1]$ is enumerated by $h_{[2n-1,1],k}$. The face of m of degree one, must be bounded by an edge e , which is a loop (in the usual graph theory sense of being doubly incident with a single vertex).

Recall that in $\delta(m)$ one end of e is chosen to be the tail. Re-attach the tail of e to one of the corners of the face of degree $2n-1$ which are adjacent to the tail of e . The new version e' of the former e , now bounds a digon. Thus the resulting map m' , as shown in Figure 7.6, has face partition $[2n-2, 2]$. (And m' still has k vertices.)

This procedure is in fact a two-to-one function, because the digon in m' has two edges, either of which could have been formed from the loop bounding the face of degree one in m . Thus two maps of face partition $[2n-1, 1]$ result in the

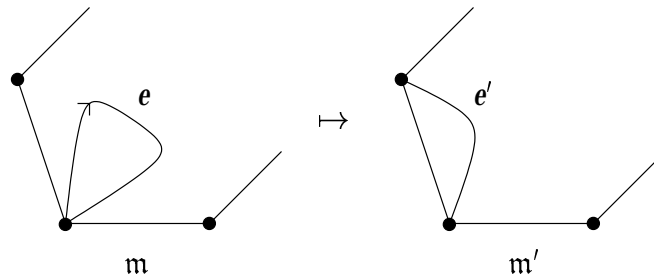


Figure 7.6: Replacing a degree one face by a digon

same map with face partition $[2n - 2, 2]$.

This action does not affect η . The edge e of m bounding the face of degree 1 makes no contribution to η , because it has either loop or border deletion type. Thus $\eta(m) = \eta(m - e)$. Note that $m' - e' = m - e$. By Lemma 7.8, $\eta(m') = \eta(m' - e')$, because e' bounds a digon. Therefore $\eta(m) = \eta(m - e) = \eta(m' - e') = \eta(m')$, as desired. \square

7.6 Summary

We defined and examined properties of a candidate Map-Jack parameter $\eta = \beta \circ \delta$. The numerical evidence as the suitability of η for the hypothetical parameter ϑ of Conjecture 1.2 is fairly convincing. We confirmed a property of η necessitated by a result from [GJ96a]. We found further properties of η which aid in simplifying its computation and provide evidence that η is a more natural parameter than the algorithm to compute η would suggest. Indeed, it would seem that η is associated with a departure from orientability of rooted maps: the number of edges whose canonical deletion type is one of cross-loop, cross-border or

cross-handle.

Moreover, concerning three properties of η , we have noted that these can be regarded as tests for the suitability of η , insofar that if any of these latter properties is proven to be false for ϑ , then the suitability of η is proven to be false. (The converse does not hold, of course; actual proof of the suitability of η requires more than the proof of these properties of ϑ .) The difficulty in testing these properties of ϑ directly is the prohibitive amount of computation required to compute all the Jack symmetric functions needed to form the generating series $\Psi^{(b+1)}$, and to compute the logarithm of the sum of scaled products of Jack symmetric functions appearing in the definition (1.5) of $\Psi^{(b+1)}$.

Chapter 8

A Bijection for Continued Fractions

Consider the numbers, $M_{v,e}$, of orientable rooted maps with v vertices and e edges. Their ordinary generating series is

$$M(y, z) = \sum_{v,e} M_{v,e} y^v z^e. \quad (8.1)$$

Previous chapters addressed enumerative results that involved the numbers (or degrees) of each of the vertices, the edges and the faces. Now information about the number of faces is suppressed, and, as a result, the numbers $M_{v,e}$ count maps without regard to genus $g = \frac{1}{2}(2 - (v - e) - f)$. While this means that the numbers $M_{v,e}$ do not count maps in such a refined way as previously considered, the generating series $M(y, z)$ has an elegant presentation as a continued fraction (8.2).

We establish a simple combinatorial interpretation of this continued fraction

as a generating series for a set of trees \mathcal{T}_l . To prove the continued fractions identity we exhibit a bijection

$$\Theta : \mathcal{M} \rightarrow \mathcal{T}_l$$

where \mathcal{M} is the set of rooted orientable maps. This bijection preserves the number of edges. Moreover, it maintains a one-to-one correspondence from vertices of a rooted map and the saturated vertices (to be defined) of trees in \mathcal{T}_l . The existence of such a bijection is implied by (8.2). The bijection Θ which we construct provides independent proof of (8.2). The problem of finding such a bijection Θ was proposed in [AB97], where (8.2) was proven with an iterative solution to a Riccati equation. Thus, Θ is a solution to that problem.

We shall define Θ by $\Theta = \lambda \circ \varepsilon$, where ε , as defined in Algorithm 4.5, sends rooted maps to edge diagrams, and λ sends edge diagrams to level labelled trees and is to be defined later. Therefore depth first search, in this chapter, as in others, has a crucial rôle. Edge deletion is applied again, not to ordered digraphs but directly to rooted maps, leading to ordinary (Ricatti) differential equations.

8.1 Continued Fractions and Trees

The main result in this chapter is a purely bijective proof the following theorem of Arquès and Didier [AB97].

Theorem 8.1 ([AB97]). *The ordinary generating series (8.1) for orientable rooted*

maps with y marking vertices and z marking edges is

$$M(y, z) = \frac{y}{1 - \frac{(y+1)z}{1 - \frac{(y+2)z}{1 - \frac{(y+3)z}{1 - \dots}}}}. \quad (8.2)$$

To prove this result bijectively with a bijection Θ , it is necessary to have another set onto which Θ sends the set of orientable rooted maps \mathcal{M} . This set consists of trees, labelled in a certain way, and is enumerated directly by the right hand side of (8.2). We now show how continued fractions are related to the enumeration of trees.

Definition 8.1. *The set $\mathcal{T}(\subset \mathcal{M})$ of rooted trees, is the set of planar rooted maps with one face.*

Rooted trees can also be characterised as rooted maps whose underlying graphs have no cycles. A rooted tree t with e edges has $e + 1$ vertices. For what follows, the set \mathcal{T} of rooted trees includes the map consisting of a single, isolated vertex (the vertex map).

Definition 8.2. *The distance (number of edges) from a vertex v of a rooted tree t from the root vertex is the level $l_t(v)$ of the vertex.*

The following well known lemma (see, for example, [GJ83]) shows that continued fractions enumerate rooted trees with respect to the number of vertices at

each level. The proof is included because it serves as the basis for the proof of Corollary 8.3.

Lemma 8.2. *Let $T = T(z, y_0, y_1, y_2, \dots)$ be the generating series for \mathcal{T} where y_i marks vertices at level i , and z marks edges. Then*

$$T = \frac{y_0}{1 - \frac{y_1 z}{1 - \frac{y_2 z}{1 - \dots}}}$$

Proof. The decomposition $\mathcal{T} \xrightarrow{\sim} \{\bullet\} \times \bigcup_{k \geq 0} \mathcal{T}^k$ is obtained by decomposing (through root vertex deletion) a tree t into its root vertex and an ordered collection of subtrees t' rooted at each neighbour of the root vertex. The root vertex is marked by y_0 . Levels in the subtree must be incremented by 1 in the tree t . ($l_t(v) = 1 + l_{t'}(v)$.) Thus, subtrees are enumerated by $T(z, y_1, y_2, \dots)$. The root vertex is joined by an edge, marked by z , to each subtree, so the decomposition for rooted trees gives:

$$T(z, y_0, y_1, \dots) = y_0 \sum_{k \geq 0} (zT(z, y_1, y_2, \dots))^k = \frac{y_0}{1 - zT(z, y_1, y_2, \dots)}.$$

This relation, when iterated, gives the result. □

The continued fraction that enumerates the set \mathcal{T} can be specialised to the right hand side of (8.2), so to accommodate this specialisation, the following modifi-

cation of the set \mathcal{T} is introduced.

Definition 8.3. *The set of level-labelled trees \mathcal{T}_l is the set of pairs (t, ℓ) where*

- $t \in \mathcal{T}$,
- $\ell : V(t) \rightarrow \mathbb{N}$ is a label function on the vertex set $(V)(t)$ of t , satisfying:
- $0 \leq \ell(v) \leq l_i(v)$ for all $v \in \mathcal{V}(t)$.

A vertex $v \in \mathcal{V}(t)$ is saturated if $\ell(v) = l_i(v)$.

A level-labelled tree t is given in Figure 8.1. This level-labelled tree has 5 sat-

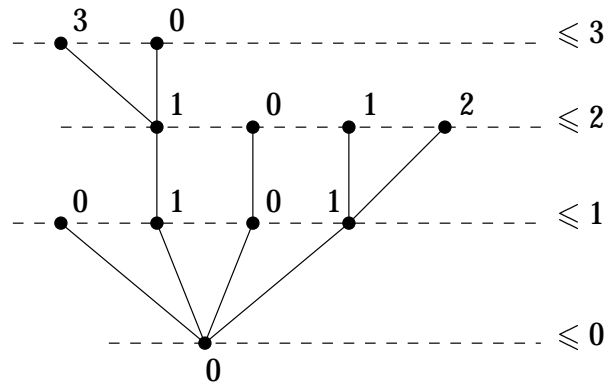


Figure 8.1: A level-labelled tree

urated vertices and 10 edges. Thus, in a generating series $T_l(y, z)$ for \mathcal{T}_l , where y marks saturated vertices and z marks edges, t is marked with $y^5 z^{10}$. The relevance of this set \mathcal{T}_l of trees lies in the following result.

Corollary 8.3. *Let $T_l(y, z)$ be the generating series for \mathcal{T}_l , where y marks saturated vertices and z marks edges. Then*

$$T_l(y, z) = \frac{y}{1 - \frac{(y+1)z}{1 - \frac{(y+2)z}{1 - \dots}}}$$

Proof. Given a rooted tree $t \in \mathcal{T}$ and a vertex $v \in \mathcal{V}(t)$ with $l_i(v) = i$, if v is to be saturated then $\ell(v) = i$, and otherwise there are the i choices for $\ell(v)$ determined by $0 \leq \ell(v) \leq i-1$. Thus y_i in T is to be replaced by $y+i$ in T_l , so $T_l(y, z) = T(z, y, y+1, y+2, \dots)$. Now apply Lemma 8.2. \square

Therefore, to prove Theorem 8.1 it suffices to find a bijection $\Theta : \mathcal{M} \rightarrow \mathcal{T}_l$ such that for all $m \in \mathcal{M}$:

- m and $\Theta(m)$ have the same number of edges, and
- the number of vertices of m equals the number of saturated vertices of $\Theta(m)$.

8.2 Ricatti Equations

We construct Θ as a composition $\Theta = \lambda \circ \varepsilon$ of two bijections. The bijection $\varepsilon : \mathcal{M} \rightarrow \mathcal{E}$, computed with Algorithm 4.5, takes orientable rooted maps into edge diagrams (without twists). The bijection $\lambda : \mathcal{E} \rightarrow \mathcal{T}_l$ takes an edge diagram to a

level-labelled tree. Crucial to construction of the second bijection λ are some decompositions for the set \mathcal{E} of edge diagrams without twists that we now develop.

Let $E(y, z)$ be the generating series for \mathcal{E} , where y marks vertices and z marks arcs (edges). Because the bijection $\varepsilon : \mathcal{M} \rightarrow \mathcal{E}$ preserves the number of vertices and edges,

$$E(y, z) = M(y, z).$$

Lemma 8.4. *The following Ricatti equation holds for $E = E(y, z)$:*

$$E = \{1 - zE\}^{-1} \left\{ y + (zE + 2z^2 \frac{\partial}{\partial z} E) \right\}$$

Proof. Decompose \mathcal{E} by considering successive leftmost arcs. A schematic dia-

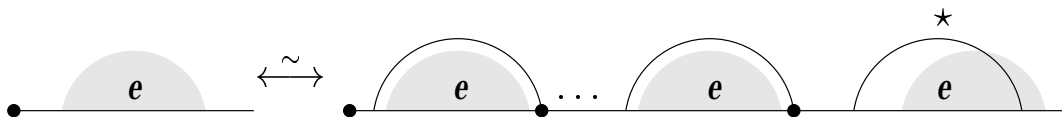


Figure 8.2: Ricatti decomposition for edge diagrams

gram for this decomposition is given in Figure 8.2. The \star indicates that terminal structure is optionally present. More precisely, if there is at least one arc, there are two cases:

1. The leftmost arc a_1 has a vertex at its right endpoint, or

2. the leftmost arc a_1 does not possess a vertex.

In the former case, no other arcs may cross a_1 . Thus a_1 encloses part of an entire edge diagram. Let a_2 be the next leftmost arc after a_1 .

Continuing, suppose a_1, a_2, \dots, a_k were all such successive leftmost arcs with vertices. Then either

- there are no more arcs to the right of a_k , or
- the next leftmost arc a_{k+1} does not possess a vertex.

Each of the enclosed edge diagrams under the arcs a_1, \dots, a_k is marked by zE , the z due to the arc a_i itself. The vertex on the arc a_i fulfils the rôle of the root vertex of the enclosed diagram.

As $k \geq 0$, the contribution from these initial arc diagrams is $\sum_{k \geq 0} (zE)^k = \{1 - zE\}^{-1}$.

If a_k is the last arc, then only the root vertex adds any further contribution. Thus the contribution is $\{1 - zE\}^{-1}y$.

If a_{k+1} exists, but does not have a vertex, consider the edge diagram e' formed by removal of the arc a_{k+1} and all the initial enclosed diagrams. If e' has n arcs, there $2n + 1$ gaps in its base line. The right endpoint of a_{k+1} could have been placed in any of these gaps, because the left endpoint is not beneath any arcs with vertices. In the terms of the generating series $E + 2z\frac{\partial}{\partial z}E$, a factor z^n is replaced with $(2n + 1)z^n$, because $(1 + 2z\frac{\partial}{\partial z})z^n = (2n + 1)z^n$. Multiply this by z to mark the arc a_{k+1} . Multiply by $\{1 - zE\}^{-1}$ for the initial enclosed edge diagrams. This completes the proof. □

The corresponding Ricatti equation was proven for $M(y, z)$ in [AB97] (by combinatorial means). It was then verified algebraically that the continued fraction solution satisfied this Ricatti equation. Because $M(y, z) = E(y, z)$, Lemma 8.4 re-proves the fact that $M(y, z)$ satisfies the corresponding Ricatti equation.

We will show how rather more can be obtained from the proof of Lemma 8.4, by using the decomposition in the proof in part of the construction of the bijection λ .

To do this, we need a second decomposition for \mathcal{E} , in terms of another set of objects. Another way to count edge diagrams in \mathcal{E} is to consider all arrangements of arcs, and then to determine how many of these arcs are permitted to possess vertices. Therefore let us consider configurations of arcs without vertices.

8.2.1 Unbroken arc configurations

Similar to, but simpler than an edge diagram, an *arc configuration* is represented by a base line, semicircular arcs attached to the same side of the base line. There are no vertices or twists, and no forbidden sub-configurations. Combinatorially, all the information in an arc configuration with n arcs is captured by a single matching $\mu \in \text{Match}(\mathcal{N}_{2n})$.

An *unbroken arc configuration* is an arc configuration such that no vertical line separates the arcs into two sets. (Or conversely, every vertical line intersecting an internal gap of the base line, also intersects an arc.) Such separating vertical lines are given for an arc configuration that fails to be unbroken in Figure 8.3. An example of an unbroken arc configuration is given in Figure 8.4. Unbroken

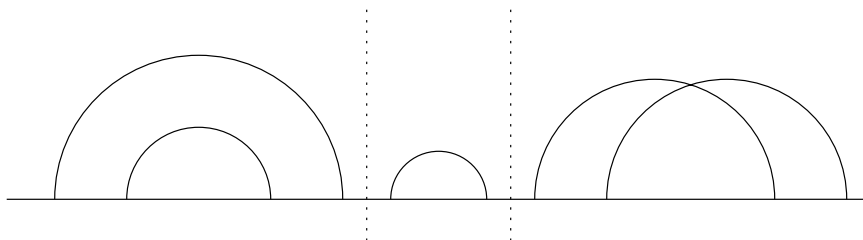


Figure 8.3: A broken arc configuration with separating vertical lines

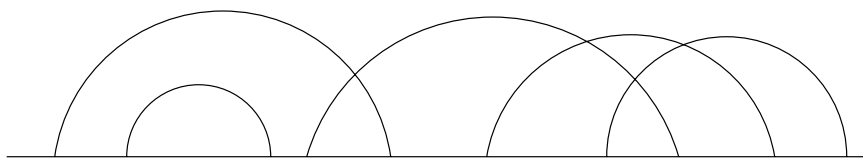


Figure 8.4: An unbroken arc configuration

arc configurations with n arcs are determined by precisely those matchings $\mu \in \text{Match}(\mathcal{N}_{2n})$ for which there does not exist $1 \leq m \leq n-1$, such that $i \leq 2m \implies \mu(i) \leq 2m$.

Let \mathcal{U} be the set of unbroken arc configurations. Let $U = U(y, z)$ be the following generating series for \mathcal{U} :

$$U(y, z) = \sum_{u \in \mathcal{U}} y^{r(u)} z^{a(u)-1}$$

where

- $r(u)$ is the number of arcs of u not crossed to the right, and therefore available to possess a vertex,

- $a(u)$ is the number of arcs of u .

For example, with u from Figure 8.4, $r(u) = 2$.

An edge diagram is formed from an arc configuration by addition of a root vertex and some vertices on certain arcs. For each arc that is not crossed to the right, it is possible to add a vertex to it or not. And since an arc configuration decomposes naturally into a chain of unbroken arc configuration, we have the following.

Lemma 8.5. $E(y, z) = y\{1 - zU(y + 1, z)\}^{-1}$.

Proof. In $U(y, z)$ each y marks a non-right crossed arc. Each of these $r(u)$ arcs may or may not have a vertex added to form an edge diagram. The former is marked by y in $E(y, z)$, the latter by 1. So, each y in $U(y, z)$ is substituted by $y + 1$.

The z in front of $zU(y + 1, z)$ ensures that the rightmost arc is marked. Then $\{1 - zU(y + 1, z)\}^{-1}$ is a geometric series, because an edge diagram breaks into a chain of unbroken configurations. Finally, the factor y marks the root vertex, which is present at the left end of every edge diagram. \square

In fact, $U(y, z)$ and $E(y, z)$ are equal. This will be shown by finding a Ricatti equation for $U(y, z)$. This Ricatti equations is proven in a way that is very similar to the the proof of the first Ricatti equation. Advantage can be taken of the comparability of the two decompositions to determine a bijection $v : \mathcal{E} \rightarrow \mathcal{U}$.

8.2.2 A second Ricatti equation

A similar Ricatti equation for $U(y, z)$ is proven with a very similar decomposition for \mathcal{u} .

Lemma 8.6. *The following Ricatti equation holds for $U = U(y, z)$:*

$$U = \{1 - zU\}^{-1} \left\{ y + (zU + 2z^2 \frac{\partial}{\partial z} U) \right\}.$$

Proof. Decompose \mathcal{u} by considering the leftmost arc a of an unbroken arc configuration u . A schematic diagram for this decomposition is given in Figure 8.5.

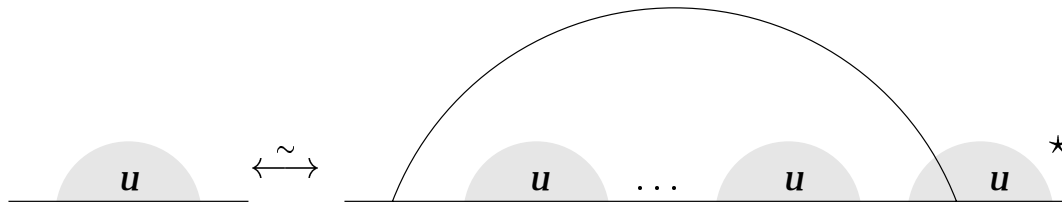


Figure 8.5: Ricatti decomposition for edge diagrams

The \star indicates that terminal structure is optionally present.

Removal of the arc a from u results in a possibly broken arc configuration. This broken arc configuration is decomposed into an ordered collection of unbroken arc configurations. There are two cases to consider for the location of the other endpoint of a .

1. The arc a intersects none of the other arcs.
2. The arc a intersects the last unbroken arc configuration.

In both cases there is a (possibly empty) ordered collection of unbroken arc configurations beneath the first arc a . These initial configurations lead to a factor of $\{1 - zU\}^{-1}$. The multiplication by z ensures all the arcs in the initial configurations are counted.

In Case 1, arc a is not crossed to the right, so is marked by y . No z is necessary, because the power of z is already $a(u) - 1$.

In Case 2, arc a is crossed to the right, so is not marked by y . We mark a by z . Since a intersects the last unbroken arc configuration u' , its right endpoint is in one of the gaps internal to u' . If u' has $n + 1$ arcs, then there are $2n + 1$ of these internal gaps. Since u' is marked by z^n in U , the term $U + 2z\frac{\partial}{\partial z}U$ counts the possible u' together with a selected internal gap. \square

As formal power series, $E(y, z)$ and $U(y, z)$ are determined uniquely by their Ricatti equations. Therefore, it follows that $E(y, z) = U(y, z)$. This equality is substituted back into Lemma 8.5 to yield:

$$E(y, z) = y\{1 - zE(y + 1, z)\}^{-1} \tag{8.3}$$

which proves immediately, in conjunction with $M(y, z) = E(y, z)$, the continued fraction in Theorem 8.1. This proof is different from that of [AB97], but not yet the bijective proof we seek.

For a fully bijective proof, we need a combinatorial decomposition corresponding to (8.3). Since we used $E(y, z) = U(y, z)$ to prove (8.3), all that is needed is a bijection $v : \mathcal{E} \rightarrow \mathcal{U}$.

8.2.3 The bijection $v : \mathcal{E} \rightarrow \mathcal{U}$

The bijection $v : \mathcal{E} \rightarrow \mathcal{U}$ is defined recursively, and by the comparability of the Ricatti decompositions for \mathcal{E} and \mathcal{U} .

Compare the decompositions for \mathcal{E} and \mathcal{U} . These are given together in Figure 8.6.

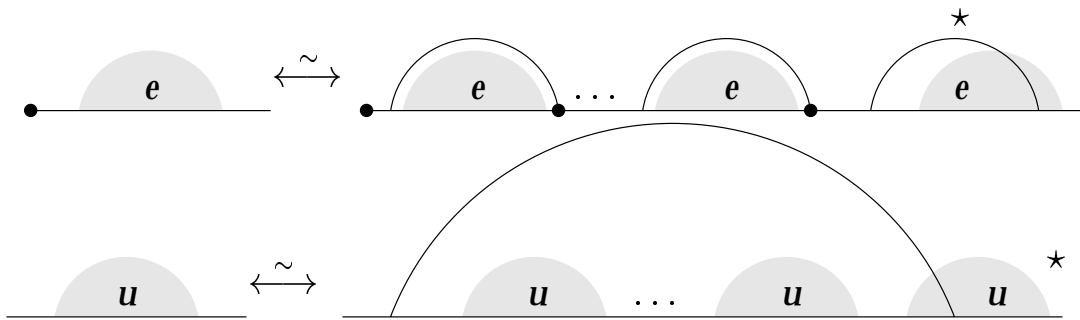


Figure 8.6: Comparison of the two Ricatti decompositions

In the decomposition for \mathcal{E} , an edge diagram e is decomposed into a sequence of edge diagrams (e_1, \dots, e_k, e^*) , where the last e^* is either absent or, if e^* has n edges, one of its $2n + 1$ gaps between its arcs is selected for the location of the right endpoint of an arc, as given in Figure 8.6.

In the decomposition for \mathcal{U} , an unbroken arc configuration u is decomposed into a sequence of unbroken arc configurations (u_1, \dots, u_k, u^*) , where the last one u^* is either absent or, if u^* has $n + 1$ arcs, one of its $2n + 1$ internal (not initial or final) gaps between its arcs is selected for the location of the right endpoint of the leftmost arc of u , as given in Figure 8.6.

In both cases, the numbers of possible selected gaps for e^* and u^* is $(2n + 1)$.

Algorithm 8.1 (Computation of $u = v(\epsilon)$). *The unbroken arc configuration $u = v(\epsilon)$ is the one whose decomposition is*

$$(v(\epsilon_1), \dots, v(\epsilon_k), v(\epsilon)^*)$$

where, if gap i of ϵ^* is selected, then $v(\epsilon)^*$ has internal gap i selected.

Moreover, in executing v , we maintain a correspondence between the vertices of ϵ and the $r(u)$ arcs of u which are not right-crossed.

Small cases of the correspondence v are given in Table 8.1. The correspon-


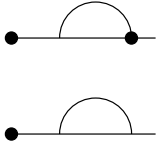
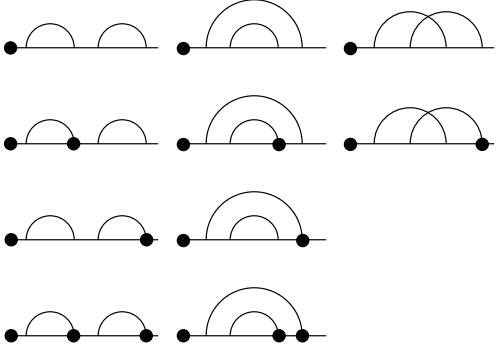

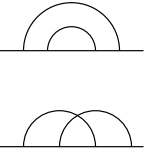

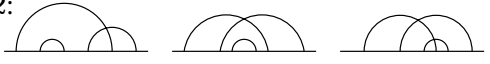
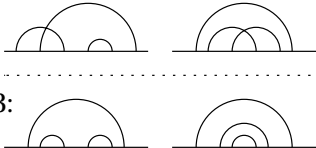
		
		<p>1:</p>  <p>2:</p>  <p>3:</p> 

Table 8.1: The correspondences $v(\epsilon)$ for ϵ with two or less edges

dence is indicated by the translated placements of the edge diagrams ϵ and unbroken arc configurations u . The parameter $r(u)$ is indicated for convenience when there are three arcs in Table 8.1.

8.3 Recursive construction of λ

Now that we have a bijection $v : \mathcal{E} \rightarrow \mathcal{U}$, we have a combinatorial decomposition corresponding to (8.3), in which an edge diagram ϵ decomposes into

1. a root vertex, and
2. an ordered collection of edge diagrams ϵ_i , each with a selected subset of vertices .

The case 2 corresponds to the substitution $y \mapsto y + 1$, and the correspondence that has been maintained in v between vertices of ϵ and non-right-crossed arcs of u . We write this as $\epsilon \mapsto (\bullet; \epsilon_1^+, \dots, \epsilon_k^+)$, where ϵ_i^+ is the edge diagram ϵ_i together with a selected subset of vertices.

There is an analogous decomposition for the set of level-labelled trees \mathcal{T}_l corresponding to the identity

$$T_l(y, z) = y\{1 - zT_l(y + 1, z)\}^{-1}.$$

A level-labelled tree (t, ℓ) decomposes into

1. a root vertex, and

2. an ordered collection of level-labelled trees (t', ℓ') , for each of which a subset of saturated vertices v has been selected to have their labels incremented by one, $\ell(v) = \ell'(v) + 1$.

Thus $t \mapsto (\bullet; t_1^+, \dots, t_k^+)$, where t_i^+ denotes a level-labelled tree t_i together with a selected subset of its saturated vertices.

Thus we have comparable decompositions for \mathcal{E} and \mathcal{T}_l , as we also have for \mathcal{E} and \mathcal{U} . From the latter pair of comparable decompositions, we formed a recursive construction of the bijection $v : \mathcal{E} \rightarrow \mathcal{U}$. We apply the same principle to define a recursive bijection $\lambda : \mathcal{E} \rightarrow \mathcal{T}_l$.

Algorithm 8.2 (Computation of $(t, \ell) = \lambda(\epsilon)$). *The level-labelled tree $(t, \ell) = \lambda(\epsilon)$ is the one whose decomposition is*

$$(\bullet; \lambda(\epsilon_1)^+, \dots, \lambda(\epsilon_k)^+)$$

where, the selected subset of vertices in ϵ_i^+ is chosen to correspond to the selected subset of saturated vertices in $\lambda(\epsilon_i)^+$.

Table 8.2 gives an example of the computation of $\Theta = \lambda \circ \epsilon$. The recursive use of λ is evident.

8.4 Specialisations and Generalisations

Let $L(b, y, z)$ be the generating series for locally orientable rooted maps, where b marks η , y marks vertices and z marks edges. Thus $L(0, y, z) = M(y, z)$. By

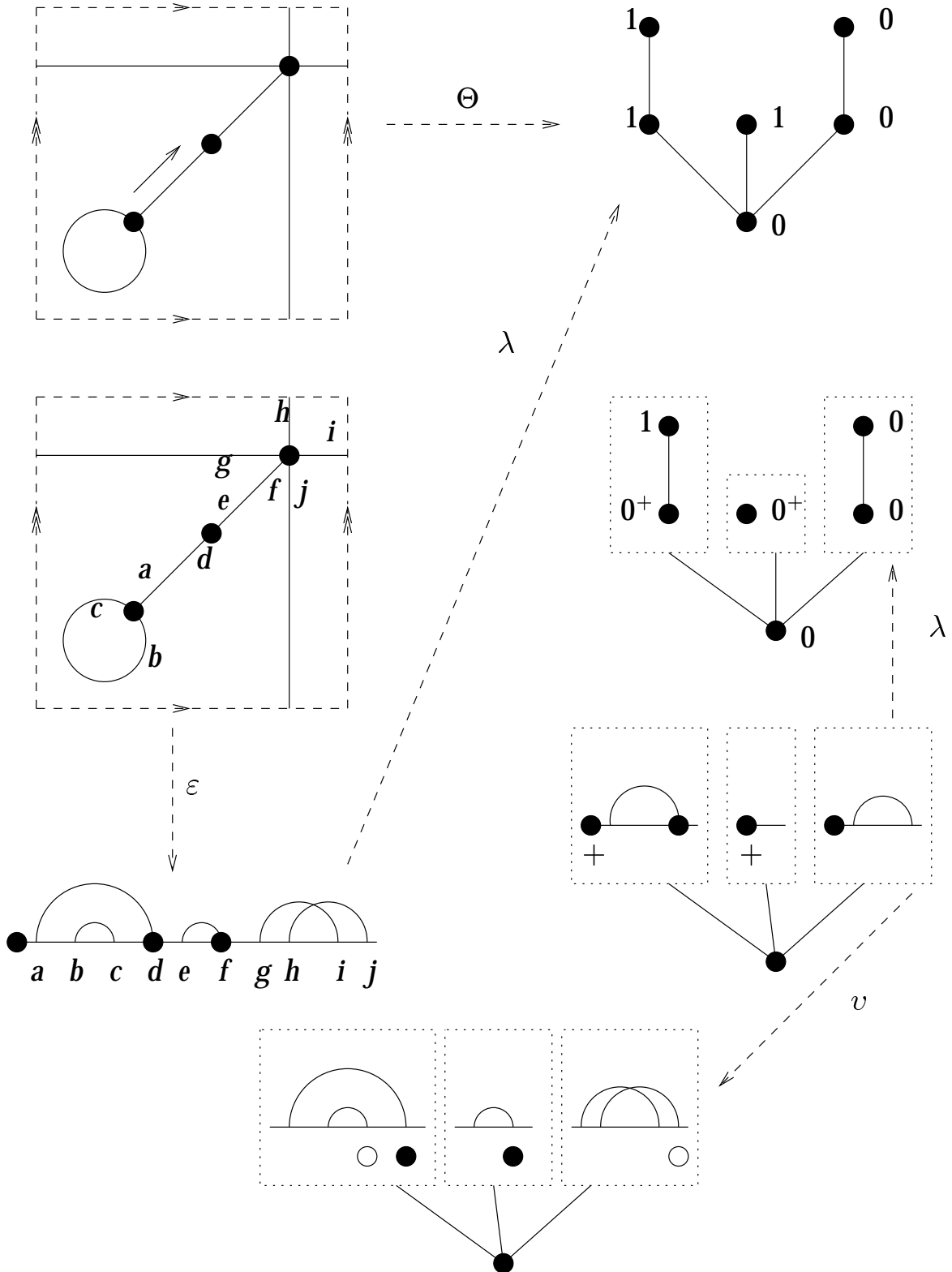


Table 8.2: Sample computation of Θ

Lemma 7.2,

$$L(b, y, z) = (b + 1)M\left(\frac{y}{b + 1}, (b + 1)z\right).$$

Moreover, letting u mark gaps not under arcs with vertices,

$$L(b, u, y, z) = (b + 1)F\left(u, \frac{y}{b + 1}, (b + 1)z\right).$$

Let $M(z) = M(1, z)$ and $L(z) = L(1, z)$. Then

$$M(z) = \frac{1}{1 - \frac{2z}{1 - \frac{3z}{1 - \dots}}} \quad (8.4)$$

and

$$L(z) = \frac{1}{1 - \frac{3z}{1 - \frac{5z}{1 - \dots}}} \quad (8.5)$$

Then $M(z) \equiv 1 \equiv 1 + 0z + 0z^2 + \dots \pmod{2}$ and $L(z) \equiv 1 \equiv 1 + 0z + 0z^2 + \dots \pmod{3}$. Hence, the numbers M_n (resp. L_n) of orientable (resp. locally orientable) rooted maps with $n \geq 1$ edges is a multiple of 2 (resp. 3). This fact can be seen

directly from considering the nature of the rightmost arc of the edge diagram. It is not clear how to prove these two divisibility results from the alternate expressions for $M(y, z)$. Moreover, (8.4) and (8.5) imply the eventual periodicity modulo m of M_n and L_n , for each modulus m , with the exception of $m = 2$ for L_n .

8.5 Alternate expressions for $M(y, z)$

The generating series $M(y, z)$ has at least three other forms besides its continued fraction form.

Derived originally [JV90a] by specialising Schur functions in the genus series for maps, there is a direct combinatorial argument to prove the following.

Lemma 8.7.

$$M(y, z) = y + 2z \frac{\partial}{\partial z} \log \sum_{n \geq 0} \frac{1}{2^n n!} z^n y^{(2n)},$$

where $y^{(2n)} = y(y+1) \cdots (y+2n-1)$, the rising factorial.

Proof. We claim that the generating series for the set of permutations $\pi \in \mathfrak{S}_N$ where y marks disjoint cycles is $y^{(N)}$. We use induction on N .

When $N = 1$, we have $y^{(N)} = y$ and $\mathfrak{S}_N = \{(1)\}$.

Consider $\pi \in \mathfrak{S}_N$ for $N > 1$.

Case 1: $\pi(N) = N$. Thus π has (N) for a cycle. The contribution is

$$y \cdot y^{(N-1)}.$$

Case 2: $\pi(N) \neq N$. Delete N from its cycle in π to get $\pi' \in \mathfrak{S}_{N-1}$. The contribution is

$$(N - 1) \cdot y^{(N-1)}$$

because π is determined by π' and $\pi(N)$, for which there are $N - 1$ choices.

This proves the claim.

An orientable rooted map m with n edges, is encoded by a $2^{n-1}(n - 1)!$ different permutations $\pi \in \mathfrak{S}_{2n}$, such that

$$\langle \pi, \varepsilon_n \rangle \tag{8.6}$$

where $\varepsilon_n = (1, 2)(3, 4) \cdots (2n - 1, 2n)$, is a transitive permutation group. Recall that this is done by assigning labels $2i - 1$ and $2i$ to the ends of the edges, with 1 at the root vertex. Then the cycles of the π are taken from the clockwise order of the labels in circulations of the vertices.

Combinatorially, if (8.6) is not transitive, π is interpreted as a rotation system, an unordered collection of labelled maps. Transitivity then is regarded as the equivalent to connectivity, with orbits becoming components.

Therefore by the claim, $\sum_{n \geq 0} \frac{1}{n!} z^n y^{(2n)}$ is the exponential generating series in z for rotation systems with n edges. The variable y is an ordinary marker for vertices.

Taking the logarithm restricts the generating series to only connected (transi-

tive) rotation systems. The differential operator $2z\frac{\partial}{\partial z}$ and scaling $z \mapsto z/2$ correct for the fact that $2^{n-1}(n-1)!$ connected rotation systems encode a single rooted map.

The term y must be added for the vertex map, which cannot be encoded by a rotation system. □

Using integer-parenthesis systems, Walsh derived [Wal71] the Ricatti equation for $M(y, z)$ in its recurrence form. Walsh then gave the solution

$$M(y, z) = \sum_{n \geq 0} z^n \frac{1 - \sqrt{1 - 4yz}}{2z} (1 - 4yz)^{-n} g_n \left(\frac{\{1 - 4yz\}^{-\frac{1}{2}} - 1}{2} \right) \quad (8.7)$$

to the recurrence, where the g_n are polynomials with positive integer coefficients satisfying another recurrence. The first few polynomials are $g_0(x) = g_1(x) = 1$, $g_2(x) = 5x + 3$, and $g_3(x) = 60x^2 + 65x + 15$.

Finally, there is an expansion of $M(y, z)$ as a continued product:

$$M(y, z) = A_0 + B_0(A_1 + B_1(A_2 + B_2(A_3 + \dots))), \quad (8.8)$$

where the A_i and B_i satisfy a simultaneous recurrence. To find and prove this system of recurrence equations we need an additional lemma.

8.5.1 An Ordinary Differential-Functional Equation

Lemma 8.8. *Let $F = F(u, y, z)$ be the generating series for edge diagrams, where u marks gaps not beneath an arc with a vertex, y marks vertices, and z marks*

edges. (Clearly $E = E(y, z) = F(1, y, z)$.) The following holds:

$$F = uy + u^3 z \frac{\partial}{\partial u} F + u^2 yz \frac{F - E}{u - 1}. \quad (8.9)$$

Proof. Let $\epsilon \in \mathcal{E}$ be an edge diagram to be enumerated by F . We decompose ϵ by attempting to remove the rightmost edge (arc). There are three cases to consider.

Case (a): There are no arcs. There is just one vertex, and one gap, as in Figure 8.7. Hence the term uy of the right hand side.



Figure 8.7: An edge diagram with no arcs

Otherwise, there is a rightmost arc a . Let $\epsilon' = \epsilon - a$. Suppose that ϵ' has h gaps not underneath an arc with a vertex.

Case (b): The rightmost arc a does not possess a vertex. The left end of a can be located in any of these h gaps. Thus the factor of u^h for the term of F counting ϵ' is multiplied by h . Furthermore, ϵ has $h + 2$ gaps not underneath an arc with vertex, as well as one more arc than ϵ' . Hence the contribution of this case is $u^3 z \frac{\partial}{\partial u} F$.

Case (c): The rightmost arc a possesses a vertex. Suppose the gaps of ϵ' are $\gamma_1, \dots, \gamma_h$. Let the gap containing the left end of a be γ_i .

Since arc a possesses a vertex, gaps $\gamma_{i+1}, \dots, \gamma_h$ are underneath an arc with a vertex, namely the arc a , and therefore is not marked by u in ϵ . One new gap

appears at the very right end of the base line. Thus ϵ has $i + 1$ gaps not under an arc with a vertex.

Thus the factor u^h marking ϵ' is replaced by $u^2 + u^3 + \dots + u^{h+1} = u^2 \frac{u^h - 1}{u - 1}$. Multiply by yz because of the new arc a and vertex on a . To do this to every term of F marking e , giving the contribution of this case, transform F into $u^2 yz \frac{F-E}{u-1}$. \square

Sometimes, the operator Δ_u is defined by $\Delta_u F = \frac{F - F|_{u=1}}{u-1}$, and the operator D_u by $D_u = \frac{\partial}{\partial u}$. Then (8.9) is rewritten as $N = uy + (b + 1)u^3 z D_u N + u^2 yz \Delta_u N$. The operator Δ_u arises in some of Tutte's equations for planar maps. But, while Tutte's equations contained a quadratic term, (8.9) contains a term with the operator D_u .

The most obvious approach for finding E from (8.9) is to eliminate F . Regard (8.9) as a first order linear differential equation in F and u , regard E as a constant, and use an integrating factor. This approach leads to a functional equation for E alone but involves a power series in u^{-1} and z^{-1} , which seems no easier to solve. Another approach, however, gives a continued product expansion of M .

8.5.2 A continued product expansion for $E(y, z)$

Let $v = u - 1$, and thus $u = v + 1$. Let F_j be determined by the expansion $F = \sum_{j \geq 0} F_j v^j$, where F_j is a constant in v , and therefore a constant in u . In particular, $F_0 = E$. Then the differential-functional equation (8.9) implies

$$\sum_{j \geq 0} F_j v^j = (v + 1)y + (v + 1)^3 z \sum_{j \geq 1} j F_j v^{j-1} + (v + 1)^2 yz \sum_{j \geq 1} F_j v^{j-1}.$$

Equating coefficients of v^j on both sides:

$$F_0 = y + z(1 + y)F_1, \quad (8.10)$$

$$F_1 = y + z(3 + 2y)F_1 + z(2 + y)F_2, \quad (8.11)$$

$$F_2 = z(3 + y)F_1 + z(6 + 2y)F_2 + z(3 + y)F_3, \quad (8.12)$$

and for $j \geq 3$:

$$\begin{aligned} F_j = & z\{(j-2)\}F_{j-2} + z\{3(j-1) + y\}F_{j-1} \\ & + z\{3j + 2y\}F_j + z\{(j+1) + y\}F_{j+1}. \end{aligned} \quad (8.13)$$

Solving for F_j in the j^{th} of these equations to get another series of equations:

$$F_j = A_j + B_j F_{j+1},$$

proves the continued product (8.8), because $M = F_0 = A_0 + B_0 F_1 = A_0 + B_0(A_1 + B_1 F_2) = \dots$.

We now describe initial conditions and the recurrence relation for the terms A_j and B_j . Firstly,

$$A_0 = y, \quad B_1 = (1 + y),$$

directly from (8.10).

Secondly, solving for F_1 in (8.11), gives:

$$F_1 = \frac{y + z(2 + y)F_2}{1 - z(3 + 2y)},$$

so that

$$A_1 = \frac{y}{1 - z(3 + 2y)}, \quad B_1 = \frac{z(2 + y)}{1 - z(3 + 2y)}.$$

Similarly, expressions can be found for A_2 and B_2 .

More generally, for $j \geq 3$, we get the simultaneous recurrence equations:

$$A_j = z \frac{(j-2)A_{j-2} + \{(j-2)B_{j-2} + 3(j-1) + y\}A_{j-1}}{1 - C_j},$$

$$B_j = z \frac{(j+1) + y}{1 - C_j},$$

where

$$C_j = z\{(j-2)B_{j-2} + 3(j-1) + y\}B_{j-1} + 3j + 2y.$$

8.6 Summary

We discussed the straightforward way that continued fractions enumerate level-labelled trees. By use of depth first search and edge diagrams, we constructed a bijection between level-labelled trees and orientable rooted maps. Such a bijection was sought in [AB97], where enumeration of rooted maps with continued

fractions was established by different means.

We note that the enumerative problem of this chapter is not as refined as in previous chapters. The generating series $M(y, z)$ contains no information about the number of faces, the genus or the degrees of faces and vertices of the rooted maps which are enumerated. Only the number of vertices and the number of edges are recorded in $M(y, z)$. For more refined problems, it is unlikely that the generating series has a form as simple as a continued fraction.

We discussed other solutions to the same enumerative problem. These formulae include: Walsh's recurrence form; the expression with logarithm of a sum containing rising factorials of Jackson and Visentin (for which we provided an elementary proof avoiding character theory); and a continued product expansion whose factors satisfied a double recurrence. It is not obvious algebraically why these four expressions for the generating series $M(y, z)$ are equal.

Appendix A

Further Work

Below are suggestions for further work.

A.1 On Double Coset Algebras

A natural interpolation corresponding the Jack parameter α between the two double cosets $D(\mathfrak{S}_{2n}, H_n)$ and $D(G_n, L_n)$ would be helpful. Efforts to realise such an algebra have been unsuccessful. Abstractly, such an interpolation may be defined using Jack symmetric functions, but nothing is gained in doing so. Perhaps a concrete realisation can be provided by an algebra similar to certain Hecke algebras which are a parameterised generalisation $\mathbb{C}\mathfrak{S}_n$ and have applications to knot theory. (In this algebra, the relations between the $n - 1$ generators $s_i = (i, i + 1)$ of \mathfrak{S}_n are modified, with a parameter q such that $q = 1$ recovers the algebra $\mathbb{C}\mathfrak{S}_n$.)

A.2 On $\tilde{\Xi}$

Clearly the aim is to find Ξ . Although $\tilde{\Xi}$ has a complicated description, it may be possible to simplify this, and even to modify in it some way to fulfil all the requirements of the Quadrangulation Conjecture.

It is promising that there is another, entirely different bijection $\kappa : \mathcal{Q} \rightarrow \mathcal{A}$, which preserves the number of edges, as $\tilde{\Xi}$ does. This bijection κ does not extend Tutte's medial bijection, because planarity is not preserved. This κ is an adaption of a bijection between embeddings of digraphs into locally orientable surfaces and projections of knots into orientable surfaces.

A.3 On β

A proof that the appropriate specialisation of $\Psi^{(b+1)}$ is a solution of the differential equation (6.2) is very desirable. Considering that Jack symmetric functions are themselves eigenfunctions to a very similar differential operator, such a proof seems plausible. Moreover, it is a hopeful indication that a very similar differential equation, for minimal transitive factorisations, has been explicitly solved in [GJ97b].

A strategy to achieve such a proof is to provide a proof for a narrower class of rooted maps, relating specialisations of the differential equation to corresponding specialisations of Jack symmetric functions. These proofs might then be extended to the fully general equation (6.2).

In two instances, Walsh's monopole formula and Tutte's formula for Eule-

rian planar maps, the solutions are sufficiently simple to be regarded as explicit in the sense of not referring to symmetric functions. These two formulae were proven by explicit verification that they satisfied the recurrence associated with specialisations of (6.2). Perhaps these two formulae could be unified to a single formula, with a unified proof by recurrence (verification of the differential equation). Then compare this with the corresponding symmetric functions expressions.

Another desirable goal is to show that Φ has integer coefficients, which would be true if $\Phi = \widehat{\Psi}^{(b+1)}$ and the Map-Jack Conjecture are true.

Macdonald has defined some symmetric functions $J_\lambda(q, t)$ with two parameters, which generalise Jack symmetric functions. One might generalise $\Psi^{(b+1)}$ of (1.5) to a generating series $\Psi(q, t)$. A quick calculation shows that in this raw form, the desired coefficients are rational functions in q and t . However, there may be a transformation, generalising the transformation $\alpha = b + 1$, which yields non-negative integer polynomials.

In §6.6 a generating series D^* is defined, where b has been replaced by two variables b_1 and b_2 . A series Φ^* could be defined from D^* in similar way to (6.24). A very speculative, further strengthening of the Conjecture 1.2 is:

Conjecture A.1. *There is a transformation $\Upsilon : \mathbb{C}^2 \rightarrow \mathbb{C}^2$, mapping (b_1, b_2) to (q, t) , the two parameters of Macdonald's generalisation of Jack symmetric functions, that is $\Phi^*|_{\Upsilon:(b_1, b_2) \rightarrow (q, t)} = \Psi(q, t)|_{y_j \rightarrow y}$.*

A.4 On η

Ideally one could prove that $\vartheta = \eta$ meets all the conditions set in the Map-Jack Conjecture. Such a proof might require new results about Jack symmetric functions. It is promising that two new characterisations of Jack symmetric functions have been recently discovered [KS97, LV95], providing independent proof of the Macdonald-Stanley Conjecture. One of these characterisations uses a new sort a tableau, which might perhaps amenable to the combinatorics of η . Perhaps the thorough investigation of the properties of η proved in Chapter 7 and of their potential analogues for $\Psi^{(b+1)}$ will lead to a proof of suitability of η .

A more modest achievement is to show that η is in fact consistent with the partial differential equation of Chapter 6, in the sense that $\Phi = H$. Considering that η used β in its definition, such a proof seems very attainable. A crucial step would be to show that depth first search is sufficient to go from ordered digraphs (β) to rooted maps (η). An even weaker aim is establish this monopoles only. For monopoles the action of the depth first search is extremely simple. The main content the canonical ordered digraph function δ when applied to monopoles, is in ordering the edges.

Because $\eta \leq 2 - \chi$ and $2 - \chi$ gives the rank of some homology groups of the surface, a more natural description of η might be found in terms of homology. Specifically, the dual of the matchings graph (as a map in the same surface) is a simplicial complex. The root position corresponds to a root simplex. So perhaps, associated with the choice of root simplex there is naturally defined subgroup of the homology group with rank η . Such a *semantic* description of η may even be

used to prove the Map-Jack Conjecture.

A.5 On Θ

The bijection Θ of Chapter 8 may have a simpler description than the one given. More interestingly, perhaps Θ could be modified so that it extends the bijection that has been found [CV81] between planar rooted maps and well-labelled trees.

Interestingly, in [Sch98] there is a bijection between rooted orientable maps and well-labelled single faced rooted maps of the same genus. These single faced maps are called *g-arbres* and generalise trees. Thus the bijection in [Sch98] is another way to extend the bijection given in [CV81].

A.6 On random matrices

An integration theory of random matrices accompanies the theory of Zonal polynomials and Schur symmetric functions [Mac95], and can be used to characterise these symmetric functions. Moreover, matrix integration can be applied directly to the enumeration of maps [Bro95, GJ97a, Jac96, Jac94]. However, the rôle of Jack symmetric functions in the matrix integration framework is not fully understood, either in the theoretical relationship of [Mac95] or in the enumerative method for maps.

Selberg's theorem, used in [GHJ99], provides an integration result for Jack symmetric functions. However, the Selberg integrals is taken over variables corresponding to the eigenvalues of matrices, after diagonalization. Matrix inte-

grals before diagonalization, like those for Schur symmetric functions and Zonal polynomials but parameterized by some parameter corresponding to the Jack parameter α , would be far more useful for a combinatorial interpretation directly useful to map enumeration. In particular, such integrals may be a means to construct a Map-Jack parameter ϑ , or to prove that η is a valid Map-Jack parameter.

Matrix integration has applications to string theory and quantum field theory [Hoo74, BIZ80] and many other areas of physics and even the Riemann hypothesis [Meh91].

A.7 Products in the Category of Rooted Maps

The definition of isomorphisms between rooted maps can be broadened to a definition of homomorphisms between rooted maps. This endows the set of rooted maps with a category structure. (Combinatorial pre-maps also form a category by similar means.) The category of rooted maps possesses a product. Properties such as regularity and orientability can be characterised in terms of this product. Moreover, the product is root dependent. Because of these features of the product, it might be useful in the Quadrangulation Conjecture or the Map-Jack Conjecture.

A.8 On Jucys-Murphy elements

Other algebraic approaches to connection coefficients of \mathfrak{S}_n , not using Schur symmetric functions, are given in [FH59], [Juc74] and [GJ94]. The second uses certain sums of transpositions called Jucys-Murphy elements. The third uses certain symmetric functions defined by Macdonald using Lagrange inversion. (These symmetric functions are distinct from Macdonald's generalisation of Jack symmetric functions [Mac95].) A close relationship between these approaches can be proved inductively [Bro98]. If these approaches can be extended to include connection coefficients of $D(\mathfrak{S}_{2n}, H_n)$, then perhaps their combinatorics can be used to find a Map-Jack parameter ϑ (at least for a subset of maps).

Appendix B

Tables of coefficients of Φ_n , for $n \leq 6$

The following sections display all the non-zero coefficients $[x_\phi y^k b^B] \Phi_n$ for $n \leq 6$. Their format is that of Table B.1. The leftmost column indicates ϕ , corresponding to the face partition. The remaining columns contain computer-generated coefficients of Φ_n . Notice that these are nonnegative integers, so could represent a number of rooted maps with corresponding properties.

The numbers in Table B.1 correspond to rooted maps with three faces, eight edges and two vertices. These numbers were computed, using the recursion obtained from the partial differential equations. Computing the analogous numbers using Jack symmetric functions would take far more time. Similarly, computing these numbers on a map by map basis, and using the parameter η , would also take an prohibitive amount of time.

Therefore, the partial differential equations approach to map enumeration gives an efficient method to compute these coefficients. (Assuming all three methods yield equal analogous coefficients.) If, however, one wants more detailed, refined numbers, the coefficients with respect to both ϕ and ν , (the face partition and vertex partition), these partial differential equations will not help.

B.1 Number of Edges = 1 ($n = 1$)

B.1.1 Number of Vertices = 1 ($k = 1$)

$\phi : B$		0	$\phi : B$		1
[1, 1]		1	[2]		1

$\phi : B$	1	2	3	4	5
[6, 5, 5]	210928	421856	890232	679304	344008
[6, 6, 4]	219496	438992	919244	699748	345316
[7, 5, 4]	452736	905472	1901728	1448992	726720
[7, 6, 3]	504480	1008960	2131184	1626704	815408
[7, 7, 2]	322448	644896	1309672	987224	478632
[8, 4, 4]	246954	493908	1032008	785054	383760
[8, 5, 3]	528688	1057376	2240432	1711744	857712
[8, 6, 2]	655256	1310512	2660560	2005304	957488
[8, 7, 1]	1206544	2413088	4899824	3693280	1777968
[9, 4, 3]	586816	1173632	2480832	1894016	936448
[9, 5, 2]	699104	1398208	2854544	2155440	1040816
[9, 6, 1]	1248224	2496448	5079600	3831376	1837712
[10, 3, 3]	353360	706720	1502376	1149016	566952
[10, 4, 2]	785904	1571808	3182536	2396632	1129128
[10, 5, 1]	1347936	2695872	5488720	4140784	1983408
[11, 3, 2]	957600	1915200	3923472	2965872	1408848
[11, 4, 1]	1533120	3066240	6227968	4694848	2216832
[12, 2, 2]	648984	1297968	2540356	1891372	858732
[12, 3, 1]	1875648	3751296	7617088	5741440	2704608
[13, 2, 1]	2595936	5191872	10161424	7565488	3434928
[14, 1, 1]	2410512	4821024	9435608	7025096	3189576

Table B.1: Coefficients $[x_\phi y^2 b^B] \Phi_8$ for $\ell(\phi) = 3$

B.1.2 Number of Vertices = 2 (k = 2)

$\phi : B$	0
[2]	1

B.2 Number of Edges = 2 (n = 2)

B.2.1 Number of Vertices = 1 (k = 1)

$\phi : B$	0	$\phi : B$	1	$\phi : B$	0	1	2
[2, 1, 1]	2	[2, 2]	1	[4]	1	1	3
		[3, 1]	4				

B.2.2 Number of Vertices = 2 (k = 2)

$\phi : B$	0	$\phi : B$	1
[2, 2]	1	[4]	5
[3, 1]	4		

B.2.3 Number of Vertices = 3 (k = 3)

$\phi : B$	0
[4]	2

B.3 Number of Edges = 3 (n = 3)

B.3.1 Number of Vertices = 1 (k = 1)

$\phi : B$	0	$\phi : B$	1	$\phi : B$	0	1	2	$\phi : B$	1	2	3
[2, 2, 1, 1]	3	[2, 2, 2]	1	[3, 3]	1	1	5	[6]	13	13	15
[3, 1, 1, 1]	2	[3, 2, 1]	12	[4, 2]	3	3	9				
		[4, 1, 1]	9	[5, 1]	6	6	18				

B.3.2 Number of Vertices = 2 (k = 2)

$\phi : B$	0	$\phi : B$	1	$\phi : B$	0	1	2
[2, 2, 2]	1	[3, 3]	9	[6]	10	10	32
[3, 2, 1]	12	[4, 2]	15				
[4, 1, 1]	9	[5, 1]	30				

B.3.3 Number of Vertices = 3 ($k = 3$)

$\phi : B$	0	$\phi : B$	1
[3, 3]	4	[6]	22
[4, 2]	6		
[5, 1]	12		

B.3.4 Number of Vertices = 4 ($k = 4$)

$\phi : B$	0
[6]	5

B.4 Number of Edges = 4 ($n = 4$)

B.4.1 Number of Vertices = 1 ($k = 1$)

$\phi : B$	0	$\phi : B$	1	$\phi : B$	0	1	2		
[2, 2, 2, 1, 1]	4	[2, 2, 2, 2]	1	[3, 3, 2]	4	4	20		
[3, 2, 1, 1, 1]	8	[3, 2, 2, 1]	24	[4, 2, 2]	6	6	18		
[4, 1, 1, 1, 1]	2	[3, 3, 1, 1]	16	[4, 3, 1]	16	16	64		
		[4, 2, 1, 1]	36	[5, 2, 1]	24	24	72		
		[5, 1, 1, 1]	16	[6, 1, 1]	20	20	60		
$\phi : B$	1	2	3	$\phi : B$	0	1	2	3	4
[4, 4]	19	19	24	[8]	21	42	181	160	105
[5, 3]	40	40	56						
[6, 2]	52	52	60						
[7, 1]	104	104	120						

B.4.2 Number of Vertices = 2 ($k = 2$)

$\phi : B$	0	$\phi : B$	1	$\phi : B$	0	1	2	$\phi : B$	1	2	3
[2, 2, 2, 2]	1	[3, 3, 2]	36	[4, 4]	15	15	53	[8]	215	215	260
[3, 2, 2, 1]	24	[4, 2, 2]	30	[5, 3]	32	32	128				
[3, 3, 1, 1]	16	[4, 3, 1]	112	[6, 2]	40	40	128				
[4, 2, 1, 1]	36	[5, 2, 1]	120	[7, 1]	80	80	256				
[5, 1, 1, 1]	16	[6, 1, 1]	100								

B.4.3 Number of Vertices = 3 ($k = 3$)

$\phi : B$	0	$\phi : B$	1	$\phi : B$	0	1	2
[3, 3, 2]	16	[4, 4]	38	[8]	70	70	234
[4, 2, 2]	12	[5, 3]	96				
[4, 3, 1]	48	[6, 2]	88				
[5, 2, 1]	48	[7, 1]	176				
[6, 1, 1]	40						

B.4.4 Number of Vertices = 4 ($k = 4$)

$\phi : B$	0	$\phi : B$	1
[4, 4]	9	[8]	93
[5, 3]	24		
[6, 2]	20		
[7, 1]	40		

B.4.5 Number of Vertices = 5 ($k = 5$)

$\phi : B$	0
[8]	14

B.5 Number of Edges = 5 ($n = 5$)

B.5.1 Number of Vertices = 1 ($k = 1$)

$\phi : B$	0	$\phi : B$	1	$\phi : B$	0	1	2
[2, 2, 2, 2, 1, 1]	5	[2, 2, 2, 2, 2]	1	[3, 3, 2, 2]	10	10	50
[3, 2, 2, 1, 1, 1]	20	[3, 2, 2, 2, 1]	40	[3, 3, 3, 1]	10	10	50
[3, 3, 1, 1, 1, 1]	5	[3, 3, 2, 1, 1]	80	[4, 2, 2, 2]	10	10	30
[4, 2, 1, 1, 1, 1]	10	[4, 2, 2, 1, 1]	90	[4, 3, 2, 1]	80	80	320
[5, 1, 1, 1, 1, 1]	2	[4, 3, 1, 1, 1]	70	[4, 4, 1, 1]	30	30	120
		[5, 2, 1, 1, 1]	80	[5, 2, 2, 1]	60	60	180
		[6, 1, 1, 1, 1]	25	[5, 3, 1, 1]	70	70	250
				[6, 2, 1, 1]	100	100	300
				[7, 1, 1, 1]	50	50	150

$\phi : B$	1	2	3	$\phi : B$	0	1	2	3	4
[4, 3, 3]	80	80	125	[5, 5]	33	66	289	256	189
[4, 4, 2]	95	95	120	[6, 4]	65	130	600	535	375
[5, 3, 2]	200	200	280	[7, 3]	70	140	690	620	450
[5, 4, 1]	340	340	450	[8, 2]	105	210	905	800	525
[6, 2, 2]	130	130	150	[9, 1]	210	420	1810	1600	1050
[6, 3, 1]	380	380	500						
[7, 2, 1]	520	520	600						
[8, 1, 1]	455	455	525						
$\phi : B$	1	2	3	4	5				
[10]	753	1506	2889	2136	945				

B.5.2 Number of Vertices = 2 ($k = 2$)

$\phi : B$	0	$\phi : B$	1	$\phi : B$	0	1	2		
[2, 2, 2, 2, 2]	1	[3, 3, 2, 2]	90	[4, 3, 3]	65	65	295		
[3, 2, 2, 2, 1]	40	[3, 3, 3, 1]	90	[4, 4, 2]	75	75	265		
[3, 3, 2, 1, 1]	80	[4, 2, 2, 2]	50	[5, 3, 2]	160	160	640		
[4, 2, 2, 1, 1]	90	[4, 3, 2, 1]	560	[5, 4, 1]	270	270	1010		
[4, 3, 1, 1, 1]	70	[4, 4, 1, 1]	210	[6, 2, 2]	100	100	320		
[5, 2, 1, 1, 1]	80	[5, 2, 2, 1]	300	[6, 3, 1]	300	300	1120		
[6, 1, 1, 1, 1]	25	[5, 3, 1, 1]	430	[7, 2, 1]	400	400	1280		
		[6, 2, 1, 1]	500	[8, 1, 1]	350	350	1120		
		[7, 1, 1, 1]	250						
$\phi : B$	1	2	3	$\phi : B$	0	1	2	3	4
[5, 5]	355	355	500	[10]	483	966	4294	3811	2589
[6, 4]	740	740	965						
[7, 3]	870	870	1180						
[8, 2]	1075	1075	1300						
[9, 1]	2150	2150	2600						

B.5.3 Number of Vertices = 3 ($k = 3$)

$\phi : B$	0	$\phi : B$	1	$\phi : B$	0	1	2
[3, 3, 2, 2]	40	[4, 3, 3]	230	[5, 5]	120	120	490
[3, 3, 3, 1]	40	[4, 4, 2]	190	[6, 4]	250	250	910
[4, 2, 2, 2]	20	[5, 3, 2]	480	[7, 3]	300	300	1140
[4, 3, 2, 1]	240	[5, 4, 1]	740	[8, 2]	350	350	1170
[4, 4, 1, 1]	90	[6, 2, 2]	220	[9, 1]	700	700	2340
[5, 2, 2, 1]	120	[6, 3, 1]	820				
[5, 3, 1, 1]	180	[7, 2, 1]	880				
[6, 2, 1, 1]	200	[8, 1, 1]	770				
[7, 1, 1, 1]	100						
$\phi : B$	1	2	3				
[10]	2200	2200	2750				

B.5.4 Number of Vertices = 4 ($k = 4$)

$\phi : B$	0	$\phi : B$	1	$\phi : B$	0	1	2
[4, 3, 3]	60	[5, 5]	215	[10]	420	420	1450
[4, 4, 2]	45	[6, 4]	380				
[5, 3, 2]	120	[7, 3]	490				
[5, 4, 1]	180	[8, 2]	465				
[6, 2, 2]	50	[9, 1]	930				
[6, 3, 1]	200						
[7, 2, 1]	200						
[8, 1, 1]	175						

B.5.5 Number of Vertices = 5 ($k = 5$)

$\phi : B$	0	$\phi : B$	1
[5, 5]	36	[10]	386
[6, 4]	60		
[7, 3]	80		
[8, 2]	70		
[9, 1]	140		

B.5.6 Number of Vertices = 6 ($k = 6$)

$\phi : B$	0
[10]	42

B.6 Number of Edges = 6 ($n = 6$)

B.6.1 Number of Vertices = 1 ($k = 1$)

$\phi : B$	0	$\phi : B$	1	$\phi : B$	0	1	2
[2, 2, 2, 2, 2, 1, 1]	6	[2, 2, 2, 2, 2, 2]	1	[3, 3, 2, 2, 2]	20	20	100
[3, 2, 2, 2, 1, 1, 1]	40	[3, 2, 2, 2, 2, 1]	60	[3, 3, 3, 2, 1]	60	60	300
[3, 3, 2, 1, 1, 1, 1]	30	[3, 3, 2, 2, 1, 1]	240	[4, 2, 2, 2, 2]	15	15	45
[4, 2, 2, 1, 1, 1, 1]	30	[3, 3, 3, 1, 1, 1]	64	[4, 3, 2, 2, 1]	240	240	960
[4, 3, 1, 1, 1, 1, 1]	12	[4, 2, 2, 2, 1, 1]	180	[4, 3, 3, 1, 1]	150	150	654
[5, 2, 1, 1, 1, 1, 1]	12	[4, 3, 2, 1, 1, 1]	420	[4, 4, 2, 1, 1]	180	180	720
[6, 1, 1, 1, 1, 1, 1]	2	[4, 4, 1, 1, 1, 1]	63	[5, 2, 2, 2, 1]	120	120	360
		[5, 2, 2, 1, 1, 1]	240	[5, 3, 2, 1, 1]	420	420	1500
		[5, 3, 1, 1, 1, 1]	132	[5, 4, 1, 1, 1]	180	180	684
		[6, 2, 1, 1, 1, 1]	150	[6, 2, 2, 1, 1]	300	300	900
		[7, 1, 1, 1, 1, 1]	36	[6, 3, 1, 1, 1]	220	220	740
				[7, 2, 1, 1, 1]	300	300	900
				[8, 1, 1, 1, 1]	105	105	315

$\phi : B$	1	2	3	$\phi : B$	0	1	2	3	4
[3, 3, 3, 3]	34	34	60	[4, 4, 4]	45	90	447	402	297
[4, 3, 3, 2]	480	480	750	[5, 4, 3]	288	576	2868	2580	2016
[4, 4, 2, 2]	285	285	360	[5, 5, 2]	198	396	1734	1536	1134
[4, 4, 3, 1]	804	804	1188	[6, 3, 3]	150	300	1598	1448	1130
[5, 3, 2, 2]	600	600	840	[6, 4, 2]	390	780	3600	3210	2250
[5, 3, 3, 1]	864	864	1272	[6, 5, 1]	708	1416	6348	5640	4068
[5, 4, 2, 1]	2040	2040	2700	[7, 3, 2]	420	840	4140	3720	2700
[5, 5, 1, 1]	816	816	1080	[7, 4, 1]	720	1440	6804	6084	4320
[6, 2, 2, 2]	260	260	300	[8, 2, 2]	315	630	2715	2400	1575
[6, 3, 2, 1]	2280	2280	3000	[8, 3, 1]	840	1680	7968	7128	5040
[6, 4, 1, 1]	1704	1704	2250	[9, 2, 1]	1260	2520	10860	9600	6300
[7, 2, 2, 1]	1560	1560	1800	[10, 1, 1]	1134	2268	9774	8640	5670
[7, 3, 1, 1]	1992	1992	2520						
[8, 2, 1, 1]	2730	2730	3150						
[9, 1, 1, 1]	1456	1456	1680						

$\phi : B$	1	2	3	4	5
[6, 6]	1215	2430	4841	3626	1695
[7, 5]	2508	5016	9996	7488	3564
[8, 4]	2721	5442	10884	8163	3780
[9, 3]	3180	6360	13004	9824	4620
[10, 2]	4518	9036	17334	12816	5670
[11, 1]	9036	18072	34668	25632	11340

$\phi : B$	0	1	2	3	4	5	6
[12]	1485	4455	24630	41835	51876	31701	10395

B.6.2 Number of Vertices = 2 ($k = 2$)

$\phi : B$	0	$\phi : B$	1	$\phi : B$	0	1	2
[2, 2, 2, 2, 2, 2]	1	[3, 3, 2, 2, 2]	180	[3, 3, 3, 3]	28	28	146
[3, 2, 2, 2, 2, 1]	60	[3, 3, 3, 2, 1]	540	[4, 3, 3, 2]	390	390	1770
[3, 3, 2, 2, 1, 1]	240	[4, 2, 2, 2, 2]	75	[4, 4, 2, 2]	225	225	795
[3, 3, 3, 1, 1, 1]	64	[4, 3, 2, 2, 1]	1680	[4, 4, 3, 1]	648	648	2760
[4, 2, 2, 2, 1, 1]	180	[4, 3, 3, 1, 1]	1158	[5, 3, 2, 2]	480	480	1920
[4, 3, 2, 1, 1, 1]	420	[4, 4, 2, 1, 1]	1260	[5, 3, 3, 1]	696	696	2952
[4, 4, 1, 1, 1, 1]	63	[5, 2, 2, 2, 1]	600	[5, 4, 2, 1]	1620	1620	6060
[5, 2, 2, 1, 1, 1]	240	[5, 3, 2, 1, 1]	2580	[5, 5, 1, 1]	648	648	2424
[5, 3, 1, 1, 1, 1]	132	[5, 4, 1, 1, 1]	1188	[6, 2, 2, 2]	200	200	640
[6, 2, 1, 1, 1, 1]	150	[6, 2, 2, 1, 1]	1500	[6, 3, 2, 1]	1800	1800	6720
[7, 1, 1, 1, 1, 1]	36	[6, 3, 1, 1, 1]	1260	[6, 4, 1, 1]	1350	1350	5046
		[7, 2, 1, 1, 1]	1500	[7, 2, 2, 1]	1200	1200	3840
		[8, 1, 1, 1, 1]	525	[7, 3, 1, 1]	1560	1560	5568
				[8, 2, 1, 1]	2100	2100	6720
				[9, 1, 1, 1]	1120	1120	3584

$\phi : B$	1	2	3	$\phi : B$	0	1	2	3	4
[4, 4, 4]	569	569	786	[6, 6]	795	1590	7468	6673	4849
[5, 4, 3]	3684	3684	5484	[7, 5]	1644	3288	15480	13836	10332
[5, 5, 2]	2130	2130	3000	[8, 4]	1785	3570	16785	15000	10737
[6, 3, 3]	2082	2082	3072	[9, 3]	2100	4200	20344	18244	13276
[6, 4, 2]	4440	4440	5790	[10, 2]	2898	5796	25764	22866	15534
[6, 5, 1]	7812	7812	10632	[11, 1]	5796	11592	51528	45732	31068
[7, 3, 2]	5220	5220	7080						
[7, 4, 1]	8460	8460	11196						
[8, 2, 2]	3225	3225	3900						
[8, 3, 1]	9888	9888	13032						
[9, 2, 1]	12900	12900	15600						
[10, 1, 1]	11610	11610	14040						

$\phi : B$	1	2	3	4	5
[12]	23178	46356	90727	67549	30669

B.6.3 Number of Vertices = 3 ($k = 3$)

$\phi : B$	0	$\phi : B$	1	$\phi : B$	0	1	2		
[3, 3, 2, 2, 2]	80	[3, 3, 3, 3]	118	[4, 4, 4]	198	198	766		
[3, 3, 3, 2, 1]	240	[4, 3, 3, 2]	1380	[5, 4, 3]	1296	1296	5544		
[4, 2, 2, 2, 2]	30	[4, 4, 2, 2]	570	[5, 5, 2]	720	720	2940		
[4, 3, 2, 2, 1]	720	[4, 4, 3, 1]	2112	[6, 3, 3]	740	740	3100		
[4, 3, 3, 1, 1]	504	[5, 3, 2, 2]	1440	[6, 4, 2]	1500	1500	5460		
[4, 4, 2, 1, 1]	540	[5, 3, 3, 1]	2256	[6, 5, 1]	2640	2640	10248		
[5, 2, 2, 2, 1]	240	[5, 4, 2, 1]	4440	[7, 3, 2]	1800	1800	6840		
[5, 3, 2, 1, 1]	1080	[5, 5, 1, 1]	1776	[7, 4, 1]	2880	2880	10656		
[5, 4, 1, 1, 1]	504	[6, 2, 2, 2]	440	[8, 2, 2]	1050	1050	3510		
[6, 2, 2, 1, 1]	600	[6, 3, 2, 1]	4920	[8, 3, 1]	3360	3360	12384		
[6, 3, 1, 1, 1]	520	[6, 4, 1, 1]	3696	[9, 2, 1]	4200	4200	14040		
[7, 2, 1, 1, 1]	600	[7, 2, 2, 1]	2640	[10, 1, 1]	3780	3780	12636		
[8, 1, 1, 1, 1]	210	[7, 3, 1, 1]	4008						
		[8, 2, 1, 1]	4620						
		[9, 1, 1, 1]	2464						
$\phi : B$	1	2	3	$\phi : B$	0	1	2	3	4
[6, 6]	4006	4006	5436	[12]	6468	12936	58856	52388	36500
[7, 5]	8352	8352	11808						
[8, 4]	8982	8982	11916						
[9, 3]	11080	11080	14952						
[10, 2]	13200	13200	16500						
[11, 1]	26400	26400	33000						

B.6.4 Number of Vertices = 4 ($k = 4$)

$\phi : B$	0	$\phi : B$	1	$\phi : B$	0	1	2
[3, 3, 3, 3]	32	[4, 4, 4]	331	[6, 6]	800	800	3046
[4, 3, 3, 2]	360	[5, 4, 3]	2508	[7, 5]	1680	1680	6792
[4, 4, 2, 2]	135	[5, 5, 2]	1290	[8, 4]	1785	1785	6591
[4, 4, 3, 1]	540	[6, 3, 3]	1398	[9, 3]	2240	2240	8416
[5, 3, 2, 2]	360	[6, 4, 2]	2280	[10, 2]	2520	2520	8700
[5, 3, 3, 1]	576	[6, 5, 1]	4404	[11, 1]	5040	5040	17400
[5, 4, 2, 1]	1080	[7, 3, 2]	2940				
[5, 5, 1, 1]	432	[7, 4, 1]	4500				
[6, 2, 2, 2]	100	[8, 2, 2]	1395				
[6, 3, 2, 1]	1200	[8, 3, 1]	5232				
[6, 4, 1, 1]	900	[9, 2, 1]	5580				
[7, 2, 2, 1]	600	[10, 1, 1]	5022				
[7, 3, 1, 1]	960						
[8, 2, 1, 1]	1050						
[9, 1, 1, 1]	560						
$\phi : B$	1	2	3				
[12]	17905	17905	22950				

B.6.5 Number of Vertices = 5 ($k = 5$)

$\phi : B$	0	$\phi : B$	1	$\phi : B$	0	1	2
[4, 4, 4]	54	[6, 6]	864	[12]	2310	2310	8178
[5, 4, 3]	432	[7, 5]	1992				
[5, 5, 2]	216	[8, 4]	1842				
[6, 3, 3]	240	[9, 3]	2400				
[6, 4, 2]	360	[10, 2]	2316				
[6, 5, 1]	720	[11, 1]	4632				
[7, 3, 2]	480						
[7, 4, 1]	720						
[8, 2, 2]	210						
[8, 3, 1]	840						
[9, 2, 1]	840						
[10, 1, 1]	756						

B.6.6 Number of Vertices = 6 ($k = 6$)

$\phi : B$	0	$\phi : B$	1
[6, 6]	100	[12]	1586
[7, 5]	240		
[8, 4]	210		
[9, 3]	280		
[10, 2]	252		
[11, 1]	504		

B.6.7 Number of Vertices = 7 ($k = 7$)

$\phi : B$	0
[12]	132

Appendix C

Numbers of Rootings of Maps

Let $\rho_{\phi,\nu}$ be the partition with one part for each unrooted map u with face partition ϕ and vertex partition ν , equal to the number of rootings of u . For example, $\rho_{[4],[4]} = [2^2 1]$, because there are three unrooted maps u with face and vertex partition $[4]$, and two of these u have two rootings and one of the u has a single rooting.

Partitions $\rho_{\phi,\nu}^o$ and $\rho_{\phi,\nu}^n$, include only those parts associated with orientable and non-orientable unrooted maps respectively. Then clearly $\rho_{\phi,\nu} = \rho_{\phi,\nu}^o \cup \rho_{\phi,\nu}^n$. Computer-generated values of $\rho_{\phi,\nu}^*$, for $* = o, n$ are given in §§C.1.1–C.8.1. The values $\rho_{\phi,\nu}^o$ are given first, for planar maps in §C.1, for maps on the torus in §C.2, and for maps on the double torus in §C.3. The values $\rho_{\phi,\nu}^n$ are given in §C.4–C.8. Since $\rho_{\phi,\nu}^* = \rho_{\nu,\phi}^*$, some values are redundant and are omitted.

These *rooting partitions* $\rho_{\phi,\nu}$ are valuable enumeratively. For example, because

$$\psi_{[4],[4],2} = 3b^2 + b + 1,$$

the value $\rho_{[4],[4]} = [2^2 1]$ implies that the hypothetical parameter ϑ for the Map-Jack Conjecture must depend in some way upon the root of a map. The values of $\rho_{[4^k],\nu}^o$ are relevant to the set $\Omega_{g,n}$ of the Quadrangulation Conjecture. When compared to the appropriate other values of $\rho_{\phi,\nu}^o$ for the set $\mathcal{A}_{g,n}$, it can be demonstrated that the hypothetical bijection Ξ must also depend on the root of map.

Many of the partitions $\rho_{\phi,\nu}^*$ given here can also be determined from the information given in [JV00], where many diagrams of maps and many tables of numbers of maps are given. Each section that follows is specific to a single surface, and numbers of edges determine the subsection. The convention from [JV00], that an orientable surface has genus $g = \frac{1}{2}(2 - \chi)$ and a non-orientable surface has genus $\tilde{g} = 2 - \chi$ is used to designate the surfaces.

The partitions $\rho_{\phi,\nu}^*$ were obtained by generating complete sets of rooted maps, and then checking for isomorphism as unrooted maps by applying the canonical position labelling algorithm. (By this means, combinatorial maps can be tested for isomorphism

in polynomial time.) Note that $\ell(\rho_{\phi,\nu}^*)$ gives the number of unrooted maps of the specific type, and $|\rho_{\phi,\nu}^*|$ gives the number of rooted of the specific type.

C.1 Surface: Genus 0 ($\chi = 2$, orientable)

C.1.1 Number of Edges: 1

$\phi : \nu$	[2]
[1, 1]	[1]

C.1.2 Number of Edges: 2

$\phi : \nu$	[3, 1]	[2, 2]	$\phi : \nu$	[4]
[3, 1]	[4]	\emptyset	[2, 1, 1]	[2]
[2, 2]	\emptyset	[1]		

C.1.3 Number of Edges: 3

$\phi : \nu$	[5, 1]	[4, 2]	[3, 3]	$\phi : \nu$	[6]
[4, 1, 1]	[6]	\emptyset	[3]	[3, 1, 1, 1]	[2]
[3, 2, 1]	[6]	[6]	\emptyset	[2, 2, 1, 1]	[3]
[2, 2, 2]	\emptyset	\emptyset	[1]		

C.1.4 Number of Edges: 4

$\phi : \nu$	[6, 1, 1]	[5, 2, 1]	[4, 3, 1]	[4, 2, 2]	[3, 3, 2]	
[6, 1, 1]	[8, 4]	[8]	[16]	\emptyset	[4]	
[5, 2, 1]	[8]	[16, 8]	[8]	\emptyset	[8]	
[4, 3, 1]	[16]	[8]	[8 ²]	[8]	\emptyset	
[4, 2, 2]	\emptyset	\emptyset	[8]	[4]	\emptyset	
[3, 3, 2]	[4]	[8]	\emptyset	\emptyset	[4]	
$\phi : \nu$	[7, 1]	[6, 2]	[5, 3]	[4, 4]	$\phi : \nu$	[8]
[5, 1, 1, 1]	[8]	\emptyset	[8]	\emptyset	[4, 1, 1, 1, 1]	[2]
[4, 2, 1, 1]	[16]	[8]	[8]	[4]	[3, 2, 1, 1, 1]	[8]
[3, 3, 1, 1]	[8]	[4]	\emptyset	[4]	[2, 2, 2, 1, 1]	[4]
[3, 2, 2, 1]	[8]	[8]	[8]	\emptyset		
[2, 2, 2, 2]	\emptyset	\emptyset	\emptyset	[1]		

C.1.5 Number of Edges: 5

$\phi : \nu$	[8, 1, 1]	[7, 2, 1]	[6, 3, 1]	[6, 2, 2]	[5, 4, 1]	[5, 3, 2]	[4, 4, 2]	[4, 3, 3]
[7, 1, 1, 1]	[10 ²]	[10]	[20, 10]	\emptyset	[20]	[10]	\emptyset	[10]
[6, 2, 1, 1]	[20, 10]	[20 ² , 10]	[20, 10]	\emptyset	[20 ²]	[20, 10 ²]	\emptyset	[10]
[5, 3, 1, 1]	[20, 10 ²]	[20, 10]	[20, 10]	[10]	[20, 10 ²]	[10]	[10]	[10]
[5, 2, 2, 1]	[10]	[20, 10]	[20, 10]	[10]	[10]	[10]	[10]	[10]
[4, 4, 1, 1]	[10 ²]	[10]	[20, 10]	[5]	[10]	\emptyset	[10]	[5]
[4, 3, 2, 1]	[20 ²]	[20 ² , 10]	[20, 10 ²]	[10 ²]	[20, 10 ²]	[20, 10]	[10]	[10]
[4, 2, 2, 2]	\emptyset	\emptyset	\emptyset	\emptyset	[10]	[10]	\emptyset	\emptyset
[3, 3, 3, 1]	[10]	[10]	\emptyset	\emptyset	[10]	[10]	\emptyset	\emptyset
[3, 3, 2, 2]	[5]	[10]	[10]	[5]	\emptyset	\emptyset	[5]	[5]

$\phi : \nu$	[9, 1]	[8, 2]	[7, 3]	[6, 4]	[5, 5]	$\phi : \nu$	[10]
[6, 1, 1, 1, 1]	[10]	\emptyset	[10]	\emptyset	[5]	[5, 1, 1, 1, 1, 1]	[2]
[5, 2, 1, 1, 1]	[20, 10]	[10]	[20]	[10]	[10]	[4, 2, 1, 1, 1, 1]	[10]
[4, 3, 1, 1, 1]	[20, 10]	[10]	[10]	[10 ²]	\emptyset	[3, 3, 1, 1, 1, 1]	[5]
[4, 2, 2, 1, 1]	[20, 10]	[20]	[10 ²]	[10]	[5 ²]	[3, 2, 2, 1, 1, 1]	[10 ²]
[3, 3, 2, 1, 1]	[20, 10]	[10 ²]	[10]	[10]	[10]	[2, 2, 2, 2, 1, 1]	[5]
[3, 2, 2, 2, 1]	[10]	[10]	[10]	[10]	\emptyset		
[2, 2, 2, 2, 2]	\emptyset	\emptyset	\emptyset	\emptyset	[1]		

C.2 Surface: Genus 1 ($\chi = 0$, orientable)

C.2.1 Number of Edges: 2

$\phi : \nu$	[4]
[4]	[1]

C.2.2 Number of Edges: 3

$\phi : \nu$	[6]
[5, 1]	[6]
[4, 2]	[3]
[3, 3]	[1]

C.2.3 Number of Edges: 4

$\phi : \nu$	[7, 1]	[6, 2]	[5, 3]	[4, 4]	$\phi : \nu$	[8]
[7, 1]	[16 ² , 8]	[16]	[8 ²]	[8]	[6, 1, 1]	[8 ² , 4]
[6, 2]	[16]	[8, 4]	[8]	[4]	[5, 2, 1]	[16, 8]
[5, 3]	[8 ²]	[8]	[8]	\emptyset	[4, 3, 1]	[8 ²]
[4, 4]	[8]	[4]	\emptyset	[2, 1]	[4, 2, 2]	[4, 2]
					[3, 3, 2]	[4]

C.2.4 Number of Edges: 5

$\phi : \nu$	[9, 1]	[8, 2]	[7, 3]	[6, 4]	[5, 5]
[8, 1, 1]	[20 ⁶ , 10 ³]	[20, 10 ³]	[20 ² , 10 ³]	[20 ² , 10, 5]	[10 ² , 5]
[7, 2, 1]	[20 ⁷ , 10]	[20 ⁴ , 10]	[20 ³ , 10]	[20, 10 ⁴]	[20, 10]
[6, 3, 1]	[20 ⁶ , 10]	[20 ² , 10 ²]	[20, 10 ³]	[10 ³]	[20, 10]
[6, 2, 2]	[20, 10]	[20, 5]	[10 ²]	[10, 5]	[5 ²]
[5, 4, 1]	[20 ⁵ , 10 ²]	[20 ² , 10]	[20, 10 ²]	[20, 10 ³]	[10]
[5, 3, 2]	[20 ² , 10 ²]	[10 ⁴]	[20, 10]	[20, 10]	\emptyset
[4, 4, 2]	[20, 10]	[10 ²]	[10]	[5]	[5 ²]
[4, 3, 3]	[10 ³]	[10, 5]	[10]	[5]	[5]
$\phi : \nu$	[10]				
[7, 1, 1, 1]	[20, 10 ³]				
[6, 2, 1, 1]	[20 ³ , 10 ⁴]				
[5, 3, 1, 1]	[20 ² , 10 ³]				
[5, 2, 2, 1]	[20 ² , 10 ²]				
[4, 4, 1, 1]	[10 ² , 5 ²]				
[4, 3, 2, 1]	[20 ² , 10 ⁴]				
[4, 2, 2, 2]	[5 ²]				
[3, 3, 3, 1]	[10]				
[3, 3, 2, 2]	[5 ²]				

C.3 Surface: Genus 2 ($\chi = -2$, orientable)

C.3.1 Number of Edges: 4

$\phi : \nu$	[8]
[8]	[8 ² , 4, 1]

C.3.2 Number of Edges: 5

$\phi : \nu$	[10]
[9, 1]	$[20^8, 10^5]$
[8, 2]	$[20^4, 10^2, 5]$
[7, 3]	$[20, 10^5]$
[6, 4]	$[20, 10^4, 5]$
[5, 5]	$[10^2, 5^2, 2, 1]$

C.4 Surface: Genus $\tilde{1}$ ($\chi = 1$, nonorientable)

C.4.1 Number of Edges: 1

$\phi : \nu$	[2]
[2]	[1]

C.4.2 Number of Edges: 2

$\phi : \nu$	[4]
[3, 1]	[4]
[2, 2]	[1]

C.4.3 Number of Edges: 3

$\phi : \nu$	[5, 1]	[4, 2]	[3, 3]	$\phi : \nu$	[6]
[5, 1]	[12, 6]	[6]	[6]	[4, 1, 1]	[6, 3]
[4, 2]	[6]	[6]	[3]	[3, 2, 1]	$[6^2]$
[3, 3]	[6]	[3]	\emptyset	[2, 2, 2]	[1]

C.4.4 Number of Edges: 4

$\phi : \nu$	[7, 1]	[6, 2]	[5, 3]	[4, 4]	$\phi : \nu$	[8]
[6, 1, 1]	$[16^2, 8^2]$	[8, 4]	$[16, 8^2]$	[8]	[5, 1, 1, 1]	$[8^2]$
[5, 2, 1]	$[16^2, 8^2]$	$[16, 8^2]$	$[16, 8^2]$	[8]	[4, 2, 1, 1]	$[16, 8^2, 4]$
[4, 3, 1]	$[16^3, 8]$	[16, 8]	$[8^2]$	$[8^2]$	[3, 3, 1, 1]	$[8^2]$
[4, 2, 2]	[8]	[8]	[8]	[4, 2]	[3, 2, 2, 1]	$[8^3]$
[3, 3, 2]	$[8^2]$	[8, 4]	[8]	\emptyset	[2, 2, 2, 2]	[1]

C.4.5 Number of Edges: 5

$\phi : \nu$	[8, 1, 1]	[7, 2, 1]	[6, 3, 1]	[6, 2, 2]	[5, 4, 1]	[5, 3, 2]	[4, 4, 2]	[4, 3, 3]
[8, 1, 1]	$[20^4, 10^7]$	$[20^4, 10^4]$	$[20^8, 10^2]$	[10, 5]	$[20^7, 10]$	$[20^2, 10^4]$	$[10^2]$	$[20^2, 10, 5]$
[7, 2, 1]	$[20^4, 10^4]$	$[20^9, 10^3]$	$[20^7, 10^2]$	$[20, 10^2]$	$[20^6, 10^2]$	$[20^4, 10^5]$	[20, 10]	$[20, 10^3]$
[6, 3, 1]	$[20^8, 10^2]$	$[20^7, 10^2]$	$[20^5, 10^2]$	$[20, 10^2]$	$[20^7, 10^3]$	$[20^3, 10^3]$	[20, 10]	$[10^3]$
[6, 2, 2]	[10, 5]	$[20, 10^2]$	$[20, 10^2]$	[10, 5]	$[20, 10^2]$	$[20, 10^2]$	[10, 5]	[10, 5]
[5, 4, 1]	$[20^7, 10]$	$[20^6, 10^2]$	$[20^7, 10^3]$	$[20, 10^2]$	$[20^3, 10^5]$	$[20, 10^2]$	$[20^2, 10]$	$[10^4]$
[5, 3, 2]	$[20^2, 10^4]$	$[20^4, 10^5]$	$[20^3, 10^3]$	$[20, 10^2]$	$[20, 10^2]$	$[20, 10^2]$	$[10^3]$	[20, 10]
[4, 4, 2]	$[10^2]$	[20, 10]	[20, 10]	[10, 5]	$[20^2, 10]$	$[10^3]$	[10]	[5]
[4, 3, 3]	$[20^2, 10, 5]$	$[20, 10^3]$	$[10^3]$	[10, 5]	$[10^4]$	[20, 10]	[5]	[5]
$\phi : \nu$	[9, 1]	[8, 2]	[7, 3]	[6, 4]	[5, 5]			
[7, 1, 1, 1]	$[20^4, 10^2]$	$[10^2]$	$[20^2, 10^3]$	[20, 10]	[20, 10]			
[6, 2, 1, 1]	$[20^8, 10^2]$	$[20^3, 10^3]$	$[20^4, 10^3]$	$[20^2, 10^2]$	$[20, 10^4]$			
[5, 3, 1, 1]	$[20^7, 10^4]$	$[20^2, 10^3]$	$[20^3, 10]$	$[20^2, 10^4]$	[20, 10]			
[5, 2, 2, 1]	$[20^3, 10^3]$	$[20^2, 10^3]$	$[20^2, 10^3]$	$[20, 10^3]$	$[10^2]$			
[4, 4, 1, 1]	$[20^4, 10]$	$[10^3]$	$[20, 10^2]$	$[20, 10^2, 5]$	[5]			
[4, 3, 2, 1]	$[20^9, 10^3]$	$[20^5, 10^3]$	$[20^3, 10^3]$	$[20, 10^6]$	$[20^2, 10]$			
[4, 2, 2, 2]	[10]	[10]	[10]	[10]	$[5^2]$			
[3, 3, 3, 1]	$[20^2]$	$[10^2]$	[10]	[10]	[10]			
[3, 3, 2, 2]	$[10^3]$	$[10^2, 5]$	$[10^2]$	[10, 5]	\emptyset			
$\phi : \nu$	[10]							
[6, 1, 1, 1, 1]	$[10^2, 5]$							
[5, 2, 1, 1, 1]	$[20^2, 10^4]$							
[4, 3, 1, 1, 1]	$[20^2, 10^3]$							
[4, 2, 2, 1, 1]	$[20^2, 10^4, 5^2]$							
[3, 3, 2, 1, 1]	$[20^2, 10^4]$							
[3, 2, 2, 2, 1]	$[10^4]$							
[2, 2, 2, 2, 2]	[1]							

C.5 Surface: Genus $\tilde{2}$ ($\chi = 0$, nonorientable)

C.5.1 Number of Edges: 2

$\phi : \nu$	[4]
[4]	$[2^2]$

C.5.2 Number of Edges: 3

$\phi : \nu$	[6]
[5, 1]	[12, 6 ²]
[4, 2]	[6, 3 ²]
[3, 3]	[3 ²]

C.5.3 Number of Edges: 4

$\phi : \nu$	[7, 1]	[6, 2]	[5, 3]	[4, 4]	$\phi : \nu$	[8]
[7, 1]	[16 ⁹ , 8 ²]	[16 ³ , 8 ²]	[16 ³ , 8 ⁴]	[16, 8 ²]	[6, 1, 1]	[16 ² , 8 ⁵ , 4 ²]
[6, 2]	[16 ³ , 8 ²]	[16, 8 ³ , 4 ²]	[16, 8 ³]	[8, 4 ²]	[5, 2, 1]	[16 ⁴ , 8 ⁴]
[5, 3]	[16 ³ , 8 ⁴]	[16, 8 ³]	[16, 8 ²]	[8]	[4, 3, 1]	[16 ³ , 8 ⁴]
[4, 4]	[16, 8 ²]	[8, 4 ²]	[8]	[4, 2 ⁴]	[4, 2, 2]	[8, 4 ⁴]
					[3, 3, 2]	[8 ² , 4 ²]

C.5.4 Number of Edges: 5

$\phi : \nu$	[9, 1]	[8, 2]	[7, 3]	[6, 4]	[5, 5]
[8, 1, 1]	[20 ²⁷ , 10 ⁶]	[20 ⁵ , 10 ¹⁰]	[20 ¹³ , 10 ⁶]	[20 ⁹ , 10 ³ , 5 ²]	[20 ³ , 10 ⁶ , 5 ²]
[7, 2, 1]	[20 ²⁸ , 10 ⁴]	[20 ¹⁵ , 10 ⁶]	[20 ¹⁴ , 10 ⁵]	[20 ⁸ , 10 ⁸]	[20 ⁶ , 10 ³]
[6, 3, 1]	[20 ²⁹ , 10 ²]	[20 ¹¹ , 10 ⁵]	[20 ⁹ , 10 ⁵]	[20 ⁶ , 10 ⁷]	[20 ⁵ , 10 ³]
[6, 2, 2]	[20 ⁴ , 10 ⁴]	[20 ³ , 10 ³ , 5 ²]	[20 ² , 10 ⁵]	[20, 10 ⁴ , 5 ²]	[10 ² , 5 ⁴]
[5, 4, 1]	[20 ²⁵ , 10 ⁴]	[20 ¹⁰ , 10 ³]	[20 ⁸ , 10 ⁶]	[20 ⁷ , 10 ⁹]	[20 ² , 10 ²]
[5, 3, 2]	[20 ¹¹ , 10 ⁸]	[20 ⁵ , 10 ¹⁰]	[20 ⁶ , 10 ³]	[20 ⁴ , 10 ⁴]	[20, 10]
[4, 4, 2]	[20 ⁵ , 10 ²]	[20, 10 ⁶]	[20, 10 ³]	[20, 10 ² , 5 ²]	[10 ² , 5 ⁴]
[4, 3, 3]	[20 ⁵ , 10 ⁶]	[20 ² , 10 ³ , 5 ²]	[20, 10 ³]	[10 ³ , 5 ²]	[10 ² , 5 ²]
$\phi : \nu$	[10]				
[7, 1, 1, 1]	[20 ⁷ , 10 ⁶]				
[6, 2, 1, 1]	[20 ¹⁴ , 10 ¹²]				
[5, 3, 1, 1]	[20 ¹³ , 10 ⁶]				
[5, 2, 2, 1]	[20 ⁸ , 10 ⁸]				
[4, 4, 1, 1]	[20 ³ , 10 ⁷ , 5 ⁴]				
[4, 3, 2, 1]	[20 ¹⁵ , 10 ¹⁰]				
[4, 2, 2, 2]	[10 ² , 5 ⁴]				
[3, 3, 3, 1]	[20 ² , 10 ²]				
[3, 3, 2, 2]	[10 ⁴ , 5 ⁴]				

C.6 Surface: Genus $\tilde{3}$ ($\chi = -1$, nonorientable)

C.6.1 Number of Edges: 3

$\phi : \nu$	[6]
[6]	[12, 6 ³ , 3 ³ , 2]

C.6.2 Number of Edges: 4

$\phi : \nu$	[8]
[7, 1]	[16 ¹⁷ , 8 ⁷]
[6, 2]	[16 ⁴ , 8 ¹¹ , 4 ³]
[5, 3]	[16 ⁵ , 8 ⁷]
[4, 4]	[8 ⁶ , 4 ³ , 2]

C.6.3 Number of Edges: 5

$\phi : \nu$	[9, 1]	[8, 2]	[7, 3]	[6, 4]	[5, 5]
[9, 1]	[20 ¹⁴⁰ , 10 ⁷]	[20 ⁵⁷ , 10 ⁹]	[20 ⁵⁶ , 10 ¹⁴]	[20 ⁴⁴ , 10 ¹⁵]	[20 ²² , 10 ⁷]
[8, 2]	[20 ⁵⁷ , 10 ⁹]	[20 ²⁷ , 10 ²⁸]	[20 ²⁵ , 10 ¹³]	[20 ¹⁸ , 10 ¹³ , 5 ⁵]	[20 ⁷ , 10 ¹⁰ , 5 ³]
[7, 3]	[20 ⁵⁶ , 10 ¹⁴]	[20 ²⁵ , 10 ¹³]	[20 ¹⁹ , 10 ⁹]	[20 ¹² , 10 ¹¹]	[20 ⁸ , 10 ⁵]
[6, 4]	[20 ⁴⁴ , 10 ¹⁵]	[20 ¹⁸ , 10 ¹³ , 5 ⁵]	[20 ¹² , 10 ¹¹]	[20 ⁷ , 10 ¹⁹ , 5 ⁵]	[20 ⁴ , 10 ¹⁰ , 5 ³]
[5, 5]	[20 ²² , 10 ⁷]	[20 ⁷ , 10 ¹⁰ , 5 ³]	[20 ⁸ , 10 ⁵]	[20 ⁴ , 10 ¹⁰ , 5 ³]	[20, 10 ²]

$\phi : \nu$	[10]
[8, 1, 1]	[20 ⁵⁷ , 10 ²⁸ , 5 ³]
[7, 2, 1]	[20 ⁷⁴ , 10 ¹⁶]
[6, 3, 1]	[20 ⁵⁶ , 10 ¹⁴]
[6, 2, 2]	[20 ⁸ , 10 ²² , 5 ⁶]
[5, 4, 1]	[20 ⁴⁹ , 10 ¹⁵]
[5, 3, 2]	[20 ²⁶ , 10 ¹⁶]
[4, 4, 2]	[20 ⁷ , 10 ¹³ , 5 ⁸]
[4, 3, 3]	[20 ⁶ , 10 ¹⁵ , 5 ³]

C.7 Surface: Genus $\tilde{4}$ ($\chi = -2$, nonorientable)

C.7.1 Number of Edges: 4

$\phi : \nu$	[8]
[8]	[16 ¹⁹ , 8 ¹⁹ , 4 ⁷ , 2 ²]

C.7.2 Number of Edges: 5

$\phi : \nu$	[10]
[9, 1]	$[20^{230}, 10^{28}]$
[8, 2]	$[20^{99}, 10^{42}, 5^8]$
[7, 3]	$[20^{81}, 10^{28}]$
[6, 4]	$[20^{57}, 10^{46}, 5^8]$
[5, 5]	$[20^{26}, 10^{23}, 5^{10}]$

C.8 Surface: Genus $\tilde{5}$ ($\chi = -3$, nonorientable)

C.8.1 Number of Edges: 5

$\phi : \nu$	[10]
[10]	$[20^{358}, 10^{100}, 5^{13}, 2^2]$

Bibliography

- [AB97] D. Arquès and J.-F. Béraud, *Rooted maps and hypermaps on surfaces*, (preprint), 1997.
- [BIZ80] D. Bessis, C. Itzykson, and J.-B. Zuber, *Quantum field theory techniques in graphical enumeration*, *Advances in Applied Math.* **1** (1980), 109–157.
- [Bro95] D. R. L. Brown, *Random matrices in the enumeration of locally orientable maps*, Master’s thesis, University of Waterloo, 1995.
- [Bro98] D. R. L. Brown, *A relationship between Jucys-Murphy elements, the Farahat-Higman ring and some symmetric functions of Macdonald*, (research notes), 1998.
- [BT64] W. G. Brown and W. T. Tutte, *On the enumeration of rooted non-separable planar maps*, *Canad. J. Math.* **16** (1964), 572–577.
- [CV81] R. Cori and B. Vauquelin, *Planar maps are well labeled trees*, *Canad. J. Math.* **33** (1981), no. 5, 1023–1042.
- [FH59] H. K. Farahat and G. Higman, *The centres of symmetric group rings*, *Proc. Roy. Soc. London Ser. A* **250** (1959), 212–221.

- [GHJ99] I. P. Goulden, J. L. Harer, and D. M. Jackson, *A geometric parameterization for the virtual Euler characteristic of the moduli spaces of real and complex algebraic curves*, Trans. Amer. Math. Soc. (1999), (to appear).
- [GJ83] I. P. Goulden and D. M. Jackson, *Combinatorial enumeration*, Wiley-Interscience Series in Discrete Mathematics, John Wiley & Sons Inc., New York, 1983, With a foreword by Gian-Carlo Rota.
- [GJ94] I. P. Goulden and D. M. Jackson, *Symmetric functions and Macdonald's result for top connexion coefficients in the symmetric group*, J. Algebra **166** (1994), no. 2, 364–378.
- [GJ96a] I. P. Goulden and D. M. Jackson, *Connection coefficients, matchings, maps and combinatorial conjectures for Jack symmetric functions*, Trans. Amer. Math. Soc. **348** (1996), no. 3, 873–892.
- [GJ96b] I. P. Goulden and D. M. Jackson, *Maps in locally orientable surfaces, the double coset algebra, and zonal polynomials*, Canad. J. Math. **48** (1996), no. 3, 569–584.
- [GJ97a] I. P. Goulden and D. M. Jackson, *Maps in locally orientable surfaces and integrals over real symmetric surfaces*, Canad. J. Math. **49** (1997), no. 5, 865–882.
- [GJ97b] I. P. Goulden and D. M. Jackson, *Transitive factorisations into transpositions and holomorphic mappings on the sphere*, Proc. Amer. Math. Soc. **125** (1997), no. 1, 51–60.

- [GS96] I. M. Gessel and B. E. Sagan, *The Tutte polynomial of a graph, depth-first search, and simplicial complex partitions*, Electron. J. Combin. **3** (1996), no. 2, Research Paper 9, approx. 36 pp. (electronic), The Foata Festschrift.
- [GT87] J. L. Gross and T. W. Tucker, *Topological graph theory*, Series in Discrete Mathematics and Optimization, Wiley Interscience, 1987.
- [GW79] I. M. Gessel and D. L. Wang, *Depth-first search as a combinatorial correspondence*, J. Combin. Theory Ser. A **26** (1979), no. 3, 308–313.
- [Hoo74] G. 't Hooft¹, *A planar diagram theory for strong interactions*, Nuclear Physics B **72** (1974), 461–473.
- [HSS92] P. J. Hanlon, R. P. Stanley, and J. R. Stembridge, *Some combinatorial aspects of the spectra of normally distributed random matrices*, Hypergeometric functions on domains of positivity, Jack polynomials, and applications (Tampa, FL, 1991), Amer. Math. Soc., Providence, RI, 1992, pp. 151–174.
- [HZ86] J. Harer and D. Zagier, *The Euler characteristic for the moduli space of curves*, Invent. Math. **85** (1986), 457–485.
- [Irv98] J. Irving, *An enumerative problem concerning products of permutations*, Master's thesis, University of Waterloo, 1998.

¹1999 Nobel Prize Winner

- [Jac94] D. M. Jackson, *On an integral representation for the genus series for 2-cell embeddings*, Trans. Amer. Math. Soc. **344** (1994), no. 2, 755–772.
- [Jac96] D. M. Jackson, *Algebraic and analytic approaches for the genus series for 2-cell embeddings on orientable and nonorientable surfaces*, Formal power series and algebraic combinatorics (New Brunswick, NJ, 1994), Amer. Math. Soc., Providence, RI, 1996, pp. 115–132.
- [JPV96] D. M. Jackson, M. J. Perry, and T. I. Visentin, *Factorisations for partition functions of random Hermitian matrix models*, Comm. Math. Phys. **179** (1996), no. 1, 25–59.
- [Juc74] A.-A. A. Jucys, *Symmetric polynomials and the center of the symmetric group ring*, Rep. Mathematical Phys. **5** (1974), no. 1, 107–112.
- [JV90a] D. M. Jackson and T. I. Visentin, *A character-theoretic approach to embeddings of rooted maps in an orientable surface of given genus*, Trans. Amer. Math. Soc. **322** (1990), no. 1, 343–363.
- [JV90b] D. M. Jackson and T. I. Visentin, *Character theory and rooted maps in an orientable surface of given genus: face-colored maps*, Trans. Amer. Math. Soc. **322** (1990), no. 1, 365–376.
- [JV99] D. M. Jackson and T. I. Visentin, *A combinatorial relationship between Eulerian maps hypermaps in orientable surfaces*, Journal of Combinatorial Theory, Series A **87** (1999), 120–150, (to appear).

- [JV00] D. M. Jackson and T. I. Visentin, *An atlas of the smaller maps on orientable and nonorientable surfaces*, CRC Press, 2000, (to appear).
- [KS97] F. Knop and S. Sahi, *A recursion and a combinatorial formula for Jack polynomials*, *Inventiones Mathematicae* (1997), no. 128, 9–22.
- [LPS95] F. Lesage, V. Pasquier, and D. Serban, *Dynamical correlation functions in the Calogero-Sutherland model*, *Nuclear Phys. B* **435** (1995), 585–603.
- [LV95] L. Lapoint and L. Vinet, *A Rodrigues formula for the Jack polynomials and the Macdonald-Stanley conjecture*, *International Mathematics Research Notices* (1995), no. 9, 419–424.
- [Mac95] I. G. Macdonald, *Symmetric functions and Hall polynomials*, second ed., The Clarendon Press Oxford University Press, New York, 1995, With contributions by A. Zelevinsky, Oxford Science Publications.
- [Meh91] M. L. Mehta, *Random matrices*, second ed., Academic Press, New York, 1991.
- [Sag91] B. E. Sagan, *The symmetric group*, Wadsworth & Brooks/Cole Advanced Books & Software, Pacific Grove, CA, 1991, Representations, combinatorial algorithms, and symmetric functions.
- [Sch94] L. Schepers (ed.), *The Grothendieck theory of Dessins d'Enfants*, London Mathematical Society Lecture Note Series, vol. 200, Cambridge University Press, 1994.

- [Sch98] G. Schaeffer, *Conjugaison d'arbres et cartes combinatoires aléatoires*, Ph.D. thesis, L'Université Bordeaux I, 1998.
- [Sta89] R. P. Stanley, *Some combinatorial properties of Jack symmetric functions*, *Advances in Mathematics* **74** (1989), 87–134.
- [Ste95] J. R. Stembridge, *A Maple package for symmetric functions*, *J. Symbolic Comput.* **20** (1995), no. 5-6, 755–768, *Symbolic computation in combinatorics Δ_1* (Ithaca, NY, 1993).
- [Tut62] W. T. Tutte, *A census of slicings*, *Canad. J. Math.* **14** (1962), 708–722.
- [Tut63] W. T. Tutte, *A census of planar maps*, *Canad. J. Math.* **15** (1963), 249–271.
- [Tut84] W. T. Tutte, *Graph theory*, *Encyclopedia of Math. and its Applications*, vol. 21, Addison-Wesley Publishing Co., Reading, Mass., 1984, With a foreword by C. St. J. A. Nash-Williams.
- [Wal71] T. R. S. Walsh, *Combinatorial enumeration of non-planar maps*, Ph.D. thesis, University of Toronto, 1971.